ANL-75-30

ANL-75-30

DIVISION OF BIOLOGICAL AND MEDICAL RESEARCH

Annual Report

1974

U of C-AUA-USERDA

ARGONNE NATIONAL LABORATORY, ARGONNE, ILLINOIS

Prepared for the U. S. ENERGY RESEARCH AND DEVELOPMENT ADMINISTRATION under Contract W-31-109-Eng-38

DISCLAIMER

The facilities of Argonne National Laboratory are owned by the United States Government. Under the terms of a contract (W-31-109-Eng-38) between the U. S. Energy Research and Development Administration, Argonne Universities Association and The University of Chicago, the University employs the staff and operates the Laboratory in accordance with policies and programs formulated, approved and reviewed by the Association.

MEMBERS OF ARGONNE UNIVERSITIES ASSOCIATION

The University of Arizona	Kansas State University	The Ohio State University
Carnegie-Mellon University	The University of Kansas	Ohio University
Case Western Reserve University	Loyola University	The Pennsylvania State University
The University of Chicago	Marquette University	Purdue University
University of Cincinnati	Michigan State University	Saint Louis University
Illinois Institute of Technology	The University of Michigan	Southern Illinois University
University of Illinois	University of Minnesota	The University of Texas at Austin
Indiana University	University of Missouri	Washington University
Iowa State University	Northwestern University	Wayne State University
The University of Iowa	University of Notre Dame	The University of Wisconsin

Printed in the United States of America
Available from
National Technical Information Service
U. S. Department of Commerce
5285 Port Royal Road
Springfield, Virginia 22161
Price: Printed Copy $7.60; Microfiche $2.25

Distribution Category:
Biology and Medicine
(UC-48)

ANL-75-30

ARGONNE NATIONAL LABORATORY
9700 SOUTH CASS AVENUE
ARGONNE, ILLINOIS 60439

DIVISION OF BIOLOGICAL AND MEDICAL RESEARCH

ANNUAL REPORT 1974

JOHN F. THOMSON, ACTING DIRECTOR

MARCIA W. ROSENTHAL, EDITOR

PRECEDING REPORT
ANL-8070, DECEMBER 1973

THIS PAGE

WAS INTENTIONALLY

LEFT BLANK

TABLE OF CONTENTS

9. BIOPHYSICS

1. INTRODUCTION

John F. Thomson, Acting Division Director

A number of significant changes took place in the Division of Biological and Medical Research during 1974:

Warren K. Sinclair, who had been Division Director since January 1, 1970, was appointed Associate Laboratory Director for Biomedical and Environmental Research on April 1. The Associate Division Director, John F. Thomson, was named Acting Director.

Allen H. Anderson elected early retirement on September 28 as Assistant Division Director, a position he had held since 1962. His duties have been assumed by Ronald L. Breyne, who transferred from the Chemical Engineering Division.

Two Senior Scientists, Theodore N. Tahmisian (Carcinogenesis) and Fritz Schlenk (Biochemistry) retired on June 30 and November 30, respectively. Both are still affiliated with the Division, the former as a consultant, the latter as a Resident Associate.

On April 1, 1974, Robert J. Flynn resigned as Co-leader of the Aging Research Group to devote full time to administration of the Animal Facilities.

Marcia W. Rosenthal became Division Editor on November 20.

Three Assistant Scientists joined the staff in 1974: Maryka H. Bhattacharyya (Modification of Radiation Effects), Ronald D. Ley (Mammalian Cell Biology), and David L. Hachey (Biophysics). In addition, Louise S. Lombard, a staff member from 1957 to 1964, returned to the Division as a Veterinary Pathologist for two programs: Radiation Toxicity in Dogs, and Neutron and Gamma-Ray Toxicity Studies.

Douglas Grahn, who had been on leave of absence since January 1973, completed his assignment at the AEC's Division of Biomedical and Environmental Research, and returned on November 1. He will continue his program in Mammalian Genetics, while at the same time he will organize a program dealing with Analysis and Assessment.

The organization of the Division at the end of 1974 is shown in Figure 1.1. The scope of the activities of the groups is as follows:

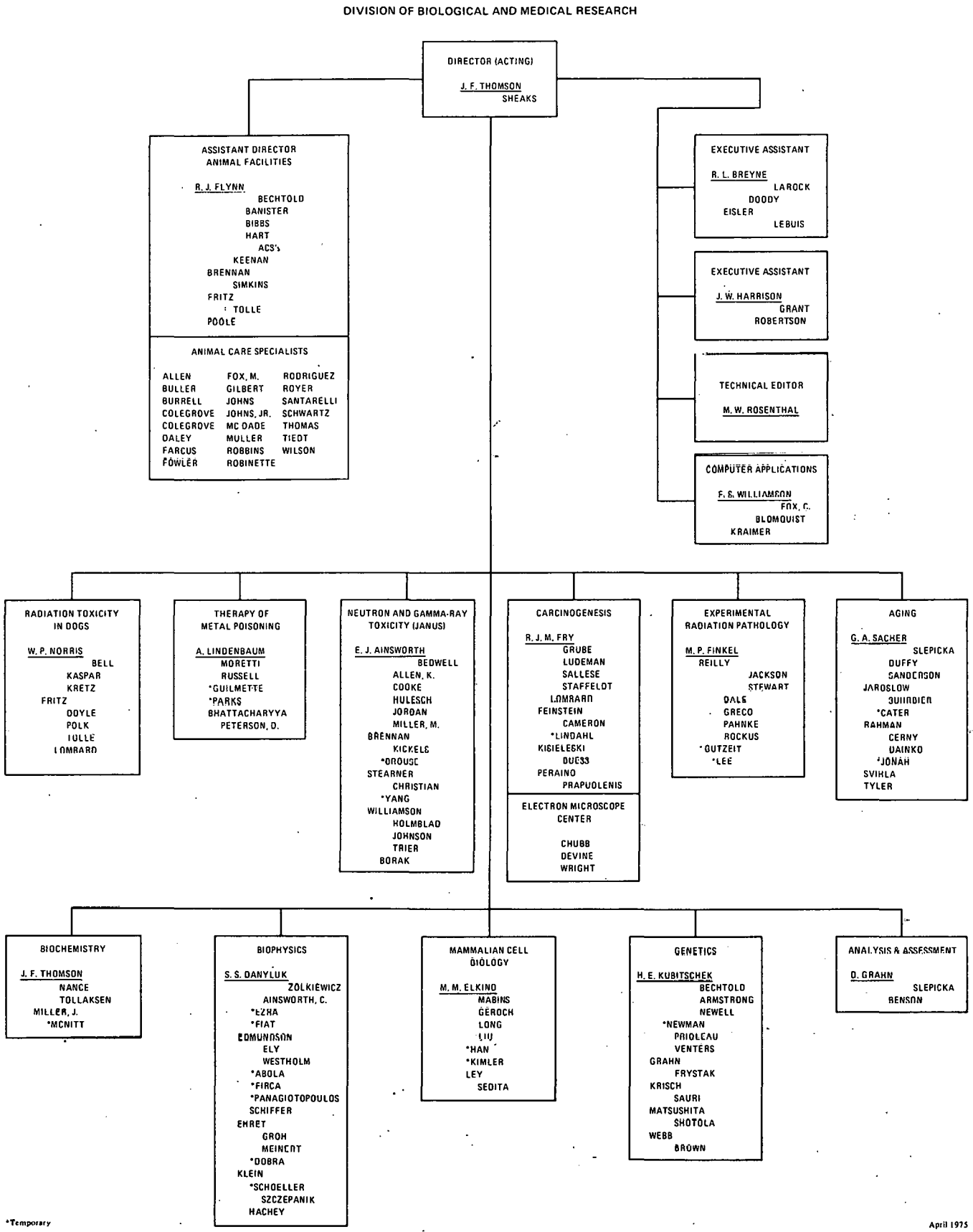

Fig. 1.1. Organizational chart.

RADIATION TOXICITY IN DOGS

The use of a long-lived animal such as the dog is an essential link in the extrapolation of radiation toxicity data from experimental animals to man. Current experiments continue to stress the effects on the beagle of low-level, continuous ^{60}Co γ-radiation at dose rates of 35, 17, 10, and 5 R/day; construction will soon begin on a new irradiation facility designed to permit exposure of dogs to 2.5, 1, and 0.4 R/day. Both duration-of-life and dose-limited exposures are planned, including *in utero* exposures during the entire gestation period. In addition, parallel experiments are planned in which pregnant bitches will be maintained on concentrations of $^{3}H_2O$ that will deliver radiation doses equivalent to 5, 2.5, 1, and 0.4 R/day of ^{60}Co radiation to the fetus.

MODIFICATION OF RADIATION EFFECTS

This program, which is concerned generally with the therapy of poisoning by radioactive and nonradioactive metals, had been a section of the Biochemistry group. This year, in recognition of the importance and increased scope of the program, it has been accorded the status of a separate group. New data are presented here on duration-of-life experiments in mice, therapeutic studies in dogs with diethylenetriaminepentaacetic acid (DTPA), therapeutic studies in mice with pyran copolymers and liposome-encapsulated chelating agents, quantitative autoradiographic analyses in dog liver, and syntheses of DTPA esters.

NEUTRON AND GAMMA-RAY TOXICITY STUDIES (JANUS)

This program is designed to provide information on radiation as an environmental hazard. The major activities are focused in two areas: one comprises experiments designed to compare the late effects of neutron and gamma radiation on mice, with principal emphasis on neoplastic and non-neoplastic disease and on life shortening; the other includes basic studies of injury and recovery at the cellular and tissue levels. The experiments are specifically designed to test the hypothesis of total dose dependence; significant departures from total dose dependence for life shortening are observed for both gamma and neutron irradiation.

CARCINOGENESIS

Since an important late effect of radiation and of other environmental hazards is an increased incidence of tumors in exposed populations, it is appropriate to study the mechanisms of induction of cancer in general, whether it develops spontaneously, or is induced by radiation, chemicals, or viruses. The primary focus of two groups, the Experimental Radiation Pathology and Oncology group and the Carcinogenesis group, is upon mechanisms of carcinogenesis. In addition, many other research groups in the Division have programs oriented toward tumorigenesis. These groups include Radiation Toxicity in Dogs, Neutron and Gamma-Ray Toxicity Studies, Aging Research, the Modification of Radiation Effects program, and also, to a lesser extent, the Biophysics and Mammalian Cell Biology programs. The Experimental

Radiation Pathology and Oncology group (see below) is engaged in studies of viruses as causative agents of bone tumors. Present concerns of the Carcinogenesis program are tumorigenesis and the enhancement of chemically induced tumors in the liver, isozymes, the effects of combined treatment with psoralen and ultraviolet light, and strain and species differences in tumor rates.

EXPERIMENTAL RADIATION PATHOLOGY

This program has evolved from a survey of the toxicity and pathological effects of a number of internally deposited radionuclides to a study of the induction of tumors by viruses. Recent emphasis has been on the search for viruses in spontaneous and radiation-induced bone tumors of mouse, dog, and man. Two osteosarcoma viruses and one osteoma virus have been isolated from mice. Current research has been devoted to determining the degree of interaction among these viruses. There is substantial evidence for the existence of a human osteosarcoma virus.

AGING RESEARCH

Another late effect of radiation, and possibly of other environmental agents as well, is the premature death of exposed animals not only from tumors, but also from assorted degenerative diseases. Like the Carcinogenesis group, the Aging Research group complements the JANUS program, and also carries out research concerned with age-dependent changes in a variety of biological systems. There are two major subprograms, one concerned with the comparative biology, genetics, and evolutionary biology of aging, and the other with the elucidation of the physiologic and biochemical mechanisms of aging. The first of these is represented by progress reports on genetic analysis of factors responsible for strain differences, and on the analysis of genotype-environment interactions, in which mice are exposed to different temperature environments. Research in the second subprogram is described in contributions on aging in the immune system, and on further applications of the technique of liposome encapsulation.

BIOCHEMISTRY

As mentioned above, the program dealing with the therapeutic removal of plutonium from mammals is now considered a separate group, administratively independent from the Biochemistry group. Another program (biochemical and cytological changes in irradiated yeast) was terminated with the retirement of the principal investigator, although reports of recent progress are presented here. The present activities of the Biochemistry group are those concerned with the isolation and characterization of cytoplasmic organelles of mammalian cells, and with the physiology of plants grown in compensated fields.

BIOPHYSICS

With the establishment of a new group, Mammalian Cell Biology (see below), there are now four major programs in Biophysics. Two programs are concerned with different approaches to the study of large molecules of biological significance: proteins by X-ray crystallographic techniques, and nucleic acids and derivatives by nuclear magnetic resonance. In the former, a major achievement has been the extension to 2.3 Å resolution of the structure of a Bence-Jones protein. In the latter, further progress has been made toward a complete NMR assignment of a trinucleotide spectrum. A third program is concerned with elucidation of mechanisms of biological clocks and circadian rhythms at the cellular level; attention is focused on the involvement of intermediary metabolic pathways in circadian regulation. The fourth program is concerned with clinical applications of stable isotopes; the main objectives are synthesis of labeled compounds for diagnostic use, instrument development, and organization of a collaborative network of clinicians to validate the use of the labeled compounds as diagnostic agents.

MAMMALIAN CELL BIOLOGY

This is a new group, derived in part from the program on the radiation biology of mammalian cells in tissue culture that hitherto was a segment of the Biophysics group. The program continues to emphasize the exploitation of cultured mammalian cells for the study of their growth, division, and metabolic processes, and to elucidate how these processes are affected by radiation and other environmental contaminants.

MOLECULAR AND RADIATION GENETICS

The four programs in Molecular Genetics, although each is directed by a different investigator, have as a common aim the understanding of the nature of genetic material and its organization, function, regulation, and replication in the living cell. These studies are essential for the understanding of more complex biological phenomena, such as the effects of radiation and other environmental agents.

The program in Mammalian Genetics has been in abeyance for the past two years during the leave of absence of the principal investigator, Douglas Grahn. With his return (see above), this research will resume.

LABORATORY ANIMAL MEDICINE

The Animal Facilities provide essential services in support of many of the research programs. The production, care, and assessment of disease status of a variety of animal species are included. Much of this work consists of applied research in microbiology, pathology, and husbandry.

EDUCATIONAL ACTIVITIES

The most significant involvement of the Division in the educational process is its postdoctoral training; the contributions of these temporary appointees are evident in every program. The Division also participates in a variety of activities ranging from summer training of local area high school students to specialized research opportunities for college and university faculty members. Programs for both undergraduate and graduate students are also provided, in cooperation with the Argonne Center for Educational Affairs. The Summer Institute in Biology has served as a model for similar activities in other divisions in the Laboratory.

Many members of the staff hold faculty appointments at universities in the Chicago area, and teach courses at the graduate and undergraduate levels. These appointments provide excellent opportunities for student contacts and faculty interactions.

ADMINISTRATIVE STAFF

John F. Thomson (Acting Director)
Ronald L. Breyne (Executive Assistant)
J. William Harrison (Executive Assistant)
Robert J. Flynn (Assistant Director, Animal Facilities)
Marcia W. Rosenthal (Editor)
Robert J. Robertson (Staff Assistant)

SUPPORT STAFF

Jeanne A. Blomquist, Programmer
Thomas J. Doody, Glassblower
William J. Eisler, Engineering Specialist
Martin R. Kraimer, Computer Scientist

2. RADIATION TOXICITY IN DOGS

SUMMARY

William P. Norris, Group Leader

During the past year we have continued to emphasize and extend our studies of the effects of continuous (22 hr/day), whole-body γ-irradiation in the pure-bred beagle dog. Our first major experiment in this area, in which dogs are being exposed continuously until death at one of four different exposure rates ranging from 5 to 35 R/day, is still in progress after 2441 days (∿ 6.7 yr) of irradiation. The experiment has narrowed to the dogs receiving 5 R/day and the controls. A group of dogs receiving one of these relatively low daily exposure rates may exhibit remarkably varied responses, both in survival times in the γ field and in ultimate causes of death. The basis for these large differences in responses of individual dogs remains mostly unexplained, but is presumed to reside in their genetic composition. The composite result in the study, however, demonstrates an orderly, step-wise appearance of clinical end points resulting from radiation-induced damage to the blood-forming tissues. About one-half the dogs exposed continuously to 10 R/day develop bone marrow aplasia and die of anemia, while the other one-half develop bone marrow hyperplasias and die of malignancies--usually myelogenous leukemias. In dogs exposed at rates greater than 10 R/day, aplastic bone marrows predominate; while hyperplastic responses are the dominant cause of death at 5 R/day. Only among the most recent deaths of dogs exposed continuously to either 10 or 5 R/day, have there appeared terminal causes of death unrelated to hematopoietic injury. These causes (degenerative and/or inflammatory disease and cancers of tissue other than bone marrow) suggest that we are now beginning to define the combinations of exposure rate and time of exposure that allow expressions of damage by tissues outside the hematopoietic system.

As dogs have died in this first experiment, the available space in the γ-ray exposure area has been utilized primarily to generate groups of dogs given predetermined total exposures ranging from 1400 to 4000 R at the same exposure rates used in the first study. It is now clear, at all these values of total exposure, that the bone marrow remains at risk from aplasia for ∿ 100 days post-termination of exposure, and from hyperplastic responses for approximately 400 days post-termination of exposure. Beyond these limits there is no suggestion, so far, that damage to the hematopoietic system will contribute importantly to ultimate causes of death.

Our earlier reports demonstrated that pregnant beagles exposed continuously to ^{60}Co γ-rays from conception to parturition, at rates ranging from 5 to 17 R/day delivered apparently normal litters. Thus, when dose rate is properly controlled, radiosensitivity during organogenesis in the fetus is about equal to that of hematopoiesis in the adult. The pups derived from these dams irradiated during pregnancy have reached the age of sexual maturity and have been observed in some detail--especially for reproductive capability. The most striking finding is that all the females have ovaries devoid of ova and show associated abnormalities in their estrous cycles and blood hormone levels. This is the most sensitive indicator of damage from continuous irradiation identified, thus far, in our work.

Plans are well-advanced to construct additional ^{60}Co irradiation facilities that will allow us to extend our measures of the effects of continuous γ-irradiation to exposure rates of 2.5, 1.0, and 0.4 R/day. The data to be derived will allow for critical interspecies comparisons of responses to continuous irradiation that should be helpful in extrapolating to effects expected in man. The new facility will also allow us to extend our current work on the effects of continuous irradiation on the developing fetus.

As a corollary to the studies of effects of continuous γ-irradiation on the fetus, we are actively preparing a facility in which to maintain pregnant bitches at constant concentrations of tritiated body water that are computed to deliver radiation doses equivalent to 5.0, 2.5, 1.0, and 0.4 R/day to the developing fetus. The exposures will begin in the current fiscal year.

RADIATION TOXICITY IN DOGS STAFF

REGULAR STAFF

Doyle, Donald E. (Scientific Assistant)
Fritz, Thomas E. (Veterinary Pathologist)
Kaspar, Lillian A. (Scientific Assistant)
Kretz, Norbert D. (Scientific Assistant)
Lombard, Louise S. (Veterinary Pathologist)
Norris, William P. (Biochemist)
Pearson, Donald L. (Scientific Assistant)
Polk, Patrick H. (Scientific Assistant)
Tolle, David V. (Scientific Assistant)

TEMPORARY STAFF DURING 1974

Stone, John P. (Postdoctoral Appointee)

THE RESPONSE OF BEAGLE DOGS TO PROTRACTED EXPOSURE TO ^{60}Co GAMMA RAYS AT 5 TO 35 R/DAY

I. SURVIVAL AND CLINICAL OBSERVATIONS

William P. Norris, Thomas E. Fritz, and Calvin M. Poole

PURPOSE AND METHODS

Our six previous annual reports (1-6) have described the initiation and progress of a study in which young adult beagle dogs of both sexes are placed in a ^{60}Co γ-ray field and kept there until they die. Daily exposure rates are either 35, 17, 10, or 5 R/22 hour exposure day. Control dogs, maintained under similar conditions, are housed immediately adjacent to the γ-ray exposure facility.

The objectives are to relate survival times, clinical signs of radiation-induced injury, and causes of death to exposure rate and to total accumulated radiation dose. The data will provide a basis for interspecies extrapolations aimed toward predicting effects in man.

Each dog is examined regularly for clinical abnormalities, with special attention to the eyes (for signs of retinal pathology and lens opacities) and body temperature (for indications of septicemia) (1). A complete hematologic examination on each animal, including a differential white cell count, enumeration of platelets, and measurement of certain biochemical parameters, is done at regular intervals. Bacteriologic examinations are performed on blood specimens from living dogs, as well as on postmortem specimens, to define the significance of bacteremia in the overall response. All decedents are necropsied, and their tissues are collected for microscopic study.

PROGRESS REPORT

On October 31, 1974, the experiment had been in progress for 2441 days. By this time, all dogs that had been exposed continuously to either 35, 17, or 10 R/day were dead, while 8 of the 24 dogs given 5 R/day were still surviving in the γ field.

The survival data, to date, for these groups of dogs are summarized in Table 2.1. An exposure rate of 35 R/day is acutely lethal to beagles, but the lower exposure rates allow continued hematopoietic function and survival for up to 3 years and more, depending on exposure rate. Mean survival time in beagles exposed continuously to 5 R/day is currently projected to be approximately 2000 days after initiation of exposure, and the minimal value from data presently in hand is 1796 days.

Table 2.1. Survival, from Initiation of Exposure up to October 31, 1974, of Beagle Dogs Maintained Continuously in a ^{60}Co γ-ray Field

Exposure Rate (R/day)	Number of Dogs	Decedents		Survivors	
		Survival Range (days)	Mean	Number of Dogs	Survival to Date (days)
35	8	45-68	57	None	
17	13	85-1061	317	None	
10	16	209-1966	692	None	
5	24	390-2441	1474	8	2441
Control	8	303		7	2442

In the 5 to 17 R/day groups, the first deaths occurred when the accumulated exposure had reached about 2000 R (Figure 2.1), but at 10 and 17 R/day the accumulated exposure at 100% mortality was about 18,000 R.

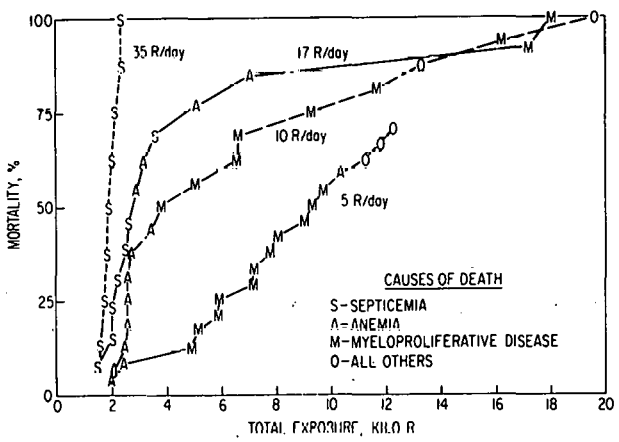

Fig. 2.1. Mortality in beagle dogs exposed continuously to either 5, 10, 17, or 35 R/day in a ^{60}Co γ field. Exposure of the 5 R/day group is still continuing.

Causes of death in these animals have been related most prominently to damage to the hematopoietic system. As can be seen in Figure 2.1, where coded symbols indicate the primary cause of death of each decedent dog, septicemia was the direct cause of death in all dogs exposed to 35 R/day as well as in the early deaths in the group exposed to 17 R/day. Septicemic deaths were followed by deaths from anemia, which occurred especially in the dogs exposed to either 17 or 10 R/day. Anemic deaths were, in turn, followed by deaths from myeloproliferative disease, especially prominent in the dogs exposed to either 10 or 5 R/day. To generalize, the responses of the hematopoietic systems in dogs exposed to 10 R/day are about equally divided between aplasia and hyperplasia. At exposure rates higher than 10 R/day, most deaths result from bone marrow aplasia; while at exposure rates below 10 R/day, hyperplastic responses of the bone marrow predominate.

It may be significant to note that two late deaths in the 10 R/day group, and the last three deaths, to date, in the 5 R/day group, were from causes other than the three just discussed. By analogy to the sequence in causes of death illustrated above, we may speculate that we are now entering the phase where extra-hematopoietic damage, more typical of the usually seen radiation-induced late effects, will begin to be prominent. The five "other causes" include two malignancies (one metastasizing mammary carcinoma and one lymphocytic leukemia) and three instances of inflammatory and/or degenerative disease (one pneumonia, one perforated intestinal ulcer, and one case of muscle abscesses).

REFERENCES

1. Norris, W. P., and C. M. Poole. ANL-7535 (1968), p. 156.
2. Norris, W. P., and C. M. Poole. ANL-7635 (1969), p. 94.
3. Norris, W. P., and C. M. Poole. ANL-7770 (1970), p. 130.
4. Norris, W. P., and C. M. Poole. ANL-7870 (1971), p. 138.
5. Norris, W. P., T. E. Fritz, and C. M. Poole. ANL-7970 (1972), p. 192.
6. Norris, W. P., T. E. Fritz, and C. M. Poole. ANL-8070 (1973), p. 31.

II. EFFECTS OF TERMINATED EXPOSURES

Thomas E. Fritz, William P. Norris, and Calvin M. Poole

PURPOSE AND METHODS

Groups of ∿ 13-month-old beagles of both sexes are being given preselected amounts of whole-body γ-irradiation at exposure rates of either 35, 17, 10, or 5 R/day (1-3). As the exposures are completed, the dogs are removed from the γ-ray field and maintained under observation in our standard kennel regimen for the remainder of their lives.

The intent is to create groups of approximately 20 dogs each that have received either 4000, 2000, or 1400 R delivered at either 10 or 17 R/day, as well as two groups receiving either 2000 or 1400 R delivered at 5 R/day, and one group receiving 1400 R at 35 R/day. It is not possible to deliver higher total exposures at 35 R/day because 1400 R is the 50% lethal dose.

PROGRESS REPORT

The data collected up to the present time are summarized in Table 2.2. The summary includes the progress of two groups of dogs exposed for 100 days at either 17 or 24 R/day in an earlier study. Dogs which are still being irradiated as of the date of this report are also included. During the coming year we should be able to begin irradiating the final dogs to bring each group up to the projected total of 20 chronic survivors in each.

Table 2.2. Interim Data on Effects of Terminated Exposures to Protracted, Whole-body γ-Irradiation in Beagles

R/day	Total Exposure (R)	Total Dogs Irrad.	No. Surviving Irrad.Period	Acute Deaths (<100 days Post-Irrad.)	Chronic Survivors (>100 Days Post-Irrad.)[a]	Decedents (Chronic) Time to Death	Decedents (Chronic) Cause of Death
35	1400	47	35	15	20 (1330-1893)	1774 1276	Endometritis Endometritis
24	2400	8	6	1	5	2024 2255 2291	Convulsive seizure Pneumonia Trauma
17	4000	24	11	1	10 (557-1135)		
17	2000	23	14	7	7 (225-569)	128	Anemia
17	2000	8	Still in field				
17	1700	8	8	3	5 (2862)	305 402 1825 2901	MPD MPD Neurofibrosarcoma Hemangiosarcoma
10	4000	32	22	2	20 (539-1680)	250 407 576 1539	MPD MPD MPD Pneumonia
10	4000	4	Still in field				
10	2000	28	26	7	19 (295-989)		
10	1400	8	8	1	7 (82)		
10	1400	12	Still in field				
5	2000	6	Still in field				
5	1400	18	18	0	18 (647)		
5	1400	6	Still in field				

[a]Values in brackets indicate the time range, post-termination of exposure, over which chronic survivors have been under observation.

The three causes of death, septicemia, anemia, and myeloproliferative disorders (MPD), previously identified in dogs exposed until death at 5 to 35 R/day, are prominent in dogs given terminated exposures. During the past year, either septicemia or anemia has continued to be the cause of death in all dogs that died within 100 days after irradiation was terminated. These must be regarded as the direct, early result of the radiation treatment.

The five cases of MPD that occurred between 250 and 405 days after terminated exposure to either 1700 R (17 R/day x 100 days) or 4000 R (10 R/day x 400 days) are still the only ones seen in dogs that received terminated exposures. No cases of MPD have yet appeared at later times in these groups or in the several other exposure groups. Deaths from other causes are too few at this time to allow any interpretation; endometritis, fatal convulsive seizures, and pneumonia are seen in untreated dogs in this colony.

A variety of non-lethal lesions have occurred and have been treated or are being followed. These include mammary tumors, cutaneous papillomas, sebaceous cysts, gingival epuli, perianal gland tumors, endometritis, and urinary calculi. All of these are also common in colony control dogs.

CONCLUSIONS

So far, the causes of death in dogs receiving terminated exposures to ^{60}Co γ-irradiation are not different from those seen in dogs irradiated continuously until death at similar exposure rates. Thus far, the minimum total exposure that produces MPD is 1700 R delivered at 17 R/day, and the induction period is about 400 days. Exposure rates higher than 17 R/day have never been related to induction of MPD.

REFERENCES

1. Norris, W. P., and C. M. Poole. ANL-7770 (1970), p. 132.
2. Norris, W. P., and T. E. Fritz. ANL-7870 (1971), p. 139.
3. Fritz, T. E., and W. P. Norris. ANL-8070 (1973), p. 33.

III. EFFECT OF CONTINUOUS IRRADIATION IN BEAGLES IRRADIATED DURING FETAL LIFE

*Thomas E. Fritz, William P. Norris, and Jack C. Wiaz**

PURPOSE AND METHODS

It is important to compare the radiosensitivity of the developing fetus to that of the adult under conditions of continuous exposure to ionizing radiation delivered at reasonably low daily exposure rates. The developing fetus is regarded as being one of the most radiosensitive of all biological objects, but is has not been studied with due regard to the relative importance of dose rate and total dose, and especially not in a large animal.

Twenty-eight adult, virgin female beagles were bred to proven sires on two successive days. They were exposed to ^{60}Co γ-irradiation at exposure rates of either 5, 10, 17, or 35 R/22-hour exposure day throughout gestation or for varying periods during pregnancy as previously described (1-3).

Growth rate, reproductive capabilities, and ultimate causes of death are being evaluated in all surviving pups.

PROGRESS REPORT

We have previously reported on the numbers of litters, litter size, survival, and other data relating to the health, growth, and reproduction of the dogs irradiated during fetal life (1-5). During the past year we have continued to observe these dogs and at the time of this report (November 1, 1974) a total of 59 dogs have reached ages ranging from 419 to 1355 days.

Of the 30 females, six (20%) have not yet been observed in estrus. These six range in age from 419 to 1346 days. Thirteen of the 24 dogs that have been in estrus have been bred one or more times. Another seven have refused to copulate when breeding was attempted. None of the 13 that have bred have conceived.

We have surgically removed one ovary from many of these females for weight data and histological examination. The weight of the single ovaries thus far removed from 21 bitches is 0.29 ± 0.02 grams (mean ± S.E.) compared with 0.77 ± 0.04 grams for the ovaries of 109 untreated dogs.

Microscopic examination of ovaries during the past year has confirmed the almost total absence of ova and developing follicles. This response of the ovary of the dog, monkey, and mouse to radiation has been previously reported, but resulting from fractionated exposures, consisting of brief daily doses either to the fetus or to the neonate (6-8).

---

*Participant in the 1974 Summer Institute in Biology, University of Illinois, Chicago.

The vasculature, connective tissue, and rete ovarii appeared normal in most ovaries but the surface epithelium often was hyperplastic. The stroma included an increased number of interstitial cells that strongly resembled luteinized cells, along with membrane-bound cords, or clusters of epithelial cells, that resembled anovular follicles or projections of the surface epithelium. The numbers of luteinized-appearing interstitial cells varied greatly from dog to dog but seemed particularly prominent in some irradiated at 17 R/day.

Because of the abnormal structure of the ovary, and the failure of many bitches to copulate although reported in estrus, more frequent and detailed observations for signs of estrus were made. These observations have suggested that many of the bitches irradiated *in utero* have atypical estrus cycles and associated signs. These abnormalities include more frequent and less pronounced physical signs of estrus and suggest a protracted but incomplete or reduced estrogen stimulation. The presence of ovarian follicles is evidently not necessary for the occurrence of estrus, a finding reported as early as 1927 (9), but not generally recognized.

Because some bitches with anovular ovaries were coming into estrus and breeding, it seemed important to evaluate the ovarian endocrine function through hormone assay. As a preliminary test, serum samples were examined by radioimmuno-assay methods for levels of estradiol, progesterone, and luteinizing hormone (LH) from three normal breeding bitches and four that had been irradiated during fetal life.* Three of the irradiated bitches had previously had one ovary removed, the other had both ovaries intact. As a further control, serum from a surgically ovariectomized, unirradiated female was also tested. Except for the latter dog, serum samples were drawn from all dogs daily for at least 14 days following the first signs of estrus and each female was tested with a male for receptivity. As shown in Figure 2.2, normal breeding bitches exhibited expected hormone changes during the estrus period, i.e., an initial increase in estradiol levels followed by a rise in progesterone levels as the estradiol content fell, and a brief spike in LH, associated with the receptive period of the bitch. In contrast, as shown in Figure 2.3, irradiated bitches had relatively constant levels of estradiol, LH, and progesterone. The estradiol levels were less than those associated with receptivity in untreated dogs. The LH levels were consistently as high as the brief peak seen in the normal, breeding bitch, indicating failure of the ovarian negative feedback mechanism. Progesterone remained constant and minimal in all irradiated dogs.

Although all 59 dogs irradiated during fetal life seem clinically normal, they appear smaller than untreated male and female dogs of the same age. To test whether there is a difference in adult body size between the irradiated dogs and untreated colony controls, the body weights of all 59 irradiated dogs were compared with those of 60 colony controls (30 male and 30 female) at 250 days of age. We have previously shown that at this age dog weights approach an asymptote which is a good criterion of adult size (10).

---

*Test results were obtained through the collaboration of the laboratory of Dr. Ernst Knobil, Department of Physiology, School of Medicine, University of Pittsburgh, Pittsburgh, Pa., supported by grants from the National Institutes of Health and the Ford Foundation.

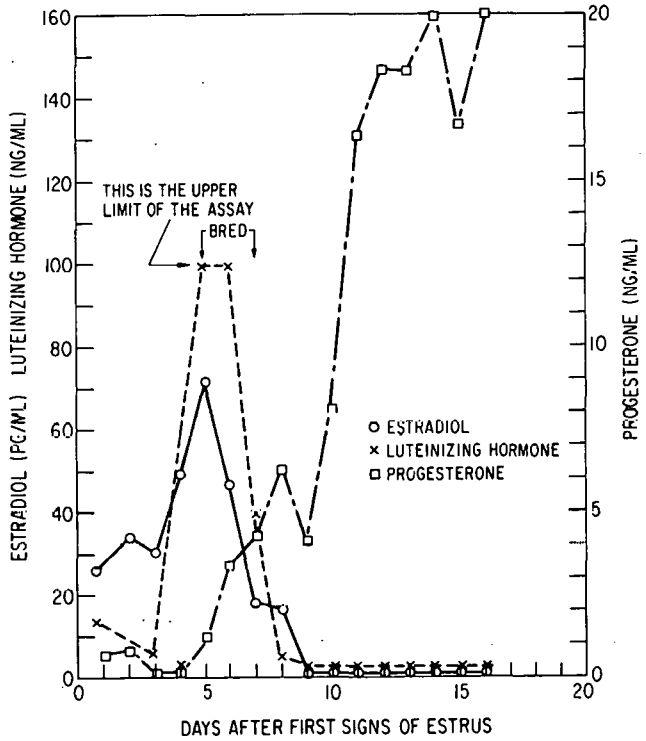

Fig. 2.2. Serum levels of estradiol, leuteinizing hormone, and progeresterone in an untreated beagle over a 2-week period beginning at the first detectable clinical signs of estrus. The bitch bred on the days indicated.

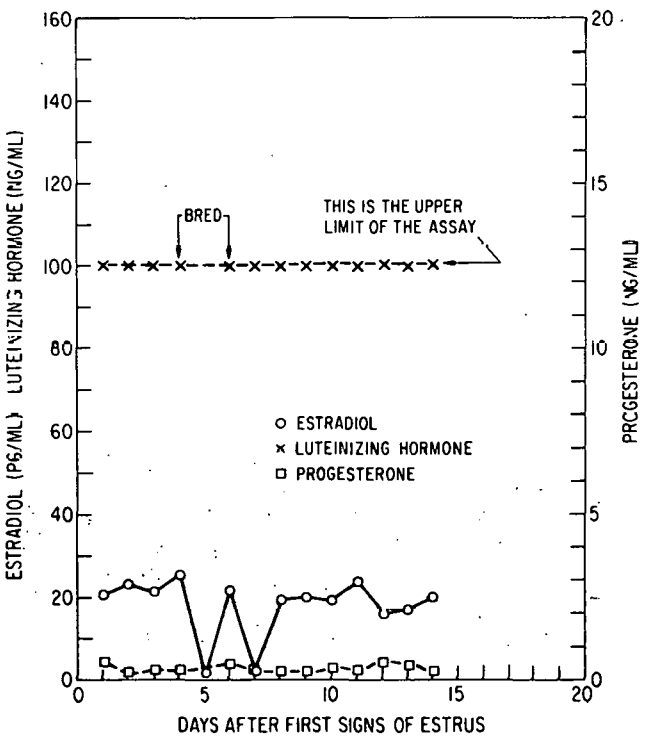

Fig. 2.3. Serum levels of estradiol, leuteinizing hormone, and progeresterone in a beagle irradiated during fetal life at an exposure rate of 17 R/22-hour day, beginning at day 20 and continuing until birth. The data are shown for a 2-week period, beginning at the first detectable clinical signs of estrus. The bitch bred on the days indicated.

The mean body weight at 250 days of age for the 29 males irradiated during fetal life was 9,879 ± 242 grams compared with 11,534 ± 288 grams for the 30 controls. These means are significantly different when compared by Student's *"t"* test ($t_{57df} = 4.38$; $P < 0.001$).

The mean body weight at 250 days of age for the 30 females irradiated *in utero* was 7621 ± 230 grams compared with 9257 ± 335 grams for 30 controls. Again the irradiated dogs are significantly smaller when the data are compared by Student's *"t"* test ($t_{58df} = 4.0$; $P < 0.001$). Although these data demonstrate a significant reduction in the size of dogs irradiated during fetal life, the contributions of several other factors that influence body size and growth, such as radiation exposure rate, parity of the bitch producing each litter, the size of each litter, and the pedigree of the dogs, require further evaluation.

CONCLUSION

Severe damage to the ovary, resulting in total reproductive failure, occurs in 100% of females exposed to as little as 5 R/day throughout uterine development. This is the most sensitive index of radiation damage yet identified in dogs exposed continuously to ^{60}Co γ-radiation.

REFERENCES

1. Norris, W. P., C. M. Poole, and T. E. Fritz. ANL-7870 (1971), p. 142.
2. Norris, W. P., and C. M. Poole. ANL-7970 (1972), p. 197.
3. Norris, W. P., and C. M. Poole. ANL-8070 (1973), p. 44.
4. Tolle, D. V., R. F. Ladove, and W. P. Norris. ANL-7970 (1972), p. 199.
5. Fritz, T. E., W. P. Norris, and M. P. Thomas. ANL-8070 (1973), p. 46.
6. Anderson, A. C., and L. S. Rosenblatt. In: Proceedings of Symposium on Dose Rate in Mammalian Radiation Biology, Eds. D. G. Brown, R. G. Gragle, and T. R. Noonan. CONF-680410, Biol. Med. (TID-4500), 1968, p. 11.1.
7. Andersen, A. E., V. G. Nelson, and M. E. Simpson. J. Med. Primatol. 1, 318 (1972).
8. Peters, Hannah. In: Advances in Reproductive Physiology Vol. 4, Ed. Anne McLaren. Academic Press, New York, 1969, p. 148.
9. Parkes, A. S. Proc. R. Soc. London, Ser. B: 101, 71 (1927).
10. Tyler, S. A., and W. P. Norris. Growth 32, 235 (1968).

NEUROFIBROSARCOMAS OCCURRING AS A LATE EFFECT IN BEAGLES GIVEN INTRAVENOUS INJECTIONS OF ^{137}CESIUM

Thomas E. Fritz, Louise S. Lombard, Patrick H. Polk, and William P. Norris

PURPOSE AND METHODS

A study of the late effects of single intravenous injections of ^{137}Cs was begun in 1961. A total of 73 dogs in three age groups received doses

near those found to be lethal within 30 days. Forty of these dogs survived more than 100 days and received integrated doses of radiation ranging from 1000 to 1400 rads during the first 100 days. The dosimetry and tissue distribution of ^{137}Cs and the early and late biologic responses have been reported (1-4).

PROGRESS REPORT

Since our last report (4), 3 of the remaining 8 dogs have died, leaving only 5 survivors at this time. One of the 3 decedents had a widely metastasizing neoplasm that has not yet been examined microscopically for classification, another had an abscess of the tongue and throat with secondary complications, and the third had extensive hepatic degeneration, nephritis, and secondary circulatory complications.

In updating the tabulation of causes of death from our last report (4) we found 6 neurofibrosarcomas and 1 neurilemmoma (schwannoma), tumors derived from the nerve sheath, in 7 of the 40 dogs (17.5%) that we have followed as chronic survivors. In 6 of the dogs the tumor was primary cause of death.

The occurrence of this high incidence of nerve sheath tumors among ^{137}Cs-treated survivors is highly significant since spontaneous peripheral nerve tumors are quite rare (5-7).

Two additional peripheral nerve tumors have been diagnosed in dogs in this colony, a neurofibrosarcoma in a beagle externally irradiated with ^{60}Co and a neurilemmoma in an untreated beagle.

Table 2.3 lists the data relevant to treatment and tissues involved in these 9 dogs with either neurofibrosarcoma or neurilemmoma. In 2 of the 9 (Nos. 392, 435), the tumor was diagnosed ante-mortem from biopsy specimens, while in the remaining 7 dogs, the tumor was diagnosed at necropsy.

In 6 of the dogs with neurofibrosarcomas, large tumor masses were found in the spleen at necropsy or on splenectomy. In 5 animals the liver was similarly involved and in 4 there was seeding of the tumor in the mesentery, omentum and/or parietal peritoneum. Because of widespread metastases the primary site has been difficult to determine. Additional examinations are being conducted to answer this question.

The characteristic histologic feature shared by all 9 tumors was the palisade arrangement of elongated, spindle-shaped nuclei. Groups of cells assumed an organoid appearance suggesting tactile corpuscles or Verocay bodies. Microcysts appeared among the bodies together with areas of serous degeneration. In the neurofibrosarcomatous tumors there were also reticulum and collagen fibers. Mitotic figures were numerous in the sarcomas and rare or absent in the pure neurilemmomas.

Recent research has shown that neurofibromas and neurilemmomas have a common cell of origin, the Schwann sheath cell (8). Mixed tumors composed of elements of both tumor types are frequently seen in man (9). Sequential studies of human neuroblastomas and ganglioneuromas have given support to the

Table 2.3. Tumors of Nerve Sheath Origin in Beagles

Dog No.	Sex	Radiation Source[a]	Dose µCi/kg	Dose Total µCi	Dose Total Rad	Age at Exposure (days)	Time after Exposure to Death (days)	Tumor Type	Tissues Involved
081	M	I.V. ^{137}Cs	1.85	15.52	742	397	2764	Neurofibrosarcoma	Leg muscle, spleen, liver
392	F	I.V. ^{137}Cs	3.45	26.77	1398	395	3319	Neurofibrosarcoma	Subcutis of neck, spleen
435	M	I.V. ^{137}Cs	3.40	35.01	1589	391	3485	Neurofibrosarcoma	Spleen, liver bone marrow
437	M	I.V. ^{137}Cs	3.46	33.57	1313	391	3351	Neurilemmoma	Small intestine
452	M	I.V. ^{137}Cs	2.68	27.91	1276	427	2369	Neurofibrosarcoma	Spleen, liver, parietal, peritoneum, diaphragm
454	M	I.V. ^{137}Cs	1.65	16.33	911	435	3037	Neurofibrosarcoma	Spleen, liver, omentum, diaphragm, heart, bone marrow, lung
471	M	I.V. ^{137}Cs	3.76	21.91	725	151	3295	Neurofibrosarcoma	Spleen, pancreas, mesentery
569	F	-	-	-	-	-	3484[b]	Neurilemmoma	Subcutis of elbow and ventral abdominal wall
954	M	^{60}Co	17 R/day x 100 days			418	1925	Neurofibrosarcoma	Spleen, liver, pancreas, omentum, mesentery, parietal peritoneum, lung

[a] I.V. = intravenously injected.

[b] Age at death (days).

concept that these tumor types may also evolve into neurofibromatous tumors (9). There has been no previous indication of radiation preferentially inducing tumors of the nerve sheath.

CONCLUSIONS

Eight tumors originating from cells of the nerve sheath (Schwann sheath cells) have been diagnosed in beagle dogs being observed for late effects from near lethal doses of irradiation. Seven of the dogs had received a single intravenous dose of ^{137}Cs and the eighth had been given whole-body irradiation from a ^{60}Co γ-ray source. With the exception of one of the tumors in the ^{137}Cs-injected dogs, all were malignant and classified as neurofibrosarcoma. The remaining ^{137}Cs-injected dog had a neurilemmoma. One neurilemmoma has also been found in an untreated colony dog. These data suggest that nerve sheath tumors are a late response to terminated exposures to ionizing radiation.

REFERENCES

1. Poole, C. M., W. P. Norris, and T. E. Fritz. ANL-7535 (1968), p. 163.
2. Norris, W. P. ANL-7770 (1970), p. 139.
3. Fritz, T. E., and W. P. Norris. ANL-7870 (1971), p. 146.
4. Fritz, T. E. ANL-7970 (1972), p. 206.
5. Frankhauser, R., and H. Luginbuhl. Pathologische Anatomie des Zentralen und Peripheren Nervensystems der Haustiere, Paul Parey, Berlin, 1968, p. 449.
6. Moulton, J. E. Tumors in Domestic Animals, Univ. of Calif. Press, Berkeley, 1961, p. 214.
7. Jubb, K. V. F., and P. C. Kennedy. Pathology of Domestic Animals, Academic Press, N. Y., 1963, p. 373.
8. Feigin, I. Acta Neuropathol. 17, 188 (1971).
9. Bolande, R. P., and W. F. Towler. Cancer (Philadelphia) 26, 162 (1970).

THE RESPONSE OF DOG PERIPHERAL LYMPHOCYTES TO CONCANAVALIN A AND PHYTOHEMAGGLUTININ

Patricia C. Brennan, Martha L. White, Kenneth G. Draper,† and Thomas E. Fritz*

PURPOSE AND METHODS

The thymus-derived (T cell) population of lymphocytes is primarily involved in cell-mediated immunity (CMI), whereas the bone marrow-derived (B cell) population is involved in the production of humoral antibodies; however, a cooperative interaction of T and B cells in the development of antibody responses to many antigens is well established (1,2). Thus, changes in the T cell population or in the functional capability of cells in that population may be correlated with alterations in cellular and humoral immune competence. Moreover, the cellular immune system is believed to form the surveillance mechanism against spontaneously arising neoplastic cells as well as influencing the rate of neoplastic tumor proliferation. The functional integrity of this system thus assumes added importance under conditions in which neoplastic disease is known to contribute significantly to the cause of death. Two such conditions are old age and irradiation at low total doses and/or low dose rate.

We have begun a series of experiments to assess the functional integrity of the cellular immune system in dogs differing in age, radiation exposure, and genetic background. The plant lectins, Concanavalin A (Con A) and Phytohemagglutinin (PHA) specifically stimulate T cells to undergo blast transformation in mice (3) and man (4) and consequently are widely used to determine the functional integrity of the cell mediated immune system.

---

*Fall 1974 participant in the Undergraduate Honors Research Participation Program, Indiana State University, Terre Haute.

†Participant in the 1974 Summer Institute in Biology, Northern Illinois University.

We are using these compounds to stimulate dog peripheral lymphocytes and have demonstrated that they are specific for T cells in the dog.

Groups of 8 to 10 adult beagle dogs of both sexes are being examined according to age, radiation exposure, and genetic background. The genetic background of interest is the degree of relatedness of each dog to a partially inbred line known as the Alabama (A) line. Dogs of the partially inbred A line have a high incidence of spontaneous thyroiditis and orchitis (5-6), which are generally considered to be autoimmune diseases and, hence, might be expected to have a T cell response different from that of outbred dogs. Of particular interest are two litters of pups of the same genetic background (10 in all) born 1 day apart that are being serially tested from 1 week of age until maturity.

Blood is collected aseptically from the jugular vein into tubes containing EDTA and the lymphocytes are separated on Ficoll-isopaque gradient (7). The lymphocytes are washed twice in complete medium and adjusted to a concentration of $\sim 1 \times 10^6/0.9$ ml in complete medium. Duplicate cultures containing each mitogen and duplicate unstimulated control cultures are prepared from each dog. Details of the culture conditions and preparation of cells for assay are described elsewhere in this report (8). We have found that final concentrations of 5 µg/ml of Con A and 1 µg/ml of PHA give maximum stimulation in 72 hours. Pretreatment of cells with rabbit anti-dog thymocyte serum and complement (9) decreases the response to that of unstimulated cultures, demonstrating the T cell specificity of these mitogens in dogs.

PROGRESS REPORT

No difference between A line dogs and comparably aged outbreds has been observed. Therefore, data from A line dogs have been included with similarly aged outbreds in Table 2.4 which shows our results to date. There is a significant decline in the responsiveness of cells from dogs 8 years of age or older to both Con A and PHA indicating an age-associated decline in T cell competence. However, although the mean stimulation index (SI) of old dogs is significantly lower than that for young dogs, three old dogs responded as well as dogs 1 to 4 1/2 years of age. This variability is similar to the variability in the humoral response of aged dogs reported by Jaroslow, et al. (10). Protracted gamma irradiation at a dose rate of 5 R/day beginning at 13 months of age (total dose $\sim$ 10,000 R) significantly decreases the response to Con A and PHA from that observed in cells from comparably aged unirradiated dogs. Again, cells from two of the eight irradiated dogs respond as well or better than their aged counterparts. It is interesting to speculate whether PHA and Con A unresponsiveness might have some predictive value in terms of neoplastic disease onset, since a majority of dogs that have died under similar conditions of irradiation had myelogenous leukemia.

Neonatal pups were uniformly unresponsive to either mitogen when assayed at 1 and 3 weeks of age. It is clear that this unresponsiveness represents functional immaturity of the peripheral T cells since immunofluorescence studies showed that $\sim$ 70% of peripheral lymphocytes are T cells regardless of age. By 5 weeks of age there is evidence of responsiveness, although the mean SI is considerably below that of adult animals.

Table 2.4. Response of Dog Peripheral Lymphocytes to Mitogens

Group	Number of Dogs	Stimulation Index[a] ± SE	
		Con A	PHA
Adult (1 to 4 1/2 years old)	19	51.5 ± 6.1	39.8 ± 4.8
Aged (> 8 years old)	15	20.5 ± 3.7	12.1 ± 2.3
5 R/day γ-irradiation (total dose = ∿ 10,000 R)	8	9.2 ± 2.8	6.9 ± 2.6
Comparably aged unirradiated	12	23.7 ± 4.8	15.5 ± 2.9
Pups: 1 week old	10	1.4 ± 0.5	1.6 ± 0.6
3 weeks old	10	1.5 ± 0.2	1.5 ± 0.2
5 weeks old	10	7.6 ± 1.8	5.4 ± 1.3

[a] Stimulation Index = $\frac{\text{Counts/min in stimulated cultures}}{\text{Counts/min in control, unstimulated cultures}}$

CONCLUSIONS

Con A and PHA stimulation can be used to assess the functional capability of dog T cells.

There is an age-associated decline in responsiveness to these mitogens which is augmented by protracted gamma irradiation.

The ability of peripheral lymphocytes to respond to Con A and PHA is immature for at least 5 weeks after birth.

REFERENCES

1. Miller, J. F. A. P., and G. F. Mitchell. Transplant. Rev. 1, 3 (1969).
2. Claman, H. N., and E. A. Chapeson. Transplant. Rev. 1, 92 (1969).
3. Greaves, M., and G. Janossy. Transplant Rev. 11, 87 (1972).
4. Geha, R. S., and E. Muler. Europ J. Immunol. 4, 193 (1974).
5. Fritz, T. E., R. C. Zeman, and M. R. Zelle. Exp. Mol. Pathol. 12, 14 (1970).
6. Fritz, T. E., L. S. Lombard, S. A. Tyler, and W. P. Norris. Pathology and familial incidence of orchitis and its relation to thyroiditis in a closed beagle colony. This report, Section 2.
7. Thorsby, E., and A. Bratlie. Histocompatibility Testing, Ed. P. I. Terasahe. Munhsgaard, Copenhagen, 1970, p. 655.
8. Brennan, P. C., W. T. Kickels, R. C. Simkins, and L. G. Daniel. Radiation effects on host defense mechanisms. This report, Section 4.

9. Stobo, J. D. Transplant Rev. 11, 60 (1972).
10. Jaroslow, B. N., K. M. Suhrbier, and T. E. Fritz. J. Immunol. 112, 1467 (1974).

PATHOLOGY AND FAMILIAL INCIDENCE OF ORCHITIS AND ITS RELATION TO THYROIDITIS IN A CLOSED BEAGLE COLONY

Thomas E. Fritz, Louise S. Lombard, Sylvanus A. Tyler, and William P. Norris

PURPOSE AND METHODS

Lymphocytic thyroiditis, resembling Hashimoto's Disease of man, occurs spontaneously in almost 20% of the untreated adult dogs in the closed beagle breeding colony in this Division (1). This disease is genetically influenced, as determined by analyses of the ancestral composition of each animal. The incidence increases with relatedness to three sibling progenitors of a partially inbred line (A-line).

During routine investigation of fertility problems in the breeding colony, reduced sperm counts related to lymphocytic infiltration and degenerative lesions of the testes were observed. These findings seemed positively correlated with the presence of lymphocytic thyroiditis and, therefore, to the degree of relatedness of affected dogs to the A-line.

Thyroiditis is generally accepted to be an autoimmune disease, and autoimmune diseases often present multiple simultaneous problems with lesions in two or more different organs or tissues (2). To determine the incidence of orchitis, its relationship to thyroiditis, and whether the incidence was genetically influenced we surveyed the histologic changes in the testes and thyroids of all untreated dogs for which we had specimens in our files. We also studied the pedigrees of each dog and attempted to make correlations between ancestry and the incidence of lesions in the testes and thyroids.

PROGRESS REPORT

A total of 69 dogs provided histological specimens of both thyroid and testes. Twenty-two of the 69 dogs had lymphocytic infiltration of the testes, of which 18 also had either atrophy or degeneration of the tubular cells. There was considerable variation in both the severity and distribution of the cellular infiltrations as well as in the tubular degenerative changes. Both nodular and diffuse infiltrations of lymphoid cells were present, with the small mature lymphocyte the predominant cell. In many cases of nodular aggregation of lymphocytes there was an obvious germinal center in the nodule. Tubular changes included focal degeneration, segmental atrophy, and diffuse atrophy of the seminiferous epithelium.

A summary of the pedigrees and clinical data of the dogs revealed several important differences between the 22 dogs with orchitis and the remaining 47 dogs. Among the dogs with orchitis 14 (64%) were 100% A-line in genetic

composition compared with 7 (15%) among the remaining dogs. Also, 17 of the 22 (77%) dogs with orchitis also had thyroiditis, while only 13 of the 47 (27%) that did not have orchitis had thyroiditis. An analyses of the incidence of each lesion, and correlations with the genetic composition of the dogs are shown in Table 2.5. A chi-square test (with total sample size fixed and all marginal totals random) of the data leads to the conclusion that the two diseases are associated ($\chi^2 = 13.059$, df = 1, $P < 0.001$).

Table 2.5. Incidence of Thyroiditis and Orchitis by Genetic Composition

Genetic Composition (% A-line)	No Lesions	Orchitis Only	Both Lesions	Thyroiditis Only	Totals
100	2	1	11	6	20
75			1		1
50	6		3	2	11
25	7	2	1	1	11
12.5	1			1	2
0	18	2	1	3	24
Totals	34	5	17	13	69
Total Orchitis			22		
Total Thyroiditis					30

CONCLUSION

Lymphocytic orchitis occurs with a high frequency among beagle dogs in this closed breeding colony. The lesions occur spontaneously, and are regarded as being the result of autoimmune mechanisms. Most cases of orchitis occur in dogs that also have thyroiditis. Both diseases are genetically influenced, and they are concentrated in dogs that form a partially inbred line within the colony.

REFERENCES

1. Fritz, T. E., R. C. Zeman, and M. R. Zelle. Exp. Mol. Pathol. 12, 14 (1970).
2. Rose, N. R. In: The Inflammatory Process, 2nd ed. Eds. B. W. Zweifach, L. Grant, and R. T. McClusky. Academic Press, New York, 1974, p. 347.

LYSOZYME LEVELS IN BLOOD SERUM OF BEAGLE DOGS

Lillian V. Kaspar

PURPOSE AND METHODS

Blood lysozyme activity has been reported to be elevated in cases of myelogenous leukemia, both in dogs (1) and man (2,3). Because myeloproliferative disease (MPD) is a common finding in our experimental dogs exposed to continuous ^{60}Co gamma radiation, a study of lysozyme levels in the various groups of dogs was begun with the hope that the results might provide a means for a more detailed evaluation of the onset and progression of the disease.

Blood was collected from the jugular vein into evacuated tubes and centrifuged at 1500 g for 5 minutes. The serum was assayed for lysozyme by the method of Osserman and Lawlor (3). A 1% solution of Noble agar in 0.066 M phosphate buffer (pH 6.8) was mixed with *Micrococcus lysodeiktieus* to achieve a concentration of 0.5 mg cells/ml agar. Ten ml aliquots of this suspension were poured into disposable petri dishes (100 x 15 mm) and stored at 2°C until needed. Seven 4-mm diameter holes were cut into each agar plate with a gel punch. Three standard solutions and two serum samples (run in duplicate) were assayed in each dish by depositing 10 µl of solution in each well. Standards were egg white lysozyme (3 x recrystallized) dissolved in distilled water at concentrations of 5, 10, 25, 50, 100, or 250 µg/ml. After a 24-hour incubation period at room temperature, the diameters of the resulting zones of lysis were measured. These diameters were plotted against the log of the lysozyme concentration and the lysozyme values of the serum samples were determined from the resultant graph.

RESULTS

Lysozyme assays on 19 male and 16 female control dogs ranging in age from a few months to 13 years showed that males and females had the same lysozyme levels in blood serum; for males the concentration was 8.7 ± 2.4 µg/ml (mean ± SD) (range 5.0-12.6) and for females it was 8.8 ± 1.9 µg/ml (range 5.0-13.0). No age-related differences in lysozyme concentrations were observed. The average WBC count for this group was 8748 ± 2065 cells/ml.

Figure 2.4 is a plot of lysozyme levels in dogs receiving ^{60}Co γ-irradiation continuously at rates of 5, 10, or 17 R/22-hour day. These data were collected over a 3-month period. In general, lysozyme levels were directly proportional to the total white blood cell count.

Lysozyme assays were also performed on a few frozen serum samples which had been collected terminally from dogs that died of radiation-induced causes. The results are shown in Table 2.6.

Table 2.6.

Dog No.	Lysozyme Level (µg/ml of Serum)	White Blood Cells/ cu. mm Blood	Cause of Death
1366	13.0	4091	Erythroid leukemia
1429	2.7	4073	Anemia
1448	122	44589	Lymphocytic leukemia
1913	170	69756	Myelogenous leukemia

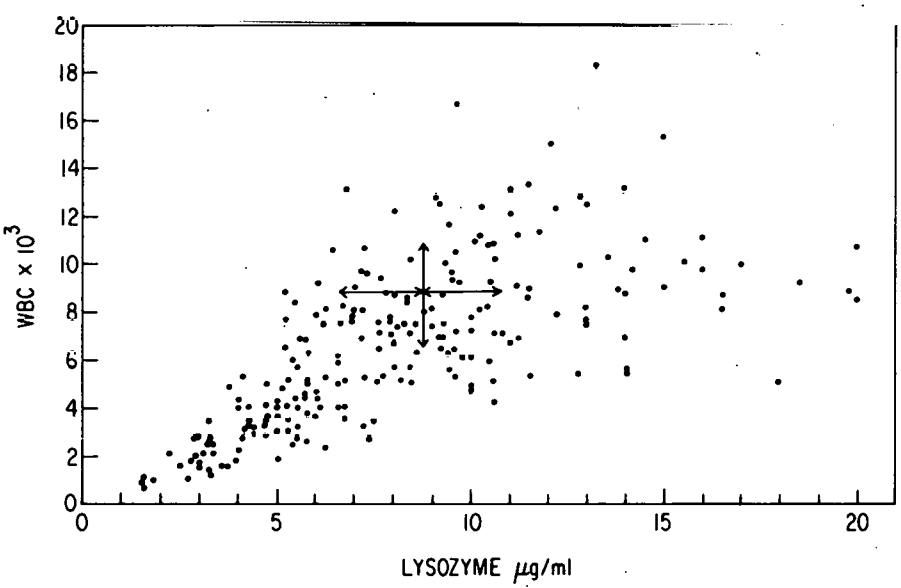

Fig. 2.4. Lysozyme levels in dogs receiving either 5, 10, or 17 R/22-hour day are directly proportional to the white blood count. White blood cells (WBC) are shown per ml of blood; lysozyme levels are shown as µg/ml of serum. The X represents the average lysozyme level of unirradiated controls (8.7 µg/ml) plotted against the average white blood cell count (8748) of the controls. The horizontal arrows represent 1 SD (2.1 µg/ml) of control lysozyme activity while the vertical arrows represent 1 SD of the control white blood count (2065).

The dogs that died of radiation-induced leukemia (1448 and 1913) and had elevated white counts also displayed elevated lysozyme levels, confirming earlier reports (1,2).

CONCLUSIONS

Sex or age did not affect the lysozyme levels in blood serum of control dogs. The lysozyme levels in blood are in general proportional to the total number of white cells present; an increase or decrease in white cell concentration is accompanied by a concomitant change in lysozyme levels.

While blood lysozyme levels may have value in diagnosis and evaluation of disease states, the significance of these changes is not clearly understood.

REFERENCES

1. Shifrine, M., C. E. Chrisp, F. D. Wilson, and U. Heffernon. Am. J. Vet. Res. 34, 695 (1973).
2. Noble, R. E., and H. H. Fudenberg. Blood 30, 465 (1967).
3. Osserman, E. F., and O. P. Lawlor. J. Exp. Med. 124, 921 (1966).

CHARACTERIZATION OF BLOOD VALUES IN NORMAL, AGING BEAGLES

Donald E. Doyle, Donald L. Pearson, and David V. Tolle

PURPOSE AND METHODS

The characterization of normal, age and sex dependent, hematology data in control dogs is a necessary preliminary to a detailed assessment of radiation-induced injury in the beagle. Routine hematological values have been obtained throughout life on animals designated as colony controls. At this time, 69 males and 58 females have contributed 2734 sets of blood values, the oldest animals among them having been followed for over 13 years.

The mean and its standard deviation were computed and plotted at 6-month increments, by sex, for five parameters: erythrocytes, leukocytes, packed cell volume, hemoglobin, and thrombocytes; additionally, the mean and standard deviation were plotted for the Wintrobe Indices--Mean Corpuscular Volume (MCV), Mean Corpuscular Hemoglobin (MCH), and Mean Corpuscular Hemoglobin Concentration (MCHC).

PROGRESS REPORT

Erythrocyte levels in puppies at 1 to 2 months of age range from 4.0 to 5.0 x 10^6 cells/mm^3, and rise to a maximum lifetime mean of 8.0 x 10^6 cells/mm^3 by 8 months of age. Thereafter there is a slow, steady decline reaching a level of 7.0 x 10^6 cells/mm^3 at 10 years of age (Figure 2.5). There is no significant differences in the mean values from the two sexes.

The packed cell volume parallels the age-related decline in the erythrocytes; however, hemoglobin levels remain relatively constant throughout life, thus allowing distinct trends in the derived Wintrobe Indices.

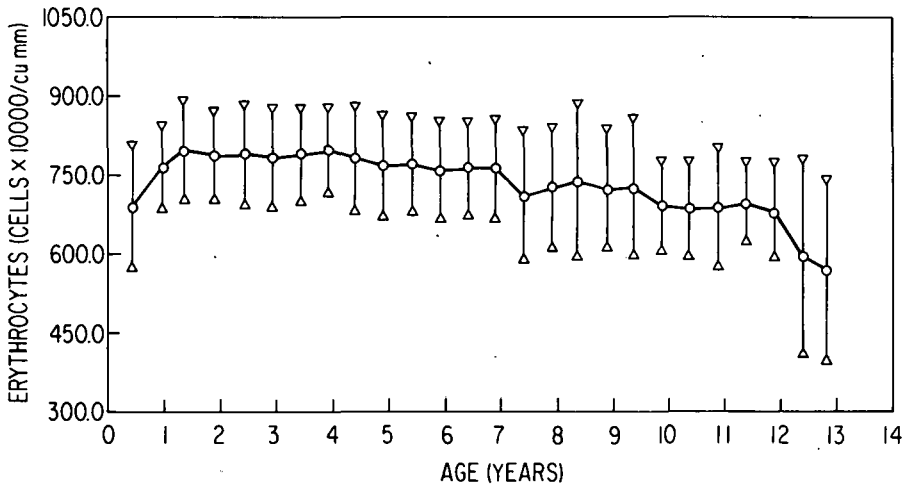

Fig. 2.5. Mean erythrocyte numbers with age in control beagles of both sexes. Ranges denote ± 1 standard deviation.

The MCH (μμg of hemoglobin per cell) response (Figure 2.6) illustrates the type of response seen in the other indices. The MCH shows a steady increase, rising from a value of 22.0 μμg/cell at 1 year of age to a maximum of 26.5 μμg/cell at 10-12 years of age.

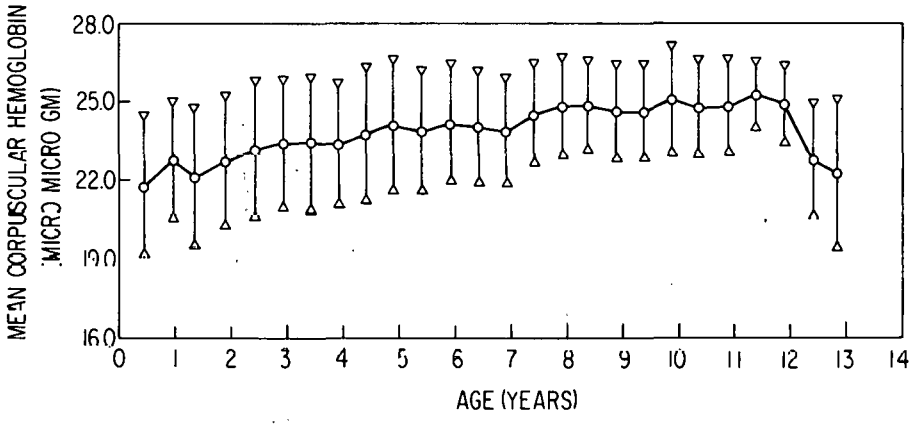

Fig. 2.6. Mean corpuscular hemoglobin with age in control beagles of both sexes. Ranges denote ± 1 standard deviation.

The MCHC (volume percent hemoglobin per cell) shows the same steady increase from 32.5% at 6 months of age to 35.5% at age 10 years.

The MCV shows a mean value of 68 μ^3 at 1 year and a steady increase in the mean to a value of 73 μ^3 at age 10 years.

Leukocyte levels at 6 months of age average 12,900 cells/mm^3 and decline sharply to 11,200 cells/mm^3 at 12 months of age, followed by a slower, steady decline to a level of 9,200 cells/mm^3 at 11 years of age.

An obvious sex difference is apparent in the thrombocyte levels. Values for females throughout life are consistently 75 to 150 thousand per mm^3 higher than in males of the same age.

CONCLUSIONS

There is an evident compensatory relationship between the total circulating erythrocytes and the hemoglobin level. The parallel and age-dependent decrease in the erythrocyte numbers and packed cell volume is not seen in the hemoglobin; both the weight (MCH) and volume percent (MCHC) of hemoglobin per cell increase steadily throughout life, thereby compensating for declining erythrocyte numbers.

Although both the erythrocyte numbers and the packed cell volume decline with age, the degree of decline is not identical in the two cases because of the increase in the mean cell volume (MCV) of the erythrocytes.

Because the blood components and indices show defined and predictable changes with age, it is essential that these changes be considered in any detailed assessment of chronic radiation injury to the hematopoietic system. With our recent innovations in data processing, more detailed and rapid analyses from our bank of hematology data are now possible.

The general trends in hematological values and indices described above for our control colony of beagle dogs form the basis for more detailed evaluations, by new methods being developed, of radiation-induced hematological changes in experimental groups.

THIS PAGE

WAS INTENTIONALLY

LEFT BLANK

3. MODIFICATION OF RADIATION EFFECTS

SUMMARY

Arthur Lindenbaum, Group Leader

In previous Annual Reports, the work described in this section was included, largely for administrative purposes, among the diverse activities being carried out by the Biochemistry Group of the Division of Biological and Medical Research. This year, however, in recognition of the importance and increased scope of the program on plutonium metabolism and therapy, the submissions are treated as a separate entity. Likewise, much diversity will be noted in the kinds of activities being carried out under this program. The unifying objective underlying the varied research activities reported here continues to be the decorporation of dangerous polyvalent radionuclides. While all radionuclides are to varying degrees hazardous when deposited in living tissue, the metals of the actinide series--and in particular, plutonium-239--represent, by any measure, one of our most serious radiological problems. Our therapeutic objectives, therefore, are mainly directed toward decorporation of plutonium. To verify that therapeutic procedures developed in a variety of small animal species will ultimately be effective in humans, a larger species, the dog, is being increasingly used as an experimental animal.

In the design of appropriate experiments, a balance has been sought among the various approaches possible. Thus, in whole animal work the mouse is the species of choice because of the relatively low cost of obtaining data. Results of particular importance are then verified in the dog, using fewer numbers of animals for economy. The results obtained in metabolic experiments have provided the basic information needed for the development of new therapeutic concepts, procedures, and drugs. Frequently, metabolic and autoradiographic studies have pinpointed specific organs, cells, or subcellular tissue components that are particularly involved in plutonium deposition and retention. Ultimately, to make full use of the information gained from the above studies, selected results must be reinvestigated and interpreted at the molecular level. Over the past year the biochemical and molecular aspects of radionuclide metabolism and therapy have received increased attention, as they will in the future.

The present report covers new results in all of the areas described above. In duration-of-life experiments with mice injected with different levels of monomeric and highly polymeric plutonium, new data have been obtained on pathological changes in various tissues and on the life-shortening

effects of these doses. These results supplement previously reported information on differences in tissue deposition and retention following administration of these two forms of plutonium.

In dogs injected with monomeric plutonium we have demonstrated (as previously shown in mice) the value of a regimen of early and prolonged treatment with DTPA (diethylenetriaminepentaacetic acid) for minimizing the plutonium burden in the soft tissues and skeleton. These results have immediate implication for DTPA treatment in man.

New studies in mice have verified the action of pyran copolymer antiviral agents in enhancing the effectiveness of DTPA for removal of polymeric plutonium from the liver. The net effect is much like that of glucan, but with the possible advantage that a water-soluble, rather than particulate, substance is injected. Time, dosage, and toxicity studies are now being carried out in preparation for therapeutic testing of the most effective of these compounds in dogs.

Continuing studies of the effectiveness of liposome-encapsulated DTPA in removing polymeric plutonium deposited in the mouse liver and skeleton are described in an abstract.

Recent application of autoradiographic procedures for quantitatively comparing short- and long-term localization of monomeric and polymeric plutonium in dog liver has shown that there is no net translocation of monomeric plutonium within the liver between 6 and 90 days following injection. In a cooperative clinical study of the possible use of a lanthanide radionuclide, ^{153}Sm, for tumor localization, the autoradiographic techniques developed for plutonium have been used to measure the differential deposition of radio-samarium in tumors and in normal tissues.

One of the molecular studies presently underway aims at synthesis of a variety of DTPA esters. The diethyl ester has already been prepared and tested for toxicity in mice. These compounds are designed to bring DTPA into contact with plutonium deposits unavailable to the action of ionic DTPA. Other synthetic work is directed toward the preparation of ^{14}C-labeled DTPA of high specific activity, to be used in elucidating the delayed action of this chelating agent and for other purposes.

Significant changes in personnel have occurred over the past year. Dr. M. W. Rosenthal has taken up other duties in the Laboratory and two new PhD-level staff members, M. H. Bhattacharyya and R. A. Guilmette, have joined our group. Their backgrounds, training, and scientific viewpoints will inevitably contribute new insights, approaches, and perhaps new directions to our program.

MODIFICATION OF RADIATION EFFECTS STAFF

REGULAR STAFF

Bhattacharyya, Maryka H. (Assistant Biochemist)
*Kalesperis, G. Steve (Scientific Assistant)
Lindenbaum, Arthur (Biochemist)
Moretti, Elizabeth S. (Scientific Assistant)
Peterson, David P. (Scientific Assistant)
†Rosenthal, Marcia W. (Biologist)
Russell, John J. (Scientific Assistant)

TEMPORARY STAFF DURING 1974

Guilmette, Raymond A. (Research Associate)
Parks, John E. (Postdoctoral Appointee)

---

*Terminated in 1974.

†Now Division Editor.

METABOLIC AND THERAPEUTIC STUDIES WITH PLUTONIUM AND AMERICIUM

*Arthur Lindenbaum, Marcia W. Rosenthal, Maryka H. Bhattacharyya, Raymond A. Guilmette, John E. Parks, G. Steve Kalesperis, Elizabeth S. Moretti, David P. Peterson, John J. Russell, and Nancy Doan**

PURPOSE AND METHODS

The broad objective of this program is to develop new approaches to the therapy of poisoning by radioactive and nonradioactive metals. Plutonium-239 and americium-241 have received major attention in recent years because of the potentially great radiological health hazard represented by alpha-emitting nuclides used for nuclear power production and allied technology. Compounds of the actinide series (as well as those of other polyvalent heavy metals) exhibit highly variable tendencies to hydrolyze and polymerize, to aggregate, and to bind to proteins and other biological components, both in solution and *in vivo*. This range in physical-chemical character has been shown to influence the deposition, retention, effectiveness of therapy, and delayed pathological effects of these nuclides. Thus, information obtained with plutonium and americium aids in understanding the behavior of other nuclides of the actinide, lanthanide, and rare earth series in living tissues. Metabolic studies of actinide compounds also provide useful information on the translocation and deposition of other colloids and macromolecules in tissues.

---

*Fall 1974 participant in the Undergraduate Honors Research Participation Program, St. Olaf College.

Previous work has demonstrated the effectiveness of chelating agents, such as diethylenetriaminepentaacetic acid (DTPA), for removal of plutonium and related elements from blood, bone, and soft tissues. Attention is now being directed toward (a) other therapeutic approaches aimed at removal of that portion of the plutonium not readily removed by DTPA, and (b) improving our understanding of the molecular interactions occurring among actinide compounds, tissue constituents, and therapeutic substances.

In past years we have used the mouse and rat to develop a variety of therapeutic procedures for removal of plutonium and to explore the mechanisms of actinide deposition and removal. Promising results with these species are now being extended to the dog. In this larger, longer-lived species there is slower bone turnover; also, the retention of plutonium in the liver is believed to resemble more closely that of man.

PROGRESS REPORT

Deposition of Polymeric Plutonium in Beagle Dogs

Although much is known about the short- and long-term pattern of deposition of monomeric plutonium in the tissues of the dog, most of our information on the deposition kinetics of polymeric plutonium has been obtained in the mouse. Accordingly, studies with polymeric plutonium are now being carried out in the dog. A group of three dogs previously injected with 0.1 μCi/kg of highly polymeric plutonium were sacrificed after 1 year to allow comparison with tissue deposition values obtained 6 and 90 days after injection of similar preparations of polymeric plutonium. The data obtained are entirely consistent with expectations based on previous results with mice and dogs: the plutonium burdens in the liver, spleen, and lymph node sample one year after injection were 73%, 5%, and 0.03% of the amount injected, respectively, approximately the same as in these tissues at 6 and 90 days. Comparison of plutonium burdens in all skeletal elements analyzed (femur, third lumbar vertebra, mandible + teeth) showed that the plutonium concentrations at one year were greater than at 90 days, which in turn were greater than at 6 days. These successive increases are presumably due to gradual translocation of plutonium from soft tissue deposition sites. Another group of dogs in this study will be sacrificed 2 years post-injection to follow these trends further and to carry out a continuing autoradiographic investigation of changes, over a 2-year period, in the microdistribution of polymeric plutonium in the liver.

Therapeutic Studies in Beagle Dogs

In comparative studies of plutonium decorporation in dogs, the effects of DTPA therapy delayed for 3 months after injection of 0.3 μCi/kg of monomeric plutonium have been compared with results of the same therapeutic regime (70 mg/kg, twice weekly, for 12 weeks) begun at 6 days. At the end of the delayed therapy about 7% of the injected plutonium remained in the liver, compared to 1.2% at the end of therapy begun at 6 days (1). The difference between these values may reflect the processes of tissue binding, intracellular incorporation, etc., that gradually sequester the plutonium and inhibit chelation by DTPA. Delayed DTPA treatment resulted in only small differences in the plutonium content of the skeletal samples from

levels found in controls or in dogs receiving early treatment. In a second comparison, DTPA treatment was begun at 6 days but continued for only 4 weeks before sacrifice. In this case, the livers contained about 9% of the injected plutonium and less removal of plutonium from the femurs and third lumbar vertebra was found than after 12 weeks of treatment. These results reinforce other data indicating the value of early, and prolonged, treatment with DTPA.

Because the skeleton undergoes a continuous process of remodeling, deposits of any bone-seeking substance gradually tend to become buried in cortical areas impenetrable by chelating agents like DTPA. In the case of plutonium, one of our therapeutic goals is to promote bone resorption, thereby exposing buried plutonium. To this end two procedures have been tested in dogs. In one, DTPA was injected intravenously as the pentasodium salt slowly (to avoid tetany) rather than as $CaNa_3DTPA$. The rationale was that plasma calcium lost in the formation of $CaNa_3DTPA$ would be replaced by skeletal calcium, in the course of which plutonium might also be removed or exposed to be chelated by the DTPA. This treatment was a part of the study, described above, in which 12 weeks of DTPA treatment was begun 3 months after monomeric plutonium. In the second approach, a corticoid drug, methylprednisolone acetate, known to increase osteoclastic activity in the skeleton with minimal effects on water balance, was administered intramuscularly with and without concomitant DTPA therapy. Injections of corticoid were given twice per week for 4 weeks, beginning 6 days after injection of monomeric plutonium (as part of a study described above). In brief, no significant additional plutonium removal from the skeleton was achieved by either approach over the removal obtained with $CaNa_3DTPA$ alone. In both experiments it is possible that treatment with either of these substances begun less than 6 days after plutonium administration, or with a different dose regimen, might have shown some effectiveness. Because of the importance of achieving maximal skeletal depletion of any of the alpha-emitting actinides, this problem will continue to be an experimental challenge; other approaches to skeletal removal are being considered.

Therapeutic Studies in Mice

The manipulation of normal physiological processes to promote additional removal of actinides from tissues beyond the amounts removed by DTPA alone is an approach to therapy that has shown promise in our hands. In recent work with mice (2-6), several new adjunct compounds or preparations have been shown to amplify the effect of DTPA in removing plutonium from the liver. One of the most promising of these adjunct compounds is designated by the supplier, Hercules, Inc., as pyran copolymer XA-124-177 (peak MW $\sim$ 36,000). It is a water-soluble compound, unlike glucan, the first such adjunct substance tested, whose particulate properties may present difficulties in intravenous injection. The pyran copolymers have been shown by others to have antiviral properties; whether these properties are related to their action in promoting plutonium removal has not yet been determined. Recent mouse studies have verified the adjunct action of pyran copolymer XA-124-177 in removing hepatic plutonium. We are now determining the optimal dosage level and treatment schedule for this drug in the mouse. (Testing in dogs would be an obvious next step.)

Although oral administration of pyran copolymer XA-124-177 was ineffective, a single intravenous injection given with concomitant DTPA therapy increased the amount of mid-range polymeric plutonium removed from the mouse liver by a factor of 2 as compared to treatment with DTPA alone [14.4% of the injected dose (ID) vs. 7.5% ID net removal due to therapy]. The effect of this same pyran compound in treating contamination by highly polymeric plutonium was even more pronounced, i.e., $\sim$ 5 times as much plutonium was removed from the liver compared to DTPA treatment alone (27.7% ID vs. 5.7% ID net removal due to therapy). Preliminary results suggest that pyran copolymers used as adjuncts to DTPA therapy are at least as effective in removing polymeric plutonium from the liver as liposome encapsulation of DTPA. The toxicities of several other antiviral drugs are being determined in anticipation of testing those that show promise for plutonium decorporation.

Effects of Physical-Chemical State of Plutonium on Lifetime Pathological Changes in Mice

The high carcinogenicity in bone of ^{239}Pu is believed due to the high local energy of its alpha radiation and its selective deposition near the cells lining the endosteal surfaces of the skeleton. Evidence indicating that these are the cells at risk in the induction of bone tumors by irradiation is based on our earlier demonstration (7,8) that monomeric plutonium, which is deposited almost entirely on bone surfaces, was at least twice as carcinogenic in bone as an equal bone deposition of a mid-range polymeric plutonium, which is located in the marrow as well as on the bone surfaces. Several years ago we initiated an experiment to extend these studies to a highly polymeric form of plutonium and to compare, under identical experimental and environmental conditions, the induction of bone tumors by monomeric plutonium and by a highly polymeric plutonium, using more exactly characterized plutonium preparations in mice of the same age from a closed, carefully controlled colony (9). This highly polymeric plutonium had a much higher deposition in liver and spleen, and a much lower deposition in bone, and on bone surfaces, than the mid-range polymeric plutonium preparation used previously. At 6 days after injection of the monomeric plutonium, the total skeletal burden was 43.2% of the injected amount (femurs x 13), and the total marrow burden was calculated from a standard sample to be 0.95%. After injection of highly polymeric plutonium, the bone burden was 3.3%, and the marrow 2.0%. Subsequent annual reports have described (a) the distribution and long-term retention of the two forms of plutonium; (b) the translocation of polymeric plutonium from liver to bone surfaces with time; (c) the development of anemia and dose-related hematopoietic deaths after polymeric plutonium; (d) reduction of survival by the highest level of monomeric plutonium; and (e) progressive shortening of the mean survival time by the three higher levels of polymeric plutonium (2, 10-12).

Analysis of morbidity data, primarily from observations at autopsy, shows that tumors of the lymphatic system (including lymphocytic leukemia, myelogenous leukemia, and reticulum cell tumors) were the primary cause of death of almost 30% of the control mice, not injected with plutonium; lesions in a number of different tissues were responsible for the other deaths. In mice given polymeric plutonium, anemia and tumors of bone and lymph were the major causes of death. Some deaths were caused by hemorrhages in the spleen, apparently related to radiation damage from the high

concentrations of the polymeric plutonium. In mice with monomeric plutonium, no large hemorrhages were observed, and either lymphatic or bone tumors were the cause of most deaths.

The total occurrence of lymphatic tumors was high in all groups of mice. These tumors occurred in 72% of the control mice. Their incidence was increased over this control level in all groups of mice receiving monomeric plutonium except the group given the highest level, but was decreased in the groups in which life-shortening was also observed.

A detailed histopathological study of all skeletal areas diagnosed as abnormal in terminal radiograms has been completed in a cooperative study with Dr. T. E. Fritz (in consultation with Dr. L. S. Lombard). Two of the 58 duration-of-life control mice (3.4%) had malignant tumors in the bone. After injection of monomeric plutonium at 0.07, 0.14, 0.27, 0.47, and 0.96 μCi/kg, the incidence of mice with malignant bone tumors increased with dose: 5.3%, 11.6%, 35.3%, 55.9%, and 61.5%, respectively. After injection of polymeric plutonium, doses of 1.1, 2.2, and 3.8 μCi/kg, which resulted in the same initial bone burdens as the three lowest levels of the monomeric form, produced a bone tumor incidence of 42%, 50%, and 25%, respectively. With both forms of plutonium, increasing dose resulted in a shortening of the latent period, and an increased age-specific death rate with bone tumors.

Most of the tumors were osteosarcomas of the osteogenic type, and consisted of well-differentiated, rapidly proliferating, bone-forming osteoblastic cells. In some tumors, however, other forms of morphologic differentiation sometimes predominated over the obvious osteoid-producing cells. No apparent relationship existed between the histologic variability in tumor type and either the form or the dose level of plutonium injected. Most of the osteosarcomas appeared to originate from the endosteal bone. Non-neoplastic osteoporotic and osteosclerotic changes were also distributed throughout the animals of the several groups, including the controls.

Interpretation of the comparative effectiveness of monomeric plutonium and highly polymeric plutonium in the induction of bone tumors in this experiment must take into consideration a number of complex and interrelated factors, including: (a) the initial microlocalization of the monomeric plutonium on bone surfaces and of two-thirds of the polymeric plutonium in the marrow; (b) the different long-term retention patterns of the two forms, particularly as regards the increasing bone levels and the continuing lay-down of plutonium on bone surfaces after administration of the polymeric form; (c) the effect of polymeric plutonium on life-shortening; and (d) radiation damage to the hematopoietic system, liver, and spleen by polymeric plutonium.

Enzymatic Dissociation of Liver Parenchymal Cells from Plutonium-Treated Mice

New biochemical studies of the association of different physical-chemical forms of ^{239}Pu with non-cellular, cellular, and subcellular components of the liver have been initiated in the mouse. It is anticipated that such studies, when extended to other species such as the dog and hamster, will aid in understanding the mechanisms responsible for the grossly longer hepatic retention half times of monomeric plutonium in these animals (and

presumably man) as compared to those in mice and rats. These studies are also expected to contribute to our knowledge of the fundamental mechanisms involved in plutonium uptake in liver and other tissues, and to aid in devising better detoxification procedures.

Data are presently being obtained on the kinetics of association of plutonium with mouse liver parenchymal cells following intravenous injection of 0.1 μCi/kg of monomeric plutonium. To carry out this work, a method has been developed for the isolation of parenchymal cells from dog and mouse livers. The technique involves incubation of a tissue mince with buffered lysozyme solution, followed by dispersion of the incubated tissue mince with gentle strokes in a Potter-Elvehjem homogenizer (clearance, 1.0 mm) to release individual parenchymal cells. The cells are then isolated by differential centrifugation. By this means, the plutonium associated with liver parenchymal cells can be isolated free from plutonium associated with Kupffer cells or contained in extracellular spaces of the liver. The role of the parenchymal cells and their subcellular components in handling the liver plutonium burden can then be investigated. Subcellular components prepared from the isolated cells can be analyzed for plutonium content without the problems presented by heterogeneous mixtures of liver cell types or by the mixing of cell-associated and non-cell-associated plutonium during the tissue homogenization step.

In preliminary tests of this procedure using dog livers, cell yields averaged 6.4×10^7 parenchymal cells isolated per gram of fresh liver. Cell yields from mice were much lower, averaging 2.3×10^6 parenchymal cells isolated per gram of fresh liver. In the case of both dogs and mice, cell yields obtained so far have been consistently lower in plutonium-treated than control animals, possibly indicating increased cell fragility in plutonium-irradiated livers.

Autoradiographic Studies

Quantitative autoradiographic measurements of the microdistribution of monomeric plutonium in the dog liver 90 days following injection, reported last year as preliminary results (3), are now complete. Both track density and the fractions of tracks associated with parenchymal or littoral cells were found to be unchanged from values obtained at 6 days. Thus, no translocation of plutonium in the liver between 6 and 90 days following injection of monomeric plutonium could be detected by autoradiographic techniques.

Autoradiographic estimation of plutonium localization in different regions of a canine liver lobe 6 days following injection of polymeric plutonium has also been completed. As reported earlier (13), particulate plutonium is phagocytized primarily by reticuloendothelial elements of the liver, namely the Kupffer cells. In the present work only a slightly higher concentration of plutonium was found in the central region of the liver lobe, as compared to the peripheral region. This is in contrast to autoradiographic results with polymeric plutonium in the dog liver reported earlier (13). This difference may be due to the use of a slightly more polymeric solution in the earlier experiment, possibly resulting in physical entrapment of some of the larger particles in addition to uptake by phagocytosis. To extend the information obtained at 6 days, the quantitative

microdistribution in liver of highly polymeric plutonium at 3 months and 1 year after injection is currently being determined.

In addition to liver studies, bone specimens from dogs sacrificed at 6 and 90 days after injection of monomeric plutonium, and at 6, 90, and 365 days after injection of highly polymeric plutonium are now being prepared for autoradiographic and histological evaluation.

In cooperation with several members of the Chemistry and Physics Divisions of ANL and some of the staff of Rush University Medical Center we are participating in the evaluation of intravenously injected ^{153}Sm citrate as a tumor-localizing agent, using ICR white mice bearing sarcoma-180 as experimental animals. Autoradiographic examination of tumor tissue sections removed 24 hours after injection show a moderately high ratio ($\sim$ 5:1) of ^{153}Sm activity associated with cells in the peripheral regions of the tumor (no activity in the necrotic central regions), as compared to activity levels in adjacent areas of normal tissue. It has been shown (14) by direct radiochemical measurement of mouse tissues that between 24 and 48 hours after ^{153}Sm injection the activity ratios of tumor/normal tissues are increased, indicating a faster rate of removal of ^{153}Sm from non-tumor tissue than from the tumors.

Use of Electron Microscopy and X-Ray Microanalysis to Detect Subcellular Localization of Plutonium

The availability of a scanning electron microscope equipped with an Ortec energy dispersive X-ray analyzer has raised the possibility of combining the visualization of tissue sections at high magnifications with high resolution detection of plutonium located in subcellular deposition sites (15). In preliminary tests of the apparatus, X-ray peaks corresponding to plutonium have been obtained from electron-dense areas located on grids to which a solution of highly polymeric plutonium had been applied. However, the detection system as used at Argonne was not sensitive enough to produce X-ray peaks corresponding to plutonium from areas of liver sections where plutonium had already been located by EM autoradiography. More sensitive X-ray detector systems are available, however, and the feasibility of using these for our purposes is presently being investigated. This technique, when developed, could locate plutonium more quickly and accurately than can α-track recording by EM autoradiography. Also, development of such a sensitive detection method would permit estimations of the cellular and subcellular deposition of other heavy metal environmental pollutants.

Molecular Studies

Synthesis of ^{14}C-DTPA. Methods for the synthesis of DTPA labeled with ^{14}C in the 2-carbon have been successfully adapted to a micro-scale (6 millimoles) preparation, with a procedure which will allow maximum label incorporation. Problems encountered in the purification have been overcome by a combination of selective precipitation and ion-exchange chromatography. These procedures are also expected to be of use in the recovery of the pure ^{14}C-labeled DTPA from excreta of experimental animals. In the course of this work, a new technique for the rapid colorimetric microanalytical determination of DTPA has been developed. A preparation of low specific

activity DTPA is in progress to determine the percent label incorporation and the radiochemical purity of the synthetic DTPA.

Synthesis of Lipid-Soluble DTPA Esters. Previous work (16) has established that esterification of DTPA can enhance its ability to promote the removal of plutonium internally deposited in the liver, presumably by facilitating the penetration of the DTPA through cellular membranes. Intracellular hydrolysis of these esters then presumably liberates the free chelating agent. Unfortunately, the toxicity of the pentaethyl ester precludes its therapeutic use. To determine whether other, possibly less toxic, DTPA esters might be of interest we have developed a procedure for the synthesis of DTPA esters in which both the number and nature of the ester groups can be varied. The key intermediates in these syntheses are acid anhydride derivatives of DTPA. The diethyl ester of DTPA has been prepared in pure form and completely characterized by chemical analysis, and by infra-red and nuclear magnetic resonance spectroscopy. Preliminary experiments have established that the toxicity of this compound is not appreciably different from that of DTPA. Small quantities of the monoethyl ester of DTPA have been isolated and a compound believed to be the triethyl ester has been obtained; modification of the syntheses to provide macroscopic quantities of these derivatives is in progress.

Vitamins A_1 and A_2 are selectively taken up by the liver. Therefore, esterification of these vitamins to DTPA may provide a liver-specific vehicle for delivery of this chelating agent. Preliminary experiments with octadecyl alcohol have indicated that the esterification of DTPA with long-chain lipid-soluble alcohols is possible; chromatographic procedures for the isolation of pure DTPA-lipid-soluble esters are being developed.

Mössbauer Spectroscopy of ^{237}Np. Mössbauer spectroscopy offers the possibility of providing chemical information about the binding of certain radioelements in intact tissue samples. In order to assess the feasibility of this approach, spectra of $^{237}Np^{4+}$ and $^{237}NpO_2^{+}$ as perchlorates were obtained in frozen aqueous solution, at concentration levels approximating those that might occur in biological specimens. Satisfactory spectra were obtained in both cases, thus demonstrating the potential utility of this technique in characterizing the binding sites for internally deposited actinide ions.

REFERENCES

1. Baxter, D. W., M. W. Rosenthal, and A. Lindenbaum. Radiat. Res. 55, 144 (1973).
2. Lindenbaum, A., M. W. Rosenthal, D. W. Baxter, N. E. Egan, G. Steve Kalesperis, E. S. Moretti, and J. J. Russell. ANL-7970 (1972), p. 121.
3. Lindenbaum, A., M. W. Rosenthal, D. W. Baxter, J. E. Parks, G. Steve Kalesperis, E. S. Moretti, and J. J. Russell. ANL-8070 (1973), p. 137.
4. Rosenthal, M. W., H. Brown, D. L. Chladek, E. S. Moretti, J. J. Russell, and A. Lindenbaum. Radiat. Res. 53, 102 (1973).
5. Rahman, Y. E., M. W. Rosenthal, and E. A. Cerny. Science 180, 300 (1973).
6. Rosenthal, M. W., Y. E. Rahman, E. S. Moretti, and E. A. Cerny. Removal of polymeric plutonium by DTPA directed into cells by liposome encapsulation. This Report, Section 3.

7. Rosenthal, M. W., and A. Lindenbaum. Radiat. Res. 31, 506 (1967).
8. Rosenthal, M. W., and A. Lindenbaum. In: Delayed Effects of Bone-Seeking Radionuclides, Eds. C. W. Mays et al. The University of Utah Press, Salt Lake City, 1969, p. 371.
9. Lindenbaum, A., M. W. Rosenthal, C. J. Lund, J. J. Russell, M. H. Smoler, E. S. Moretti, and H. Brown. ANL-7535 (1968), p. 60.
10. Lindenbaum, A., M. W. Rosenthal, J. J. Russell, E. S. Moretti, and M. A. Smyth. ANL-7635 (1969), p. 186.
11. Lindenbaum, A., M. W. Rosenthal, J. J. Russell, E. S. Moretti, and D. Chladek. ANL-7770 (1970), p. 149.
12. Lindenbaum, A., M. W. Rosenthal, D. W. Baxter, N. E. Egan, D. Chladek, E. S. Moretti, and J. J. Russell. ANL-7870 (1971), p. 83.
13. Baxter, D. W., M. W. Rosenthal, J. J. Russell, E. Moretti, D. Chladek, and A. Lindenbaum. Radiat. Res. 54, 556 (1973).
14. Sullivan, J. C., A. M. Friedman, G. V. S. Rayudu, E. W. Fordham, and P. C. Ramachandran. Int. J. Nucl. Med. Biol., in press.
15. Barbi, N. C., and J. C. Russ. Proc. Electron Microscopy Society of America, Ed. C. J. Arceneaux. Claitor's Publishing Division, Baton Rouge, La., 1974, p. 110.
16. Markley, J. F. Int. J. Radiat. Biol. 7, 405 (1963).

REMOVAL OF POLYMERIC PLUTONIUM FROM DOGS WITH DTPA AND GLUCAN*

Marcia W. Rosenthal, Arthur Lindenbaum, David W. Baxter, G. Steven Kalesperis, Elizabeth S. Moretti, and John J. Russell

A highly polymeric preparation of plutonium-239 was injected intravenously into five groups of beagle dogs. An untreated control group was killed at six days after injection. The four treated groups, killed at 90 days, received one of the following by intravenous injection: a) 15 mg/kg of glucan on days 6, 34, and 62; b) 100 mg/kg of $CaNa_3DTPA$, twice-weekly for 12 weeks, beginning on day 6; c) both of these treatments; or d) saline. Between days 6 and 90 the level of plutonium in the liver decreased from 92.2% to 85.6% of the injected dose (ID) after saline, to 81.6% after glucan, to 77.8% after DTPA, and to 71.0% after both glucan and DTPA. The decrease to 71.0%, an approximately additive effect, was statistically significant. In dogs treated with either saline or glucan, the bone, and soft tissues other than the liver, had increased plutonium levels that did not occur in animals treated with DTPA. The 90-day excretion of plutonium in feces was low in all groups (3.3% ID, or less), while urinary plutonium was 3.5% ID after saline, 4.0% after glucan, 13.4% after DTPA, and 21.1% after glucan plus DTPA. These results confirm in dogs, as previously determined in mice, the action of glucan as an adjunct to DTPA in removal of polymeric plutonium from the liver.

*Abstract of a paper to be published in Radiation Research.

REMOVAL OF POLYMERIC PLUTONIUM BY DTPA DIRECTED INTO CELLS BY LIPOSOME ENCAPSULATION*

Marcia W. Rosenthal, Yueh-Erh Rahman, Elizabeth S. Moretti, and Elizabeth A. Cerny

DTPA (diethylenetriaminepentaacetic acid) encapsulated within lipid spherules (liposomes) removes more plutonium from the liver and femurs of mice injected with polymeric plutonium than conventional nonencapsulated DTPA. A single intravenous injection, at 3 days after plutonium, of 100 mg/kg of $CaNa_3DTPA$ encapsulated in liposomes made with phosphatidylcholine and cholesterol (3:1) reduced the plutonium in liver to 43-51% of the control level at 10 days, compared to 60% after nonencapsulated DTPA. In the femurs, the plutonium was reduced to 60.4-62.5% of the control level compared to 83-113%. Liposomal DTPA was equally effective when given intraperitoneally, or when stored for 3 days before use. Liposomal DTPA at doses as low as 25 mg/kg was not significantly less effective than a higher dose of 100 mg/kg. Four once-weekly injections of liposomal DTPA continued to give improved removal of plutonium compared to conventional DTPA. When given 24 days after plutonium, liposomal DTPA had a greater advantage over nonencapsulated DTPA in the liver than at 3 days and removed 22% of the plutonium from the femurs, compared to no removal by the nonencapsulated form. To date, DTPA liposomes made with lipids other than phosphatidylcholine and cholesterol, or with different surface charges, offer no advantage for plutonium removal.

---

*Abstract of a paper to be published in Radiation Research.

4. NEUTRON AND GAMMA-RAY TOXICITY STUDIES

SUMMARY

E. John Ainsworth, Group Leader

The major program activities are focused in two areas: (1) late effects experiments with large populations of mice which compare the effectiveness of neutron and gamma radiation for production of neoplastic and non-neoplastic diseases and life shortening, and (2) basic studies of cellular and functional indices of radiation injury, which provide the opportunity for fundamental new contributions to the understanding of late radiation effects in the vascular, immune, and hematopoietic systems.

During the past year effort has been devoted to (1) initiation of new late effects experiments with $B6CF_1$ mice to provide a dose-response matrix that will allow the effects of low doses of neutron or gamma radiation, protracted over extended periods of the animals' lifespan, to be precisely measured; and (2) analysis and evaluation of results which are now available from our initial study, JM-2, which began in 1971. Most of the animals in JM-2 are dead and most probable cause of death is being assigned to each animal when analysis of histopathology and/or gross pathology information is completed. The results from JM-2 show a departure from total dose dependence for fractionated doses of both neutron and gamma radiation administered over 24 weeks. When total dose and instantaneous dose rate are held constant and the dose is given in 72, 24, or 6 fractions, the groups that received 6 doses of neutrons showed less life shortening and those that received 6 doses of gamma radiation showed more life shortening than did animals which received 24 or 72 doses. Another departure from additivity observed in neutron-irradiated animals, namely the increase in life shortening and age-specific tumor rate that are produced by dose fractionation, in comparison with the same single dose, is not singularly attributable to induction-promotion of lethal pulmonary tumors, a frequently occurring neoplasm in irradiated $B6CF_1$ mice. The role of age on sensitivity to radiation-induced life shortening produced by a single dose was evaluated in JM-2 and the results show the neutron RBE to be higher at 280 days of age than at 110 days.

Both structural and functional changes in the vasculature have been observed during the second year after irradiation. The structural changes in the pinna include collapse of arteries, arterioles, and some veins along with alterations in the smooth musculature and accumulation of significant fibrosis. Late ultrastructural changes observed in myofibrils involve the endoplasmic reticulum and mitochondria. Other recently initiated work on cardiac muscle also shows alteration in the size and number of mitochondria, and fibrosis

within 75 days after irradiation. The fibrotic reaction, which is especially pronounced in neutron-irradiated animals, indicates a deficiency in repair or proliferative capability. Capillary efficiency, measured by the clearance of subcutaneously injected ^{133}Xe, is influenced by age and by irradiation, and the basis for late qualitative differences in clearance between neutron- and gamma-irradiated animals may become clear when evaluation of structural changes is completed.

Differences in repair or repopulation potential after neutron and gamma radiation are also evident from studies of susceptibility to respiratory infection with *Pasteurella pneumotropica*, and repopulation of splenic lymphocytes which bear the theta antigen. Both end points provide evidence for slower repopulation or restitution of function after a single neutron dose when the dose ratio of gamma to neutron was 2.6. Studies of the age-related decline in cellular immune capability, which provide basic information for the design of other experiments with irradiated animals, show a decrease in the mitogen response of spleen cells cultured *in vitro* which correlates with the previously observed decline in theta antigen.

Studies of early and late injury to the hematopoietic system have continued with particular attention paid to effects of dose fractionation and instantaneous dose rate. The most interesting results concern a sparing effect of low neutron dose rate on repopulation of hematopoietic stem cells (CFU) in the femur, reappearance of circulating platelets, and on the restitution of certain organ weights; however, no dose rate effect on CFU killing, based on D_o, was observed. Thus the effect of neutron dose rate on cell killing and repopulation vary independently in this test system. Since a sparing effect of low neutron dose rate could result from decreased killing of stem cells, measurements of D_o were made for spleen and femur CFU irradiated *in situ*. No differences in D_o were observed at 1.5 and 15 rad/min. This observation is unprecedented. The CFU studies led to experiments which show a significant effect of low neutron dose rate on $LD_{50/30}$ and $LD_{50/7}$.

Work in two areas has been temporarily suspended due to competing activities and/or personnel changes; no reports on transmissible leukemia or radiation effects on microbial systems are presented. The transmissible leukemia was exploited as one model system by which to study the effects of radiation or age on cell-mediated immunity.

Two experiments conducted to evaluate the sensitivity of *Escherichia coli* K12 mutants to JANUS neutrons confirmed and extended the results presented in the 1973 Annual Report. The results show that one mutant which lacks the capacity for both recombination repair and excision repair is markedly sensitive to neutrons. Moreover, since no increase in mutation rate was observed, JANUS neutrons are lethal but not mutagenic in this test system. If funds for continuation of this work are provided, new information will be obtained on the mode of DNA damage produced by neutrons.

During this year, effort has been devoted to several important supportive activities. Preparation for interspecies comparisons which involve the white-footed mouse, *Peromyscus leucopus*, and the beagle are in progress. During the next year, experiments with these species will begin. Our data management systems and data analysis capability which utilize the IBM 370/195 computer are being expanded. Performance of the neutron- and gamma-radiation facilities continues to be excellent, and new hardware procured for gamma

irradiation provides far greater dose rate flexibility than was previously available. In the area of dosimetry, several procedures have been evaluated for calculation of deflection or scatter of gamma rays, and Monte Carlo calculations provide new insight into the influence of radiation configuration or exposure geometry on neutron-gamma dose distribution. Finally, depth dose measurements are reported for a negative pi meson beam produced by the Argonne Zero-Gradient Synchrotron; this study was conducted to evaluate the beam for purposes of biological experimentation.

NEUTRON AND GAMMA-RAY TOXICITY STUDIES STAFF

REGULAR STAFF

Ainsworth, E. John (Biologist)
Allen, Katherine H. (Scientific Associate)
Brennan, Patricia C. (Biologist)
Christian, Emily J. B. (Scientific Associate)
Cooke, Eugenia M. (Scientific Assistant)
Hulesch, Jane L. (Scientific Assistant)
Jordan, Donn L. (Scientific Associate)
Kickels, Wayne T. (Scientific Assistant)
Miller, Marietta (Scientific Associate)
Stearner, S. Phyllis (Biologist)

DOSIMETRY AND DATA MANAGEMENT STAFF

Borak, Thomas B. (Assistant Physicist)
Holmblad, Gordon L. (Scientific Assistant)
Johnson, Emil G. (Engineering Assistant)
Trier, Joseph E. (Engineering Assistant)
Williamson, Frank S. (Physicist)

TEMPORARY STAFF DURING 1974

Yang, Vivian V. (Postdoctoral Appointee)

LATE EFFECTS OF NEUTRON OR GAMMA RADIATION

E. John Ainsworth, R. J. Michael Fry, Frank S. Williamson, Katherine H. Allen, Jane S. Hulesch, Donn L. Jordan, Anthony R. Sallese, and Everett F. Staffeldt

PURPOSE AND METHODS

The objective is to compare the late effects produced by protracted or a single exposure to fission neutrons or ^{60}Co gamma radiation. The information obtained is used to test existing models or develop new models with the aim of predicting (1) any excess risk which results from population exposures to low radiation doses, and (2) the consequences of occupational, therapeutic, or inadvertent exposure to low- or high-LET radiations. The experimental program compares the hazards of low-LET gamma radiation and high-LET neutron

radiation for the induction of late radiation injury, namely neoplastic and non-neoplastic disease, to which excess risk of death is attributable. The principal focus is on determination of dose-response relationships in mice for neoplastic, degenerative, and infectious diseases, and of impairments in physiologic function which occur late in life after low radiation doses administered over long periods of time. Effects of (low) dose rate, dose fractionation, and the portion of the lifespan over which animals are irradiated are evaluated to determine the extent to which estimates of excess risk are dependent on these factors. Any repair or recovery processes operative at low dose rates, or between radiation doses, that serve to diminish late injury are identified.

PROGRESS REPORT

A series of interrelated late effects experiments is currently in progress with $B6CF_1$ mice given either fractionated or single doses of fission neutron or gamma radiation. Results continue to emerge from the first experiment, JM-2, which began in the spring of 1971 (1-5). Most of the animals that received fractionated neutron or gamma doses have died, but many survivors remain among sham-irradiated controls and animals that received low single doses.

Current estimates of mean survival time (MST) after a single radiation dose or the first fractionated dose, administered at $\sim$ 110 days of age, are shown in Table 4.1. Surviving animals are not included in the MST calculations and groups in which current survival is sufficient to alter the MST estimate are indicated with asterisks. Survival among controls is sufficiently great that the current MST is based on decedents from only the first five replicates which entered the experiment, i.e., half the control sample.

The results in Table 4.1 conform to our previous predictions (2,3), which were based primarily on analysis of results obtained from only three of the ten replicates involved in the experiment, with regard to the following points: (1) under conditions of fractionated exposures administered over 6 months, the neutron RBE for life shortening is $\sim$ 10, since similar life shortening, $\sim$ 20%, is produced by 24 weekly doses of 3.3 neutron and 35.7 gamma rad; (2) in the case of single doses, RBE is dose-dependent and is greater than 4.5 at 20 rad and is less than 3.6 at 240 rad; (3) multifractionation of a gamma radiation dose results in a sparing effect on life shortening; the extent of this sparing effect is estimated at approximately threefold, based on days of life shortening per rad and the similar percent life shortening produced by a single dose of 285 rad and the multifractionated doses which total approximately 855 rad; (4) multifractionation of the neutron dose increases, rather than decreases, life shortening; the enhancing effect is statistically significant in both sexes at the total dose of 240 rad and in males that received a total dose of 80 rad.

The mechanism whereby neutron dose fractionation increases life shortening and age-specific tumor rates is not yet clear and is the focus of supporting basic studies reported elsewhere (3). Note that the extent of enhancement is conservatively estimated in Table 4.1 since the MST values are cued from the time of the first fractionated neutron dose.

Table 4.1. Mean Survival Time after Fractionated or Single Doses of Neutron or Gamma Radiation; Experiment JM-2

	Neutron[a]								Gamma[a]							
			Mean Survival Time		Days Lost/Rad		Life Shortening (%)				Mean Survival Time		Days Lost/Rad		Life Shortening (%)	
Group	Total Dose	Fract.[b]	M[c]	F[d]	M	F	M	F	Total Dose	Fract.[b]	M[c]	F[d]	M	F	M	F
A	240	72x3.3	551±13.5	505±11	1.18	1.37	34	39	855	72x11.9	716±12	690±13	0.14	0.17	14	17
B	240	24x10	523±11.5	500±10	1.29	1.39	37	40	855	24x35.7	690±13	676±12	0.17	0.19	17	19
E	240	24x10	545±12	501± 9	1.20	1.38	35	40	855	24x35.7	697±12	694±10	0.16	0.16	16	17
H	240	6x40	575±12	530±10	1.07	1.26	30	36	855	6x143	666±12	642±11	0.20	0.23	20	23
D	80	24x3.3	666±13	675±12	2.1	2. 0	20	19	1140	24x47.5	619±12	612±11	0.19	0.20	26	27
Pooled ABEH		6,24,72	549± 6	510± 5	1.18	1.35	34	39		6,24,72	693± 6	674± 6	0.16	0.19	17	19
S1*	20	1	788±10	761±10	2.2	3.6	5	9		1	806± 9	789± 9	0.28	0.49	3.1	5.3
S2*	80	1	725±13	667±13	1.4	2.1	12	20		1	728±13	704±12	0.39	0.48	12.5	15.5
S3	240	1	633±13	581±13	0.83	1.1	24	30		1	497±15	479±14	0.43	0.45	40.3	42.5
Con-trols*			832±11 (reps. 1-5)	833±11 (reps. 1-5)							832±11 (reps. 1-5)	833±11 (reps. 1-5)				

[a] Based on average absorbed dose/frame.

[b] Number of fractions x dose/fraction; see Table 4.2 for dose rate/fraction.

[c] Males.

[d] Females.

* Several survivors.

Analysis of autopsy and histopathology data and assignment of most probable cause of death permit the conclusion that the enhancing effect of neutron dose fractionation is not solely attributable to lethal pulmonary tumors (LPT), a late-occurring neoplasm observed in approximately 8% of unirradiated control animals and 8-18% of the animals that received fractionated doses of neutron or gamma radiation (Table 4.2). The enhancing effect of neutron dose fractionation is observed both when all causes of death are included in the MST computation, or when animals which died from lethal pulmonary tumors are excluded. The contribution of LPT to survival time is estimated by a decrementation procedure. Results in Table 4.3 show that in unirradiated controls, and in irradiated groups (other than that which received a single dose of 240 rad), when decrementation for LPT was made, the MST was 6-8% longer than in the original sample. The 3% increase in MST produced by decrementation of LPT animals from the group that received the single dose of 240 rad, compared with a 6-7% increase for animals which received fractionated neutron exposures, may indicate: (1) LPT contributes to some extent to the enhancing effect of fractionation; or (2) neutron dose fractionation may decrease the killing of potentially neoplastic cells and thereby permit a greater expression of neoplastic potential than does the same single dose. Comparison of age-specific occurrence rates for LPT in irradiated and unirradiated animals indicates that acceleration of tumor expression is an important component of radiation-induced life shortening. With further analysis of the pathology data, as they become available, it should be possible to evaluate the relative contribution of acceleration-promotion and induction of other neoplasms in irradiated animals.

Table 4.2. Percent Incidence of Lethal Pulmonary Tumors in Irradiated $B6CF_1$ Female Mice

Controls %	Gamma	Dose Rate/ Min	%	Neutron	Dose Rate/ Min	%
	143 rad x 6	0.8	15	40 rad x 6	0.2	16
8	48 rad x 24	1.0	10	3.3 rad x 24	0.07	18
	36 rad x 24	0.8	8	10 rad x 24	0.2	15
	12 rad x 72	0.8	13	3.3 rad x 72	0.2	13
	36 rad x 24	0.1	10	10 rad x 24	0.03	13

Table 4.3. Male $B6CF_1$ Mice Irradiated with Fission Neutrons

Cause of Death	Mean Survival Time (days) Group and Dose				
	Controls[a]	Single Dose 240 rad[b]	Fractionated 240 rad[c]	Single Dose 80 rad[d]	Fractionated 80 rad[e]
All causes	838±13	636±13 [24][g]	553±6 [34]	728±13 [13]	671±13 [20]
All causes other than LPT[f]	906±13 <1.08>[h]	652±13 [28] <1.03>	594±7 [34] <1.07>	768±14 [15] <1.06>	721±13 [20] <1.07>
LPT only	1039±17	919±9	824±8	933±12	879±14

[a] Replicates 1-5.

[b] Replicates 1-10; no survivors.

[c] Replicates 1-10; no survivors.

[d] Replicates 1-10; 12 survivors.

[e] Replicates 1-10; 1 survivor.

[f] LPT = lethal pulmonary tumors.

[g] [ ] % life shortening compared with appropriate control.

[h] < > ratio all causes other than LPT/all causes.

Other new information is now available regarding the additivity of neutron or gamma radiation doses. As detailed above, neutron doses are not simply additive in the sense that fractionation, in comparison with a single dose, increases both life shortening and tumor rates. In addition, the mode of neutron dose fractionation also influences life shortening and thus indicates a second departure from additivity. Significantly less life shortening results in male mice that received 6 doses of 40 rad (1 each 4 weeks) than in animals that received the same total dose, 240 rad, in 24 weekly doses of 10 rad (Table 4.1). The same trend is observed in females.

Although the sparing effect is small, and amounts to a 7% reduction in life shortening in males, the existence of such a phenomenon may indicate either that there is a recovery component which is operative when doses are separated by 4 weeks or that the enhancement is less effectively produced by 6 as compared with 24 or 72 neutron doses. In contrast to the small sparing effect observed when neutron doses are administered in doses separated by 4 weeks, in gamma-irradiated animals this fractionation regimen produces significantly greater life shortening, approximately 6%, than is observed when the same total dose is administered in 72 fractions (3 fractions/week of 12 rad) over 24 weeks (Table 4.1). Since instantaneous dose rate was identical in the 6 and 72 dose groups, the difference in survival time is attributable to dose per fraction or radiation free time. Whatever the mechanism, the results indicate a departure from total dose dependence and identify a recovery component that is operative when the dose per fraction is at a level expected to be on the shoulder of a cell survival curve for gamma radiation.

The matter of comparative susceptibility of male and female mice to radiation-induced life shortening requires further analysis. Significantly shorter survival times are observed among neutron-irradiated females than males in some single and fractionated dose groups. A similar, but not significant, trend is observed among gamma-irradiated mice. Sex-related differences in body weight, which would have a greater effect on dose-distribution in neutron-irradiated animals, may account in part for the apparent sex difference.

Age-susceptibility to life shortening after single doses of neutron or gamma radiation is being evaluated in male mice between the ages of 110 to 278 days. This is the age span over which the fractionated doses in JM-2 were administered. Although several animals remain alive, two interesting trends are clear: (1) irradiation at 194 or 278 days of age causes less life shortening than at 110 days in both neutron- and gamma-irradiated animals; and (2) at 278 days of age, neutrons are more effective than gamma radiation for production of life shortening. When given at 110 days of age, single doses of 80 neutron and 285 gamma rad result in essentially the same MST (725 and 728 days, respectively, or 13% life shortening). When these doses are administered at 278 days of age, the MST after neutron irradiation is significantly shorter than after gamma radiation; thus, life shortening is greater for neutron radiation and age *per se* affords less of a protective effect for neutron than for gamma radiation.

CONCLUSIONS

1. The most probable cause of death has been determined for many of the decedents in JM-2, and it is now possible to evaluate the role of lethal pulmonary tumors in the enhancing effect of fractionated neutron irradiation. Since enhancement is observed when animals with lethal pulmonary tumors are excluded from the data base used for analysis, it is now clear that enhancement is not singularly attributable to promotion or induction of this disease.

2. Departures from total-dose dependence are observed among animals which receive fractionated doses of either neutron or gamma radiation. In the case of neutron radiation, 6 radiation doses produce less life shortening

than do the other dose fractionation protocols (72 or 24 fractions), and in the case of gamma radiation, 6 fractions produce more life shortening than do the other dose protocols. These results identify recovery parameters or departures from simple additivity which are operative under conditions of fractionated neutron or gamma irradiation.

3. Somewhat greater life shortening is observed in irradiated female mice than in male mice. Body size and dose distribution may contribute to this effect.

4. Preliminary results from an experiment designed to evaluate the role of age on sensitivity to radiation-induced life shortening produced by a single dose indicate that the neutron RBE is higher at 278 days of age than at 110 days.

REFERENCES

1. Ainsworth, E. J., R. J. M. Fry, D. Grahn, F. S. Williamson, and J. H. Rust. Proc. Second European Symp. on Late Effects of Radiation (ESLER TWO), Casaccia, Italy, 1972. In press.
2. Ainsworth, E. J., R. J. M. Fry, D. Grahn, F. S. Williamson, and J. H. Rust. Radiat. Res. 55, 531 (1973).
3. Ainsworth, E. J., R. J. M. Fry, D. Grahn, F. S. Williamson, P. C. Brennan, S. P. Stearner, A. V. Carrano, and J. H. Rust. In: Biological Effects of Neutron Irradiation, IAEA, Austria, 1974, p. 359.
4. Ainsworth, E. J., and R. J. M. Fry. Radiat. Res. 59, 314 (1974).
5. Fry, R. J. M., E. J. Ainsworth, E. Staffeldt, A. Sallese, and K. Allen. Radiat. Res. 59, 222 (1974).

EARLY AND LATE INJURY TO THE HEMATOPOIETIC SYSTEM: INFLUENCE OF DOSE RATE AND DOSE FRACTIONATION

E. John Ainsworth, Eugenia M. Cooke, Donn L. Jordan, Jane S. Hulesch, Wayne T. Kickels, and Marietta Miller

PURPOSE AND METHODS

The study of hematopoietic function is important on three counts: (1) the contribution of residual hematopoietic injury to late radiation morbidity and death is unclear; (2) hematopoietic control systems and factors which influence them are fundamental to a disease of considerable interest, leukemia; and (3) the hematopoietic stem cell, evaluated by the spleen colony or colony-forming unit (CFU) technique, offers an excellent model system for studies of injury, repair, proliferation, and subsequent differentiation of stem cell progeny; both the number and functional capability of stem cells can be evaluated independently. The stem cell model has been (1-4) and continues to be exploited in basic studies which focus on an improved understanding of the effects of dose fractionation and dose rate on proliferative tissues. These studies complement the work on life shortening and carcinogenesis (5) and may provide a means by which late effects, such as the

enhanced life shortening produced by fractionated neutron irradiation, may be understood in terms of cellular responses. Methodology utilized in these studies is described elsewhere (6,7).

PROGRESS REPORT

Our previous studies (8) indicated that stem cell repopulation, based on colony-forming units in the femur, occurred earlier in neutron- than in gamma-irradiated animals when the doses given were in proportion to the RBE of 2.6 for 30-day lethality or D_0 for CFU. The advantage observed in neutron-irradiated animals also involved repopulation of peripheral lymphocytes and restitution of spleen weight. This experiment has been repeated, with particular attention to the phase of hematopoietic recovery that occurs between 30 and 180 days after irradiation. The peripheral hematology data are not yet reduced, but the CFU results now available generally confirm our previous observations and indicate that the femur CFU content is higher in neutron-irradiated animals at four sample times between 30 and 60 days. Other new data indicate that the earlier population in neutron-irradiated animals is not attributed to a reduction of the "post-irradiation dip" in femur CFU content in neutron-irradiated animals (9). After single doses of 96 neutron or 247 gamma rad, the dip at 6 hours after exposure is as great, on a percentage basis, in neutron-irradiated as in gamma-irradiated animals and amounts to a 34-36% decline below the femur CFU content at 15 minutes after irradiation. Results from this experiment provide evidence for an earlier onset of femur CFU repopulation in neutron-irradiated mice since by 24 hours the femur CFU content increased significantly compared with the 6-hour content, but in gamma-irradiated animals the femur CFU content did not increase between 6 and 24 hours. When the same total doses of 288 neutron or 744 gamma rad are administered in nine equal fractions over a period of 3 weeks the situation is reversed, compared with the response after a single exposure, and gamma-irradiated animals show an advantage in CFU repopulation. The greater sparing effect of gamma dose fractionation is consistent with expectations and our previous observations which concentrated on the first few weeks after fractionated irradiation (4,10).

We have also repeated our original observation that CFU repopulation is influenced by decreasing the neutron dose rate from 13.1 to 1.5 rad/min (8). Selected data from two experiments are shown in Table 4.4. In both experiments, mice exposed to neutrons at the low dose rate (LDR) of 1.5 rad/min showed a numerical advantage in femur CFU content at some sample times between 12 and 21 days after irradiation. The higher CFU content in animals exposed at the LDR was correlated with higher platelet counts (Table 4.5). Similar sparing effects of low dose rate neutron irradiation are observed at certain sample times for both spleen and thymus weights.

The neutron dose rate effect observed on CFU repopulation presents the requirement to determine if the effect is attributable to a decrease in CFU killing at the LDR or, alternatively, if the effect of neutron dose rate on cell killing and on repopulation varies independently. The effect of neutron dose rate on D_0 for CFU has been determined by irradiating donor animals with the test dose, sacrificing the animals, and measuring the number of surviving CFU. With this experimental design the CFU are irradiated *in situ* rather than after they have been sequestered in the spleen following intravenous

Table 4.4. Colony-Forming Units (CFU) in the Femur after 288 Rad of Neutron Radiation Administered at 13.1 (HDR) or 1.5 (LDR) Rad/Min. At Each Sample Time Marrow from 2 to 4 Donors was Pooled and Injected into 15 to 20 Recipient Animals

Days after Irradiation	Means and 95% Confidence Limits			
	High Dose Rate (HDR)		Low Dose Rate (LDR)	
	Experiment 2	Experiment 3	Experiment 2	Experiment 3
0	6152 (5248-7057)	7345 (6599-8090)	-	-
12	464 (391-538)	583 (511-654)	653 (564-743)[a]	519 (428-609)
14	784 (615-954)	810 (655-954)	1246 (1047-1446)[a]	1460 (1210-1710)[a]
16	821 (671-972)	927 (794-1059)	1839 (1439-2240)[a]	1580 (1385-1776)[a]
18	1695 (1352 2038)	1145 (924-1366)	2602 (2086-3118)[a]	1440 (1192-1688)
21	1369 (1119-1619)	-	2376 (2019-2733)[a]	-

[a]Significantly higher than HDR at the .05 level.

Table 4.5. Platelet Counts in Peripheral Blood after 288 Rad of Neutron Radiation Administered at 13.1 (HDR) or 1.5 (LDR) Rad/Min. Group Sizes in Experiments 2 and 3 were 15 and 20 per Sample Time, Respectively

Days after Irradiation	Means and 95% Confidence Limits			
	High Dose Rate (HDR)		Low Dose Rate (LDR)	
	Experiment 2	Experiment 3	Experiment 2	Experiment 3
0	1325 (1236-1414)[a]	1365 (1345-1491)[a]	1334 (1250-1419)[a]	1368 (1293-1443)[a]
12	109 (92-127)	96 (81-111)	198 (160-236)	168 (145-191)
14	232 (198-265)	191 (163-220)	339 (297-382)	343 (314-371)
16	422 (373-510)[b]	340 (313-367)	556 (461-651)	570 (504-636)
18	632 (526-738)	522 (471-573)	867 (758-977)	843 (773-912)
21	884 (803-965)[b]	-	980 (908-1051)	-

[a]Four separate control groups, which totalled 65 animals, were evaluated.

[b]Difference between HDR and LDR is not significant; all other differences within Experiments 2 and 3 are significant ($P < 0.05$).

injection of marrow. The results available at this time indicate no significant effect of neutron dose rate on D_o for femur or spleen CFU. The current estimates are 39 ± 4 and 41 ± 1.3 rad for femur CFU and 31 ± 1 and 31 ± 1 rad for spleen CFU irradiated at low and high dose rates, respectively. The absence of a dose rate effect for fission neutrons from JANUS on CFU survival is consistent with earlier observations by Sinclair with Chinese hamster cells *in vitro*, who found no effect of dose rate on D_o (11).

Since injury to the hematopoietic system contributes significantly to neutron lethality in the $LD_{50/30}$ dose range, the higher CFU content in animals exposed at the LDR would predict some sparing effect or increase in $LD_{50/30}$ at 1.5 rad/min providing femur CFU content is correlated with survival and if the acceleration of recovery occurs at a sufficiently early time to benefit the irradiated animal. The results in Table 4.6 show a small, ∿ 7%, reproducible, and statistically significant increase in $LD_{50/30}$ at the LDR. In the experiment dated 9/74, confinement stress was controlled by retaining the animals exposed at the high dose rate (HDR) of 13.1 rad/min in the containers in which they were irradiated for the maximum period of confinement required to deliver the highest dose given at the LDR, e.g. ∿ 6 hrs. Since confinement stress produced no detectable effect on $LD_{50/30}$ at the high dose rate, the inference is that the 7% increase in $LD_{50/30}$ is specifically attributable to the decrease in dose rate. The results in Table 4.6 show that both $LD_{50/6}$ and $LD_{50/7}$ are increased at the LDR, and the percentage increase, 13%, is relatively greater than is observed for $LD_{50/30}$. This conforms to general expectations regarding repair capacities of hematopoietic and intestinal stem cells, respectively. The increase in $LD_{50/7}$ at the LDR is statistically significant and the change in $LD_{50/6}$ is borderline.

Table 4.6. Effect of Neutron Dose Rate on 6-, 7-, and 30-Day Mortality in $B6CF_1$ Male Mice

End Point	Dose Rate (rad/min)	LD_{50} (rad) and 95% Confidence Limits — Individual Determinations		Pooled LD_{50} Estimate
6-Day Lethality	1.5	4/74 678 (569-792) 9/74 638 (595-682)		662 (608-717)
	15	1/73 565 (395-737) 4/74 606 (575-637)	4/73 545 (510-581) 9/74 612 (578-647)	586 (561-611)
7-Day Lethality	1.5	4/74 628 (556-699)	9/74 616 (585-648)	626 (591-662)
	15	1/73 559 (509-609) 4/74 562 (516-609)	4/73 497 (456-540) 9/74 580 (554-607)	553 (541-567)
30-Day Lethality	1.5	8/73 479 (461-498) 9/74 475 (462-490)	1/74 465 (458-474)	474 (469-478)
	15	1/73 456 (442-471) 4/74 442 (410-435)	12/73 442 (425-459) 9/74 445 (438-453)	443 (437-451)

These results which show a significant effect of neutron dose rate on $LD_{50/30}$ are at variance with earlier reports by Vogel et al. (12), and a more recent report by Gottlieb and Gengozian (13). Although fission spectrum neutrons were used in the present experiments as well as those cited above, spectral differences as well as the use of different mouse strains may contribute to the differences between the present and the earlier observations. Since the gamma radiation component of the total dose sustained by animals exposed in the JANUS reactor facility is lower than the gamma component encountered in other exposure facilities, including those cited above,

difference in the amount of low-LET radiation in the radiation fields cannot account for the difference between the present and earlier observations. This matter requires further consideration and must be viewed with full cognizance of the fact that not all of the dose deposited by recoil protons, produced by neutron interactions in hydrogenous matter, is densely ionizing.

Other continuing studies of the hematopoietic system concentrate on functional studies that reveal late-occurring deficiencies which are not necessarily correlated with low peripheral blood counts or reductions in the size of the stem cell compartment. We previously reported (1) that by 280 days after 288 neutron or 741 gamma rad the femur and spleen stem cell content in irradiated animals did not differ significantly from aged unirradiated controls, but that the irradiated animals showed a significantly reduced ability to respond to bacterial endotoxin with CFU proliferation in the marrow or spleen. These results were confirmed in a replicate experiment. An experiment conducted at 350 days after fractionated doses of neutron or gamma radiation (total doses of 288 neutron or 741 gamma rad given in 9 equal doses over 21 days) shows generally similar phenomenology (Table 4.7). A difference between these and the previous observations after a single irradiation concerns the femur and spleen CFU content of animals before endotoxin injection. Femur CFU content in the animals that received fractionated neutron or gamma irradiation was significantly lower than in aged controls. This could indicate incomplete repopulation, or an accelerated decline in the stem cell population, both of which we have observed previously (1). Moreover, the endotoxin response in irradiated animals, reflected by reduced rather than increased CFU content, differs significantly from the response of aged controls between 3 and 5 days after injection. In irradiated survivors, both neutron- and gamma-irradiated, endotoxin produced a significant decline in femur CFU content which occurred more rapidly and to a lower level than in aged controls. The spleen response was similar to that observed at 280 days after a single irradiation; namely, some delay in the increase in CFU content in irradiated animals. The basis for these differences in proliferative response to endotoxin, which constitute some mode of residual injury, is unknown at this time, but results of Roy Vigneulle,* a graduate student in our laboratory, show that the late lesion may not reside with the stem cell *per se*. His work shows that the proliferation rate, e.g. doubling time, of stem cells from aged irradiated survivors and aged animals, after transplantation into young supralethally-irradiated recipients, does not differ significantly, although the femur content of CFU from the original irradiated donor animals was reduced in comparison with aged controls. Thus, late injury to "control systems" or stroma, rather than a component of injury to CFU *per se* may account for these results. Experiments designed to test that hypothesis are planned.

*Laboratory Graduate Program Participant, University of Illinois, Urbana.

Table 4.7. Femur and Spleen Content of Colony-Forming Units (CFU) in $B6CF_1$ Mice Injected with 0.1 ml Typhoid Vaccine at Approximately 350 Days after Irradiation[a]

Days after Injection	Organ	Aged Controls	Neutron	Gamma
1	Bone Marrow	5179 (4049-6308)	5700 (4485-6915)	4167 (3091-5243)
	Spleen	2383 (1840-2927)	2300 (1877-2723)	2288 (1792-2785)
2	Bone Marrow	5066 (3655-6478)	3653 (2778-4529)[b]	3666 (2187-5146)
	Spleen	5600 (4668-6532)	3813 (3259-4368)[b]	4615 (3349-5882)
3	Bone Marrow	6143 (4745-7541)	3700 (2871-4529)[b]	2167 (1437-2897)[b]
	Spleen	5627 (4468-6785)	6213 (5003-7426)	5200 (4132-6268)
4	Bone Marrow	5333 (4382-6285)	2733 (2089-3377)[b]	3153 (2389-3918)[b]
	Spleen	5464 (4141-6787)	4800 (3740-5860)	4420 (3729-5110)
5	Bone Marrow	4321 (3163-5479)	3071 (2153-3990)	2808 (2013-3603)
	Spleen	4343 (3549-5137)	4027 (3213-4840)	2400 (1610-3190)[b]
No Injection[c]	Bone Marrow	7071 (5934-8208)	4500 (3201-5799)[b]	4692 (3493-5892)[b]
	Spleen	2900 (2332-3468)	3883 (3330-4437)	1468 (1222-1714)[b]

[a]The fractionated irradiation schedule consisted of 9 doses of 10.7 neutron rad or 27.4 gamma rad administered over 3 weeks. The dose rates were 0.6 and 1.5 rad/min for neutron and gamma radiation, respectively. Total doses were 96 neutron and 247 gamma rad. The first radiation fraction was administered at 110-120 days of age.

[b]Significantly different from aged controls.

[c]460-470 days of age.

REFERENCES

1. Ainsworth, E. J., R. J. M. Fry, D. Grahn, F. S. Williamson, and J. H. Rust. Proc. Second European Symp. on Late Effects of Radiation (ESLER TWO), Casaccia, Italy, 1972. In press.
2. Ainsworth, E. J., R. J. M. Fry, D. Grahn, F. S. Williamson, and J. H. Rust. Radiat. Res. 55, 531 (1973).
3. Ainsworth, E. J., R. J. M. Fry, D. Grahn, F. S. Williamson, P. C. Brennan, S. P. Stearner, A. V. Carrano, and J. H. Rust. In: Biological Effects of Neutron Irradiation, IAEA, Vienna, 1974, p. 359.
4. Ainsworth, E. J., and R. J. M. Fry. Radiat. Res. 59, 314 (1974).
5. Ainsworth, E. J., R. J. M. Fry, F. S. Williamson, K. H. Allen, J. S. Hulesch, D. L. Jordan, A. R. Sallese, and E. F. Staffeldt. Late effects of neutron or gamma radiation. This Report, Section 4.
6. Ainsworth, E. J., and R. M. Larsen. Radiat. Res. 40, 149 (1969).
7. Ainsworth, E. J., R. J. M. Fry, D. Grahn, F. S. Williamson, J. H. Rust, P. C. Brennan, A. V. Carrano, D. L. Jordan, M. Miller, K. H. Allen, M. P. Nielsen, E. Cooke, E. Staffeldt, and A. Sallese. ANL-7970 (1972), p. 13.
8. Miller, M., E. Cooke, and E. J. Ainsworth. Radiat. Res. 51, 473 (1972).
9. Broerse, J. J. Curr. Top. Radiat. Res. Q. 8, 305 (1973).
10. Ainsworth, E. J., R. J. M. Fry, F. S. Williamson, W. E. Kisieleski, D. L. Jordan, M. P. O'Malley, M. Miller, E. M. Cooke, A. Sallese, and P. C. Brennan. ANL-7870 (1971), p. 19.
11. Sinclair, W. K. ANL-7770 (1970), p. 29.
12. Vogel, H. H., Jr., J. W. Clark, and D. L. Jordan. Radiat. Res. 6, 460 (1957).
13. Gottlieb, C. F., and N. Gengozian. J. Immunol. 109, 711 (1972).

STRUCTURAL CHANGES IN THE MICROVASCULATURE IN THE AGING, IRRADIATED MOUSE

S. Phyllis Stearner, Rosemarie L. Devine, and Emily J. B. Christian

PURPOSE AND METHODS

Damage to small blood vessels is frequently associated with injury from radiation, from other environmental pollutants, and also from normal aging. Serious vascular damage may be produced by radiotherapy in tissues near the tumor or surrounding it. This injury can endanger the patient even when the tumor has been successfully treated. Heart failure, for example, is recognized as a potential hazard months or years after irradiation of the heart during treatment of tumors of breast or lung.

Long-term studies of the vascular effects of low-level radiation exposures are in progress as part of the JANUS Program. These studies include direct microscopic observations of the circulation in the mouse pinna, estimations of capillary efficiency (i.e., capillary blood flow) in selected tissues, and ultrastructural observations of the microvasculature. Observations are scheduled at approximately 6-month intervals. Longitudinal studies over the lifespan of individual animals will make possible comparisons of vascular changes with radiation treatment and with the effects of fractionation. The most characteristic effects, observed *in vivo* with the light microscope, include constriction or segmental stenosis of arterioles and dilatations or tortuosities of venules. Our study of ultrastructural changes, correlated with *in vivo* observations, includes evaluation of the radiation effects that occur at approximately the time of maximum decrease in the circulatory efficiency, at about 18 months. These observations are preliminary and only tentative correlations can be made with radiation treatments at this time.

Direct microscopic observations of the vasculature in the mouse pinna were recorded photographically on 35-mm film and 16-mm movie film strips for later comparative evaluations. Selected individuals were sacrificed at about 24 months of age for fine-structural study of specific regions of the pinna that *in vivo* studies had previously identified to be of special interest. The radiation dose groups from which electron microscopic studies are reported include fission neutron exposures to 240 rad, the same neutron dose fractionated over a 24-week period, ^{60}Co gamma rays (855 rad) also delivered over 24 weeks, and unirradiated controls. Details of procedures have been described (1).

RESULTS

The major artery in the pinna should probably be classified as an arteriole. It contained at least one complete elastic layer, a layer of smooth muscle of varying thickness, and a continuous endothelium. At higher magnifications, electron-microscope observations showed that the elastic lamina has a homogeneous and rather uniform appearance. Smooth muscle cells had few dilated vacuoles, and in general appeared to undergo little alteration with age. The major venule of the pinna, which parallels the arteriole, was composed of a layer of continuous endothelium, some collagen fibers outside the basement membrane, and a more or less continuous layer of smooth muscle.

The components of capillaries, present in varying abundance in different regions of the pinna, included a continuous endothelium, a thin basement lamina surrounding the endothelium, and an occasional adjacent pericyte.

After a single exposure to 240 rad fission neutrons, marked ultrastructural effects on arterioles and venules were seen in animals sacrificed about 20 months after exposure. Arterioles were frequently completely collapsed, the lumen barely discernible. The endothelium appeared continuous (no open junctions or breaks), but the surrounding elastica was markedly changed. Instead of having a homogeneous appearance, the elastica contained myelin figures and regions of fibrosis. In general, thicker layers of collagen were present around both types of vessels. Venules also tended to be collapsed and the muscle layer was frequently discontinuous. The venular endothelium was intact, but showed a variety of changes. Frequently, electron-lucent cells were present adjacent to electron-dense endothelium. The endothelium was surrounded by an increased amount of basement lamina material.

In groups that received fractionated neutron doses, segmental arterial stenosis was especially prominent, marked ultrastructurally by regions of extensive fibrosis in the smooth muscle layer. Frequently myofibrils were completely replaced by fibers presumably collagenous in nature. There were also numberous vacuoles, dilated endoplasmic reticulum, and degenerated mitochondria. Endothelium was frequently irregular. The elastica contained vacuoles, fibrillar material, and myelin figures, all of which represented marked changes from the normal homogeneous appearance. The larger venules contained a disordered array of collagen fibers and only occasional bits of smooth muscle. Generally, the endothelium was continuous with little indication of irregularities.

In contrast to the extensive vascular change in neutron-irradiated animals, fractionated exposures to 855 rad of ^{60}Co gamma radiation resulted in less prominent alterations. Arterioles from comparable regions of the pinna showed few changes; the endothelium was intact, smooth muscle layers were complete, and only minimal alterations were present in the elastic lamina. The large, thin-walled venules adjacent to the arterioles, however, sometimes showed discontinuous endothelium, partial atrophy or disappearance of the muscle layer, and increased collagen accumulation. Capillaries tended to be swollen, with enlarged endothelial vacuoles that frequently occluded the lumen. Thickened basement laminae were again prominent. Of special interest was the appearance of endothelial proliferation in arteries. The resulting projections contained significant amounts of elastic material in addition to endothelium and led to obstruction of blood flow in effected vessels. There was also an unusual amount of pinocytosis.

CONCLUSION

In neutron-irradiated animals, fibrosis was much more notable than in gamma-irradiated animals and there was apparently less cell proliferation for injury repair. Segmental stenosis, a characteristic late radiation effect, most prominent after neutron radiations, appeared to be a consequence of smooth muscle changes. Smooth muscle degeneration and fibrosis appeared to be more marked after fractionated than after single neutron exposures.

Development of irregularly dilated venous segments, associated with aging as well as radiation damage, appeared to be the result of degeneration of the smooth muscle of the vessel wall. Capillaries were frequently occluded by swollen endothelium.

REFERENCE

1. Stearner, S. P., and R. L. Devine. ANL-8070 (1973), p. 22.

FINE STRUCTURE OF THE IRRADIATED HEART

S. Phyllis Stearner and Vivian V. Yang

PURPOSE AND METHODS

Radiation effects on the heart are recognized as a possible cause of complications associated with various procedures in radiotherapy. Some years ago, Kohn et al. described changes in the mouse heart a year or more after exposure to whole-body X-radiation (1). In general, however, this organ is considered to be fairly radioresistant and has received little attention in studies of radiation effects of relatively low-level total-body exposures. Observations in the chicken (2) indicated that late appearance of myocardial atrophy and pericardial fibrosis frequently resulted from whole-body exposures to ^{60}Co gamma radiations at or near the acute lethal range. In addition, rabbits and mice showed histological evidence of myocardial damage after partial-body exposures to 1000 or 2000 rad X-radiation (3-5). In connection with long-term observations of gamma and fission neutron effects in the JANUS Program, studies are in progress to determine ultrastructural changes in the myocardium and myocardial microvasculature associated with age and with radiation treatment. These changes will be compared with vascular effects in the pinna.

The animals in this study received a single, total-body dose of 240 neutron rad, or 285 or 855 gamma rad, or were unirradiated controls. Animals were sacrificed by ether inhalation at 4, 30, 75, and 180 days after irradiation. The thorax was opened, and the heart was perfused through the left ventricle with Karnofsky's paraformaldehyde-glutaraldehyde fixative, pH 7.4. After perfusion, cross-sections of the major vessels (aorta and inferior vena cava) were removed. The heart was sectioned below the auricles, perpendicular to the long axis, and blocks of tissue were taken from the left and right ventricles, using a constant sampling site in all animals. All specimens were fixed in fresh Karnofsky's fixative for 3 to 5 hours at 4°C. After overnight wash in buffer, tissues were post-fixed with osmium tetraoxide, dehydrated in alcohol, stained *en bloc* with uranyl acetate in 75% alcohol, and embedded in Epon-Araldite mixture. Survey sections cut at 1-μm thickness and stained with toluidine blue were prepared for light microscopy. Thin sections were examined and photographed in the Siemens electron microscope.

RESULTS

Ultrastructural changes in cardiac muscle were seen at 4 days after irradiation. Myocardial cells showed fibrillar disorganization, accumulation of myelin figures, and lysosomal-like bodies. Z-lines and mitochondria were generally unchanged. At 75 days, fibrillar degeneration was more advanced, with loss of entire myofibrils. Many of these areas contained double-membrane vesicles, electron-dense debris, dispersed ribosomes, and partially vacuolated mitochondria. In some myofibrils, Z-bands showed total destruction. Some muscle fibers had disrupted intercalated disks. Interstitial fibrosis surrounding the muscle fibers was also observed at 75 days. There appeared to be slightly greater injury in the neutron-irradiated than in the gamma-irradiated animals. At 4 and 75 days post-irradiation, the myocardial capillaries also showed a variety of ultrastructural changes. Endothelial cell swelling varied from capillary to capillary and in some instances was also markedly different in adjacent endothelial cells. In addition to swelling, endothelial cells also showed extensions and blebbing, myelin-like figures, and vacuolated mitochondria. Thrombi were frequently observed adhering to irregularities of the endothelial surface.

Only preliminary observations of other treatment groups have been completed. It is anticipated that quantitative evaluations can be made of the extent of myofibrillar degeneration and of capillary abnormalities. Changes in the size and number of mitochondria in the muscle fibers, suggested by preliminary evaluations, will receive further study.

REFERENCES

1. Kohn, H. I., R. F. Kallman, C. C. Berdjis, and K. B. DeOme. Radiat. Res. 7, 407 (1957).
2. Stearner, S. P., and E. J. B. Christian. Radiat. Res. 52, 179 (1972).
3. Fajardo, L. F., and J. R. Stewart. Lab. Invest. 29, 244 (1973).
4. Khan, M. Y. Am. J. Pathol. 73, 133 (1973).
5. Khan, M. Y., and M. Ohanian. Am. J. Pathol. 74, 125 (1974).

RADIATION EFFECTS ON CIRCULATORY EFFICIENCY

S. Phyllis Stearner and Emily J. B. Christian

PURPOSE AND METHODS

Studies of alterations in circulatory function in the mouse have been carried out in connection with studies of structural changes in the vasculature resulting from radiation exposures and from natural aging (1). The clearance of locally administered radioactive xenon, Xenon-133, is a rapid and non-destructive method for determination of capillary blood flow in specific tissue regions. It can be carried out conveniently in the mouse. Radioactive xenon in saline solution is injected into a subcutaneous tissue region, from which it enters the circulating blood through the capillary

endothelium. It is then removed from the region by means of venous outflow to the lungs where about 95% of the injected amount is expired in the first circulation.

The amount of injected ^{133}Xe for each determination was about 0.02 ml containing 50 to 100 μCi. A Packard 400-channel analyzer equipped with a sodium iodide crystal was used to count the 80 keV gamma ray emitted. The entire mouse was monitored at a position 21 cm from the face of the crystal to determine the loss from the subcutaneous region. Counting was continuous for more than 30 minutes during injection and the subsequent washout period. The time per channel was 5 seconds. The dose groups for which mean clearance values are reported here include single doses of 240, 80, and 20 rad of fission neutrons, and 855 and 285 rad of ^{60}Co gamma rays. Additional dose groups will be reported later.

RESULTS

Clearance of locally injected radio-xenon from a subcutaneous region was usually adequately fitted by a single exponential in both controls and irradiated mice. The mean half time was approximately 10 minutes in unirradiated controls, up to about 20 months of age.

The effect of irradiation and of age on capillary efficiency are shown in Figures 4.1 and 4.2. In controls from 24 to 30 months, the circulatory efficiency decreased, as indicated by an increase in half time of xenon clearance to 13 to 14 minutes from the earlier level of 10 minutes. After this, however, when group mortality exceeded 50%, there was an increase in capillary efficiency as a preterminal condition was reached. In the various irradiated groups, capillary efficiency also tended to increase at approximately the time at which group mortality had exceeded 50%. In individuals nearing a terminal state clearance was frequently even more rapid than in young controls. Following a neutron dose of 240 rad, there was an early increase in capillary efficiency and at 3 days after exposure mean clearance half time was only about 5 minutes. At 4 days, however, the mean values returned to the control level and remained at this level through 30 days. After some months, clearance in the neutron-exposed groups tended to be only slightly slower than in controls and there was no clear dose-dependence. All groups showed a preterminal increase in capillary efficiency (faster clearance) that paralleled the control response. After a ^{60}Co gamma dose of 855 rad, there was an early increase in capillary efficiency that was sustained through 7 days. Clearance was much slower than in controls during the 3- to 12-month period after gamma irradiation. Again there was no clear dose-dependence. A preterminal increase in clearance time, corresponding to the time of increased mortality, was observed as in the control and neutron-irradiated groups.

CONCLUSIONS

Clearance times of subcutaneously injected Xenon-133 generally increased with age in all irradiated groups and, to a lesser degree, in controls. There was a more rapid clearance in neutron- than in gamma-irradiated groups that suggested a qualitatively different change was operative in these groups.

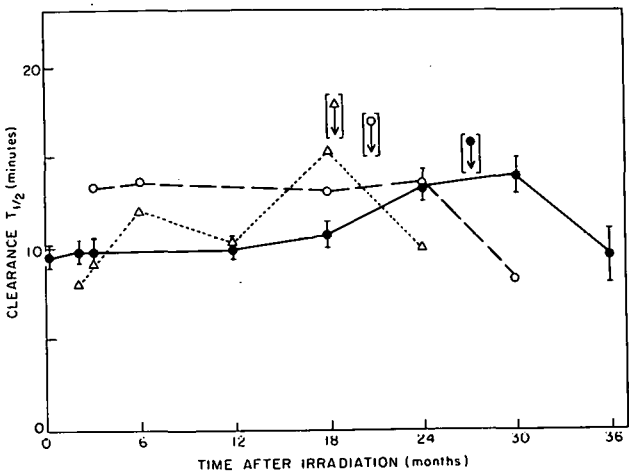

Fig. 4.1. Effect of single-dose, total-body irradiation with fission neutrons on capillary efficiency, indicated by the half time ($T_{1/2}$) of ^{133}Xe clearance from the subcutaneous region in the mouse. Arrows indicate the time at which mortality reached 50% in each of the treatment groups. Error bars represent 1 SE.

- ● Control
- o 80 rad
- Δ 240 rad

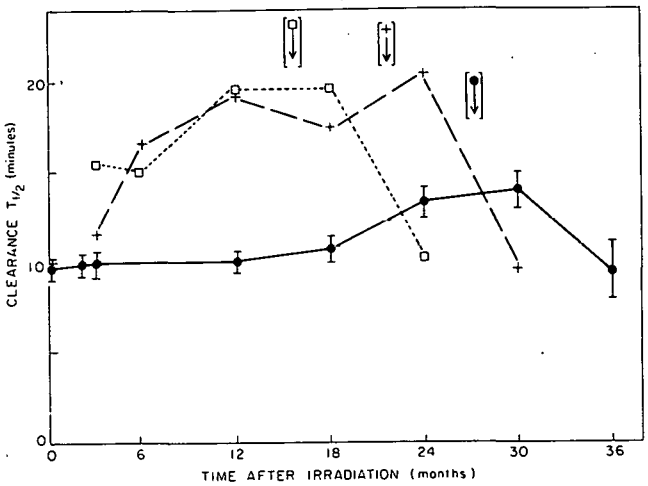

Fig. 4.2. Effect of single-dose, total-body irradiation with ^{60}Co γ-rays on capillary efficiency, indicated by the half time ($T_{1/2}$) of ^{133}Xe clearance from the subcutaneous region in the mouse. Arrows indicate the time at which mortality reached 50% in each of the treatment groups. Error bars represent 1 SE.

- ● Control
- \+ 285 rad
- □ 855 rad

A contributing factor to decrease in capillary efficiency (that is, the longer clearance time) may be the fibrosis that is commonly observed after radiation (1). A more efficient circulation in the preterminal period is not a unique response associated with irradiation, but is also seen in unirradiated controls.

Interpretation of factors influencing changes in capillary efficiency in irradiated mice will require information from related studies ongoing in the JANUS Program. Correlation with structural findings will be of value.

REFERENCE

1. Stearner, S. P., R. L. Devine, and E. J. B. Christian. Structural changes in the microvasculature in the aging, irradiated mouse. This Report, Section 4.

RADIATION EFFECTS ON HOST DEFENSE MECHANISMS

*Patricia C. Brennan, Wayne T. Kickels, Richard C. Simkins, and Linda G. Daniel**

PURPOSE AND METHODS

Resistance to disease depends as much on the integrity of host defense mechanisms as on the invasive and/or toxic properties of the disease-producing agent. The ability to mount an adequate cellular defense may determine the outcome of exposure to certain viral, bacterial, and mycotic infections. Similarly, cellular immune competence is believed to influence tumor cell proliferation as well as forming the surveillance system that eliminates tumor cells when they arise spontaneously. Resistance to other diseases may depend more on the ability of specialized host cells to phagocytize and kill the invading microorganism, to mount a humoral response, or to produce interferon. Any injury which impairs one or more of the many interacting host defense mechanisms can upset the delicate balance that exists between health and disease.

While it is well known that increased susceptibility to infectious disease, and hence impaired host defense, follows acute mid-lethal exposure to low-LET radiation, little is known about the effect on host defense of chronic low-level exposure or about either acute or chronic exposure to high-LET radiation.

We are assessing the integrity of host defense mechanisms of the irradiated $B6CF_1$ mouse by determining: (1) the functional state of the pulmonary antibacterial system, measured by clearance of *Pasteurella pneumotropica;* (2) the ability to mount a cellular and humoral response to challenge with *Mycoplasma pulmonis*; (3) cellular immune competence by spleen thymus-derived (T) cell content and response to T-cell mitogens; (4) humoral immune competence by response to the B-cell mitogen, bacterial lipopolysaccharide (LPS). Experiments have also been initiated to study cellular immune competence in *Peromyscus leucopus* and the beagle dog (see Section 2, Radiation Toxicity in Dogs). With the exception of the *in vitro* response to mitogens, details of the methods have been previously reported (1-4).

The response of cultured spleen cells to mitogens is determined by measuring the incorporation of tritiated thymidine into DNA after 72 hours culture with optimum doses of the T-cell mitogens, Concanavalin A (Con A) and Phytohemagglutinin (PHA), and the B-cell mitogen LPS.

PROGRESS REPORT

Table 4.8 shows the clearance of *P. pneumotropica* from the lungs of mice 5, 11, and 21 days after single doses of 288 neutron rad or 740 gamma rad. Little repair is evident in neutron-irradiated mice; 85% were unable to clear the organism when challenged as long as 21 days after irradiation, whereas only 25% of gamma-irradiated mice failed to eliminate *P. pneumotropica*.

---

*Summer 1974 participant in the Undergraduate Honors Research Participation Program, Clark College.

Table 4.8. Clearance of *Pasteurella pneumotropica* from the Lungs of Neutron- or Gamma-Irradiated Mice

Time of Challenge[a]	Radiation Dose (rad)[b]	Viable *P. pneumotropica* Recovered/Lung (10^2)[c]	Percentage of Mice Unable to Clear *P. pneumotropica*
5 days	fn 288	29.0 ± 12.2	70.4
	γ 740	4.2 ± 2.2	72.0
11 days	fn 288	280.0 ± 83.0	93.1
	γ 740	5.1 ± 1.8	66.0
21 days	fn 288	38.0 ± 13.0	85.2
	γ 740	0.27 ± 0.09	25.0
5-21 days	0	0.05 ± 0.005	7.3

[a]Groups of 30 mice were challenged with 3×10^5 viable *P. pneumotropica* and their lungs cultured 4 days later.

[b]Factors used to convert exposures to midline tissue dose were 0.80 for JANUS neutrons and 0.95 for ^{60}Co gamma radiation.

[c]Values are the mean ± 1 SE.

These data suggest an RBE of > 2.6 for this end point. Immunofluorescent-stained lung sections at all time intervals were strikingly similar among neutron- and gamma-irradiated and unirradiated mice. Alveolar macrophages were swollen with fluorescent *P. pneumotropica* cells and macrophages surrounding the bronchi and in the bronchial exudate were also intensely fluorescent. The immunofluorescence data coupled with the culture data indicate that while pulmonary macrophages in the irradiated host are capable of engulfing invading *P. pneumotropica* cells, the ability to kill them is impaired.

We have continued our efforts to develop more sensitive tests for the detection of antibody to *M. pulmonis*. A radioimmunoprecipitation (RIP) test has been developed which is more sensitive than the mycoplasmacidal test we reported previously (4). The RIP test has the added advantage that levels of different immunoglobulin classes can be determined. We are presently determining the level of anti *M. pulmonis* IgG in the serum and anti *M. pulmonis* IgA in nasal washings of experimentally infected mice.

During this reporting period, we have completed a study of the early changes in T-cell spleen populations following neutron or gamma irradiation. Results 5, 11, and 21 days after single doses of 288 neutron or 740 gamma rad are shown in Figure 4.3. In gamma-irradiated mice, the T-cell content is depressed by 70% at 5 days, but returns to normal by 21 days. In neutron-irradiated animals, the T-cell content is depressed by 82% 5 days after

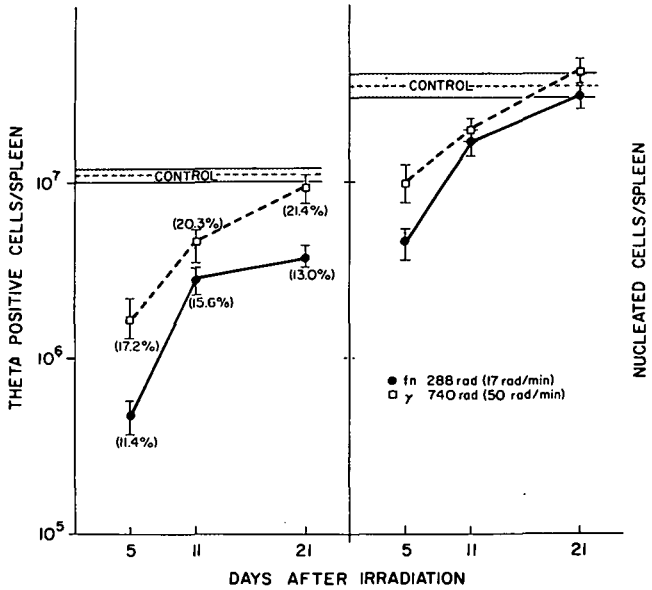

Fig. 4.3. The effect of irradiation on the spleen T-cell content and on total spleen cellularity 5, 11, and 21 days after irradiation, with the associated standard error. The percentage of T cells is shown in parentheses.

irradiation and by 21 days is still 20% below normal, although the total spleen cellularity has returned to normal. An experiment to determine the T-cell content at later times after a single dose of 240 neutron or 855 gamma rad is in progress. Eight to 10 weeks after irradiation the T-cell content in gamma-irradiated mice is depressed by 33%, whereas that in neutron-irradiated mice is depressed by 42%. Twenty, 36, and 44 weeks after neutron irradiation the spleen T-cell content is depressed by ∿ 30%, whereas 20 weeks after gamma irradiation the T-cell content is only depressed 18%. Data from later time periods after gamma irradiation are incomplete. We have examined some selected single-dose mice from the JM-2 experiment 78 to 116 weeks after irradiation. The T-cell content in gamma-irradiated mice is not significantly different from that in control mice, whereas that of neutron-irradiated mice is ∿ 50% that of comparably aged controls. These data suggest an RBE of > 3.6 at these later time points.

Since our future plans involve interspecies comparisons with *P. leucopus*, we have determined that *P. leucopus* T cells carry the θ AKR allele, in contrast to $B6CF_1$ mouse T cells which carry the θ C_3H allele. High titer anti θ AKR serum has been prepared which will allow us to compare the spleen T-cell content of irradiated *P. leucopus* with that of $B6CF_1$ mice.

Studies on the response of cultured mouse spleen cells to mitogens have been initiated during this reporting period. Preliminary experiments were designed to determine the optimum culture conditions and the mitogen concentration that gives maximum stimulation. We have found that culture of 1.5×10^6 viable nucleated spleen cells in RPMI 1640 medium supplemented with 2 mM glutamine, 10% heat-inactivated fetal calf serum, and 100 μg/ml of penicillin and streptomycin for 72 hours is optimal. The cells are suspended in 0.9 ml medium, and mitogen diluted in 0.1 ml medium is added at 0 time. The cultures are then incubated for 48 hours at 37°C in 5% CO_2. They are then pulsed with 1 μCi of tritiated thymidine (specific activity, 6 Ci/mM) and re-incubated for 18 hours. The cells are collected on Millipore filters, and the DNA precipitated with cold TCA. After drying, the filters are counted

in a liquid scintillation counter. We have found that the final concentration of Con A and PHA that gives maximum stimulation is 2 μg/ml. For LPS (Piromen, Flint Laboratory) the dose is 0.2 μg/ml. Table 4.9 shows preliminary data on the age and radiation related response of cultured spleen cells to mitogen stimulation. There is a significant decline in the response to Con A and PHA between 160 and 415 days of age. This decline parallels our previously reported decline in theta antigen with age (3). A similar decline is inferred in the response to the B-cell mitogen LPS from comparison of the tritiated thymidine activity of cells from 100-day-old mice and from 415-day-old mice. There was no significant difference to mitogen stimulation between irradiated and unirradiated control animals 250 days after gamma irradiation, or 415 days after neutron irradiation; however, the sample sizes were very small.

Table 4.9. Mitogen Stimulation of $B6CF_1$ Spleen Cells

Age (days)	Radiation[a]	Response to Mitogen[b]		
		Con A (2 μg/ml)	PHA (2 μg/ml)	LPS (0.2 μg/ml)
100	0	195,313 ± 23,878	52,826 ± 3,878	17,362[c]
160	0	137,625 ± 13,954	56,702 ± 7,503	-
250	0	57,219 ± 9,376	-	-
	855 γ	73,528 ± 6,953	-	-
330	0	95,703 ± 19,951	-	-
415	0	76,354 ± 8,762	31,164 ± 2,996	5,928 ± 2,954
	240 fn	84,908 ± 18,055	59,116 ± 11,244	9,110 ± 1,544

[a]Mice were irradiated at 110 days of age with a single dose of either 240 fn at a dose rate of 17 rad/min or 855 γ at a dose rate of 50 rad/min.

[b]The response is shown as the increase in counts per minute of tritiated thymidine from unstimulated control cultures ± 1 standard error.

[c]Only one determination at this age; 5-10 mice were used at other ages.

CONCLUSIONS

Single doses of 288 neutron rad or 740 gamma rad interfered with the ability of the host to kill a challenge dose of *P. pneumotropica* 5, 11, and 21 days after irradiation. Neutron-irradiated mice showed little repair by 21 days, but some repair was evident in gamma-irradiated mice. The same doses of radiation dramatically depressed the spleen T-cell content. The T-cell content in gamma-irradiated mice returned to normal by 21 days, but that in neutron-irradiated mice did not.

An age-related decline in the response of cultured spleen cells to mitogen stimulation was observed which closely paralleled the decline of Θ antigen previously reported (3).

REFERENCES

1. Ainsworth, E. J., R. J. M. Fry, D. Grahn, F. S. Williamson, P. C. Brennan, S. P. Stearner, A. V. Carrano, and J. H. Rust. In: Biological Effects of Neutron Irradiation IAEA, Austria, 1974, p. 359.
2. Brennan, P. C., and W. T. Kickels. The JANUS Project Semiannual Report No. 5, p. 58 (Jan., 1973).
3. Brennan, P. C., and B. N. Jaroslow. Cell. Immunol. 15, 51 (1975).
4. Brennan, P. C., R. C. Simkins, and R. T. Collins. ANL-8070 (1973), p. 20.

AGE-ASSOCIATED DECLINE IN THETA ANTIGEN ON SPLEEN THYMUS-DERIVED LYMPHOCYTES OF $B6CF_1$ MICE*

Patricia C. Brennan and Bernard N. Jaroslow

The proportion of theta-bearing cells in spleen cell suspensions of normal $B6CF_1$ mice of both sexes, from 1-900 days of age was determined using indirect immunofluorescence. By 25 days of age theta positive cells constituted ∿ 32% of the population and this proportion remained constant to 183 days of age. Between 183 and 650 days of age the proportion of theta positive cells declined linearly. The amount of theta antigen per cell also decreased with age. Theta was visualized as a continuous ring on cells from young mice and changed to a patchy distribution to faintly visible incomplete rings by 600 days of age.

The age-associated decline in theta antigen suggests that the amount of theta on the cell surface is an indicator of, and perhaps a contributor to, the functional capability of the thymus-derived cell.

---

*Abstract of a paper published in Cellular Immunology 15, 51 (1975).

A UNIQUE AND VERSATILE GAMMA IRRADIATION FACILITY

Frank S. Williamson, Gordon L. Holmblad, Joseph E. Trier, and Emil G. Johnson, Jr.

PURPOSE AND METHODS

Experience with the JM-2 experimental series has emphasized the desirability of a gamma irradiation facility which combines a capacity of at

least 400 mice per exposure with a range of dose rates encompassing at least a factor of 1000.

PROGRESS REPORT

An Atomic Energy of Canada Gammabeam 650 panoramic irradiator has been installed in the High Level Gamma Room and calibrated. As manufactured, this unit has 12 source tubes containing 12 sources which may be exposed in any combination. Furthermore, the pitch-circle diameter of the exposed sources may be adjusted so as to irradiate a central volume at high dose rates with good uniformity.

The unit was ordered with a novel source loading (Cobalt-60). The 12 sources specified were:

5000, 5000, 5000, 5000, 2500, 1250, 625, 320, 160, 80, 40, 20 Curies.

Hence, by using only 1 source we can obtain an intensity in the range 20-5000 Ci, by factors of 2. By using 2 or 4 sources of 5000 Ci the range is similarly extended to 20,000 Ci.

Panoramic Geometry

These combinations add valuable new dimensions but complicate the dosimetry. For example, no single source is ever at the center of the room and it is not feasible to mark the floor with a coordinate grid for each separate source.

A floor grid has been laid out in polar coordinates originating at the center of symmetry of the source system. A computer program has been written to calculate exposure rates from the various sources, allowing for floor scatter. In setting up an irradiation using load frames which hold mouse containers, this information is used to narrow down the zone in which exposure-rate measurements are made. A second program calculates exposure-rate distribution in the load frame, with the mean, and is used to estimate the target exposure rate, at the frame center, that will produce the desired mean. The required orientation of the frame with respect to the floor grid is also computed.

Typical conditions, showing the estimated worst-case deviation from the mean of the exposure to a single mouse, are shown in Table 4.10. A continuously variable exposure rate from 0.04 to 23 R/min is available to irradiate 500 mice in a 10-frame load, with a worst-case deviation from the mean exposure to one mouse of better than 7%.

Central Geometry

The four strongest sources are disposed in tubes so that, when exposed, they are equidistant on the circumference of a circle. In typical geometries (sources in November, 1974):

Sources on 14-cm diam circle - central exposure rate 30,000 R/min.
Sources on 30-cm diam circle - central exposure rate 8960 R/min.

In a volume 8-cm high by 8-cm diameter, the exposure rate is uniform to ± 2%.

Table 4.10. High Level Gamma Room in Panoramic Geometry Source Strength on October 17, 1974

Source Ci	Distance from Source Axis cm	Exposure Rate R/min	No. of Frames	No. of Mice	Maximum Deviation from the Mean %
16.4	300	0.037	10	500	-2.7
16.4	170	0.108	10	500	-6.1
3253	170	22.7	10	500	-6.1
12941[a]	238[b]	45.5	4	200	-3.4

[a]Four sources.

[b]From center of irradiator.

CONCLUSION

This new gamma irradiation facility provides an extremely wide range of exposure rates and will go far toward fulfilling the diverse requirements of this Division for acute and fractionated exposures.

DOSIMETRY OF A π^- BEAM AT THE ZERO GRADIENT SYNCHROTRON

Thomas B. Borak, Gordon L. Holmblad, and Frank S. Williamson

The unique electromagnetic and nuclear properties of the negative pi (π) meson make it a particularly good candidate for use in radiotherapy (1,2). Considerable radiobiological data need to be accumulated, however, before clinical applications can be inaugurated. We, therefore, participated in a particle production survey to determine if existing accelerator facilities at Argonne are adequate for a research program in pion radiobiology.

The experiment was conducted at secondary beam line 42 in the west experimental hall of the Argonne Zero Gradient Synchrotron (ZGS). This beam was designed to transport 200 MeV/c charged particles every ZGS pulse. Pilot-B plastic scintillation detectors were placed at several locations downstream of the momentum selection slit. The distance between the first and last paired coincidence counters was sufficient to allow for time of flight separation of light particles (electrons) and heavy particles (pions and muons).

Due to the pulsed nature of the beam and uncertainties in intensity, dosimetry measurements were made with a small (1.0 cm x 1.0 cm x 0.32 cm) plastic scintillator. This detector was placed at a focal point about 40 cm downstream from the last quadropole doublet, and was surrounded by a movable

water phantom. The light emitted when a charged particle passes through or interacts in the detector was sampled by a photomultiplier tube. The output was amplified and transferred into a 512 channel pulse height analyzer gated by the time of flight system.

Figure 4.4 shows several energy deposition spectra as a function of depth. Note that at zero depth both pions and muons are minimum ionizing, and therefore indistinguishable. At greater depths the pions begin losing energy more rapidly than do the muons and the resulting heavier ionization is characterized by a progressive shift toward higher energy deposition. Finally near the end of the pion range the high LET nuclear fragments deposit large amounts of energy, whereas the muons are just beginning to slow down. The small shoulder at low energies is produced by minimum ionizing electrons.

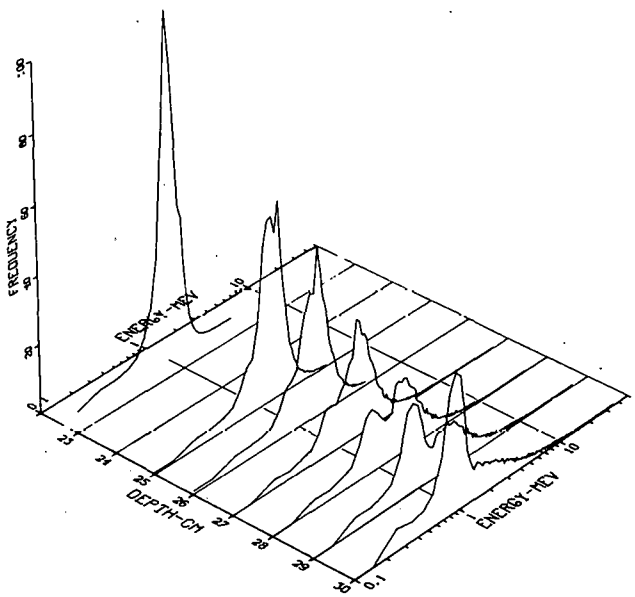

Fig. 4.4. Differential energy-deposition spectra of 200 MeV negative pions at various depths in a water phantom.

These differential energy spectra can be integrated to yield absorbed dose in the plastic as a function of depth in the phantom. Figure 4.5 shows the relative depth dose properties observed in this experiment. The characteristic peak at the pion end of range is clearly evident. However, the slope of the "plateau" region is much steeper than reported elsewhere (3,4).

A calculation incorporating multiple Coulomb scattering (MCS) and nuclear collisions was made to aid in interpreting the observed slope. We assumed a parallel beam with intensities weighted by transverse beam profile measurements. MCS was incorporated in the form of an energy dependent gaussian with ionization energy loss according to the work of Sternheimer (5,6). A polynomial fit was used for the nuclear scattering cross section, noting that the incident energy (104 MeV) lies within the P_{33} π-nucleon resonance region (7).

The results of this calculation, shown by the dashed curve in Figure 4.5, are in excellent agreement with a Monte Carlo computation also using a parallel beam (8). The divergence between the calculated and measured data

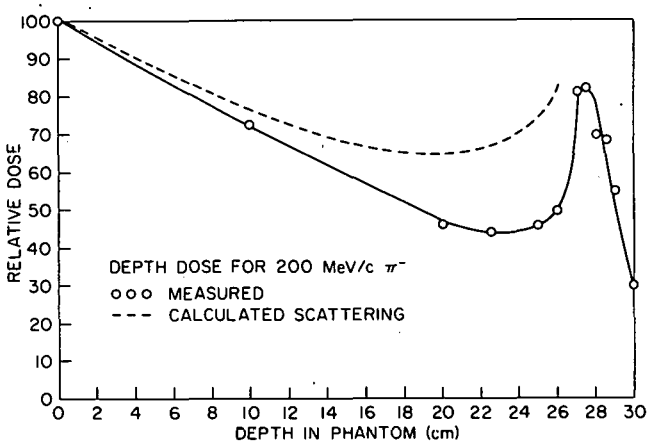

Fig. 4.5. Measured and calculated depth dose distributions for 200 MeV negative pions.

suggests that the greater slope may be caused by the large geometrical fluctuations of the beam at the focal point of the magnetic lens.

Using the measured value of absolute intensity per pulse and a duty cycle of 1 pulse every 4.6 seconds, we arrived at a dose rate in the stopping region of 1.2 ± 0.3 mrad/min. Attempts to measure the dose with ionization chambers were unsuccessful because of the extremely small signals produced by this beam intensity.

CONCLUSIONS

The dose rate of 1.2 mrad/min is several orders of magnitude below that convenient for radiobiological experiments. This could be increased by a factor of 4 by increasing the external proton beam current on the beam 42 production target. The secondary particle contamination in a 100 MeV pion beam produced from a 12 GeV source deserves strict attention. Reliability and tolerance levels of all beam components must be carefully scrutinized since biological specimens, as opposed to fast electronics, cannot "gate-off" after each beam separator failure.

ACKNOWLEDGMENT

We wish to acknowledge the cooperation of the Argonne Accelerator Facilities Division.

REFERENCES

1. Fowler, P. H., and D. H. Perkins. Nature (London) 180, 524 (1961).
2. Fowler, P. H. Proc. Phys. Soc. (London) 85, 105 (1965).
3. Sullivan, A. H., and J. Baarli. CERN Rep. DI/HP/148 (1972).
4. Dutrannois, J. R., R. N. Hamm, J. E. Turner, and H. A. Wright. Phys. Med. Biol. 17, 765 (1972).
5. Sternheimer, R. M. Phys. Rev. 91, 256 (1953).
6. Sternheimer, R. M. Phys. Rev. 103, 511 (1956).
7. Lock, W. O., and D. F. Meadsay. Intermediate Energy Nuclear Phys, Metheun, London, 1970.
8. Wright, H. A. Oak Ridge National Laboratory. Personal communication (1974).

A QUALITY CONTROL TECHNIQUE FOR GEOMETRICAL REPRESENTATIONS IN THE BIM-130 MONTE CARLO TRANSPORT CODE

Thomas B. Borak

PURPOSE AND METHODS

The BIM dosimetry group maintains a large Monte Carlo neutron-gamma ray transport code titled BIM-130 (1). This code is used to compliment and in some instances supplement physical measurements. It has the capacity to trace the intersection and scattering of particles through 45 geometric regions, each of which has a chemical composition containing up to 15 elements.

The 45 regions are mathematically defined in the program through a three-dimensional Cartesian coordinate system. The boundaries are prescribed by input data containing the central location and orthogonal half widths. With this type of arrangement there is always a problem of quality control; mainly, is the information on the data cards correctly converted into the true geometrical pattern of interest within the program? A small error could be drastic and expensive!

We have developed a test code to check and confirm the shapes of the regions described by the input data. The program, called BIMBOX, uses the actual portion of the Monte Carlo code which makes geometrical decisions. To this is coupled an arsenal of idealized particle sources which can be aimed with chosen directions and locations. The intersections of these particles with respective regions is scored and stored in appropriate arrays. These arrays are then displayed in the form of printer plots and if desired on a Calcomp plotter using the ANL DISSPLA package.

Figure 4.6 shows the configuration of an irradiation room (15.5 x 5.0 m^2) filled with nested cylinders whose axes of rotation are parallel to the Z direction. The central region is reduced to a straight line, but can be magnified by using the ZOOM characteristics of the program.

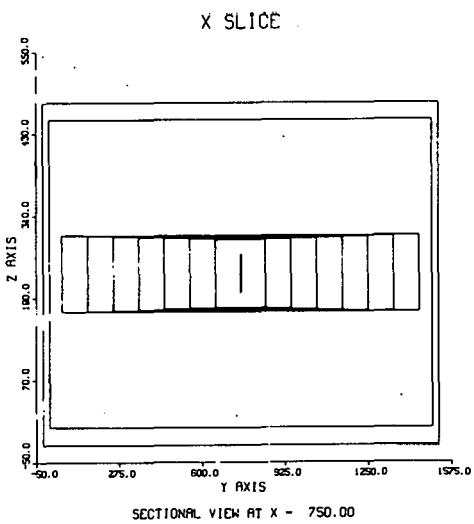

Fig. 4.6. Elevation view of an irradiation facility filled with concentric cylinders. The vertical line in the center contains the ^{60}Co source.

Figures 4.7 and 4.8 show two magnified views of the central region which represents the capsulated ^{60}Co source in an AECL Gamma Beam 150.

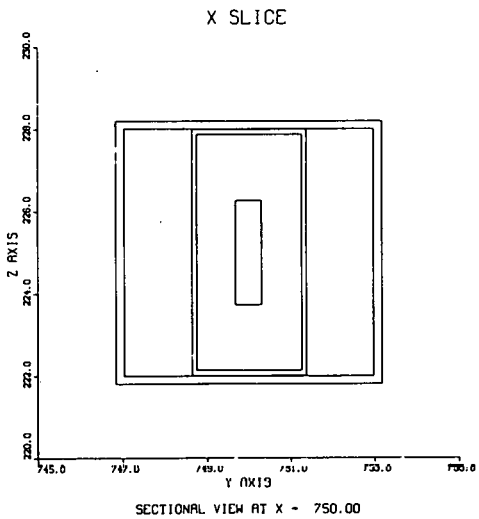

Fig. 4.7. Magnified elevation view of the ^{60}Co source and container shown in Figure 4.6.

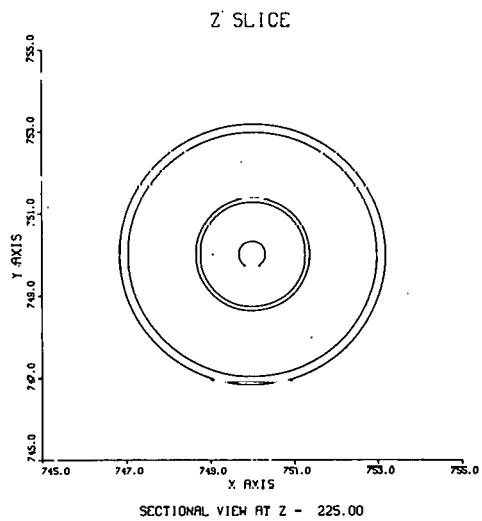

Fig. 4.8. Plan view of the ^{60}Co source and container shown in Figure 4.7.

The correct nesting sequence can be confirmed in the printer plots where the boundaries of each region are identified with coded characters. Execution for this example of 16 regions was performed within 250 K bytes of core in less than 30 seconds on an IBM 370/195.

REFERENCE

1. Frigerio, N. A., R. F. Coley, and M. H. Branson. Phys. Med. Biol. 18, 53 (1973).

A SIMPLE APPROACH TO CALCULATING GAMMA RAY SKYSHINE FOR REDUCED SHIELDING APPLICATIONS

Thomas B. Borak

PURPOSE AND METHODS

New irradiation facilities at ANL (1) and elsewhere are being designed with the minimum radiation shielding. Usually the first victim of these austerity measures is the roof. This increases the amount of radiation escaping skyward and atmospherically reflected toward neighboring facilities. Below we present a simplified single scatter treatment of SKYSHINE. The pessimistic case with forward shielding wall and source reduces to a single summation which can be performed on a desk calculator.

Given a monoenergetic isotropic source of gamma rays, the intensity of singly scattered photons at distance X can be represented by (see Figure 4.9):

$$I = \frac{SN}{4\pi X} \int_{\psi_o}^{\pi-\phi_o} d\psi \int_{\phi_o}^{\pi-\psi} d\phi \int_{0}^{A_z} dAz \; \frac{d\sigma}{d\Omega}(\theta = \psi + \phi) \qquad (1)$$

where

S = photons/second emitted by source
N = number of electrons/cm^3 in air
$\frac{d\sigma}{d\Omega}(\theta)$ = differential Compton scattering cross section (cm^2/electron)
A_z = Azimuthal acceptance of scattering volume
X = distance from source to detector in cm.

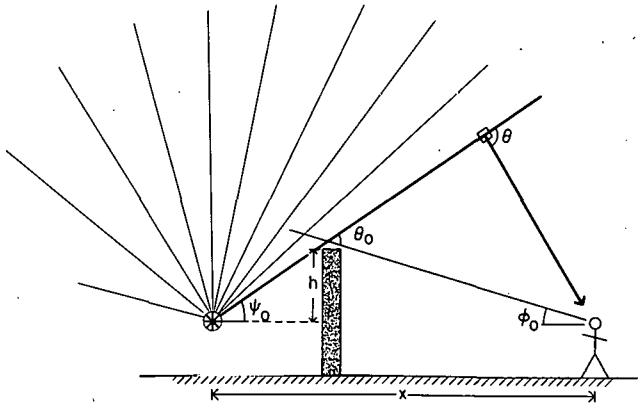

Fig. 4.9. Schematic diagram illustrating the symbols and angles defined by equations 1-5. The wall in all cases is perpendicular to the vector along X, with effective height above source equal to h.

For the pessimistic case of full hemispherical scattering volume ($A_z = \pi$), the elevation of the shielding wall reduces to a semicircle of radius h. The photon energy scattered into the detector at X is:

$$I_E = \frac{E_\gamma SN}{4X} \Delta\theta^2 \sum_{\theta = \psi_o + \phi_o}^{179} (\theta + 1 - \psi_o - \phi_o) \frac{d\sigma_E}{d\Omega}(\theta) \qquad (2)$$

Here the sum is carried over integral degree values but the differential increment remains in radians ($\Delta\theta = 0.0175$). All energy units are in MeV. The energy scattered Compton formula can be obtained graphically (2) or calculated:

$$\frac{d\sigma_E}{d\Omega} = 3.97 \times 10^{-26} [F^2 + F^4 - F^3 \sin^2 \theta] \qquad (3)$$

$$F = \frac{E}{E_\gamma} = \left[1 + \frac{E_\gamma}{.511} (1 - \cos \theta)\right]^{-1} \qquad (4)$$

Realistically the azimuthal acceptance is limited by the size of the forward wall or side walls. For the case of a semi-infinite wall of height h, the limits of integration depend on ψ, but can easily be incorporated yielding:

$$I_E = \frac{E_\gamma SN}{4\pi X} \int_{\psi_o}^{180-\phi_o} d\psi \int_{\phi_o}^{180-\psi} d\phi \; 2 \cos^{-1}\left(\frac{h \sin(\psi + \phi)}{X \sin(\psi) \sin(\phi)}\right) \frac{d\sigma_E}{d\Omega}(\psi + \phi) \qquad (5)$$

where now a double sum must be performed.

The dose rate can be obtained by multiplying the results by the appropriate first collision flux to dose conversion factors. Although complex in appearance these sums can easily be made and dose rates rapidly calculated to obtain the potential hazard at various locations outside of the structure.

REFERENCES

1. Norris, W. P., Argonne National Laboratory. Personal communication (1974).
2. Segré. E. Nuclei and Particles, W. A. Benjamin Inc., New York, 1964, p. 55.

5. CARCINOGENESIS

SUMMARY

R. J. Michael Fry, Group Leader

The current studies in this program are concerned with hepatic tumorigenesis and the enhancement of chemically induced tumors, isozymes, the effects of treatment with psoralen and ultraviolet light, and strain and species differences in both spontaneous and induced tumor rates. While the range of these studies seems diverse we have concentrated on three main tissues, namely liver, lung, and skin.

The approaches are interrelated and they have been selected to investigate major aspects of tumorigenesis, such as the factors determining susceptibility, the control of gene expression and the alterations with tumorigenesis, and the role of specific molecular lesions in initiation, acceleration, and co-carcinogenesis.

Most experiments designed to investigate the mechanisms and other aspects of tumor induction take considerably longer than the interval between these reports. Despite that there are some interesting new results in the various reports that follow.

The results from our study of skin tumors on the question of a causal relationship between photoadducts, resulting from exposure to UV light after treatment with psoralen are now accumulating. One interesting aspect of these studies is the attempt to use various cell and tissue responses as assays of the dose so that we can meaningfully compare the effects of different wavelength spectra. The current results suggest that the psoralen bifunctional adducts are not, at least by themselves, the molecular lesion responsible for the skin tumors. On the other hand, the results underline the possible importance of synergistic lesions induced by different wavelengths. These studies of skin tumors benefit from the information being obtained on cells *in vitro* by the Mammalian Cell Biology section and the findings on the effects of exposure to near UV by members of the Genetics group.

It is becoming increasingly clear that much has to be done on both the synergistic and co-carcinogenic effects of combinations of various chemical compounds and also of chemical agents and exposure to light. In the case of chemical co-carcinogenesis, the liver tumor test system, using a brief period of administration of 2-acetylaminofluorene (AAF) to weanling rats, has proven

an excellent method for testing agents for enhancing or co-carcinogenic potential. The future studies on the mechanism of co-carcinogenesis have been helped by the finding that of the two compounds, phenobarbital and amobarbital, which are similar both in structure and many of their pharmacological actions, only phenobarbital is an enhancer. It is now possible to eliminate from consideration a number of metabolic activities which are common to the two drugs and therefore to narrow the choice of possible activities that could be associated causally with enhancement.

The detection of changes in the isozyme patterns in various tumors is being used to study the changes in gene expression accompanying the events that result in malignant transformation of cells. Of considerable interest is the finding that changes in the aldehyde dehydrogenase isozyme patterns occur prior to the detection of any histological evidence of tumor formation. Not only have the studies on aldehyde dehydrogenase isozymes in liver tumors been continued, but the investigations of gene expression and tumorigenesis, as detected by isozyme patterns, have been extended to both thymic lymphomas and lung tumors. In these studies, every opportunity will be taken to probe the possible differences between the advancement of the time of appearance of tumors by various agents, such as in murine lung tumors, and the induction of tumors.

Again this year, the productive collaboration with other groups, divisions, and institutions is evident from some of the following reports, such as "A comparison of the incidence of tumors obtained by two methods of sampling" and "Microscopic tracing of deuterium," and also from reports that are included in Chapters 4 and 7 of this report.

CARCINOGENESIS STAFF

REGULAR STAFF

Buess, Evelyn M. (Scientific Assistant)
Cameron, Erma C. (Scientific Assistant)
Chubb, G. Theodore (Scientific Assistant)
Devine, Rosemarie L. (Scientific Assistant)
Feinstein, Robert N. (Senior Biochemist)
Fry, R. J. Michael (Senior Physiologist)
Grube, Donald D. (Scientific Assistant)
Kisieleski, Walter E. (Chemist)
Ludeman, V. Ann (Scientific Assistant)
Peraino, Carl (Biochemist)
Prapuolenis, Aldona M. (Scientific Assistant)
Sallese, Anthony R. (Scientific Assistant)
*Staffeldt, Everett F. (Scientific Assistant)
*Tahmisian, Theodore N. (Senior Biologist)

TEMPORARY STAFF DURING 1974

Lindahl, Ronald G. (Postdoctoral Appointee)
Morris, J. Emory (Visiting Scientist)

---

*Retired June 30, 1974.

COMPARATIVE ENHANCING EFFECTS OF PHENOBARBITAL, AMOBARBITAL, DIPHENYLHYDANTOIN, AND DDT ON 2-ACETYLAMINOFLUORENE-INDUCED HEPATIC TUMORIGENESIS IN THE RAT

R. J. Michael Fry, Carl Peraino, and Everett Staffeldt

PURPOSE AND METHODS

Last year we reported the initial results of the experiment designed to compare the enhancing or co-carcinogenic effects of amobarbital, diphenylhydantoin, DDT, and butylated hydroxytoluene (BHT) with those of phenobarbital (1). These studies have used a sequential feeding of chemicals. Weanling rats are fed for a brief period the hepatocarcinogen 2-acetylaminofluorene (AAF) at a dose level which produces a significant but low incidence of liver tumors within one year. The chemicals under test for effects on tumorigenesis are then included in the diet for the rest of the lifetime. The experiment is now complete, and the histological examination and classification of all the lesions has been carried out.

The lesions involving hepatocytes have been classified into the following types: 1) Hyperplasia and hypertrophy; while these lesions appear to represent a new cell population with altered proliferation rate and glycogen metabolism, the main characteristics of normal liver structure are maintained. 2) Adenomas; the characteristics of these lesions are an increased cell proliferation and highly differentiated cells, but abnormal liver cords and loss of lobular structure. The tumors, while they may grow to replace most of the normal tissue, do not show the characteristic invasive properties indicative of malignancy, nor do they appear to metastasize. 3) Hepatocellular carcinomas; these malignant tumors include types that have been called trabecular, because of the thickness of the liver cords; types called adenomatous, because the cell arrangement is acinar; and lastly, a mixture of both these types. The degree of pleomorphism, the degree of proliferation, the frequency of obviously abnormal mitoses, and the incidence of metastases all vary considerably.

RESULTS

The incidence of adenomas and carcinomas has been separated in Figure 5.1, but pooled in Figure 5.2. In Figure 5.1, it is clear that up to 482 days the enhancing effects of phenobarbital and DDT are mainly restricted to the more highly differentiated tumors. The data suggest, perhaps, that growth control rather than some of the other aspects of neoplastic change is involved. The increase in malignant tumors at the end of the experimental period raises the question of whether these compounds also increase the malignant tumor rate. Furthermore, it is not clear whether a progressive increase in the incidence of malignant tumors would have occurred in time, either due to progression of benign tumors to a malignant state or due to a late appearance of malignant tumors induced earlier.

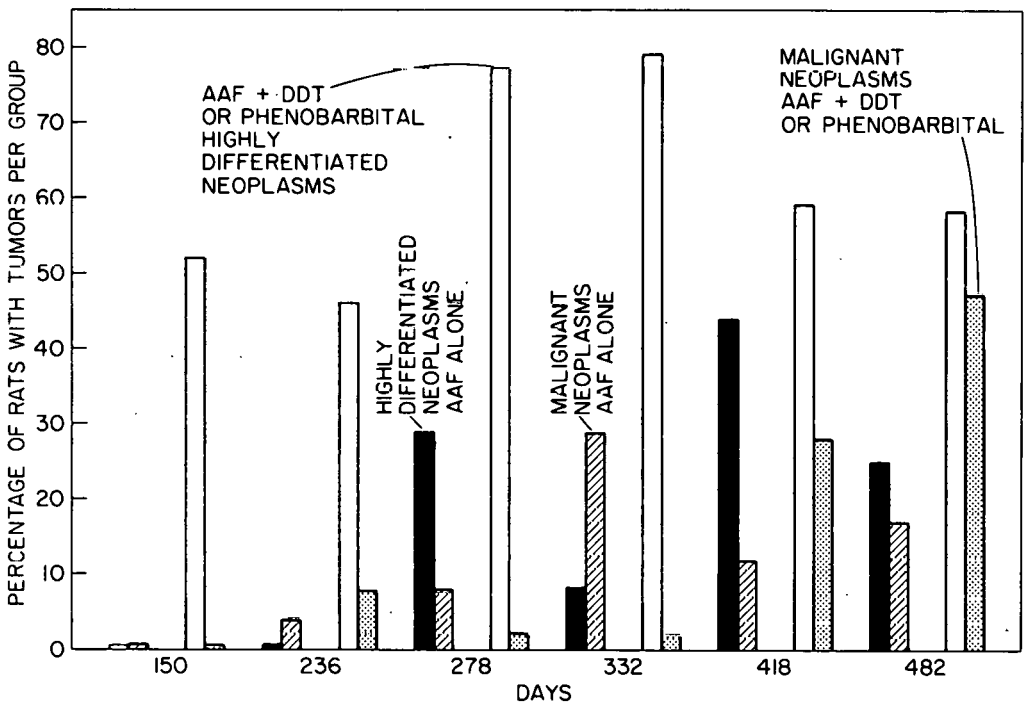

Fig. 5.1. The percentage of rats bearing tumors at intervals after the cessation of treatment with AAF. The incidence of adenomas and carcinomas are recorded separately. The data for the groups of rats given AAF followed by DDT and AAF followed by phenobarbital have been pooled. Thus, the data are based on 23, 48, 48, 48, 44, and 25 rats, respectively, for the times indicated.

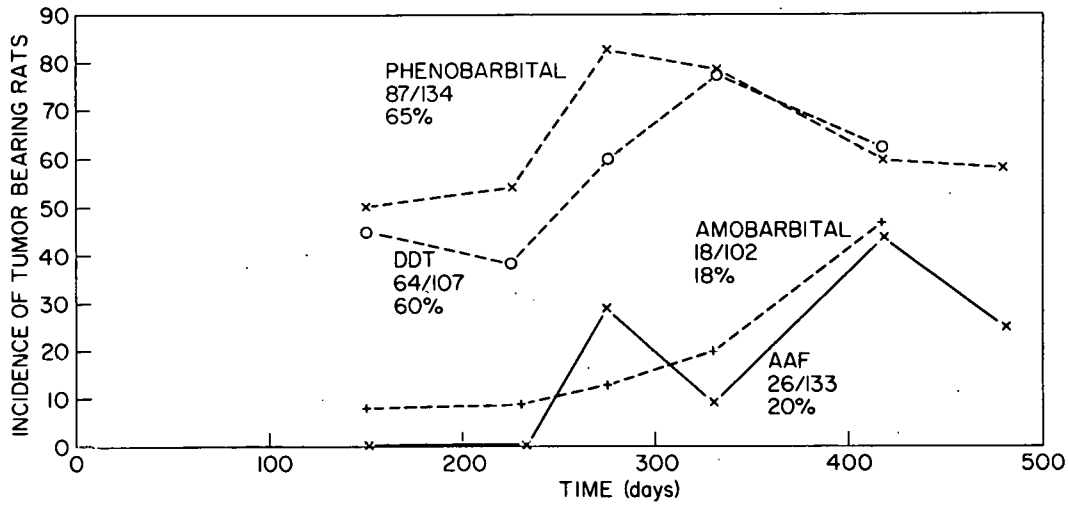

Fig. 5.2. The percentage of rats with either adenomas or carcinomas as a function of age. The data have been obtained from about 24 rats killed within 3 weeks of the time intervals indicated. Also shown are the total number of rats and tumor-bearing rats in the various experimental groups.

Figure 5.2 illustrates the effect of phenobarbital and DDT compared to amobarbital; it is clear the latter does not enhance the tumor incidence. It was also found that neither diphenylhydantoin nor BHT acted as co-carcinogenic agents.

CONCLUSIONS

1. The sequential feeding of chemical agents is a useful technique for investigating co-carcinogenesis.

2. Judicious selection of agents, based on both chemical structure and pharmacological action, provides a method for probing the mechanisms involved in co-carcinogenesis. We are currently using this method. In addition, we are studying the specific effects on liver cell metabolism of enhancers or co-carcinogens, in comparison to the effects of similar compounds without any co-carcinogenic activity.

REFERENCES

1. Peraino, C., R. J. Michael Fry, and E. Staffeldt. ANL-8070 (1973), p. 65.
2. Stewart, H. L. In: The Physiopathology of Cancer, Ed. F. Homburger. Paul B. Hoeber Inc., New York, 1953, p. 85.

EFFECTS OF PHENOBARBITAL AND 2-ACETYLAMINOFLUORENE ON HEPATIC CELL TURNOVER

Carl Peraino, Walter E. Kisieleski, and R. J. Michael Fry

PURPOSE AND METHODS

Previous studies have shown that dietary phenobarbital enhances 2-acetylaminofluorene (AAF)-induced hepatic tumorigenesis in the rat (1,2). Among the potential mechanisms for this enhancement is the possible prolonged, low-level toxic effect of extended phenobarbital feeding on liver cells. If such toxicity exists and is sufficiently severe, it might be manifested in rats fed phenobarbital alone. A marginal degree of toxicity, however, might only become apparent in cells sensitized by prior exposure to AAF. In either case expression of such toxicity should be characterized by increased cell loss and replacement occurring throughout the period of phenobarbital treatment. The enhancing effect of phenobarbital on tumorigenesis might then be ascribed in part to the creation of such a proliferative milieu.

One hundred eighty male rats, 24 days old, were each given four daily intraperitoneal injections of tritiated thymidine (0.2 μCi/g body weight). On the first injection day (Day 1), 90 of these rats were placed on a diet containing 0.02% AAF and the remainder were placed on a control diet. Five rats from each group were killed on Day 5 and their livers were analyzed for DNA labeling (see below). On Day 18, the rats receiving AAF were shifted to the control diet. On Day 20, another 5 rats from the AAF and control groups were analyzed. On Day 25, forty of the rats that had received AAF and forty that had been fed only the control diet were shifted to a diet containing 0.05% phenobarbital; the remaining rats were kept on the control diet. No further dietary changes were made during the experiment.

Five rats from each group were killed at the intervals shown in Figures 5.3 and 5.4, their livers were removed, and hepatocyte nuclei were isolated (3). Nuclear samples were prepared for autoradiography. Trichloroacetic acid insoluble radioactivity was determined on additional samples of nuclei and on aliquots of whole liver homogenate.

PROGRESS REPORT

Figure 5.3 shows the kinetics of DNA loss from the liver during the experiment. After an initial loss of DNA, which was greater for rats receiving AAF, the DNA labeling for both the AAF-treated and control rats remained relatively constant during the remainder of the experiment. The feeding of phenobarbital to rats previously fed the control diet produced a short-lived decrease in labeling after which the labeling pattern paralleled that of the controls. In rats previously fed AAF, phenobarbital feeding did not alter the DNA retention pattern from that seen in rats treated with AAF alone, i.e., neither group showed a long-term progressive loss of DNA.

Figure 5.4 shows the change in the ^{3}H level per 10^{6} nuclei during the experiment. Reduction in the ^{3}H level could reflect loss of cells from the liver and/or increased proliferative activity with growth or in response to injury. The likelihood that both cell loss and increased proliferation are

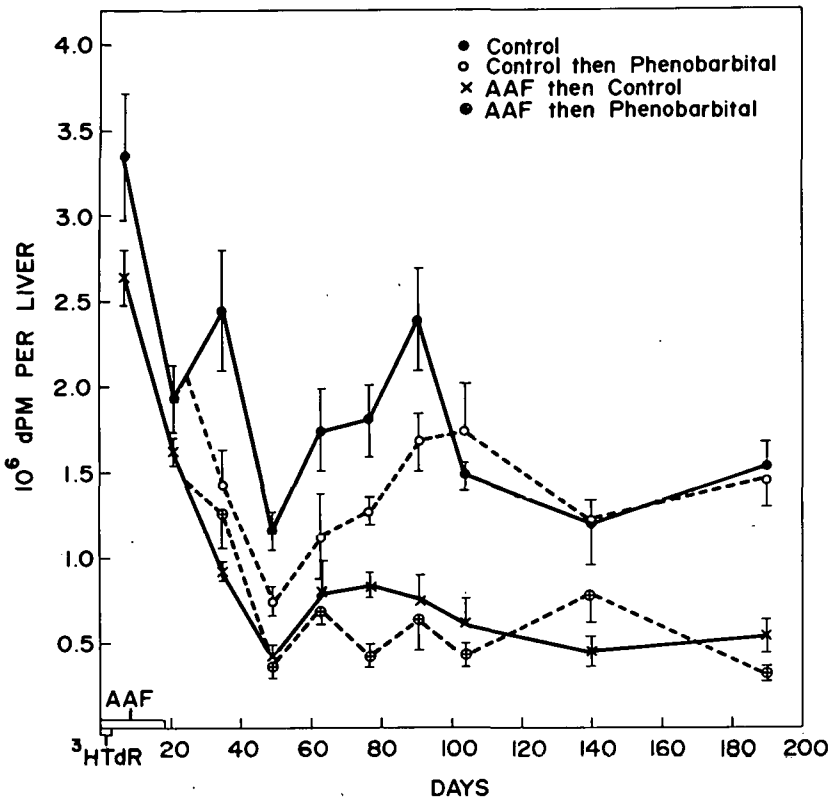

Fig. 5.3. Effects of dietary AAF and/or phenobarbital on the loss of prelabeled DNA from the liver.

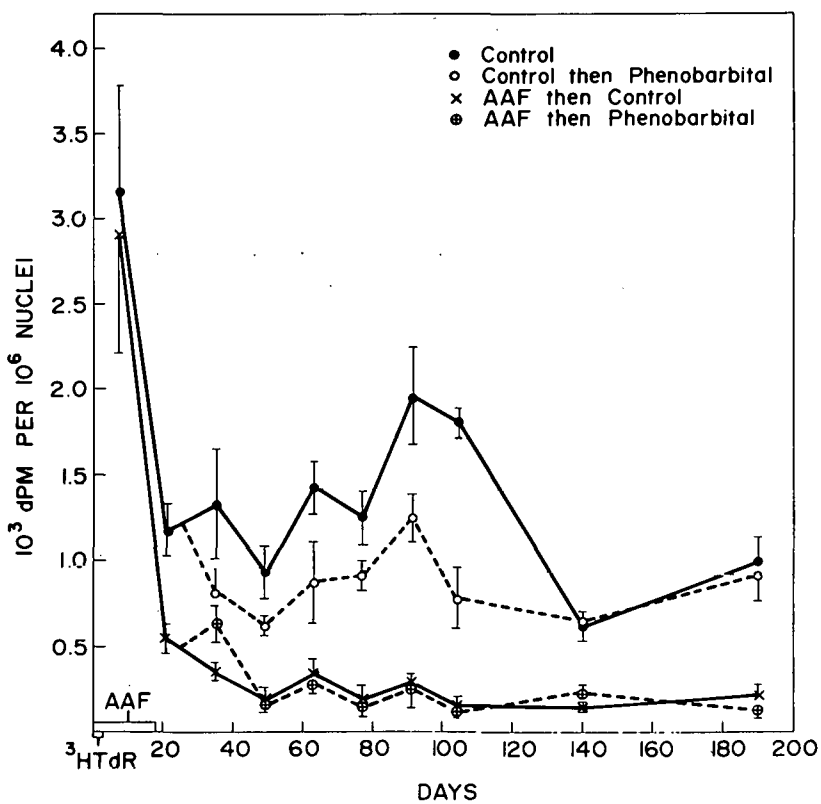

Fig. 5.4. Effects of dietary AAF and/or phenobarbital on the concentration of prelabeled hepatocyte nuclei in the liver.

occurring is suggested by a comparison of the kinetics of label retention in Figures 5.3 and 5.4 during the first 20 days after labeling. Thus, the decrease in the proportion of nuclear label during this period (Figure 5.4) substantially exceeded the decrease in total labeled DNA retention (Figure 5.3), the difference being attributable to hepatocyte proliferation. After approximately 40 days, the amount of label per cell in all groups (Figure 5.4) remained virtually constant, as did the total retention (Figure 5.3). This similarity indicates that proliferative activity as well as cell loss was not significant after approximately 40 days in any of the groups.

CONCLUSIONS

1. Significant cell loss (measured as a decrease in the retention of labeled DNA) and increased proliferative activity (indicated by a larger decrease in the proportion of nuclear label) occur in the livers of rats during the first 40-60 days after weaning (22 days of age). Subsequently, however, these processes virtually cease, resulting in the retention of a constant level of prelabeled DNA and a constant proportion of nuclear label.

2. Feeding AAF for 18 days during the period of cell proliferation and cell turnover described above increases both processes, but does not influence the subsequent cessation of cell loss and proliferation.

3. Phenobarbital feeding to rats not previously given AAF produces brief increases in cell loss and cell proliferation, but has no long-term effects on these processes even though fed continuously. Phenobarbital feeding to rats previously fed AAF has no effect on cell loss or proliferation. Thus, continuous exposure to dietary phenobarbital does not appear to produce any evidence of prolonged low-level toxicity that might be expressed as a continuing turnover of hepatocytes, whether or not these hepatocytes have been previously exposed to AAF.

REFERENCES

1. Peraino, C., R. J. M. Fry, and E. Staffeldt. Cancer Res. 31, 1506 (1971).
2. Peraino, C., R. J. M. Fry, E. Staffeldt, and W. E. Kisieleski. Cancer Res. 33, 2701 (1973).
3. Blobel, G., and V. R. Potter. Science 154, 1622 (1966).

EFFECTS OF DIETARY PHENOBARBITAL ON THE BINDING OF 2-ACETYLAMINOFLUORENE TO RAT LIVER NUCLEAR DNA*

Phillip S. Mushlin† *and Carl Peraino*

Previous studies have shown that dietary phenobarbital reduces 2-acetylaminofluorene (AAF)-induced hepatic tumorigenesis when fed simultaneously with the carcinogen, but enhances tumorigenesis when fed after the cessation of AAF feeding. Since DNA may be a primary target of chemical carcinogens, the effects of phenobarbital on the binding *in vivo* of AAF metabolites to hepatic nuclear DNA were investigated. The results show that the prolonged feeding of phenobarbital prior to the injection of AAF-9-^{14}C reduced the binding of label to DNA, but the binding of label was not reduced if phenobarbital feeding was begun after the injection of AAF.

---

*Abstract of a paper appearing in the Proceedings of the Society for Experimental Biology and Medicine 145, 859 (1974).

†Spring 1973 participant in the Undergraduate Honors Research Participation Program, The Colorado College.

"NOTHING DEHYDROGENASE" IN THE MOUSE THYMUS AND IN MOUSE THYMIC LYMPHOMAS

Robert N. Feinstein and Erma C. Cameron

PURPOSE AND METHODS

"Nothing dehydrogenase" (N.D.) is the designation applied to a widely distributed enzyme activity, of unknown nature, which has the ability to transfer electrons to certain acceptors even in the absence of added substrate. Whatever may be its exact nature, preliminary observations suggested that the isozyme pattern of N.D. in thymic lymphoma sometimes differed from the pattern of normal thymus, and it is this phenomenon that we have briefly investigated.

PROGRESS REPORT

Because the N.D. is commonly detected in a system consisting of NAD, PMS (phenazine methosulfate), and NBT (nitroblue tetrazolium), plus an enzyme source, we have attempted to establish, by a series of color reactions, whether or not the electron donor might actually be NAD, PMS, or NBT, acting in some hitherto unconsidered fashion. The results have thus far been inconclusive; the experiments are continuing.

From the oncological point of view, the original observation has been confirmed: the thymus of a mouse bearing a thymic lymphoma exhibits a nothing dehydrogenase isozyme pattern which often, but not invariably, shows fewer than the five bands regularly observed in the normal mouse thymus.

CONCLUSIONS

Although not a completely consistent phenomenon, the thymus of a mouse bearing a thymic lymphoma often shows fewer isozyme bands of "nothing dehydrogenase" than does the thymus of a normal mouse.

GLUCOSE-6-PHOSPHATE DEHYDROGENASE (G6PD) AND 6-PHOSPHOGLUCONATE DEHYDROGENASE (6PGD) ACTIVITIES OF NORMAL MOUSE LUNG AND OF MOUSE LUNG TUMORS

Robert N. Feinstein and Erma C. Cameron

PURPOSE AND METHODS

Our preliminary screening of several animal tissues, normal and tumorous, for a variety of dehydrogenases, suggested that a mouse lung tumor differed from the normal lung in the activity and electrophoretic pattern of G6PD. The assay used was one commonly employed: using glucose-6-phosphate (G6P) as substrate and NADP as coenzyme, the G6PD activity is measured as the increase in A_{340} as NADP is reduced to NADPH. Electrophoresis was performed on polyacrylamide gels, the location of the G6PD being detected by incubation in a mixture of G6P, NADP, phenazine methosulfate, and nitroblue tetrazolium.

PROGRESS REPORT

It has become evident that results were being confused by two previously unconsidered factors:

(a) The enzyme activity is relatively unstable. Considerable losses apparently occur upon storage in the ultra-deep freeze (ca. -80°C) for several months, and great losses are also occasioned by the use of ultrasonic treatment of a lung homogenate. In future studies, lungs will be examined after no more than two weeks storage at -80°C, and they will be homogenized but not sonicated.

(b) The assay system, as originally employed, gives invalid results. G6P is converted by its enzyme, G6PD, to 6-phosphogluconate (6PG), with the concomitant reduction of NADP to NADPH. The 6PG in turn can be further oxidized by the enzyme 6-phosphogluconate dehydrogenase (6PGD) [6-phospho-D-gluconate:NADP oxidoreductase (decarboxylating), EC 1.1.1.44] to ribulose-5-phosphate, with the concomitant reduction of more NADP to NADPH. Thus, what we first considered the straightforward assay of a single enzyme activity proves to measure the sum of the G6PD and 6PGD reactions. A new assay system has now been devised, in which the system is loaded with 6PG, and the production of NADPH is measured in the absence, and in the added presence, of G6P. In this way we are able to measure the two enzyme activities separately.

Although few data have yet been obtained with these new techniques, preliminary results suggest that lung tumor tissue may regularly have a greater activity of both enzymes than is found in normal lung. G6PD activity is

apparently the more strongly affected. The results of acrylamide gel electrophoresis thus far indicate that the changes are quantitative only; no qualitative differences between the isozyme pattern of normal lung and lung tumor tissue have been observed.

CONCLUSIONS

After we modified certain points of technique, preliminary results suggest that mouse lung tumor has a higher activity of glucose-6-phosphate dehydrogenase, and of 6-phosphogluconate dehydrogenase, than does normal mouse lung.

FURTHER STUDIES ON ALDEHYDE DEHYDROGENASE ISOZYMES IN THE AAF-INDUCED HEPATOMA OF SPRAGUE-DAWLEY RATS

Robert N. Feinstein and Erma C. Cameron

PURPOSE AND METHODS

In a previous report (1), we pointed out that the hepatoma induced in the Sprague-Dawley rat by acetylaminofluorene (AAF) contained aldehyde dehydrogenase (Ald D) isozymes which differed both qualitatively and quantitatively from those of normal liver. The new forms were more stable and more active than the normal forms, and they also differed in coenzyme and substrate specificity. The present report continues the earlier studies and describes further refinements in assessing the differences between the two sorts of isozyme. Part of the refinement was brought about by recognition of previously unconsidered complications in the test system, and part by the use of the LKB "Multiphor" equipment, which separates isozymes by their isoelectric point (pI) as they migrate through polyacrylamide gel; the resulting definition is much finer than can be achieved by the use of polyacrylamide gel electrophoresis alone.

PROGRESS REPORT

The polyacrylamide gel electrophoresis (PAGE) system has been used to obtain more complete and more accurate information than previously by the recognition of two previously unconsidered findings: First, not all bands observed in our standard PAGE test system are true Ald D isozymes; some of them prove to be aldehyde oxidase, and some are "nothing dehydrogenase," an enzyme activity of unknown nature which exhibits bands in the standard test system even if no substrate has been added. Second, despite the use of ordinarily sufficient precautions, cross-contamination by slightly volatile substrates gives erroneous bands on some gels. The development of complete controls and extraordinary precautions now enables us to identify true Ald D with assurance.

Regard for these extremely stringent precautions, together with the use of the Multiphor apparatus for fine-line separation by pI, now permits the following statements:

Two distinct sets of Ald D isozymes, distinguishable by isoelectric point, are to be found in Sprague-Dawley rat liver and hepatoma. One set, with pI about 6.8-7.1 (the "neutral" isozymes), is the heavily predominant set in the tumor and exists very weakly or not at all in normal liver. These isozymes can use either NAD or NADP as coenzyme. The other set of isozymes has a pI of 6.2-6.4 (the "acid" isozymes). The acid set of isozymes is found in both normal liver and hepatoma, and its activity has an absolute requirement for NAD.

CONCLUSIONS

Based on the above, and on some earlier studies on cellular distribution, we conclude that the carcinogenic change, in the particular tumor under discussion, brings about the production of a large activity of an entirely new set of molecular forms of aldehyde dehydrogenase. The tumor also produces the normal set of isozymes, but they now represent a minor fraction of the total activity. The new forms probably exist in the cytoplasm; the normal forms, in microsomes and mitochondria.

REFERENCE

1. Feinstein, R. N., and E. C. Cameron. ANL-8070 (1973), p. 63.

PURIFICATION AND CHARACTERIZATION OF ALDEHYDE DEHYDROGENASE FROM NORMAL RAT LIVER AND FROM AAF-INDUCED RAT HEPATOMAS

Ronald Lindahl and Robert N. Feinstein

PURPOSE AND METHODS

In normal Sprague-Dawley rat liver, different isozymes of aldehyde dehydrogenase (aldehyde:NAD oxidoreductase, EC 1.2.1.3) are present in subcellular particles in the cytoplasm. In the acetylaminofluorene (AAF)-induced liver tumors of these rats, however, the predominant forms of aldehyde dehydrogenase are three major and two minor forms of the related enzyme aldehyde: NAD(P) oxidoreductase, EC 1.2.1.5; the tumor in addition shows traces of the normal liver isozyme forms. (In what follows, the abbreviation Ald D refers to either or both of EC 1.2.1.3 and 1.2.1.5). To determine whether these hepatoma Ald D isozymes are the result of derepression of a normally repressed gene(s), or the result of post-translational modification of otherwise normal enzyme species, isozymes from both normal liver and hepatoma must be isolated and characterized.

The purification procedure for both normal liver and hepatoma Ald D consists of $(NH_4)_2SO_4$ fractionation, DEAE-Sephadex chromatography, and preparative isoelectric focusing. The isoelectric focusing step isolates the individual isozymes as single homogeneous species.

PROGRESS REPORT

The hepatoma Ald D isozymes have been purified 30-fold. At this stage of purity the five isozymes are uncontaminated by any other protein species. The isolation of the five isozymes together has been necessary, as the molecular weights and subunit composition of these species are unknown. Determination of molecular weights by G-200 gel filtration yields a molecular weight of 105,000 ± 2000 daltons for the functional species. Subunit molecular weight determined by SDS-gel electrophoresis is 53,000 daltons, indicating that the functional species is a dimer. Due to precipitation of the isozymes, efforts to determine the number of different subunit types by reversible denaturation in guanidine-HCl or urea have been unsuccessful. Monomerization of the dimers by acid-gel electrophoresis (pH 2.3) suggests that all of the hepatoma isozymes may be composed of a single subunit type.

Purification of the normal aldehyde dehydrogenase has proven considerably more difficult than that of hepatoma Ald D. This difficulty appears to be due in part to a possible interconversion of Ald D with aldehyde oxidase, in a manner similar to that described by Della Corte and Stirpe (1) for xanthine dehydrogenase and xanthine oxidase. In part, the difficulty is due to an inherent instability of the normal enzyme forms.

CONCLUSIONS

The hepatoma Ald D isozymes isolated from AAF-induced hepatomas in Sprague-Dawley rats are similar in molecular weight and subunit composition to the cytoplasmic portion of the Ald D isozymes isolated from the liver of several mammalian species. The determination of whether or not these hepatoma isozymes are identical to the cytoplasmic Ald D in normal Sprague-Dawley liver awaits the purification of normal Ald D. The possibility is suggested that an interconversion may be possible between aldehyde dehydrogenase and aldehyde oxidase.

REFERENCE

1. Della Corte, E., and F. Stirpe. Biochem. J. 108, 349 (1968).

REGULATION OF ORNITHINE AMINOTRANSFERASE AND SERINE DEHYDRATASE SYNTHESIS IN RAT LIVER

Carl Peraino, J. Emory Morris, and Aldona Prapuolenis*

PURPOSE AND METHODS

In previous studies of the mechanisms of enzyme regulation in rat liver (1-3) it was shown that the activities of two amino acid catabolizing enzymes,

*Visiting Scientist, State University College of New York, Brockport.

ornithine aminotransferase (OAT) and serine dehydratase, increase in rats changed from a low to a high protein diet. When these rats were subsequently injected with glucocorticoids a further increase in serine dehydratase activity occurred, but ornithine aminotransferase activity fell to low levels although the high protein diet was continued (1-3). The possibility that this divergent behavior constitutes a useful tool for probing the mechanism by which glucocorticoids regulate gene expression in liver has been investigated.

Both enzymes were crystallized and inoculated into goats. The resultant antibodies were used to determine the rates of synthesis of both enzymes in rats subjected to appropriate dietary and hormonal stimuli. This was done by measuring antibody precipitable radioactivity in liver extracts from rats injected with 100 μCi of ^{3}H leucine 40 minutes before they were killed.

PROGRESS REPORT

Shifting rats from a 15% casein diet to one containing 60% increased the level of ornithine aminotransferase 10- to 15-fold and increased the rate of synthesis 3- to 4-fold. Serine dehydratase levels were increased 20- to 30-fold and the synthetic rate was increased 2- to 2.5-fold. This response in serine hydratase level and synthetic rate was also produced by glucocorticoid (triamcinolone) treatment of rats on a 15% casein diet. Under the latter conditions, however, ornithine aminotransferase levels only doubled and the synthetic rate decreased slightly.

When rats were fed a 60% casein diet for 5 days and were given a single glucocorticoid injection on the morning of day 6, the synthetic rate for serine dehydratase rose approximately 4-fold within 9 hours and declined to nearly pre-injection levels by 18 hours. A second wave of synthesis then occurred, reaching a peak (7-fold increase) by 36 hours with a subsequent shallower decline and further increase. The overall pattern could be characterized as a damped oscillation. The 7-fold increase in synthetic rate of serine dehydratase under these conditions was accompanied by only a 3-fold increase in the level of enzyme.

In contrast to the waves of serine dehydratase synthesis described above, ornithine aminotransferase synthesis in the same rats fell within 9-12 hours to approximately 25% of its rate prior to the glucocorticoid injection. The level of the enzyme did not begin to decline significantly for another 9 hours. The reduced rate of synthesis was maintained for the remainder of the experiment (72 hours).

When inhibitors of RNA synthesis (actinomycin D or α amanitin) were administered with the steroid to rats on the 60% casein diet, both the increase in serine dehydratase synthesis and the decrease in ornithine aminotransferase synthesis were blocked.

Measurement of body weight and food intake in rats receiving the high protein + steroid regime showed that the rats shifted into negative nitrogen balance and lost weight (8 g average/rat) during the first day after the steroid injection even though their food intake was 80% of that in uninjected rats, which gained 8 g during this period. (During the first 6 hours, when marked changes in the synthesis of both enzymes was occurring in the steroid

treated animals, both the treated and control rats ate approximately 10% of their total intake for that day). On the second and third days of the experiment the injected rats continued to lose weight and their food intake was approximately 60% that of the uninjected controls.

CONCLUSIONS

1. When both enzymes are at low levels, increasing the dietary protein intake raises the rate of enzyme synthesis and also reduces enzyme degradation, resulting in a rapid and marked accumulation of both enzymes. Of the two, serine dehydratase is stabilized to a greater extent than is ornithine aminotransferase and reaches higher absolute levels, although the rate of synthesis of ornithine aminotransferase shows a comparatively greater increase.

2. Glucocorticoid treatment in rats on a low protein diet also enhances the stability of both enzymes, but only increases the synthesis of serine dehydratase; the synthesis of ornithine aminotransferase actually decreases slightly, but the stabilization effect leads to a net accumulation of enzyme.

3. Young rats on a high protein diet are in positive nitrogen balance and gaining weight. Both serine dehydratase and ornithine aminotransferase synthesis and activity are elevated under these conditions, presumably to maintain homeostatic levels of serine and ornithine (the latter probably serving to regulate the functioning of the urea cycle). Administration of glucocorticoid shifts the rats to negative nitrogen balance (loss of body protein), causing them to lose weight while eating enough to produce weight gain in untreated rats. The metabolic changes involved in the steroid-mediated shift to negative nitrogen balance include further elevation of serine dehydratase synthesis to process additional incoming serine. (This response is characteristic of amino acid catabolizing enzymes in general.) The synthesis of ornithine aminotransferase, however, is concomitantly reduced, which allows ornithine accumulation and consequent maintenance of the urea cycle at a level sufficient to process the increased ammonia produced by the catabolism of other amino acids. Ornithine aminotransferase, therefore, apparently plays a pivotal role in the regulation of nitrogen metabolism.

4. mRNA synthesis is required for both the induction of serine dehydratase and repression of ornithine aminotransferase by glucocorticoid. In the latter case, this requirement means that the steroid must be inducing either a repressor for ornithine aminotransferase translation or a specific nuclease which degrades the mRNA for this enzyme.

5. Further comparison of transcriptional and translational events in the responses of these enzymes to regulatory stimuli should increase our understanding of the mechanisms by which gene expression is controlled in mammalian liver.

REFERENCES

1. Peraino, C. J. Biol. Chem. 252, 3860 (1967).
2. Peraino, C. Biochim. Biophys. Acta 165, 108 (1968).
3. Rahman, Y. E., and C. Peraino. Exp. Gerontol. 8, 93 (1973).

MOLECULAR WEIGHT OF RAT LIVER ORNITHINE-KETOACID AMINOTRANSFERASE*

J. Emory Morris,† *Carl Peraino, and Dana Strayer*‡

The molecular weights of ornithine-ketoacid aminotransferase in pure form and in crude extracts of rat liver were compared. The molecular weight of the pure enzyme was concentration-dependent. At concentrations of 10 mg per ml its molecular weight was 202,000 daltons, but this value was reduced to 116,000 daltons when the enzyme was diluted and allowed to equilibrate at a concentration of 0.1 mg/ml. The crude enzyme preparation also had a molecular weight of 116,000 daltons. The molecular weight of the enzyme subunit was 52,000 daltons and the pure enzyme contained one pyridoxal phosphate moiety per subunit. The data suggest that the enzyme may exist as a dimer *in vivo*.

---

*Abstract of a paper appearing in the Proceedings of the Society for Experimental Biology and Medicine 147, 706 (1974).

†Visiting Scientist, State University College of New York, Brockport.

‡Participant in the 1972 Summer Institute in Biology, State University College of New York, Brockport.

STUDIES ON THE EFFECTS OF PSORALEN AND ULTRAVIOLET LIGHT

Donald Grube, Ronald D. Ley, and R. J. Michael Fry

During exposure to ultraviolet light, 8-methoxypsoralen photoreacts with pyrimidine bases producing lethal, mutagenic, and oncogenic effects (1,2). We have initiated studies in skin carcinogenesis using such a combined treatment as an approach to determine whether the specific and mutagenic photoproducts ascribed to psoralen are causally related to tumorigenesis.

In earlier studies we have characterized the spectral dependence of some of the acute photosensitizing effects of 8-methoxypsoralen (8-MOP) in the skin of hairless mice, using 3 wavelength spectra (Figure 5.5). Irradiation with the broad wavelength spectra, i.e., 300-400 nm and 320-400 nm, was $\sim$ 4 times more effective than 365 nm (3) for producing cell depletion and delay of progression through the cell cycle.

This report is concerned with ongoing studies characterizing the spectral dependence of the photobinding of psoralen to epidermal DNA, including the relationships to the erythema and cytological action spectra, as well as subsequent neoplastic change.

With the exception that ethanol was the vehicle used in these studies, the protocol was the same as described earlier (3). In experiments conducted to determine the formation of bifunctional photoadducts (psoralen cross-linkages in epidermal DNA), HRS/J/An1 and SKH:hr-1 hairless mice were injected

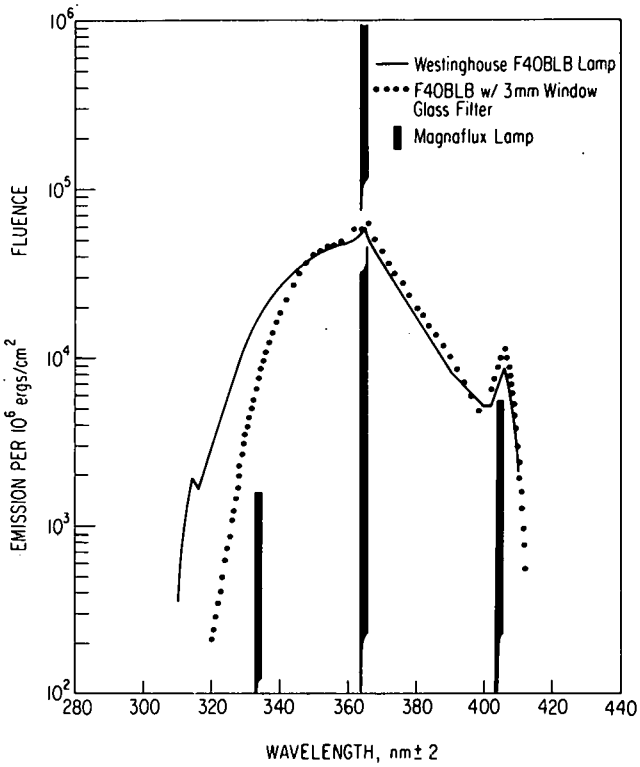

Fig. 5.5. Comparison of the spectral energy distribution from the Westinghouse F40BLB fluorescent lamp and Magnaflux Mercury Vapor lamp. [Unpublished data (1974), courtesy of R. B. Webb, Molecular Genetics Group.] These values represent average measurements from a calibrated Gamma Scientific Spectroradiometer, without correction for the fixed slits, or the scattered light components.

with ^{3}H-Tdr every 6 hours for a 42-hour period prior to a single exposure to ultraviolet light in skin photosensitized with $\sim$ 33/µg/cm^2 8-MOP. Subsequently, epidermal DNA was isolated and changes in the relative fractions of heat denatured (single-stranded) and reversibly renaturable (cross-linked) labeled DNA were determined using hydroxylapatite chromatographic separation.

PROGRESS REPORT

Preliminary data on the formation of psoralen bifunctional photoadducts in photosensitized skin indicate that 8-MOP photoreacts with epidermal DNA forming interstrand cross-linkages analogous to those observed *in vitro*. In addition, differences in the cross-linking efficiency of the respective wavelength spectra, i.e., 300-400 nm, 320-400 nm, and 365 nm, was closely paralleled by the same relative spectral differences in efficiencies for erythemal and cytological effects. This has been suggested by indirect evidence reported by others (4). The cross-linking (CL) efficiency for irradiance with 320-400 nm and 300-400 nm was similar, but with irradiance at principally 365 nm, the effect per unit dose was $\sim$ 4 times less.

The exposure regimes selected for each wavelength spectrum in tumor studies are shown in Figure 5.6. On the assumption that the acute biological parameters studied were appropriate, the daily irradiance levels as shown have been adjusted taking into account the $\sim$ 4-fold difference in spectral effectiveness for cell and tissue damage (3), as well as the formation of psoralen cross-linkage in epidermal DNA. If the basis for these adjustments is correct, any differences in tumor incidences cannot be attributed singularly to psoralen-DNA cross-linkages.

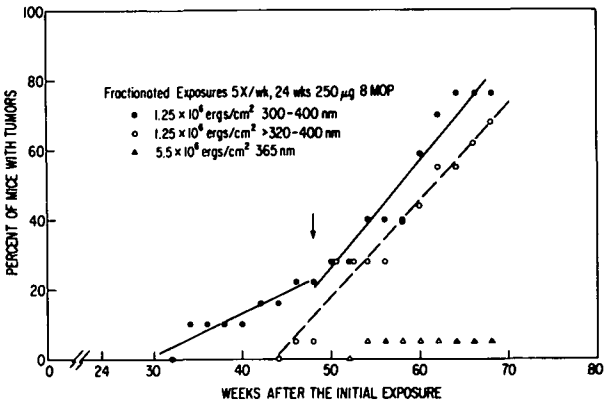

Fig. 5.6. Cumulative incidence of epidermal carcinoma in SKH:hr-1 mice treated daily with 250 µg 8-MOP and subsequently exposed at the fluence shown for the respective wavelength spectra. The daily incident dose used in these comparative studies approximate cell and tissue damage, as well as the formation of psoralen cross-linkage in epidermal DNA of photosensitized skin.

The results to date clearly demonstrate a spectral dependence in the oncogenic effects of combined treatment. No erythematous or neoplastic response was observed during the 24 weeks of fractionated exposures to a combined treatment of 8-MOP and ultraviolet light. Subsequently, at ~ 28-30 weeks after the initial exposure, there was a progressive appearance of epidermal eruptions, focal ulceration, and the onset of tumors. Animals bearing one or more epidermal carcinomas were first observed in SKH:hr-1 hairless mice photosensitized with 8-MOP and exposed to the 300-400 nm wavelength spectrum. The cumulative incidence of tumors with time in this group does not appear to be a simple linear relationship. However, except for differences in the initial appearance of tumors, the rate of appearance of tumors in mice exposed to both broad wavelength spectra (300-400 nm and 320-400 nm) is similar, as shown by the calculated regression lines. In contrast, only a low incidence of epidermal carcinomas, after an extended latent period, has been observed in SKH:hr-1 mice exposed to principally 365 nm wavelength from the Magnaflux lamp, even though the initial and secondary cutaneous responses were comparable in all groups.

CONCLUSIONS

Interpretations of these studies depend on the final results from these and replicate experiments in progress. The data to date demonstrate a spectral dependence in oncogenic effects, which must be related in part to the formation of some psoralen photoproduct, since the exposure to wavelengths 320-400 nm is carcinogenic only in photosensitized skin. However, it tentatively appears unlikely that the photoproduct involved is the bifunctional adduct.

Whether the different responses for tumor induction are related to differences in an "initiating" event which can be ascribed to specific photoproducts, or represent differences in enhancement is not resolved. Studies are currently underway to examine these questions, as well as dose-response relationships.

REFERENCES

1. Musajo, L., and G. Rodighiero. Photophysiology VII, p. 115 (1972).
2. Griffin A. C., R. E. Hakim, and J. Knox. J. Invest. Dermatol. 31, 289 (1958).
3. Grube, D. D., and R. J. M. Fry. ANL-8070 (1973), p. 58.
4. Dall'Acqua, F., S. Marciani, D. Vedaldi, and G. Rodighiero. Biochim. Biophys. Acta 353, 267 (1974).

STRAIN-DEPENDENT CELL PROLIFERATION AND TUMORIGENESIS

Donald Grube and R. J. Michael Fry

Species and tissue differences in susceptibility to oncogenic agents may reflect differences in the induction or expression of neoplastic changes. One of the long-term objectives in our studies of skin carcinogenesis is to determine the relationship of cell proliferation to tumor induction. For these purposes we have chosen to use two strains of hairless mice: HRS/J/An1 and SKH:hr-1 which, in comparison, has a significantly shorter latent period for ultraviolet light-induced tumors than does the HRS/J strain (1).

This report is concerned with an investigation of strain differences in the proliferative activity and turnover times in untreated epidermis. Mice 12-14 weeks of age were injected intraperitoneally with 0.5 μCi/g body weight of ^{3}H-TdR (specific activity 0.36 Ci/mM) every 6 hours for intervals up to 120 hours. At selected times, groups of two or three mice from each strain were killed 30 minutes after injection. Autoradiograms of dorsal epidermis were prepared from 4-μm transverse sections stained with Mayer's haematoxylin. The percentage of labeled nuclei in the basal and superficial cell layers were determined by scoring at least 1500 epithelial cells in the interfollicular epidermis of each mouse. Nuclei were considered labeled when they were overlaid by four or more grains.

Figure 5.7 illustrates changes in the percentage of labeled nuclei in the basal and differentiating cell layers as a function of time under conditions considered to be continuous labeling. The data indicate strain differences in both the rate of entry of cells into DNA synthesis (S), as well as in the rate of cell turnover.

In both groups, the percentage of labeled basal cells increased at a linear rate during the initial 60-72 hours of labeling. Subsequently, as the values approached 100%, there was a reduction in the rate at which the indices increased, with the initial change apparent at about the time of onset in the movement of labeled cells into the suprabasal layers. The mean rate of increase in labeled cells between 0-60 hours in the HRS/J/An1 mice was estimated as $\sim$ 0.91%/hr of the total basal cell population; a value comparable to previous estimates of the flux of cells into S in HRS/J/An1 mice using a double-labeling technique (2). The proliferative activity in the epidermis of SKH:hr-1 mice was greater (1.08%/hr) but the strain difference was not statistically significant at the 0.05 level. In both strains of mice, the

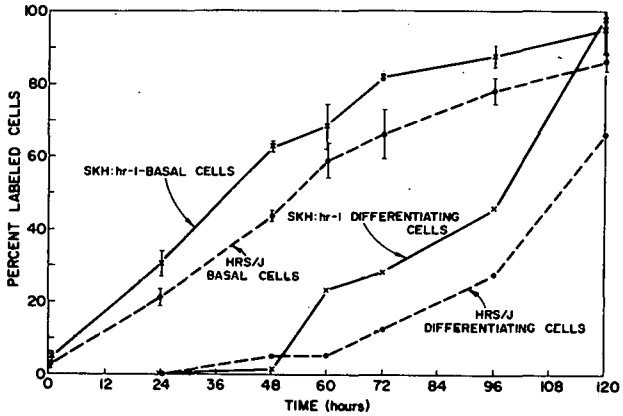

Fig. 5.7. Changes in the percentage of labeled basal cells and differentiating cells in interfollicular epidermis as a function of time under conditions of continuous labeling. Each point represents the mean value (± SE) derived from section autoradiographs from two or three animals. The lines are best fit by eye.

proportion of labeled basal cells approached 100% at ∿ 120 hours. Changes in the rate of proliferation as values approach 100% have been previously observed (3), but there is insufficient evidence to determine whether these changes reflect variability in cell cycle times or different cell populations.

Cell turnover times have been estimated from the rate of cell transit through the superficial layer. Again strain differences are apparent. After an initial delay of ∿ 48-60 hours, the estimated rates of migration of basal cells through the superficial cell layers (HRS/J ∿ 0.89%/hr, SKH:hr-1 ∿ 1.18%/hr) closely parallel the rates of proliferation. The mean turnover time for interfollicular epidermis of HRS/J/An1 mice was estimated to be ∿ 113 hours, as compared to ∿ 85 hours in the SKH:hr-1 mice. The data show that in both strains of mice, cells do not migrate from the basal layer randomly during the cell cycle. While the movement of basal cells into the suprabasal layers appears to be random in another stratified epithelium (4), our findings of delayed progression in dorsal epidermis have been observed by others (3).

CONCLUSION

The rate of cell proliferation and cell turnover is greater in the untreated interfollicular epidermis of the SKH:hr-1 mice as compared to the HRS/J/An1 strain. These studies will be extended to comparative experiments in skin carcinogenesis to examine whether differences noted in UV-induced tumorigenesis are related to the differences in proliferation kinetics.

REFERENCES

1. Forbes, P. D., Temple University, Philadelphia. Personal communication (1972).
2. Grube, D. D., Auerbach, H., and Brues, A. M. Cell Tissue Kinet. 3, 363 (1970).
3. Iversen, O. H., Bjerknes, R., and F. Devik. Cell Tissue Kinet. 1, 351 (1968).
4. Brockwell, P. J., and R. J. M. Fry. Biometrics 29, 837 (1973).

A COMPARISON OF THE INCIDENCE OF TUMORS OBTAINED BY TWO METHODS OF SAMPLING

R. J. Michael Fry, George A. Sacher, Sylvanus A. Tyler, E. John Ainsworth, Katherine H. Allen, and Everett Staffeldt

Tumors found at death may be the cause of death or have contributed little or nothing to lethality. Age-specific mortality rates can give a precise actuarial description of the lesions that are the cause of death; whereas prevalence rates, obtained by serial killing, are necessary for "non-lethal" tumors to describe either a) the spontaneous incidence, or b) the effects of experimental procedures on the incidence or the time of appearance. However, in many experiments these two types of data for some tumors are not clearly separated but are confounded.

The present study was undertaken to compare the data for the incidence of lymphomas in female $B6CF_1$ mice obtained, in one case, at the time of natural death and, in the second, by serial killing at approximately 100-day intervals. The proportion of animals with lymphoma in a population alive at a given age is the prevalence of lymphoma at that age (1).

The mice allowed to live out their lifespan were from five replicates of unirradiated controls of one experiment in the JANUS program. The mice killed to obtain the prevalence rates were similar in every important aspect.

PROGRESS REPORT

For this preliminary analysis we have pooled data from all types of lymphomas. We presume that the more rapidly developing tumors are lymphoblastic-lymphocytic lymphomas, whereas the majority of the lymphomas occurring late in life are reticulum cell sarcomas. The histological classification of the lymphomas which is being carried out will allow separate analyses and comparisons for each lymphoma type.

The data on incidence of lymphomas in the serial killing study and in the necropsied life table population are given in Table 5.1. Age-specific prevalence values were estimated using the formula

$$P_x = l_x/S_x$$

where l_x is the number of mice sacrificed at age x that bear lymphomas, and S_x is the total number sacrificed at age x. The age-specific lymphoma mortality rate is found by

$$\mu_{x+\frac{1}{2}h} = \frac{1}{h}\{\ln[L_x - \tfrac{1}{2}(d_x - m_x)] - \ln[L_x - \tfrac{1}{2}(d_x + m_x)]\} .$$

Here L_x is the number living at age x, d_x is the number dying from all causes in the following interval of length h, and m_x is the number dying of lymphoma in the following interval. This is a provisional formula. The estimation for the final report will be done by another method.

The lymphoma mortality rate is too low to estimate before 500 days of age, and after 600 days it increases in log-linear fashion with a doubling time of about 150 days (Figure 5.8). The mean number of tumors per animal, estimated as $-\ln(1-P_x)$, is also given in Figure 5.8. It can be seen to have a roughly parallel trend. This quantity is the reciprocal of the natural logarithm of the proportion of tumor-free animals in the age sample.

The mean duration of the recognizable disease, or residence time, can be estimated by

$$T_x = (\text{mean no. tumors per animal})/(\text{tumor death rate per animal})$$
$$= -\ln(1-P_x)/\mu_x \quad .$$

Table 5.1. Incidence of Lymphomas in $B6CF_1$ Female Mice

	Natural Death			Sacrificed	
Age (days)	Number Alive L_x	Number of Tumor-bearing Mice m_x	Number of Mice Dying d_x	Number of Tumor-bearing Mice l_x	Number of Mice Killed S_x
0- 299				0	212
300- 399				2	128
400- 499	169	0	2	0	121
500- 599	167	1	6	2	100
600- 699	161	3	12	6	124
700- 799	149	11	22	13	148
800- 899	127	13	23	23	107
900- 999	104	15	39	21	107
1000-1099	65	21	36	43	114
1100-1199	29	10	22	5	14
1200-1299	7	1	7	55	101

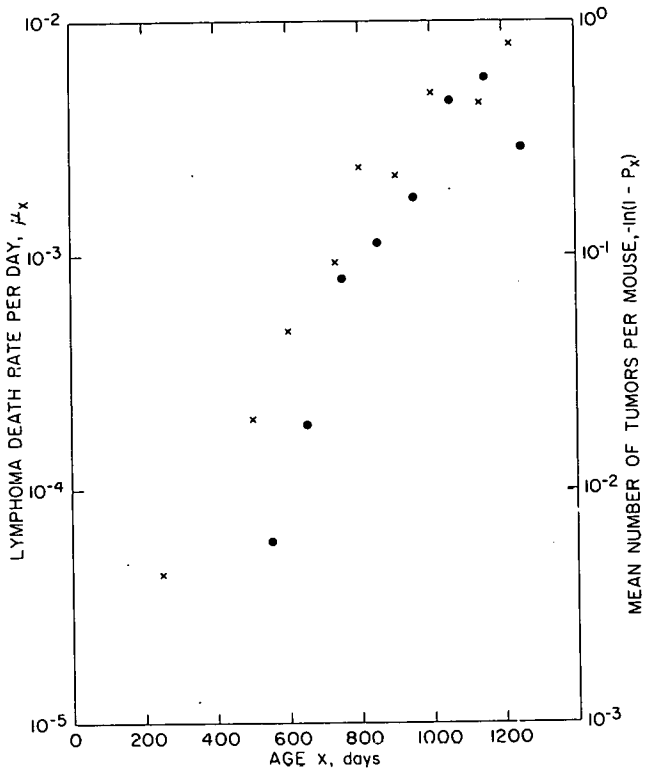

Fig. 5.8. Age-specific death rate (filled circles) and mean number of tumors per animal (crosses) for reticular tissue tumors of $B6CF_1$ mice. The data are from Table 5.2.

The residence times are given in the right-hand column of Table 5.2. If we ignore the two extreme estimates, which are based on small samples, the T_x values fluctuate between 104 and 273 days. Since there is no trend, it can be provisionally concluded from this analysis that mean residence time is constant at about 200 days throughout most of the period of lymphoma mortality. However, this estimate is too high because it fails to take the exponential increase into account. A better estimation formula is being developed.

CONCLUSION

The mean time for lymphoma to progress from its earliest detectable stage to death is somewhat less than 200 days for the female $B6CF_1$ mouse. This estimate will be improved in several ways when work in progress is completed. The population for mortality rates will be larger, and tumors will be separated into the categories of lymphoblastic-lymphocytic and reticulum cell sarcoma.

Table 5.2. Death rate, Prevalence, and Residence Time for Lymphoma in $B6CF_1$ Female Mice

Age (days) x	Tumor Prevalence P_x	Mean Number of Tumors $\ln(1-P_x)$	Lymphoma Death Rate ($\times 10^6$) u_x	Mean Tumor Residence Time (days) T_x
300- 399	.016	.016		
400- 499	.000	.000	0	
500- 599	.020	.020	61	328
600- 699	.048	.048	192	250
700- 799	.088	.092	798	115
800- 899	.215	.242	1126	215
900- 999	.196	.218	1780	122
1000-1099	.377	.473	4540	104
1100-1199	.357	.442	5710	77
1200-1299	.545	.786	2880	273

REFERENCE

1. MacMahon, B., T. F. Pugh, and J. Ipsen. Epidemiologic Methods, Little, Brown and Co., Boston, 1960.

INSTRUMENTATION FOR FORWARD-DIRECTION FLUORESCENCE DETECTION IN SEM STUDIES OF BIOLOGICAL MATERIALS

Daniel G. Oldfield, G. Theodore Chubb, and William R. Cole†*

PROGRESS REPORT

The instrumentation for fluorescence studies of biological materials with the scanning electron microscope (SEM) described previously (1) has been appreciably modified and improved in order to eliminate significant deficiencies (specifically, low fluorescence-detection sensitivity and specimen self-shadowing) and to extend performance capability to include spectral analysis of the fluorescence.

*Faculty Research Participant, DePaul University.

†Central Shops, Argonne National Laboratory.

The major modification made was conversion of the fluorescence detector from a mirror-system collecting fluorescence emitted in the backward direction (relative to the incident electron beam) to a fiber optics system collecting fluorescence emitted in the forward direction.

The modified system thus consists of: (a) a special stub having one or more holes; (b) a thin glass chip (carrying the biological specimen) cemented over the hole in the stub; (c) a bundle of 64 plastic fibers with one end of the bundle directly below the hole in the stub to collect fluorescence emitted by the specimen, and with the other end of the bundle fed through an expoxy vacuum seal (as a vertical fiber array) leading from the specimen chamber to a wedge interference filter and photomultiplier; (d) a small stainless fixture (attached to the SEM stage and moving with it) which clamps the fiber-optics bundle in position under the stub hole, and that fixes the vertical height and guides the axial rotation of the stub (the latter being returned in the stub socket).

The above arrangement reduces specimen self-shadowing. Absorption of fluorescence in the specimen will, of course, still occur in the forward-fluorescence system but may decrease as beam penetration depth increases. The detection sensitivity for fluorescence is higher since light is now collected over a greater solid angle. Detection sensitivity has been additionally improved by replacing the external amplifier initially used with an amplifier (Keithley 427) having a relatively short rise-time (60 microseconds) even at high gain (10^8 volts per ampere). Thus, the time required for photographing fluorescence traces on the oscilloscope can be held to under about 5 minutes.

Since the system described here is still under test, no firm estimates of detection efficiency can be made at this time. It should be noted that a forward-direction fluorescence system can be combined, if desired, with a backward-direction system to obtain a higher detection efficiency than is possible with either system alone. But the ease with which stub-changes can be made and the feasibility of tilting the specimen if desired when the forward-direction system is used suggests that it merits investigation in its own right.

REFERENCE

1. Oldfield, D. G., and G. T. Chubb. ANL-7970 (1972), p. 66.

THE ANALYTIC DETERMINATION OF INTRACELLULAR STRUCTURES FROM THREE-DIMENSIONAL SCANNING MICROSCOPY LUMINESCENCE DATA*

Daniel G. Oldfield†

This paper examines various sets of conditions under which intracellular structures can be quantitatively characterized as to general chemical type, size, and location within the cell using luminescence data obtained by scanning electron or proton microscopy.

The physical basis of the method is provided by the differences in luminescence spectra produced at each of two or more different depths of beam penetration into the specimen (corresponding to two or more initial beam energies incident on the specimen). For the analysis, we define a luminescence function $L(x,y,z,U,\omega,\lambda)\, dVdUd\omega d\lambda$ as the probability per unit time that a luminescence photon in the wavelength range $d\lambda$ at λ is emitted into the solid angle $d\omega$ at ω from the specimen volume element $dV = dxdydz$ at x,y,z when an increment of energy in the range dU at U is absorbed in that volume. For an incident beam of initial energy E_1^o and scan position x^o, y^o, applying expressions for beam scattering and specific energy loss to the luminescence function L yields an expression $S_1(\omega,\lambda,E_1^o,x^o,y^o, \{i_1\})$ for the luminescence spectrum emitted from the specimen when the integration limits for energy deposition within the specimen are $\{i_1\} = x_1', y_1', z_1', x_1'', y_1'', z_1''$. Applying luminescence-detector and object-image relationships in the scanning microscope to S_1 then yields the function $M_1(\lambda,E_1^o, \{i_1\}, u, v)$ which specifies the luminescence spectrum expected at the image point u,v of an intensity-modulated display synchronized with the scan beam. Finally, the difference M_2-M_1 determines the luminescence spectrum of that portion of the specimen bounded by the integration limits $\{i_2\}$ and $\{i_1\}$.

When the spectra produced by various portions of the specimen are compared, and assuming that a specific set of spectra uniquely characterizes a specific structure, sensitive chemical specification and high-resolution spatial localization of intracellular structures become feasible in favorable cases. Some preliminary experimental data will be presented as applications of the methods discussed.

---

*Summary of paper to be published in the proceedings of the Fourth International Congress for Stereology, Gaithersburg, Md. September 4-9, 1975.

†Faculty Research Participant, De Paul University.

CLEFT PALATE INDUCTION: QUANTITATIVE STUDIES OF ^3H CORTICOIDS IN A/JAX MOUSE TISSUES AFTER MATERNAL INJECTIONS OF ^3H CORTISOL*

Kenneth M. Spain, Walter Kisieleski, and Norman K. Wood†

Pregnant A/Jax mice were injected intramuscularly with a solution of 50 µCi of ^3H cortisol and 10 mg of cortisone acetate as cold carrier on day 12 of gestation. Animals were sacrificed at each of the following time intervals after injection: 0.5, 1.0, 1.5, 2.0, and 3.0 hours. Maternal liver, placenta, yolk sac, and fetal jaws were analyzed for total tritium content. The percentages of total radioactivity were determined for ^3H cortisol, ^3H cortisone, and ^3H corticoid metabolites in the various tissues utilizing thin layer chromatography techniques in conjunction with oxidative combustion and liquid scintillation counting. Results clearly show that not only were significant amounts of ^3H cortisone and other ^3H cortisol metabolites identified at the 0.5 interval, but significant levels were maintained through the 3.0 hour interval in all tissues. Comparable results obtained for yolk sac and placenta suggest that both of these organs may act as a quantitative barrier for the passage of corticoids to the fetus. Results of this study support the thesis that these corticoids may induce clefts by an individual or combined direct action on the fetal jaws and palatal shelf tissue.

---

*Abstract of a paper to be published in the Journal of Dental Research. The paper was part of a research thesis prepared by Dr. Spain in partial fulfillment of the Master of Science Degree requirements in the Department of Oral Biology, Loyola University School of Dentistry, Maywood, Illinois.

†Loyola University School of Dentistry, Maywood, Illinois.

MICROSCOPIC TRACING OF DEUTERIUM*

G. Roy Ringo† *and Walter E. Kisieleski*

The objective of this program is to develop an ion-microprobe analyzer that will be useful in two applications in biology. (1) It will permit the mapping of stable isotopes, particularily tracers, in biological materials to an accuracy better than 500 Å. (2) It will permit analysis of the mass spectrum of ionic molecular fragments knocked out by the primary beam; this may be a useful indication of the chemical composition of the spot being bombarded.

To demonstrate this technique, we have made ion micrographs at mass 1 and 2 of a section of liver from a deuterated animal. In the ion micrographs, discrimination between the deuterium rich and deuterium poor tissues is fairly

---

*Abstract of a paper submitted to the Journal of Microscopy.

†Physics Division, Argonne National Laboratory.

easy by comparison of the two micrographs. This discrimination illustrates clearly the practicality of using an ion microprobe to find the location of deuterium in biological materials.

The development of the ion-microprobe analyzer (1) has raised the possibility that stable isotopes can be followed with microscopic resolution in biological and other materials. This technique should permit the use of deuterium as a practical tracer with a resolution of about 1 μm in the plane of the section and 20 Å in the depth dimension with available instruments.

This technique for mapping deuterium must of course be compared with that recently developed by F. H. Geisler, et. al. (2), which uses nuclear reactions with ∿ 200 KeV tritium ions. The chief advantage of the ion-microprobe analyzer is the high resolution it gives in depth. In other respects -- sensitivity, speed, complexity, and cost -- the two methods are at least roughly comparable. The choice might well depend on whether an ion probe or a 200 KeV accelerator were more available.

REFERENCES

1. Andersen, C. A., and J. R. Henthome. Science 175, 853 (1972).
2. Geisler, F. H., K. W. Jones, J. S. Fowler, H. W. Kraner, A. P. Wolf, E. P. Cronkite, and D. N. Slatkin. Science 186, 361 (1974).

SPARK COMBUSTION OF ^{3}H AND ^{14}C LABELED SAMPLES SUITABLE FOR LIQUID SCINTILLATION COUNTING*

John Noakes[†] *and Walter E. Kisieleski*

A new method of combusting labeled ^{3}H and ^{14}C samples is accomplished through continuous spark ignition. Liquid, wet tissue and powdered samples are combusted in disposable steel planchets. Radioisotope collection is in liquid scintillation cocktails as $^{3}H_2O$ and $^{14}CO_2$. Quantitative collection and minimum memory is enhanced through controlled combustion rates. Comparison of the spark ignition method is made with presently available commercial equipment.

Present capabilities of the instrument allow for the combustion of samples up to 40 millimoles of carbon dioxide for ^{14}C samples and up to 85 millimoles of water for ^{3}H samples. Analytical recovery of the ^{14}C and ^{3}H labeled thymidine filter papers show results in the 97-98% range with a precision of ± 1.5%. Memory and spillover values recorded for these standards were 0.05% and 0.07% for ^{14}C and 0.2% and 0.8% for ^{3}H. Counting efficiency of the collecting cocktails for the combusted labeled thymidine samples showed 60% for ^{14}C and 47% for ^{3}H.

*Abstract of a paper by Noakes, J. E., and W. Kisieleski. In: Liquid Scintillation Counting: Recent Developments, Eds. P. E. Stanley and B. A. Scoggins. Academic Press, Inc., New York, 1974, p. 125.

†Geochronology Laboratory, The University of Georgia, Athens, Georgia.

6. EXPERIMENTAL RADIATION PATHOLOGY AND ONCOLOGY

SUMMARY

Miriam P. Finkel, Group Leader

The goal of the Experimental Radiation Pathology program is to provide basic data for use in evaluating the hazard to man from exposure to radionuclides deposited within the body. In the initial approach to this goal, a variety of radionuclides were tested in a variety of laboratory animals with the objective of obtaining relative dose-response information. When it became apparent that all radionuclides are oncogenic, experiments were undertaken to determine how radiation causes cancer. The approach to this second objective involves the induction of bone cancer when the physical, biological, and temporal parameters of dosage are altered. A third objective, to determine the role of oncogenic virus in radio-oncogenesis, was added to the program when it became apparent that viruses can cause tumors in mice. The approach has been the search for virus in spontaneous and radiation-induced bone cancer of mouse, dog, and man.

Major emphasis during the past year was devoted to determining the degree of interaction between the three murine bone tumor viruses previously isolated in this laboratory. Two of these viruses came from CF#1 mice, and the third from the X/Gf strain. Although we had previously isolated a virus that produces tumors of the reticular tissues in the latter strain, we have only recently been successful in obtaining cell-free passage of CF#1 reticular-tissue tumors. This new isolation provides us with both sarcoma and leukemia viruses for the two mouse strains so that we now have a more complete system for examining viral oncogenesis.

The initial phase of our search for a human osteosarcoma virus is nearing completion, and there is strong evidence for the existence of such an agent.

EXPERIMENTAL RADIATION PATHOLOGY AND ONCOLOGY STAFF

REGULAR STAFF

Dale, Phylis J. (Scientific Assistant)
Finkel, Miriam P. (Senior Biologist)
Greco, Isabel I. (Scientific Assistant)
Pahnke, Vernon A. (Scientific Assistant)
Reilly, Christopher A., Jr. (Microbiologist)
Rockus, Gabriele (Scientific Assistant)

TEMPORARY STAFF DURING 1974

Lee, Chung K. (Postdoctoral Appointee)

VIRAL ETIOLOGY OF BONE CANCER*

Miriam P. Finkel, Christopher A. Reilly, Jr., and Birute O. Biskis

There is now adequate proof that viruses play an important role in the etiology of a number of animal tumors. Some viruses are specific for one kind of tumor while others induce a variety of histologic types, including osteosarcomas.

At present there are three viruses that cause only bone tumors in mice. Two were derived from spontaneous bone tumors of the CF#1 strain. One of these, FBJ, induces parosteal osteosarcomas; the other, RFB, induces osteomas. The third virus, FBR, was derived from a ^{90}Sr-induced osteosarcoma of an X/Gf mouse, a strain that is highly tumor resistant under natural and most experimental conditions. This virus, like FBJ of CF#1 mice, induces parosteal osteosarcomas. All three agents are RNA, type C viruses.

The evidence for a human osteosarcoma virus, though not conclusive at this time, is very suggestive. The incidence of mesenchymal tumors in hamsters inoculated soon after birth with extracts of tissues from patients with bone tumors or from hamsters previously inoculated with such extracts is much higher than the incidence in untreated hamsters; there are type C particles in human osteosarcomas and in the sarcomas appearing in treated hamsters; and some of the hamster sarcomas have been shown to react antigenically with human osteosarcoma serum, as measured both by indirect immunofluorescence and by cytotoxicity assays.

---

*Summary of a paper presented at the Tenth Annual Cancer Symposium of the West Coast Cancer Foundation, Inc. To be published in Frontiers of Radiation Therapy and Oncology, Vol. 10, "Bone Cancer: The Multidiscipline Disease." University Park Press, Baltimore.

PATHOGENESIS OF RADIATION AND VIRUS-INDUCED BONE TUMORS*

Miriam P. Finkel, Christopher A. Reilly, Jr., and Birute O. Biskis

Areas for Continuing Research

In the preceding pages we have attempted to summarize our experiences relating to the induction of bone tumors by radiation and oncogenic viruses. It is somewhat discouraging that after 30 years of research so little is known about the manner in which bone-seeking radionuclides bring about neoplastic change. The answers probably will be found in the course of careful investigations of the latent period, not in further work with dose-response relationships, a type of research that is likely to be just as fruitless in the future in elucidating mechanisms of oncogenesis as it has been in the past. An important clue may be that oncogenesis by the two murine osteosarcoma viruses occurs very quickly, tumors being recognized roentgenographically as early as three days after newborn mice have been inoculated with virus. In this case the animal is overwhelmed with the oncogen. Perhaps in the case of radiation the oncogenic information present in each cell must first be properly activated, then amplified, and finally produced in such abundance that the usual mechanisms for repressing neoantigens are no longer effective against the new growth. That FBJ-antigen has been demonstrated in some ^{90}Sr-induced osteogenic sarcomas and that FBR virus was isolated from a ^{90}Sr-induced osteogenic sarcoma in a mouse strain that rarely develops tumors of any kind lend support to this view.

---

*Conclusion of a paper presented at the VIth International Symposium of the Gesellschaft zur Bekampfung der Krebskrankheiter Nordrhein-Westfalen E.V. To be published in Recent Results in Cancer Research: "Malignant Bone Tumors." Springer/Press, Berlin - Heidelberg - New York.

TUMOR INDUCTION IN SYRIAN HAMSTERS BY EXTRACTS OF HUMAN BONE TUMORS*

Miriam P. Finkel, Christopher A. Reilly, Jr., Birute O. Biskis, and Douglas J. Pritchard†

Three viruses that induce bone tumors in mice have been isolated in our laboratory from murine osteosarcomas and osteomas. To determine whether similar agents are present in human bone cancer, extracts of tissues from 109 patients with bone tumors were injected into approximately 2500 newborn Syrian hamsters, which are being maintained to assess tumor induction. The 109 cases consist of 100 osteosarcomas, 5 chondrosarcomas, 3 fibrosarcomas, and 1 giant-cell tumor. Approximately 500 control hamsters were inoculated with extracts of normal human abdominal muscle or balanced salt solution.

To date, 46 sarcomas, 7 osteomas, and 1 giant-cell tumor have been diagnosed in the experimental hamsters. Mesenchymal tumors are very rare in Syrian hamsters, and only one, a fibrosarcoma, has appeared among our control animals. The incidence of tumors of the reticuloendothelial system, which are relatively common in this species, and of carcinomas has not been influenced by the experimental procedures.

At this time, extracts of tissues from 27 of the 109 bone-tumor patients (25%) have produced one or more hamster sarcomas, osteomas, or giant-cell tumors; these tumors appeared in 54 of approximately 2500 experimental hamsters (2%). The control incidence is 0.2% (1/500).

These data support the view that there is an oncogenic agent in human bone cancer. Other lines of evidence are cross-reactivity of some of the hamster sarcomas with human osteosarcoma sera and the cytotoxic behavior of human osteosarcoma sera upon a tissue-culture line of one of the hamster sarcomas.

---

*Abstract of a paper presented at the XIth International Cancer Congress. Published in XIth International Cancer Congress, Abstracts Vol. 1 - Conferences, Symposia, Workshops, pp. 242-243 (1974).

†Mayo Clinic and Mayo Foundation, Rochester, Minnesota.

BIOLOGICAL RELATIONSHIPS OF THREE MURINE BONE TUMOR VIRUSES*

Christopher A. Reilly, Jr. and Miriam P. Finkel

The three bone tumor viruses isolated from mice in our laboratory are now being examined to determine their host ranges, immunologic similarities, and biological interactions. They are particularly useful for studying tumor induction by virus because of the way in which they share several important characteristics. FBJ osteosarcoma virus was isolated from a spontaneous parosteal osteosarcoma of a CF#1 mouse, FBR osteosarcoma virus from a ^{90}Sr-induced osteogenic sarcoma of a X/Gf mouse, and RFB osteoma virus has been repeatedly isolated from spontaneous osteomas of CF#1 mice.

The two osteosarcoma viruses are very potent oncogenic agents in their respective strains of origin. However, each is only weakly oncogenic in the other strain, even though FBJ virus is very oncogenic in all other mouse strains in which it has been tested. The CF#1 osteoma virus (RFB) readily induces benign bone tumors in CF#1 and CBA mice, and it is moderately oncogenic in X/Gf mice. Serum from mice bearing tumors induced by any one of these three viruses neutralizes the respective inducing virus. There is no cross-neutralization in the case of the two osteosarcoma viruses, but serum from CF#1 mice bearing RFB osteomas does have some neutralizing capacity against FBJ virus, the osteosarcoma agent of the same strain. Interference studies also indicate interaction and competition between these two native CF#1 viruses.

It appears that the two CF#1 viruses, which were isolated from spontaneous bone tumors, are oncogenic in most mouse strains, share common antigenic determinants, and may also share host cells. In contrast, the X/Gf virus, which was isolated from a radiation-induced osteogenic sarcoma, seems to be unique in host range and antigenicity.

---

*Abstract of a paper presented at the XIth International Cancer Congress. Published in XIth International Cancer Congress, Abstracts Vol. 2 - Panels, p. 82 (1974).

IN VIVO INTERFERENCE OF NATURALLY OCCURRING MURINE BONE TUMOR VIRUSES

Christopher A. Reilly, Jr., Phylic J. Dalo, and Miriam P. Finkel

We have isolated two viruses from spontaneous bone tumors of CF#1 mice: FBJ virus induces parosteal osteosarcomas, and RFB virus induces osteomas. To determine whether these two agents might interfere with each other, five groups of newborn CF#1 mice were inoculated with virus preparations. Group I received FBJ osteosarcoma virus only, Group II received RFB osteoma virus only, Group III received FBJ followed in 24 hours with RFB, Group IV received RFB followed in 24 hours with FBJ, and Group V received a mixture of

FBJ and RFB. Animals were selected for autopsy and bone tumors were scored when the tumors interfered with normal activities. The average time of sacrifice with FBJ osteosarcomas was 54 days in Group I. RFB osteomas grow more slowly; the first mouse of Group II was taken at 90 days. Group III mice responded as if they had received only FBJ, most succumbing to osteosarcomas before osteomas usually appear. In both Groups IV and V the present data for RFB osteomas is similar to that in Group II, but the incidence of FBJ osteosarcomas is much less than that in Group I, and the time to sacrifice is longer. This marked interference with FBJ osteosarcoma induction when RFB osteoma virus is injected either first or along with FBJ virus suggests that these two agents share a common host cell.

7. AGING RESEARCH

SUMMARY

George A. Sacher, Group Leader

The program of the Aging Research group can be divided into two major subprograms, one of which is concerned with the comparative biology, genetics, and evolutionary biology of aging, and the other with the elucidation of the ontogenetic aging processes in mammals, especially in the cell membrane and the immune system.

The evolutionary-comparative research activity is focused on discovering how the disparate life tables of different mammalian species evolved. The basic postulate is that increased lifespan evolved under the action of selective forces, as a concomitant of the evolutionary trend toward large brain size and body size. Enough evidence has been adduced in support of this thesis to justify the next step of searching for some of the specific genetic determinants of longevity differences. The mammalian life table is determined by two parameters, one of which governs the species rate of aging and the other which governs the initial constitutional vigor and vulnerability to disease. So far as is known, the differences in longevity within species are due to variation in the vulnerability parameter, so that genetic analysis of the factors governing rate of aging is not now possible by the classical procedures of reproductive genetics. This presents a serious methodological problem. Our proposed attack is to begin the analysis of interspecies differences in aging rate at the physiological and biochemical levels so that interspecies genetic analysis can proceed as the tools become available. However, genetic analysis of the factors responsible for strain differences in the vulnerability parameter can be carried out, and an experiment is under way, using inbred mouse strains and their hybrids.

An additional approach to the dissection of the factors involved in longevity and aging is the analysis of genotype-environment interactions. Such a study is under way, in which mice are exposed to different temperature environments.

The studies in the cellular biology of aging are concerned with the factors involved in the control of enzyme biosynthesis and with the properties of nerve membranes, especially in regard to transport of metabolites. The nerve membrane studies will be made using a newly developed *in vitro* system consisting of isolated presynaptic bulbs, or synaptosomes. These studies were sidetracked in the past year while the membrane research team pursued the development of artificial liposomes as a means of transporting otherwise impermeable molecules into the interiors of specific target cells. This

procedure is being applied to the decorporation of heavy metals and the transport of anti-tumor drugs into tumor cells. This is appropriate because these test situations permit short-term experiments. In a later phase of this research, when liposome technology is better understood, long-term experiments with anti-aging drugs will be justified.

The studies of aging in the immune system are concerned with identifying the cell population primarily responsible for the loss of immunological responsiveness with age. Approaches include: a) characterizing the differences in the kinetics of the primary and secondary response in young and old beagle dogs and mice; and b) measuring the age changes in populations of thymus-derived immunocytes (T-cells) in mice. The latter project lends itself to comparative study and genetic analysis, and an experiment on the relation of T-cell population parameters to aging and disease vulnerability between strains and species is in its startup phase.

An investigation of the suppression and enhancement of immune response in the mouse by a product of murine lymphoma cells, now nearing completion, has theoretical implications in regard to the interaction of normal and abnormal populations of immune cells, and practical importance in regard to the new controls that must hereafter be imposed when immunological studies are done with old mice.

The next phase of this work will examine the hypothesis that the enhancement-suppression phenomena arise from an essential aspect of the interactive regulation of immunocyte populations, which may be one of the specific vulnerable points in the aging of the immune system.

AGING RESEARCH STAFF

REGULAR STAFF

Cerny, Elizabeth A. (Scientific Assistant)
*Duffy, Peter H. (Scientific Assistant)
Flynn, Robert J. (Senior Veterinarian)
Jaroslow, Bernard N. (Immunologist)
Rahman, Yueh-Erh (Biologist)
Sacher, George A. (Senior Biologist)
Sanderson, Margaret (Scientific Associate)
Suhrbier, Katherine M. (Scientific Assistant)
Svihla, George (Biologist)
Tyler, Sylvanus A. (Mathematician)
Wright, Betty Jean (Scientific Assistant)

TEMPORARY STAFF DURING 1974

Cater, Jerome (Research Associate)
Jonah, Margaret M. (Postdoctoral Appointee)

---

*Returned to full time duties as Assistant Division Director for Animal Facilities.

COMPARATIVE METABOLISM OF AGING

George A. Sacher, Robert J. Flynn, and Peter H. Duffy

PURPOSE AND METHODS

A fundamental problem in the biology of aging is to understand why there are genetically related species of mammals that are alike in body size, dentition, diet, and ecological habitat, but differ greatly in longevity. For example, the two small wild rodent species *Mus musculus* (house mouse) and *Peromyscus leucopus* (white-footed mouse), both weigh about 25 grams, but *Mus* lives about 3 years while *Peromyscus* lives about 8 years. The major goal of the comparative program is to determine the physiological and biochemical mechanisms responsible for such differences in longevity, and the nature of the genetic control of those mechanisms.

Chronological age is not necessarily the best measure of the aging process, especially when interspecies comparisons are to be made. A better parameter is the lifetime metabolic activity of an organism. Therefore, this study is concerned with the lifetime oxygen utilizations, activities, and deep body temperatures of several species of wild and laboratory rodents, and with the relations of these parameters to longevity.

The comparative metabolism program is divided into three major segments: a) Metabolism of Wild Rodents, b) Metabolism of Thermally Stressed Rodents, and c) Genetics of Energy Metabolism of Inbred and Hybrid Mice. Variables measured in specific experiments include resting, daily average and maximum metabolic rate, rectal temperature, and food and water consumption. All of the above experiments have been, or will be, run on an open system utilizing a paramagnetic oxygen analyzer, in conjunction with a vibration-sensitive activity monitor. In some cases deep body temperatures were measured simultaneously by means of implantable temperature transducers.

PROGRESS REPORT

Resting and diurnal metabolic rates have been measured for 13 species of wild rodents maintained in our laboratory: *Peromyscus boylei, P. californicus insignis, P. crinitis, P. eremicus, P. floridanus, P. gossypinus, P. leucopus, Praomys natalensis, Baiomys taylori, Mus musculus, Oryzomys palustris, Mesocricetus auratus, and Sigmodon hispidus.* They range in weight from 8 to 150 grams. On comparing the relationship of logarithm of resting metabolic rate to logarithm of body weight for these species, one obtains a slope of -0.49, which is steeper than the slope of -0.26 in Kleiber's relation for mammals generally (1).

An experiment has been completed in which resting and average metabolic rates of *M. musculus* and *P. leucopus* were measured as a function of age on a cross-sectional basis. It was found earlier that the resting metabolism of *Mus* decreases by 40% by 2 years of age. *P. leucopus* has a slower rate of decline of resting metabolism than *Mus*, even if the decline is expressed per unit of lifespan, rather than per day. Figure 7.1 displays the resting, average, and maximum oxygen consumption of *P. leucopus* throughout a good part

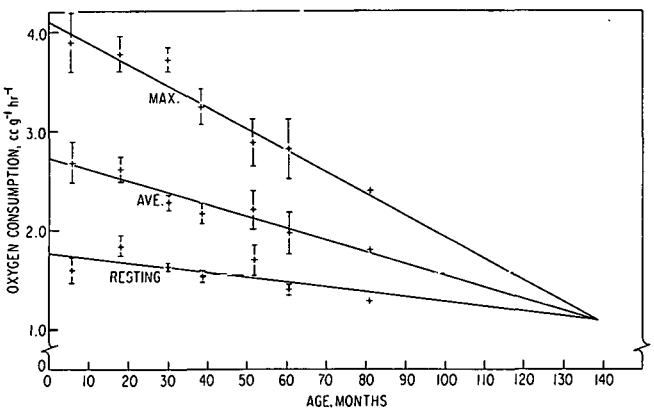

Fig. 7.1. Resting (mean daytime minimum), 24-hour average, and mean night-time maximum oxygen consumption, in ml per gram per hour for *Peromyscus leucopus*, as a function of age. Sample size, ten animals per point, except that there are seven at 60 months and one at 80 months. The three lines are fitted by least squares, and their intersection at 140 months is not forced. The maximum lifespan of *P. leucopus* in the laboratory is 100 months, and the life expectation from birth is 50 months.

of the lifespan. Comparison of the upper two lines with the resting metabolism line indicates that the metabolism of activity falls off more steeply with age than resting metabolism. Measurements of the age dependence of peak metabolism by either epinephrine injection or exposure to cold, will be undertaken to fill in the developing picture of aging of energy metabolism.

Collection of data for a genetic analysis of the metabolism of mouse genotypes in the 5 x 5 diallel design (discussed in Reference 2) has been completed. Two 6- to 8-month old males of each of the 25 genotypes in this design were measured for resting and average oxygen consumption, and food and water consumption. A preliminary analysis has been made of resting oxygen utilization as a function of body weight. The data will be analyzed by the procedure for the genetic analysis of variance (2).

REFERENCES

1. Kleiber, M. The Fire of Life, John Wiley & Sons, New York, 1961.
2. Sacher, G. A., S. A. Tyler, P. H. Duffy, and R. J. Flynn. Genetics of longevity in laboratory mice. This Report, Section 7.

COMPARATIVE MORPHOLOGY OF AGING

George A. Sacher, Robert J. Flynn, and Peter H. Duffy

PURPOSE AND METHODS

A prerequisite to a comparative approach to aging is the definition and standardization of each species to be used. This includes the measurement of the basic morphological parameters. Some information is known about growth functions of murid rodents such as the laboratory rat, *Rattus norvegicus*.

Rattus continues to grow until at least 2 years of age. Since *Mus musculus* is also a murid rodent, the question should be asked if this extended growth period is also representative of this species. *P. leucopus* is a member of the family Cricetidae. Unfortunately, the information concerning growth in this family of rodents is limited, especially concerning growth after maturity. Therefore, a study was made of growth during adult life of laboratory-bred wild-type *Mus musculus*, and *Peromyscus leucopus*. Head-plus-body length, tail length, and body weight were measured for the two species in a longitudinal series taken over a 2-year period, and in cross-sectional samples over all ages in the colony at a given time. Head-plus-body length and tail length were measured by two methods, manual and radiographic.*

PROGRESS REPORT

Four sets of longitudinal measurements have been made on the *M. musculus* and *P. leucopus* colonies at 6-month intervals, which confirm previous evidence that *Mus* continues to grow in both head-plus-body length and in tail length. Radiographic measurements on this species yielded an almost identical increase in skeletal length, confirming that the increase in length is due to bone growth. *P. leucopus*, in contrast, showed little or no growth of body weight or length after maturity. There are no evident differences between the longitudinal and cross-sectional measurements, but statistical tests remain to be done. These differences in growth parameters, and in the underlying endocrine mechanisms of growth control may have relevance to the cancer susceptibility patterns of the two species. Plans are being made to measure post-maturity growth in an inbred laboratory mouse strain, the C57BL/6 mouse, to determine whether this inbred has the indefinite growth characteristic of the wild-type mouse.

---

*The radiographic measurements were made by Ronald Douglas of St. Louis University, a participant in the 1974 Argonne Summer Institute in Biology.

COMPARATIVE STUDIES OF THE NERVOUS SYSTEM

George A. Sacher, George Svihla, Margaret H. Sanderson, Peter H. Duffy, and Robert J. Flynn

PURPOSE AND METHODS

Previous annual reports (1,2) have described the initiation and progress of a study comparing the number of myelinated fibers in optic and cervical vagus nerves of *Peromyscus leucopus*, a long-lived rodent, and *Mus musculus*, a short-lived rodent, as a function of age. Each species' lifespan is divided into seven age periods, beginning at 4 months, when the animals are young adults. Three to six animals of each sex are included in each group. Nerve sections are prepared and counted as previously described (2).

PROGRESS REPORT

The enumeration of myelinated fibers in optic and cervical vagus nerves of these species as a function of age has been completed. Since there is no statistical difference in fiber counts in the nerves studied based on sex, the mean values include all animals at each sampling period.

All optic nerve fibers are myelinated in these animals. In *P. leucopus*, optic nerve fiber counts average between 64,000 and 72,000 for the first 4 years (Figure 7.2). After 4 years, fiber counts as low as half or less the previous values are observed. Two-thirds of the animals at 5 and 6 years have counts lower than 50,000; the lowest value at 5 years is 13,000, and at 6 years, 7,000. The single 8-year-old has as many fibers as the higher 6-year-old animals. Optic nerve fibers of *Mus* average 30,000 to 40,000 and do not decrease in number through 30 months of age.

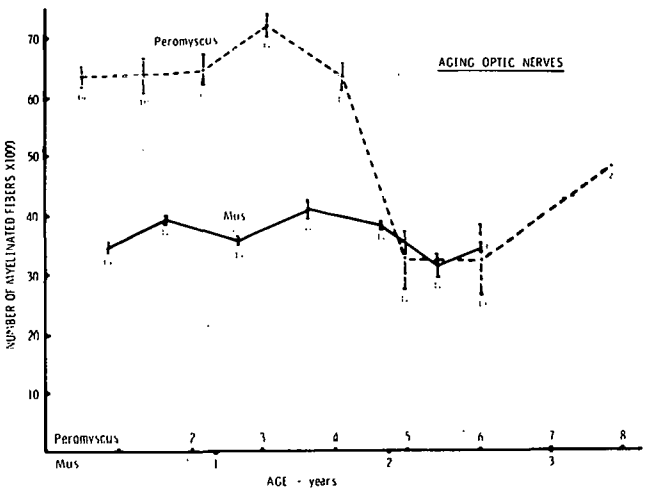

Fig. 7.2. Mean numbers of fibers in optic nerves of *Peromyscus leucopus* and *Mus musculus*, as a function of age. Vertical bars represent standard errors. Numbers of optic nerves, and animals, in the samples are also given.

In cervical vagus nerves of mammals, myelinated fibers make up 10% to 20% of the total fiber number (3,4,5). Although the number of myelinated fibers in the cervical vagus within age groups varies considerably in both *P. leucopus* and *M. musculus*, there appears to be no loss of fibers with age (Figure 7.3). Fiber counts are about 20% higher in *P. leucopus*. The apparent decrease in fibers in *P. leucopus* at 15-17 months is thought to be due to sampling variation. These data do not support the hypothesis that there is a significant rate of random loss of neural elements, at least insofar as these cranial nerve afferents and efferents are concerned. The question is still open in regard to brain neurons, but no existing technique is adequate to answer it.

Statistical analyses of size distribution and cross-sectional area of the nerve fibers as a function of age are in progress.

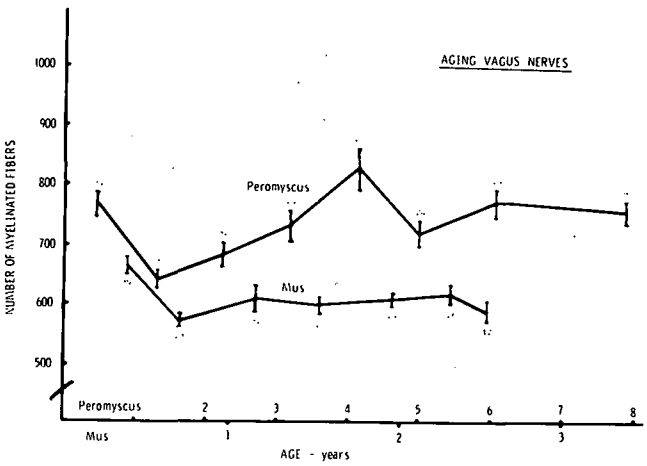

Fig. 7.3. Mean numbers of myelinated fibers in vagus nerves of *Peromyscus leucopus* and *Mus musculus* as a function of age. Bars are standard errors. Numbers of fibers, and animals in each sample are given.

REFERENCES

1. Sacher, G. A., R. J. Flynn, G. Svihla, M. H. Sanderson, and P. H. Duffy. ANL-7970 (1972), p. 74.
2. Sacher, G. A., R. J. Flynn, G. Svihla, M. H. Sanderson, B. J. Wright, and P. H. Duffy. ANL-8070 (1973), p. 86.
3. Evans, D. H. L., and J. G. Murray. J. Anat. 88, 320 (1954).
4. Friede, R. L., and T. Samorajski. J. Comp. Neurol. 130, 223 (1967).
5. Hoffman, H. H., and H. N. Schnitzlein. Anat. Rec. 139, 429 (1961).

COMPARATIVE STUDIES OF IMMUNOLOGY AND AGING

George A. Sacher, Bernard N. Jaroslow, George Svihla, and Margaret H. Sanderson

PURPOSE AND METHODS

Single-cell suspensions of mammalian spleen and brain contain cells that are functionally different, but show little morphological heterogeneity. Identification and quantitative enumeration of the subpopulations of these cells appears to be possible by taking advantage of specific antigens present in the surface structure of some of these cells. The antigenic sites can be labeled with specific fluorescent antibody and the fluorescent cells enumerated by flow-microfluorometry. Theta antigen has proved to be a useful marker for dividing splenic lymphocytes into two immunologically distinct groups: thymus-derived (T) cells, which have the antigen, and bone marrow-derived (B) cells, which lack it. We plan to apply the technique in a new way, to determine the sizes of the T and B cell populations as a function of age in short- and long-lived animal populations. Such determination is important as part of the search for the parameters of the immune system that are associated with long life. This kind of assay might also be useful for the assessment of the sizes of T and B cell populations in relation to diseases of the immune system and blood dyscrasias.

In our study of the comparative biology of aging in the nervous system of rodents, total and differential cell counts of the brain are needed in order to measure neuron loss and change of neuron:glia ratio as a function of age. Existing methods are highly inaccurate. By employing immunofluorescent labeling techniques, it may be possible to develop the methodology for enumerating neurons and glial cells directly from suitably prepared brain suspensions.

A Cytograph-Cytofluorograph (Bio/Physics Systems, Inc.) is now being standardized for photometric analyses of spleen cell suspensions. In these instruments, suspended cells flow in single file through a laser beam focused on a photosensor system. The cytograph counts, sorts by size, and differentiates unstained or stained cells, utilizing the light absorbance and scattering properties of cells. The cytofluorograph counts, sorts by size, differentiates, and characterizes cells based on light scatter and fluorescence. Total and selected counts are displayed digitally, and a multi-channel distribution analyser stores the information for histogram display on a cathode ray tube, digital printout, or x-y plot. Optimum counting rate is about 1,000 cells per second.

PROGRESS REPORT

The basic instruments have been delivered and set up. They are undergoing tests to provide operator experience and to uncover weaknesses in the instruments. Several components have failed, and have been replaced. Capabilities of the instruments are being assessed, and standardization is in progress. The comparative study of the number of T and B cells in spleens of selected rodent species as a function of age will begin in the near future. Studies of macrophage populations in the peritoneal fluid have begun, and the frequency distributions of the size parameter have a reproducible pattern of multiple modes, which is influenced by age, past history, and the health status of the animals.

ENVIRONMENTAL PHYSIOLOGY OF INTERSPECIES LONGEVITY IN MYOMORPH RODENTS

Howard W. Braham, George A. Sacher, and Sylvanus A. Tyler*

PURPOSE AND METHODS

One of our aims in research on the comparative biology of aging is to ascertain if differences in longevity between seemingly closely related species can be explained in terms of their capacities for regulation of certain basic physiologic processes.

The maintenance of internal physiological stability in animals (such as myomorph rodents) is conditioned by the need to adjust to annual, daily, and periodic variations in temperature and to random meteorological and microclimatic fluctuations. The internal stability has been shown to be in part a

---

*Thesis Parts Student, Ohio State University.

result of cycles of metabolism, activity, and body temperature that are entrained to environmental temperature and light, and are thus important in maintaining the metabolic adaptation of animals to their environments. Some of these physiological parameters, such as oxygen consumption and physical activity, seem to be more closely correlated to environmental temperature variability than with seasonal changes in temperature levels, light intensity or day length (1). Basic metabolic cycles may also change during and after exposure to ionizing radiation, but little is known about the action of radiation upon metabolic cycles.

Progressive imperfection of homeostatic invariance is believed to be an important mechanism in the aging process. It may also be important in the relative differences in longevity between species. We believe that differences in species longevity are in part a function of their capacities for metabolic adaptation to varying environments, and thus hypothesize that longer-lived rodents respond more "adaptively," by means of physiological adjustments, to complex changes in ambient conditions. The hypothesis also implies that the variance in metabolic regulations is an important factor in species longevity.

This study centers around the comparative physiological adaptive capabilities of two mammalian species (Order: Rodentia) in response to a) ambient temperature phase-changes, and b) their adjustive capacities during recovery from injury by ionizing radiation. The wild house mouse, *Mus musculus* (Family Muridae), and the white-footed mouse, *Peromyscus leucopus* (Family Cricetidae) are being used as representative myomorphs. *Mus musculus* lives to a maximum age of approximately 36 months in the laboratory; *Peromyscus leucopus* to approximately 100 months (Argonne National Laboratory rodent colony life tables).

To determine how each species adjusts to environmental temperature perturbations, it is first necessary to analyze its steady state capabilities under conditions in which the animals are entrained to consistent daily patterns. These patterns include fixed light-dark regimes, ambient temperature within or near the thermoneutral zone, and *ad libitum* food. Parameters measured include oxygen consumption, spontaneous motor activity, and deep body temperature. The response capabilities to changes in ambient temperature will be tested by varying the ambient temperature above or below the thermoneutral zone in single increments, both in phase and out of phase with the entrainment to the light-dark cycle. The animals are thereby required to respond to two imposed cycles, thus making two independent yet physiologically linked adjustments. The degradation of performance caused by aging will be compared to the degradation produced by exposure to a sublethal dose of gamma rays.

The statistical analysis will compare the time-lag correlations of metabolic responses to fluctuations in environmental temperature in the two species.

PROGRESS REPORT

Collection of data has been completed, and analysis has begun. Preliminary data show that there is significant within- and between-animal variation of metabolism, body temperature, and activity in the unperturbed condition.

REFERENCE

1. Hart, J. S. In: Comparative Physiology and Thermoregulation, Vol. II, Ed. G. C. Whittow. Academic Press, New York, 1971, p. 1.

MATURATION AND LONGEVITY IN RELATION TO CRANIAL CAPACITY IN HOMINID EVOLUTION*

George A. Sacher

Longevity of mammals is highly correlated with brain weight and body weight. This relation holds equally well for primates, and accurately predicts the lifespans of the great apes and man. The regression formula is used to estimate the lifespan of australopithecines, pithecanthropines and neanderthals. The estimates are compared with published age determinations based on skeletal changes. A factor analysis of the dimensions of 12 brain regions of 63 insectivore and primate species is reported, and it is shown that lifespan has significant partial regressions on three structural factors. It is shown that the length of the gestation period in mammals is governed by brain size, and the ages of sexual maturity of extinct hominids are estimated on the basis of brain size. Evidence is given that the adult brain:body ratio in mammals has an upper limit of 4%, so it would be possible for man's brain to increase from its present value of 2%, either by eugenic or euphenic means. The rapidity of the expansion of brain size is taken to be evidence against the hypothesis that a major reorganization of the brain took place during hominid evolution.

*Abstract of a paper to be published in the Proceedings of the IXth International Congress of Anthropological and Ethnological Sciences, Chicago, August 28-September 8, 1973.

THE USE OF ZOO ANIMALS FOR RESEARCH ON LONGEVITY AND AGING*

George A. Sacher

The role of zoos in aging research is examined in three perspectives. First, the development of new model species with desirable physiological characteristics, such as marsupials in particular. Second, the identification of species that are good models for research in degenerative or neoplastic diseases. Third--and perhaps the area providing greatest scope--comparative research, which can be done with no more invasion than a skin biopsy or a blood sample, on species differences in the mechanisms of protection and repair of DNA and other informational molecules.

*Abstract of a paper published in Research in Zoos and Aquariums, National Academy of Sciences, Washington, D. C., 1975, p. 191.

GENETICS OF LONGEVITY IN LABORATORY MICE

George A. Sacher, Sylvanus A. Tyler, Peter H. Duffy, and Robert J. Flynn

PURPOSE AND METHODS

This research program was undertaken to learn about some of the constitutive biochemical, physiological, and anatomical traits that are genetically related to length of life. The initial step was to select five inbred mouse strains and set up a 5 x 5 mating design to produce the male and female progeny to be used in a 5 x 5 diallel design. Samples of these F_1 genomes are used in a series of studies, of which the following are either under way or completed.

1. Survival and disease incidence under the conventional conditions of environment and husbandry in our animal facility (the "conventional environment" study).
2. Survival and pathology under environmental loads, including chronic gamma irradiation and low ambient temperature.
3. Anatomical measurements: body weight and length, and weights of eight organs of physically mature mice.
4. Metabolic measurements: resting and average oxygen consumption, food and water intake, and rectal temperature measured at physical maturity and at 18 months of age.
5. Population sizes of thymus-derived immunocytes, in young and old mice.

Further investigations are planned in a continuing, open-ended research program. In effect, the diallel design is our defined experimental population, filling much the same role in our research planning as some single inbred strain does in the typical aging study, with the added advantage that each experiment also adds to our knowledge about the genetic determination of longevity and aging.

The five inbred strains used in this program are listed in Table 7.1, together with the abbreviated codes used in the text and tables.

The sample size in the present experiment is approximately 12 mice of each genotype and sex. All possible crosses of the five inbred strains are included. A control group and two duration-of-life Co^{60} gamma exposure groups (43 R/day and 125 R/day) were maintained. The total experimental design entailed 5 x 5 x 2 x 12 x 3 = 1800 mice (the actual number was 1814). The complete experimental plan provides for three equal replications of the control group set up at intervals of about a year. The second replication is under way and the third is being recruited.

Table 7.1. Inbred Strains Used in the Diallel Study, Giving Standardized Nomenclature and Provenance

Standard Nomenclature	Code	Source
A/JAnl	A	ANL (Grahn)
BALB/cJAnl	C	ANL (Grahn)
C3Hf/JAnl	H	ANL (Grahn)
C57BL/6JAnl	B	ANL (Grahn)
DBA/1J	D	Jackson Lab.

All hybrids are coded as dam x sire:
A/JAnl ♀ x BALB/cJAnl ♂ F_1 is AC.

STATISTICAL METHODS

Each dose group is analyzed separately. The general design used is a modification of one developed by Griffing (1) and used by Kidwell and Howard (2). However, the analytical approach will follow "Analysis of Variance" (ANOVA) procedures, rather than the comparable "Regression" techniques, in order to exhibit more explicitly the various components of variance with specific relevance to a genetic analysis.

The ANOVA design assumes that the variables under investigation are fixed. This assumption is appropriate because they are genetically determined quantities. Tables 7.2 and 7.3 give the complete partition of components for control, 43 R, and 125 R groups. "Breeding type" distinguishes between inbred and hybrid genomes. The effect of "Crosses within sex" component in Table 7.2 is further partitioned into the contribution to the variance attributable to differences in reciprocal effects and to combining ability between genotypes (Table 7.3).

PROGRESS REPORT

The data of Table 7.2 indicate that the genetic factors governing length of life in the conventional, minimum stress environment are different from those that determine survival under lifetime exposure to medium- and high-level gamma-ray fields, and the difference increases as the level of exposure increases. For example, the term "breeding type," which is a measure of heterosis or hybrid vigor, is non-significant for the controls and highly significant for the chronically irradiated groups. Similarly, the "sex" term gets progressively larger as daily dose increases.

The analysis of variance for the 20 hybrid genomes in Table 7.3, which gives information about the inheritance of strain-specific characteristics, bears out the findings in Table 7.2. The terms for "Maternal Effect" and "Reciprocal" are large in controls and get progressively smaller in both sexes with increase of daily dose, while "General Combining Ability" and "Specific Combining Ability," vary in more complex ways.

Table 7.2. Cross-Nested ANOVA Design

Component	df	Mean Square		
		Control	43 R/day	125 R/day
Sex	1	.0015	.0056	.0970
Breeding Type	1	.0017	.0920	.0467
Sex x Breeding Type	1	.0073	< .0001	.0010
Strain	4	.0186	.0156	.0073
Strain x Sex	4	.0041	.0032	.0025
Within Genotype	( )[a]	.0010	.0009	.0004
		(536)	(566)	(562)

[a]The degrees of freedom for controls and each dose group are enclosed in parentheses.

Table 7.3. Orthogonal Partition of Male Crosses and Female Crosses

Component	df	Mean Square		
		Control	43 R/day	125 R/day
Male Crosses	19	.0043	.0040	.0018
General Combining Ability	6	.0038	.0066	.0033
Specific Combining Ability	3	.0041	.0065	.0036
Maternal Effect	4	.0040	.0014	.0006
Reciprocal Effect	6	.0051	.0020	.0003
Female Crosses	19	.0040	.0031	.0037
General Combining Ability	6	.0047	.0039	.0055
Specific Combining Ability	3	.0015	.0049	.0084
Maternal Effect	4	.0046	.0025	.0013
Reciprocal Effect	6	.0041	.0018	.0011

We can account for the greater part of the variance of survival times of the 25 genomes, 2 sexes, and 3 dose levels by means of 2 genetic factors (Figure 7.4). These are the "Male Longevity Factor," which is so named because control males have the highest loading on it, and the "Radiation Survival Factor," defined by the high loadings of males and females at 125 R/day. The two sexes at 43 R/day have intermediate loadings on both factors. Survival of control females is not governed by these two factors.

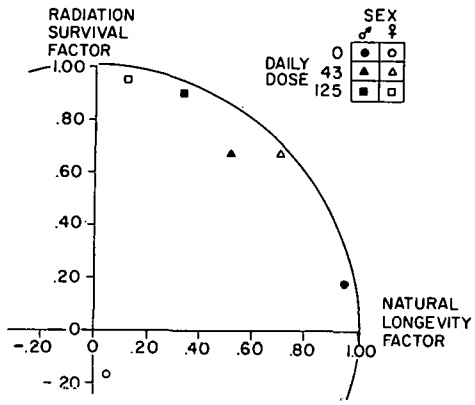

Fig. 7.4. Two-factor relationship of general combining ability for survival of 25 mouse genomes as a function of daily gamma ray dose and sex.

The findings to date are highly encouraging for our program of analyzing the complex genetics of longevity by assigning the genetic-longevity variance to physiological and anatomical factors that can then be further analyzed genetically. Some anatomical correlates have already been found, relations to metabolic factors are now under study (3), and the study of small environmental modifications will shortly begin with the setting up of a diallel design in the cold-environment chamber, which is now operational after the completion of some major improvements in humidity control. Introduction of long-term experiments is now waiting for the installation of animal cage racks.

REFERENCES

1. Griffing, B. Aust. J. Biol. Sci. 8, 463 (1956).
2. Kidwell, J. F., and A. Howard. Growth 33, 269 (1969).
3. Sacher, G. A., R. J. Flynn, and P. H. Duffy. Comparative metabolism of aging. This Report, Section 7.

DRUG DEPRESSION OF CNS MEMBRANE TRANSPORT*

Harold H. Harsch† *and Yueh-Erh Rahman*

Several anesthetics and drugs are known to depress the respiration of brain homogenates or brain slices. However, specific effects of these drugs on neurons have not been proved.

The existence of a unique high-affinity, carrier-mediated glucose transport system in rat synaptosomes was reported by Diamond and Fishman (Nature, London 242, 122, 1973). In the present study, various neuropharmacological drugs were examined for their effect on the high-affinity sugar transport system that was also found to be present in mouse synaptosomes. Synaptosomes

*Abstract of a paper published in Clinical Research and Texas Reports of Biology and Medicine, 1974.

†Participant in the 1973 Summer Institute in Biology, Medical College of Wisconsin.

were isolated from mouse cerebral cortex by a modified Ficoll-sucrose gradient method. Transport activity was measured by monitoring the uptake of tritium-labeled 2-deoxyglucose (^{3}H-2-DG) by the synaptosomes in specific incubation media. The half-maximal uptake (Km) of ^{3}H-2-DG was 0.22 mM. Pentobarbital and chlorpromazine at 0.1 mM depressed the ^{3}H-2-DG uptake. Further studies, utilizing synaptosomes from pentobarbital-anesthetized mice, indicated that the transport of glucose is depressed *in vivo* by this anesthetic.

TISSUE UPTAKE OF LIPOSOMES VARYING IN SURFACE PROPERTIES

Margaret M. Jonah and Yueh-Erh Rahman

PURPOSE AND METHODS

Delivery of a drug to a specific target tissue is an important problem in chemotherapy. Intracellular penetration as well as increased tissue uptake and retention of liposome-encapsulated drugs have been demonstrated in mice (1,2). Selective tissue distribution of drugs encapsulated in liposomes (lipid spherules) might be achieved by varying liposomal surface properties, such as surface charge or membrane fluidity. Addition of lipids bearing charged functional groups or alteration of liposomal cholesterol content are typical means of varying these liposomal surface properties. Some *in vitro* effects of liposomal membrane charge or fluidity reported by other workers include: preferential interaction of aggregated ("membrane active") immunoglobulin G with positively charged liposomes (3), and calcium dependent induction of fusion of cells in culture by negatively charged liposomes which possess fluid bilayers (4). However, there has been no *in vivo* examination of interactions between specific, competing tissues and liposomes of various lipid compositions.

Basic variations of liposomal charge and fluidity can be achieved by using different types of lipid to form the lipid bilayers of the liposomes. Synthetic phospholipids with defined fatty acid content and position are available. Bacterial phospholipids with branched chains or cyclopropane fatty acids can be similarly studied to test bilayer fluidity effects. Different types of polar lipids, such as phosphatidylinositol, glycolipids lacking formal charge, and o-aminoacyl phosphatidylglycerols, might produce greater tissue specificity.

Incorporation of lipid-soluble drugs into liposomal bilayers introduces new possibilities for specific drug delivery. Actinomycin D can be incorporated into either the lipid bilayers or the aqueous compartments of liposomes; tissue distributions of these two types of liposomes are very different (5). The use of lipid-soluble steroid hormones, which themselves are recognized by specific tissues, might confer specificity upon liposomes. A hormone on the bilayer surface might then direct another drug, encapsulated within the liposome, to a hormone sensitive target tissue.

A series of liposomes containing ^{14}C-ethylenediaminetetraacetic acid (^{14}C-EDTA) with different lipid compositions was prepared: electrophoretically

neutral liposomes made of phosphatidylcholine and varying proportions of cholesterol; negatively charged liposomes made of phosphatidylserine, phosphatidylcholine, and in some cases, cholesterol; and positively charged liposomes made of stearylamine, phosphatidylcholine and cholesterol. Each liposome preparation was injected intravenously into CF#1 mice and tissue levels of ^{14}C-EDTA were determined at intervals between 5 minutes and 24 hours. Permeability of the different liposomes to ^{14}C-EDTA was measured after *in vitro* incubation at 37°C for intervals between 0 minutes and 18 hours. Other liposomes containing different phospholipids, steroid hormones, α-tocopherol, and stearylamine with aqueous actinomycin D were also tested *in vitro*.

PROGRESS REPORT

Neutral liposomes made with mixtures of phosphatidylcholine and cholesterol, either in 3:1 or 1:1 weight ratio, show a greater uptake in certain tissues, particularly the spleen, than liposomes made only with phosphatidylcholine. Uptake of ^{14}C-EDTA by spleen and marrow was highest from negatively charged liposomes. Uptake of ^{14}C-EDTA by lungs was highest from positively charged liposomes; lungs and brain retained relatively high levels of EDTA from these liposomes between 1 and 6 hours after injection. Liver uptake of EDTA from positively or negatively charged liposomes was similar.

The *in vitro* leakage of ^{14}C-EDTA from all neutral liposomes was never greater than 6%, after 18 hours incubation, of the total incorporated activity; neutral liposomes lacking cholesterol showed slightly greater permeability than those with cholesterol. Negatively charged liposomes made of phosphatidylserine, phosphatidylcholine, and cholesterol released up to 46% of incorporated ^{14}C-EDTA after 6.5 hours. Positively charged liposomes containing stearylamine, phosphatidylcholine, and cholesterol released only 18% of incorporated radioactivity in 6.5 hours.

Other common phospholipids were tested for feasibility of use in liposome preparation; cardiolipin, phosphatidic acid, and phosphatidylinositol could all be incorporated into liposomes containing phosphatidylcholine. Inclusion of cholesterol into these liposome preparations occasionally prevented liposome formation.

Liposomes containing α-tocopherol, estrone, progesterone, testosterone, and testosterone acetate in the lipid phase were successfully prepared. A pilot study of *in vivo* distribution of neutral liposomes containing ^{3}H-testosterone indicated measurable tissue levels of the hormone 30 minutes after liposome injection.

The effect of pH on incorporation of ^{14}C-EDTA and $^{45}CaNa_2DTPA$ into neutral liposomes as well as on incorporation of ^{3}H-actinomycin D into positively charged liposomes containing stearylamine was tested. No definite pH optima were observed.

DISCUSSION

The greater tissue uptake of neutral EDTA liposomes containing cholesterol is probably due chiefly to the stabilizing effect of cholesterol on lipid

bilayers, with resultant decrease in bilayer permeability, although a degree of preferential cellular membrane interaction with cholesterol-containing liposomes cannot be ruled out. Because cell surfaces bear a net negative charge, greater uptake of a drug encapsulated in positively charged liposomes might be expected; this was observed in lung, but not in spleen and marrow. There is evidence, however, for non-homogeneous distribution of negatively charged groups on both normal and ascites cell surfaces (6,7), as well as for a mediating influence of Ca^{++} in cellular and liposomal membrane fusion (4). Furthermore, interactions of some proteins with positively (3) or negatively (8) charged liposomes require prior conformational changes in the protein. Preferential interaction of some tissues with negatively charged liposomes may therefore be a specific property of the cell surfaces in question.

CONCLUSIONS

Selective tissue uptake of liposome-encapsulated drugs is possible. Further development of drug-liposome systems is required to understand the observed variations in tissue distribution and the interactions of liposomal and cellular membranes. Knowledge of specific cellular-liposomal interactions and ability to prepare liposome-encapsulated drugs with desired surface properties could provide powerful tools both for chemotherapy and basic research.

REFERENCES

1. Rahman, Y. E., and B. J. Wright. J. Cell Biol. 59, 276a (1973).
2. Rahman, Y. E., M. W. Rosenthal, E. A. Cerny, and E. S. Moretti. J. Lab. Clin. Med. 83, 640 (1974).
3. Weissman, G., A. Brand, and E. C. Franklin. J. Clin. Invest. 53, 536 (1974).
4. Papahadjopoulos, D., G. Poste, and B. E. Schaeffer. Biochim. Biophys. Acta 323, 23 (1973).
5. Rahman, Y. E., W. E. Kisieleski, E. M. Buess, and E. A. Cerny. Tissue distribution of liposomes containing actinomycin D. This Report, Section 7.
6. Weiss, L., R. Zeigel, O. S. Jung, and I. D. J. Bross. Exp. Cell Res. 70, 57 (1972).
7. Weiss, L., O. S. Jung, and R. Ziegel. Int. J. Cancer 9, 48 (1972).
8. Calissano, P., S. Alemà, and P. Fasella. Biochemistry 13, 4553 (1974).

PREPARATION OF LIPOSOME-ENCAPSULATED DRUGS

Elizabeth A. Cerny and Yueh-Erh Rahman

PURPOSE AND METHODS

The usefulness of some drugs is limited by their low uptake into cells, their excessive toxicity, or their rapid excretion from the animal body. The chelating agent ethylenediaminetetraacetic acid (EDTA) has been found to have increased tissue uptake and retention time when encapsulated within liposomes.

The liposome-encapsulated chelating agent was more effective in removing toxic metals from mice (1). These studies suggest that the method of liposome encapsulation could be beneficially applied to other drugs as well. We have studied the possibilities of liposome encapsulation of three classes of drugs: (a) chelating agents in addition to EDTA; (b) anti-tumor drugs; and (c) radioprotective agents.

In our standard procedure for preparation of liposomes, we first dry the chloroform-dissolved lipids to give a thin, even film on the inside wall of a round bottom flask. An aqueous electrolyte solution, usually containing the drug, is then added to the flask with constant stirring by a small magnetic mixer. The flask is rotated to bring each area of the film into contact with the stirring aqueous phase until all of the film is removed from the glass wall. This process is carried out in a water bath on a hot plate mixer to control the temperature at 37°C. The liposomes thus prepared contain the drug in the aqueous center and between the lipid bilayers of the liposomes and are called aqueous phase liposomes (APL).

Modifications of this standard procedure are sometimes necessary for the preparation of liposomes with different characteristics or for the successful encapsulation of a given drug. First, the lipid constituents or proportions may be altered. Phosphatidylcholine (PC) and cholesterol, varying from 3:1 to 1:1 by weight have been used in most cases (1,2). We have used phosphatidylserine or stearylamine to prepare liposomes with either negative or positive surface charge. We also have used synthetic PC with known fatty acids. Second, the electrolyte used in the aqueous phase may be changed depending on the drug used. We have found the divalent cations of Ca^{2+} necessary with some drugs, while the monovalent cations of Na^{1+} give better results with other drugs. Most of our liposome preparations are made at 37°C, but with the saturated phospholipids such as dipalmitoyl PC, a temperature of 60°C is used. Third, a drug can be incorporated into the lipid bilayers of the liposomes, rather than in the aqueous phase, if the drug is soluble in lipid solvents. In this case a mixture of drug-lipid in chloroform is dried on the flask and the resulting liposomes are called lipid phase liposomes (LPL).

Our criteria for a successful liposomal preparation are mainly morphological. A drop of the preparation is examined under a phase contrast polarizing microscope. A good preparation has many liposomes which are round and fairly uniform in size and are well separated from each other. The liposomes should also show the typical lipid birefringence under the polarized light. The presence of clumps of liposomes, very large and irregularly-shaped liposomes, or a lack of birefringence indicate a poor preparation. When a radioactively labeled drug is used, the amount of drug incorporated into the liposomes can be measured and morphologically good preparations usually have higher incorporation than do poor preparations.

PROGRESS REPORT

The chelating agents we have used are DTPA and penicillamine, in addition to EDTA. Both have been successfully encapsulated within liposomes, and the DTPA liposomes have been used to treat ^{239}Pu and ^{210}Pb-injected mice. The DTPA encapsulated in liposomes was more effective in removing both plutonium and lead from mouse tissue than was free DTPA solution (1). The following

anti-tumor agents were successfully encapsulated within liposomes: actinomycin D (act. D), daunorubicine (daunomycin), mitomycin D, puromycin, cycloheximide, mechlorethamine (Mustargen), cytarabine (Cytosar), and doxorubicin (adriamycin). Most of these anti-tumor agents have so far only been prepared in aqueous solutions. For act. D and adriamycin, the lipid phase liposomes have also been successfully prepared. We found that purity of the lipids used is a crucial factor for satisfactory preparations of liposomes. Partially degraded or oxidized phospholipids are unsuitable for liposome-drug preparations.

The radioprotective drugs that we have tested for incorporation into liposomes are: glutathione, cysteine, cystamine, cysteamine, AET, MEA, WR638H, WR2721C, WR2529, and WR1065. Of these, only glutathione could be encapsulated within liposomes. These are all very reactive drugs and apparently quickly react with the lipids in such a fashion that the bilayer arrangement of the lipids is no longer preserved so that liposomes cannot be formed. The reactive sulfur atoms in many of these drugs are probably involved.

CONCLUSIONS

A number of chelating agents and anti-tumor agents can be encapsulated within liposomes. Actinomycin D and adriamycin can be incorporated into either the aqueous or lipid phases of the liposomes. However, most radioprotective agents cannot be encapsulated within liposomes. The benefit of drug incorporation into liposomes lies in increasing the level and biological life of the drug within the cells of the animal, resulting in more efficient treatment. So far, studies have been done only with liposomal EDTA, or DTPA, and liposomes containing act. D. Studies with other chelating agents and anti-tumor drugs will be initiated.

REFERENCES

1. Rahman, Y. E., M. W. Rosenthal, and E. A. Cerny. Science 180, 300 (1973).
2. Rahman, Y. E., M. W. Rosenthal, E. A. Cerny, and E. S. Moretti. J. Lab. Clin. Med. 83, 640 (1974).

MORPHOLOGICAL IDENTIFICATION OF CELL TYPES CAPABLE OF LIPOSOME UPTAKE

Betty Jean Wright and Yueh-Erh Rahman

PURPOSE AND METHODS

Drugs, such as chelating agents or anti-tumor agents, have been successfully encapsulated within liposomes (1,2). A radioactive chelating agent incorporated into the liposome demonstrates a higher concentration and longer retention time within certain tissues (3). Liposome encapsulation of drugs has been shown to be useful in the treatment of metal poisoning and cancer (1,2).

In order to apply liposome-encapsulated drugs successfully in therapy it is important to identify the types of cells that take up liposomes. Morphological identification of these cell types by electron microscopy has been initiated.

Liver, lungs, and spleen, tissues that have been shown to contain a high concentration of the liposome-encapsulated ethylenediaminetetraacetic acid (EDTA) (3), were selected for electron microscopic study. Tissue samples were obtained at chosen time intervals from mice injected intravenously with liposome-encapsulated EDTA. Standard electron microscope preparations of these tissues were made and examined. In addition, one representative type of tumor cell, the Ehrlich ascites tumor cell, was treated with liposome-encapsulated actinomycin D and examined by electron microscopy (4).

PROGRESS REPORT

In the liver, liposomes are found in the cytoplasm of both the parenchymal cells and the Kupffer cells within 15 minutes after injection. In the lungs, most of the liposomes are found in the lumen of the capillaries, but liposomes have been noted in some eosinophils. Although liposomes were expected within the alveolar phagocytes, they have not thus far been firmly identified within these cells. The spleen exhibits a wider variety of cell types that contain liposomes--lymphocytes and both fixed and free reticuloendothelial cells. Liposomes are also found in the cytoplasm of the Ehrlich ascites tumor cell.

Liposomes have been identified within all the tissues examined. These preliminary studies using only liposomes composed of lecithin and cholesterol, and containing EDTA, show that not all of the different cell types within a tissue appear to take up liposomes. Nevertheless, they provide morphological evidence for the direct delivery of the encapsulated drugs to their site of action. This morphological study thus yields qualitative information which complements the quantitative studies using gradient centrifugation techniques for cell fractionation of various tissues (5,6).

REFERENCES

1. Rahman, Y. E., M. W. Rosenthal, and E. A. Cerny. Science 180, 300 (1973).
2. Rahman, Y. E., E. A. Cerny, S. L. Tollaksen, B. J. Wright, S. L. Nance, and J. F. Thomson. Proc. Soc. Exp. Biol. Med. 146, 1173 (1974).
3. Rahman, Y. E., M. W. Rosenthal, E. A. Cerny, and E. S. Moretti. J. Lab. Clin. Med. 83, 640 (1974).
4. Wright, B. J., G. Svihla, and Y. E. Rahman. Liposome-encapsulated actinomycin D and increased effectiveness in Ehrlich ascites tumor killing. A morphological study. This Report, Section 7.
5. Thomson, J. F., S. L. Nance, S. L. Tollaksen, E. A. Cerny, and Y. E. Rahman. Incorporation of liposomes into spleen cells. This Report, Section 8.
6. Thomson, J. F., S. L. Tollaksen, S. L. Nance, E. A. Cerny, and Y. E. Rahman. Liver fractionations using sucrose gradients to study mechanism of drug release from liposomes. This Report, Section 8.

LIPOSOMES CONTAINING CHELATING AGENTS. CELLULAR PENETRATION AND A POSSIBLE MECHANISM OF METAL REMOVAL*

Yueh-Erh Rahman and Betty Jean Wright

Electron microscopic studies were done on mouse liver, 5 minutes through 8 weeks after an intravenous injection of liposomes containing EDTA. Liposomes were shown to be phagocytized by hepatocytes as well as by Kupffer cells within minutes after the injection. Initially, there was a close contact between the liposomal membrane and the cellular membrane, followed by an invagination of the latter and the formation of a distinct vesicle surrounding a single liposome or a cluster of several liposomes. Between 15 minutes to 6 hours after liposome injection, the Kupffer cells showed an increased number of lysosomes and autophagic vacuoles. Within the latter, morphologically intact liposomes or remnants of liposomes could be seen. At 12 hours after injection, a striking increase in macrophages was observed in the sinusoids; within these macrophages, remnants of liposomes could occasionally be observed. However, the origin and the physiological role of these cells are unknown. In the hepatocytes, morphological changes were first observed 24 hours after injection; there were large numbers of autophagic vacuoles and some cells showed extensive areas of focal cytoplasmic degeneration. The morphology of the liver cells returned to normal about 7 days after injection. A possible mechanism through which the liposome-encapsulated chelating agents can successfully remove intracellular toxic metals is discussed. The use of liposomes as carriers seems to be a useful tool for intracellular delivery of chelating agents or drugs in general.

---

*Abstract of a paper published in the Journal of Cellular Biology, 65, 112 (1975).

LIPOSOME-ENCAPSULATED ACTINOMYCIN D: POTENTIAL IN CANCER CHEMOTHERAPY*

Yueh-Erh Rahman, Elizabeth A. Cerny, Sandra L. Tollaksen, Betty Jean Wright, Sharron L. Nance, and John F. Thomson

Actinomycin D, when encapsulated within liposomes, is less toxic to mice than the nonencapsulated form. A single dose (0.75 mg/kg) or multiple doses (1 x 0.50, 4 x 0.25 mg/kg) significantly increased the mean survival time of mice inoculated with Ehrlich ascites tumor cells. Liposomes containing actinomycin D were found in tumor cells and cell degeneration and death were subsequently observed.

---

*Abstract of a paper published in the Proceedings of the Society for Experimental Biology and Medicine 146, 1173 (1974).

STUDIES ON THE TOXICITY OF LIPOSOME-ENCAPSULATED ANTI-TUMOR DRUGS

Yueh-Erh Rahman, Elaine H. Callahan, Elizabeth A. Cerny, Jane L. Hulesch, and E. John Ainsworth*

PURPOSE AND METHODS

Anti-tumor drugs are highly toxic. Their toxicity is commonly manifested in the rapidly dividing cell systems such as the bone marrow and the intestinal epithelium. Liposome-encapsulated actinomycin D was found to be less toxic to mice than the nonencapsulated form (1). The mechanism of this decrease in toxicity is unknown. We are therefore conducting comparative studies on the toxicity of an anti-tumor drug in its liposome-encapsulated and nonencapsulated forms. The toxicity studies are divided into three categories: 1) gross toxicity--as measured by survival time and altered physiological symptoms; 2) cellular toxicity--this study involves the histological examination of the blood forming cells, the intestinal epithelial cells, and also the heart tissues, since this latter organ is known to be especially sensitive to some anti-tumor drugs; 3) toxicity at the molecular level--this study involves comparison of the inhibition of nucleic acid synthesis in various tissues known to be sensitive to anti-tumor drugs.

The methods used are: cell counts of blood cells and bone marrow cells; histological examination of the tissues relevant to the study; examination of the capacity of stem cell formation in the bone marrow and the spleen by the method of spleen colony unit (CFU) formation; and biochemical methods for determination of nucleic acid synthesis.

PROGRESS REPORT

Table 7.4 shows the effect of actinomycin D (24 hours after injection of 0.4 mg/kg) on mouse peripheral blood cells, bone marrow cells, and stem cells of the spleen and the bone marrow. No difference was found in red blood cell numbers among control mice and those receiving either the nonencapsulated or the liposome-encapsulated actinomycin D. However, a striking protective effect of liposome encapsulation was found for white blood cells (WBC), bone marrow cells (BMC), and stem cells from spleen and bone marrow.

The effects of actinomycin D on WBC and BMC 1, 2, 3, 4, 6, and 8 days after injection of 0.4 mg/kg were also studied. For WBC, there was about 60% inhibition by the nonencapsulated actinomycin D from day 1 through day 3, a slight recovery at day 4, but still an inhibition of 40% at day 8 after injection. In mice receiving liposome-encapsulated actinomycin D, there was about 20% inhibition of the WBC compared to the control mice, between day 2 and day 6. However, complete recovery was found at day 8. For BMC, from day 1 through day 3, there was 40% inhibition in mice receiving the nonencapsulated actinomycin D, significant recovery at day 4, and complete recovery at day 6. In mice receiving the liposome-encapsulated actinomycin D, there was only 15% inhibition from day 1 through day 4, and complete recovery at day 6.

---

*Participant in the 1974 Summer Institute in Biology, Monmouth College.

Table 7.4. Effect of Actinomycin D on Mouse Peripheral Blood Cells, Bone Marrow Cells, and Stem Cells of the Spleen and the Bone Marrow 24 Hours after Injection of 0.4 Mg/Kg

	RBC/µl ($\times 10^{-6}$)	WBC/µl ($\times 10^{-3}$)	BMC/Tibia ($\times 10^{-6}$)	CFU/Spleen[a]	CFU/Femur[a]
Control	7.73	3.68	7.34	2357 (1909-2805)	5743 (5009-6476)
Free Actinomycin D	7.76	2.66	4.61	180 (108-252)	2147 (1861-2432)
Liposomal Actinomycin D[b]	8.13	4.49	6.20	1980 (1491-2462)	6257 (5340-7175)

[a]Average value, with range shown in parentheses.

[b]Actinomycin D was encapsulated within the aqueous phase of liposomes.

CONCLUSIONS

Significant protection of the blood-forming system by liposome-encapsulation of an anti-tumor drug, actinomycin D, was found. So far only liposomes with actinomycin D incorporated in the aqueous phase have been studied. Similar studies with actinomycin D in the lipid phase of the liposomes will be conducted. Toxicity on the intestinal epithelium as well as comparative studies of actinomycin D in nonencapsulated and liposome-encapsulated forms on the nucleic acid synthesis in various tissue systems will be initiated.

REFERENCE

1. Rahman, Y. E., E. A. Cerny, S. L. Tollaksen, B. J. Wright, S. L. Nance, and J. F. Thomson. Proc. Soc. Exp. Biol. Med. 146, 1173 (1974).

TISSUE DISTRIBUTION OF LIPOSOMES CONTAINING ACTINOMYCIN D

Yueh-Erh Rahman, Walter E. Kisieleski, Evelyn M. Buess, and Elizabeth A. Cerny

PURPOSE AND METHODS

Actinomycin D, an antibiotic with known inhibitory effect on certain tumors (1,4), has been encapsulated within liposomes in two different ways: 1) When actinomycin D is encapsulated in the aqueous solution existing in the center and between the lipid bilayers of the liposomes, the liposomes are called "aqueous phase liposomes" (APL). 2) When actinomycin D is incorporated

as part of the lipid bilayers which form the outer shells of the liposomes, the liposomes are called "lipid phase liposomes" (LPL). APL and LPL are obviously different in their surface properties. A comparative study of their distribution in mouse tissues might therefore give us some insight into the problem of tissue selectivity, which could eventually lead to the ability to deliver a liposome-encapsulated drug to a specific tissue.

Liposomes were prepared with ^{3}H-actinomycin D either in the aqueous phase or in the lipid phase. They were injected intravenously or intraperitoneally into mice, and groups of 4 mice were killed at different time intervals up to 48 hours after the injection. Liver, lungs, spleen, thymus, brain, kidneys, the entire intestine, samples of blood, bone marrow from both tibias, urinary bladder, and in some animals, samples of muscle and skin were taken for radioactivity analysis. Each sample, wrapped in a filter paper, was pressed in a pellet press before combustion in a Packard 305 sample oxidizer. Tritium activity was analyzed in a Beckman liquid scintillation counter.

PROGRESS REPORT

After intravenous or intraperitoneal injections, the disappearance from blood of actinomycin D transported in LPL was faster than the disappearance of actinomycin D transported in ALP. In mice receiving LPL, all the tissues analysed had a significantly higher concentration of actinomycin D than tissues of mice receiving APL, with the exception of the kidneys and the intestine, where negligible actinomycin D was found in LPL-injected mice. After intravenous injection, there was a strikingly high concentration of the LPL actinomycin D in the lungs which persisted for as long as 24 hours. The highest uptake of LPL actinomycin D in the spleen and the bone marrow was at 24 hours after the liposome injection, when the actinomycin D concentration in the liver and lungs had started to decline.

CONCLUSION

Actinomycin D can be incorporated either in the aqueous or in the lipid phase of the liposomes. The two types of liposomes gave a different distribution pattern in mouse tissues. This tissue selectivity provides us with a useful tool to unravel the complex problems of tissue and cell membrane specificity.

REFERENCES

1. Farber, S. In: Ciba Foundation Symposium on Amino Acids and Peptides with Antimetabolic Activity, Eds., G. E. W. Wolstenholme and C. M. O'Connor. Little, Brown, Boston, 1958, p. 138.
2. Colebatch, J. H., R. Howard, A. L. Williams, G. R. Kurrle, and A. C. L. Clark. Acta Unio Int. Contra Cancrum 20, 491 (1964).
3. Ross, G. T., L. L. Stolbach, and R. Hertz. Cancer Res. 22, 1015 (1962).
4. Oettgen, H. R., P. Clifford, and D. Burkitt. Cancer Chemother. Rep. 28, 25 (1963).

LIPOSOME-ENCAPSULATED ACTINOMYCIN D AND INCREASED EFFECTIVENESS IN EHRLICH ASCITES TUMOR KILLING. A MORPHOLOGICAL STUDY

Betty Jean Wright, George Svihla, and Yueh-Erh Rahman

PURPOSE AND METHODS

The actinomycins, antibiotics derived from *Streptomyces*, inhibit the growth of certain tumors both in animals and man. However, most anti-tumor agents, including actinomycin D, are extremely toxic, even in therapeutic doses. A liposome-encapsulated chelating drug, ethylenediaminetetraacetic acid (EDTA), has demonstrated a selective uptake (1) in certain tissues. Therefore, an attempt has been made to encapsulate other drugs within liposomes. Tissue specificity for liposome-encapsulated drugs could permit an increased therapeutic effect and a decreased systemic toxicity.

The successful encapsulation of actinomycin D into liposomes and its reduced toxicity to mice has been reported by Rahman et al. (2). Further, the effectiveness of actinomycin D as an anti-tumor agent in mice bearing Ehrlich ascites tumor cells appears to be enhanced when it is encapsulated within liposomes (2).

Microscopic studies on the Ehrlich ascites tumor cell were undertaken for two purposes: first, to demonstrate morphologically the uptake of liposomes containing actinomycin D in the aqueous phase by a tumor cell known to be phagocytic; and second, to follow morphologically the kinetics of tumor cell killing by encapsulated and nonencapsulated actinomycin D. Female CF#1 mice were inoculated by intraperitoneal injection with 20×10^6 Ehrlich ascites tumor cells. Five days after inoculation the mice were injected, by the same route, with one of the following: 1) 0.4 ml 8 mM $CaCl_2$, 2) nonencapsulated actinomycin D (1 mg/kg) in 8 mM $CaCl_2$, or 3) liposome-encapsulated actinomycin D (1 mg/kg). At intervals of 1, 3, 6, 12, 24, and 48 hours after treatment and also at 5 and 7 days for the group given liposome-encapsulated actinomycin D, 0.2 ml of ascitic fluid was aspirated with a syringe from the abdominal cavity of the mouse. A drop of the undiluted fluid was examined immediately with the light microscope and representative fields were photographed. Standard electron microscope preparations of the remaining fluid from each treatment group at each time interval were made.

PROGRESS REPORT

Morphological changes in the tumor cells can be seen as early as 1 hour after administration of actinomycin D. Liposomes are found in the cytoplasm of the cells. Both treatment groups have dead or dying cells, as indicated by the condensation of the nucleolus and chromatin and by the presence of ribosome-like particles in the nucleus. The cytoplasm contains clumps of ribosomes, an increase in lipid droplets, lysosomes and autophagic vacuoles, and a decrease in microvilli. At 6 hours after actinomycin D treatment, there are considerably fewer cells present in preparations from liposome-encapsulated actinomycin D treated animals. The same types of degenerating cells are present as at earlier times. By 12 hours, the number of Ehrlich ascites tumor cells has decreased in both actinomycin D treatment groups, but the effect of

liposomal actinomycin D is more pronounced at the ultrastructural level. Significant repopulation of Ehrlich ascites tumor cells in both actinomycin D treatment groups has occurred at 48 hours after treatment. Damaged cells are still present and the liposome-treated cells show more extreme degenerative changes. Animals receiving free actinomycin D do not survive much beyond 48 hours after injection due to the toxicity of such a high dose of actinomycin D. Mice treated with liposome-encapsulated actinomycin D survive over 7 days post-injection. Cells from animals treated 5 or 7 days previously do not show any morphological changes different from those observed at earlier times.

CONCLUSIONS

Liposomes containing actinomycin D are readily taken up by Ehrlich ascites tumor cells. This morphological study shows that Ehrlich ascites tumor cells treated with liposome-encapsulated actinomycin D exhibit more severe ultrastructural damage than tumor cells treated with free actinomycin D, although the basic cellular responses are similar. Liposomal actinomycin D has a higher and earlier cell killing capacity than free actinomycin D. Liposome-encapsulation of anti-tumor agents provides a means for effective direct delivery to the target cell. The results of this study, using a model tumor cell and one anti-tumor drug, are sufficiently encouraging to justify trials with other liposome-encapsulated anti-tumor agents on other tumor cell populations.

REFERENCES

1. Rahman, Y. E., M. W. Rosenthal, E. A. Cerny, and E. S. Moretti, J. Lab. Clin. Med. 83, 640 (1974).
2. Rahman, Y. E., E. A. Cerny, S. L. Tollaksen, B. J. Wright, S. L. Nance, and J. F. Thomson. Proc. Soc. Exp. Biol. Med. 146, 1173 (1974).

RESTORATION OF ANTIBODY-FORMING CAPACITY IN AGING MICE

*Bernard N. Jaroslow and Rosanne Fidelus**

PURPOSE AND METHODS

The decline of immune responsiveness with age has been well documented and reviewed (1). The major factors in this decline are: a) a decrease in the number of cells that respond to an initial antigenic stimulus (2); b) the lower proliferative capacity of the responding cells (3); and c) an unfavorable host environment and immunosuppressive diseases that interfere with the responsiveness of immunocompetent cells (4,5).

---

*Spring 1974 participant in the Undergraduate Honors Research, Participation Program, College of St. Francis, Joliet, Ill.

In an earlier study (3) we demonstrated that multiple injections of bacteriophage restored antibody-forming capacity in aging beagles. To determine the universality of the phenomenon we attempted to restore antibody-forming capacity in aging mice immunized with sheep red blood cells (SRBC).

C57BL/6 mice were immunized with single or multiple injections of SRBC over a 100-fold range of antigen doses. Spleens were assayed for antibody-forming cells by the Jerne plaque assay (6). To obtain the peak response for IgM producing cells, we assayed on days 4, 5, and 6 after the first injection of SRBC; and for peak IgG producing cells, we assayed on days 11, 13, and 15. In all experiments, a group of mice given a single injection was treated and assayed at the same time with a group given multiple injections.

PROGRESS REPORT

We determined the mean log peak production of IgM plaque-forming cells (PFC) per spleen in groups of 5 young and 5 old mice. They were given one injection, four injections in 36 hours, or six injections in 10 hours, of SRBC at six doses over a range from 1.6×10^8 to 1×10^{10} SRBC/injection. The young mice produced more IgM plaque-forming cells than did the old mice at all the antigen doses and with both injection protocols shown in Figure 7.5. The results were the same in more limited experiments with six injections and with 500- as well as 600-day-old mice instead of 700-day-old mice.

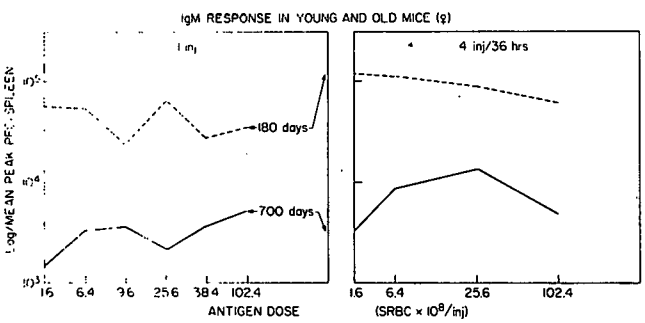

Fig. 7.5. Peak IgM plaque-forming cell production in young (225-day-old) and old (700-day-old) mice given single or multiple injections of sheep red blood cells over a 100-fold dose range.

When we tested the restorative effects of multiple antigen injections on IgG plaque-forming cells we observed complete restoration of antibody-forming capacity in old mice at two antigen doses and with two multiple injection protocols (Figure 7.6). The response to single injections was, as expected, higher in 225-day-old than in 585-day-old mice.

CONCLUSIONS

The continued presence of antigen can maintain IgG antibody-forming cells in the proliferative phase in mice given SRBC as well as in dogs given coliphage (3). We could not correct the age-associated defect for IgM plaque-forming cells. Our results extend the earlier observation that the IgM response of mice to a single injection of SRBC over a similar dose range did not overcome the defect (2).

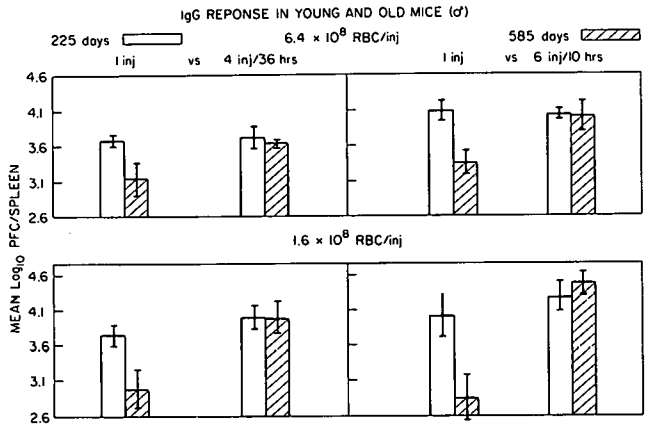

Fig. 7.6. Peak IgG plaque-forming cell production in young (225-day-old) and old (585-day-old) mice given single or multiple injections of sheep red blood cells. Each cell in the figure represents a single experiment. The error bars represent 1 SE.

REFERENCES

1. Makinodan, T., E. H. Perkins, and M. G. Chen. Adv. Gerontol. Res. 3, 1/1 (1971).
2. Price, G. B., and T. Makinodan. J. Immunol. 108, 403 (1972).
3. Jaroslow, B. N., K. M. Suhrbier, and T. E. Fritz. J. Immunol. 112, 1467 (1974).
4. Price, G. B., and T. Makinodan. J. Immunol. 108, 413 (1972).
5. Jaroslow, B. N., K. M. Suhrbier, R. J. M. Fry, and S. A. Tyler. *In vitro* suppression of immunocompetent cells by lymphomas from aging mice. This Report, Section 7.
6. Jerne, N. K., and A. A. Nordin. Science 140, 405 (1963).

SUPPRESSION AND ENHANCEMENT BY LYMPHOMA CELLS OF THE IMMUNE RESPONSE IN CULTURE

Bernard N. Jaroslow and Katherine M. Suhrbier

PURPOSE AND METHODS

Our earlier studies (1) showed that spontaneous mouse lymphomas inhibit the immune response of mouse spleen cells assayed in culture. The response of spleen cells in culture showed an accelerated decline in responsiveness at 600 days of age when the prevalence of lymphoma became significant. To determine the mechanism by which a lymphoma inhibits immunocompetent cells we switched from using spontaneous lymphomas, which come in several different varieties, to a single transplantable lymphoma, L-1V, a radiation-induced B cell lymphoma (2).

In this report we described the suppressive effect of live lymphomatous cells and the enhancing effect of an aqueous extract of the same cells on mouse spleen cells in culture.

The immune response was initiated with the addition of sheep red blood cells (SRBC) to $B6CF_1$/Anl mouse spleen cells in cultures prepared by Click's

technique (3). Four days later the cultures were harvested and the number of antibody-forming cells was determined by the Jerne plaque technique (4).

PROGRESS REPORT

We did two dose response experiments testing the suppression of immunocompetent spleen cells by L-1V cells added to a standard culture. The results shown in Figure 7.7 indicate that suppression is seen when as few as 3000 L-1V cells are added to 2 x 10^7 spleen cells in culture.

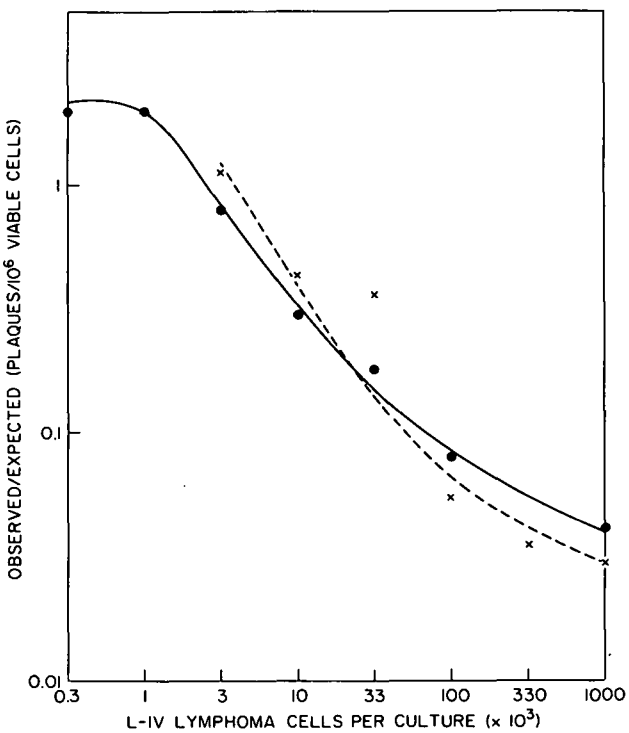

Fig. 7.7. Suppression of immunocompetent cells in culture by varying numbers of L-1V cells. The ordinate shows the fraction of the control response, in cultures of 2 x 10^7 spleen cells, achieved in similar cultures to which different numbers of live L-1V cells have been added. The dashed and solid lines represent the results of two separate experiments.

In a large number of experiments we found that an aqueous extract of a concentrated suspension of L-1V cells markedly enhanced the response of the spleen cells when added to the culture with SRBC. In a single experiment, we compared the effects of 10^6 live L-1V cells, the extract of L-1V cells, and the extract of normal spleen cells added at different times before and after antigen. The results are shown in Figure 7.8. Live cells inhibit the response when added from 24 hours before antigen to 24 hours after. Extract of these cells enhances the response from 24 hours before to 72 hours after antigen and normal mouse spleen-cell extract has no significant effect.

CONCLUSION

Earlier studies (5) showed that the first 24 hours of the immune response in culture are primarily devoted to the complex series of events associated with induction of the immune response. Subsequently, the stimulated B cells

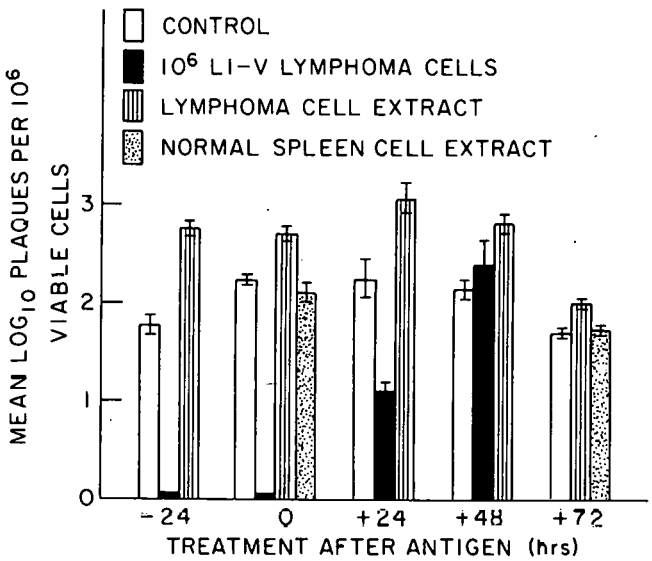

Fig. 7.8. Suppression by live L-1V cells and enhancement by extract of L-1V cells of the immune response of 2 x 10^7 mouse spleen cells in culture. Addition of appropriate preparations was made from 24 hours before to 72 hours after SRBC was added. Each control group was given culture medium at the appropriate time. The error bars represent 1 SE.

differentiate and proliferate into antibody-forming plasma cells. Our present results suggest that the inhibitory factor produced by live L-1V cells interferes with some phase of the induction process and that enhancement by the extract of L-1V cells is associated with the proliferative phase of the immune response in culture.

REFERENCES

1. Jaroslow, B. N., K. M. Suhrbier, R. J. M. Fry, and S. A. Tyler. *In vitro* suppression of immuno-competent cells by lymphomas from aging mice. This Report, Section 7.
2. Ainsworth, E. J., P. C. Brennan, R. J. M. Fry, A. V. Carrano, and W. T. Kickels. ANL-8070 (1973), p. 15.
3. Click, R. E., L. Benck, and B. J. Alter. Cell Immunol. 3, 264 (1972).
4. Jerne, N. K., and A. A. Nordin. Science 140, 405 (1963).
5. Ortiz-Ortiz, L. and B. N. Jaroslow. Nature (London) 221, 1153 (1969).

IN VITRO SUPPRESSION OF IMMUNOCOMPETENT CELLS BY LYMPHOMAS FROM AGING MICE*

Bernard N. Jaroslow, Katherine M. Suhrbier, R. J. Michael Fry, and Sylvanus A. Tyler

Antibody-forming capacity in mice declines in old age. The incidence of lymphoma in spleens of $B6CF_1$ mice (C57BL/6 ♀ x BALB/c ♂) increases with age. We studied the effect of lymphomas on immunologic responsiveness of spleen cell cultures to sheep red cells. The cultures were assayed for antibody-forming cells (AFC). Cultures of 20×10^6 normal spleen cells produced hundreds of AFC whereas similar cultures of lymphomatous spleen cells produced less than 10 AFC. Immunosuppression of normal spleen cells was observed in mixed cultures containing 5% lymphomatous spleen cells. These results demonstrate that lymphoma cells inhibit the response of normal spleen cells to antigenic stimulation *in vitro*. The age response for male mice gave a biphasic decline with a steeper second phase. The break point of 630 days coincides with the time of increasing incidence of lymphomas in aging mice. Our findings indicate that a major portion of the decline of immune responsiveness in aging $B6CF_1$ mice may result from the immunosuppressive activity of spontaneous lymphomas.

*Abstract of a paper to be published in the Journal of the National Cancer Institute.

EARLY AND LATE RADIATION EFFECTS ON ANTIBODY FORMATION IN AGING BEAGLE DOGS

*Bernard N. Jaroslow, William P. Norris, and Rosanne Fidelus**

PURPOSE AND METHODS

The rising levels of environmental radiation make the study of the short- and long-term effects of protracted radiation exposure particularly important. The immune system is a particularly valuable tool in such a study, as a model for a proliferative tissue and because of its importance to survival as a defense against disease.

In the extensive literature of radiation effects on immune response [reviewed by Taliaferro, Taliaferro, and Jaroslow (1)], it was shown that the response could be suppressed or enhanced, depending upon when the animals were given a single large dose of radiation during the immune response. In a short-term study of protracted exposure of rabbits to 2000 R of ^{60}Co γ-radiation at 25 R/day, Draper (2) observed that the rate of antibody production was delayed and slowed but the antibody-forming capacity was only slightly suppressed. An investigation by Jaroslow and Miller (3) of the long-term

*1974 Honors Research Participant, College of Saint Francis, Joliet, Ill.

effects of single exposure showed an accelerated loss of immune responsiveness with age in mice given 150 rad of neutrons 600 days before immunization.

In the previously completed portion of this study, we reported (4) that dogs given 2000 R of ^{60}Co γ-radiation at 17 R/day showed a delay and a decreased rate of antibody synthesis when immunized within a week after removal from the radiation field. A group of dogs given 4000 R at 17 R/day showed a distinct loss of immunologic capacity when immunized at 4 1/2 years of age, 2 years after removal from the radiation field.

To complete this study and to provide an age control for the second group of irradiated dogs, 4 1/2 year-old control dogs were immunized with a single intramuscular injection of alum-precipitated T_2 coliphage, a bacteriophage of *Escherichia coli* B. Serum samples were collected 13 times in the 48 days after the first phage injection and 8 times during the 2 weeks after a second phage injection, given 48 days after the first. The serum samples were assayed for phage-inhibiting activity. Care and handling of the dogs is discussed in detail by Norris et al. (5) and the detailed description of the assay procedure is given by Jaroslow et al. (6).

PROGRESS REPORT

Five 4 1/2 year-old dogs were immunized according to the same protocol as for the 4 1/2 year-old dogs that had been out of the radiation field for two years after exposure to 4000 R at 17 R/day. Figure 7.9 shows that the group of irradiated dogs gave a primary immune response that was somewhat later, slower, and less than seen in their age controls. They show a group distribution intermediate in response between their age controls and 7 1/2 year-old unirradiated dogs (6). As in the aging study, the secondary response of the irradiated dogs was as vigorous as in the controls.

CONCLUSION

The late effects of 4000 R at 17 R/day of ^{60}Co γ-radiation on the immune response resemble an accelerated loss of immune capacity with age.

REFERENCES

1. Taliaferro, W. H., L. G. Taliaferro, and B. N. Jaroslow. Radiation and Immune Mechanisms, Academic Press, New York (1964).
2. Draper, L. R. In: Ionizing Radiations and Immune Processes, Ed., C. A. Leone. Gordon and Breach, New York, 1962, p. 221.
3. Jaroslow, B. N., and M. Miller. In: Advances in Radiation Research, Biology and Medicine, Vol. 1, Eds. J. F. Duplan and A. Chapiro. Gordon and Breach, London, 1973, p. 23.
4. Jaroslow, B. N., W. P. Norris, and A. Seymour. ANL-8070 (1973), p. 41.
5. Norris, W. P., T. E. Fritz, C. E. Rehfeld, and C. M. Poole. Radiat. Res. 35, 681 (1968).
6. Jaroslow, B. N., K. M. Suhrbier, and T. E. Fritz. J. Immunol. 112, 1467 (1974).

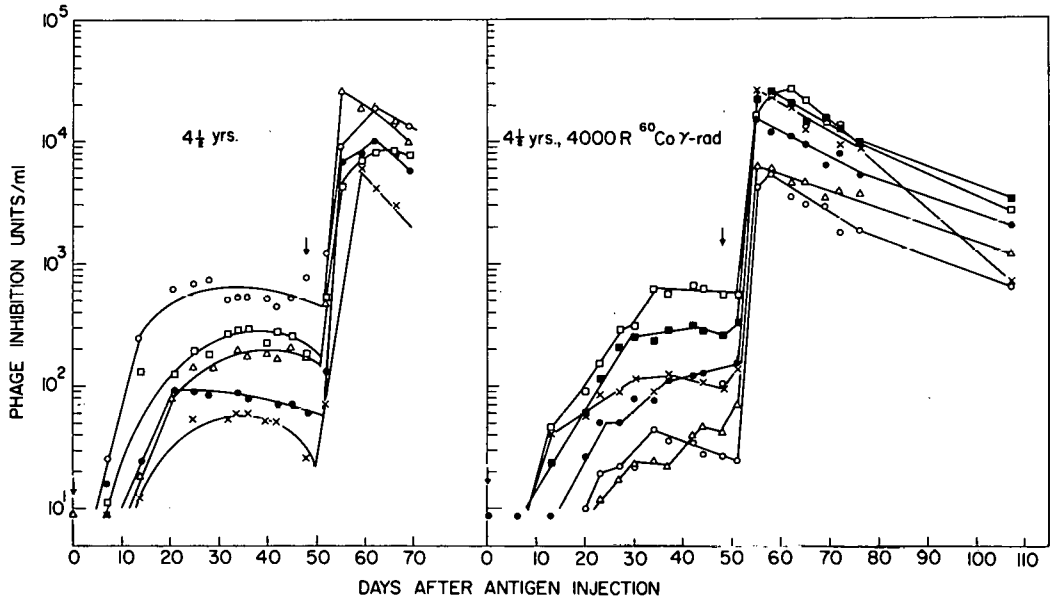

Fig. 7.9. The primary and secondary responses to a single injection of T_2 coliphage, given at times shown by arrows. Five unirradiated dogs with a median age of 4 1/2 years and six dogs immunized 2 years after 4000 R. Median age 4 1/2 years.

THE DECLINE OF CELL-MEDIATED IMMUNITY IN AGING MICE*

Mira Menon,† *Bernard N. Jaroslow and R. Koesterer*‡

The influence of aging on cell-mediated immunity (CMI) was studied in mice by two tests of allograft immunity: 1) By an *in vitro* cytotoxicity assay measuring ^{51}Cr release from tumor cells specifically lysed by splenic immunocytes, we observed a decline in CMI with $t_{1/2} \sim 7$ months. From studies of the kinetics of cytolysis we concluded that the spleens of older sensitized animals have fewer immunocytes without a loss of potency per cell. 2) The response to skin allografts showed that older (2 years) unsensitized animals had slower rejection rates for allografts than the younger animals (5-6 months), while sensitized animals, both young and old, had equal rejection rates. The slower rejection rate in older unsensitized mice is in accord with the explanation that they produce fewer immunocytes. The age-associated loss in CMI may contribute to increased carcinogenesis; but it may be beneficial to old transplant recipients who might thereby require less immunosuppressive therapy.

---

*Abstract of a paper published in the J. Gerontol. 29, 494 (1974).

†Present address: Radiological and Environmental Research Division, Argonne National Laboraotry.

‡Present address: Department of Zoology, Kenyatta University, Nairobi, Kenya.

8. BIOCHEMISTRY

SUMMARY

John F. Thomson, Group Leader

Since the results of the program concerned with the therapy of poisoning by radioactive and nonradioactive metals are now reported in a separate section of the report (Section 3), this Section covers progress in three programs: (a) the preparation and properties of single cells and subcellular particles, (b) biochemical manifestations of radiation damage in yeast cells, and (c) hormonal and metabolic bases of radiation response in plants.

The first of these programs is represented by four reports. The first describes a spectrophotometric assay for catalase with perborate as the substrate, the second deals with applications of H_2O/D_2O gradients to zonal centrifugation, and the other two represent collaborative work with members of the Aging Research Group on uptake of liposomes by splenic and hepatic cells.

The contributions of the second of the three programs are three reports, one on the biochemical effects of γ-radiation on yeast cells, one on the isolation and biological activity of compounds related to S-adenosylmethionine, and the third on the synthesis of 2-methyl-DL-homoserine, a new amino acid analogue and possible antagonist of homoserine.

The plant radiobiology program presents six abstracts and progress reports on a variety of subjects in the field of plant physiology, biochemistry, and morphology. Five of these contributions deal with various aspects of gravitational sensing and the geotropic response; the other describes measurements of the action spectra for phototropism and growth inhibition.

BIOCHEMISTRY STAFF

REGULAR STAFF

Dainko, Julia L. (Scientific Assistant)
*Nance, Sharron L. (Scientific Assistant)
Schlenk, Fritz (Senior Biochemist)
Shen-Miller, Jane (Botanist)
Thomson, John F. (Senior Biologist)
Tollaksen, Sandra L. (Scientific Assistant)

*Retired during 1974.

TEMPORARY STAFF DURING 1974

*Hinchman, Ray R. (Postdoctoral Appointee)
†McNitt, Rand E. (Postdoctoral Appointee)
†Nakamura, Kenji D. (Postdoctoral Appointee)

---

*Now in Environmental Statement Project, Argonne National Laboratory.
†Terminated during 1974.

SPECTROPHOTOMETRIC ASSAY OF CATALASE WITH PERBORATE AS SUBSTRATE

John F. Thomson, Sharron L. Nance, and Sandra L. Tollaksen

PURPOSE AND METHODS

In our studies on intracellular localization of enzymes, as determined by density-gradient and zonal centrifugation, it is necessary to assay a number of enzymes on as many as 40 samples. For many enzymes, we have used spectrophotometric assays with the spectrophotometer coupled to a key punch (1). For catalase, however, the spectrophotometric assays that have been described, using hydrogen peroxide as substrate (2,3), are not suitable for assays of numerous tissue samples that by their nature are highly impure; problems such as instability of the substrate, latency of particle-associated catalase, and high blank values made this approach unsatisfactory for our purposes.

Perborate was introduced as a substrate for catalase by Feinstein (3). We used a colorimetric adaptation of this procedure (4) in several studies on catalase distribution (4,6). Solutions of perborate are relatively stable, and the problems of latency are minimal when the assay is carried out at room temperature or higher (7). However, the method is time-consuming, of doubtful accuracy for samples with low activity, and not readily adaptable to our data-processing system.

This report describes the use of perborate as a substrate in a spectrophotometric assay of catalase in mouse liver fractions.

The reaction mixture consisted of 0.05 M phosphate buffer, pH 7.0, and 0.01 to 0.05 ml of an appropriately diluted tissue sample to a final volume of 2.5 ml. The reaction was started by the addition of 0.5 ml of 0.2 N sodium perborate, neutralized to pH 7.0 with 85% H_3PO_4 (4). Blanks without perborate were prepared for each sample. Assays were carried with two different volumes of sample.

Assays were carried out in quartz cuvettes specially cleaned to minimize the adhesion of bubbles to the surface of the glass (8). Spectrophotometric measurements were made at 228 nm, at intervals of 20-25 seconds for a period of 2-3 minutes, with the apparatus described elsewhere (1).

To test the efficacy of the method, 3 ml of a mouse liver homogenate (1:10 in 0.25 M sucrose) was layered over a 42 ml sucrose gradient (0.29-0.88 M) containing 1% ethanol in a 50 ml polycarbonate centrifuge tube. The tube was centrifuged at 4100 rev/min for 70 minutes; fifteen fractions of 3 ml each were collected and assayed. Details of gradient preparation and fraction collection have been previously presented (9). Catalase activity was calculated by computing the least-squares fit of a plot of the natural logarithm of the optical density vs. time. The slopes of these lines were converted to "k" values in terms of the total sample volume of 3 ml. Uricase activity was also measured in the same fractions.

PROGRESS REPORT

Figure 8.1 shows the results obtained with the original homogenate and with various fractions of the gradient. It is apparent that (a) the reaction obeys first-order kinetics over the assay period, (b) in each case the lines obtained by least-squares fit extrapolate to nearly the same intercept, and (c) the slopes of the lines for a given sample are proportional to the volume of the sample used.

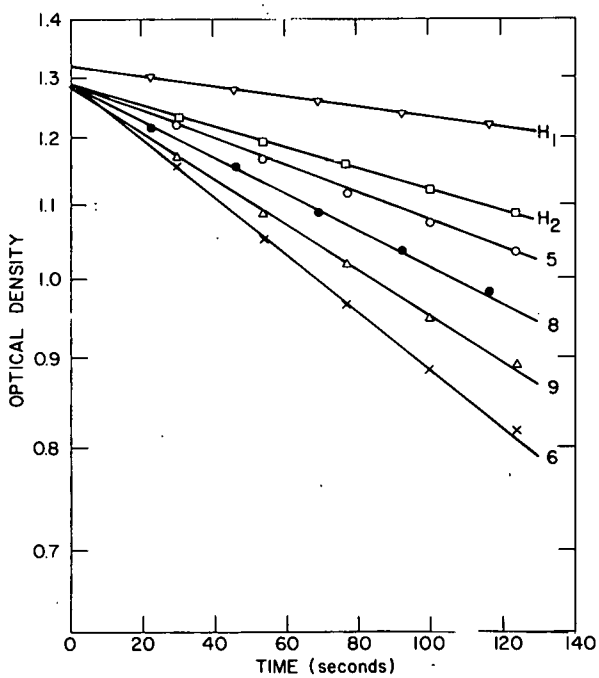

Fig. 8.1. Catalase assays on a mouse liver homogenate and on four fractions recovered after density-gradient centrifugation. The homogenate was diluted 1:30 in 0.05 M, pH 7.0, phosphate buffer; then assayed with 0.01 ml (H_1) and 0.02 ml (H_2) of the dilutions. The fractions were assayed with 0.01 ml (5), 0.02 ml (6 and 8), or 0.04 ml (9).

Table 8.1 lists the slopes (with standard errors) and intercepts for assays on the various fractions, calculated on the basis of the total fraction volume of 3 ml. The high values for fractions 1 and 2 represent the soluble catalase from the blood entrapped in the liver. Fraction 15 is the pellet. The recovery in fractions 1 through 15 is 108.4% of the original homogenate activity. The average value of the intercepts is 0.2518 ± 0.0174 (1.286 ± 0.022 optical density units).

Table 8.1. Parameters of Catalase Assays in Mouse Liver Homogenate and Fractions

Fraction	k ± SE (Slope/3 ml)	Intercept
1	-0.8586 ± 0.0422	0.2677
2	-0.5297 ± 0.0202	0.2687
3	-0.3944 ± 0.0145	0.2760
4	-0.4460 ± 0.0103	0.2622
5	-0.5188 ± 0.0133	0.2618
6	-0.5250 ± 0.0188	0.2582
7	-0.3857 ± 0.0122	0.2640
8	-0.3441 ± 0.0054	0.2353
9	-0.2214 ± 0.0067	0.2592
10	-0.1298 ± 0.0049	0.2232
11	-0.0800 ± 0.0033	0.2549
12	-0.0423 ± 0.0020	0.2206
13	-0.0364 ± 0.0022	0.2294
14	-0.0308 ± 0.0011	0.2344
15	-2.0053 ± 0.0979	0.2524
Total	-6.5485	
Homogenate	-6.0390 ± 0.0929	0.2611

Figure 8.2 presents the data in Table 8.1 as the distribution in terms of particle size, together with the distribution pattern of uricase, measured in the same experiment. The midpoints are nearly identical, 0.430 mμ for catalase and 0.442 mμ for uricase.

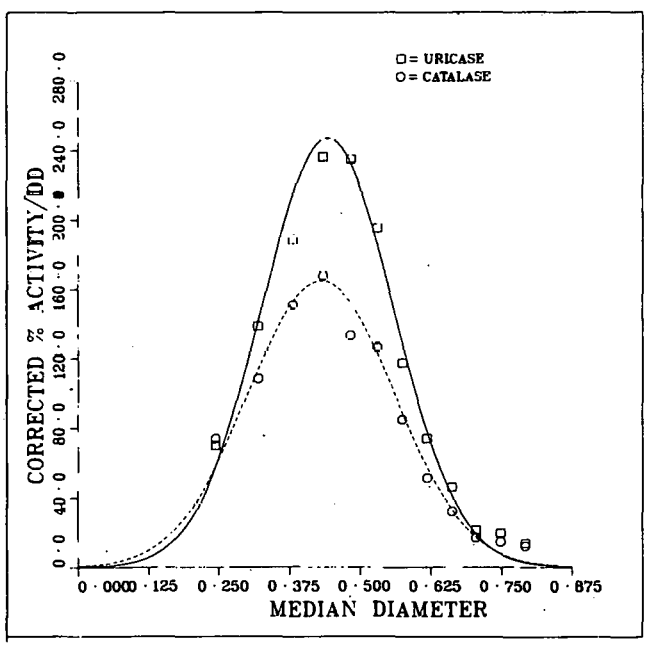

Fig. 8.2. Distribution of catalase and uricase in mouse liver homogenate as functions of particle size.

CONCLUSIONS

The use of perborate as a substrate for the spectrophotometric assay of catalase seems entirely feasible, and superior in many respects to the use of hydrogen peroxide. The principal advantages are (a) the stability of perborate solutions, which obviates the need for repeated standardization and for correction for spontaneous decomposition, and (b) the avoidance of latency problems. (It may be noted that the use of Triton X-100 as an activating agent is precluded because of its high UV absorption.)

The spectrophotometric assay is also superior to the titrimetric and colorimetric methods in which measurements are made at a single time point, and in which zero-order kinetics is generally assumed.

REFERENCES

1. Swick, R. W., J. L. Stange, S. L. Nance, and J. F. Thomson. Biochemistry 6, 737 (1967).
2. Chance, B. Methods Biochem. Anal. I, 408 (1955).
3. Feinstein, R. N. J. Biol. Chem. 180, 1197 (1949).
4. Thomson, J. F., and F. J. Klipfel. Cancer Res. 18, 229 (1958).
5. Thomson, J. F., and F. J. Klipfel. Arch. Biochem. Biophys. 70, 224 (1957).
6. Thomson, J. F., S. L. Nance, and S. L. Tollaksen. Proc. Soc. Exp. Biol. Med. 145, 1174 (1974).
7. Feinstein, R. N. Arch. Biochem. Biophys. 79, 309 (1959).
8. Beers, R. F., Jr., and I. W. Sizer. J. Biol. Chem. 195, 135 (1952).
9. Thomson, J. F., S. L. Nance, and S. L. Tollaksen. Radiat. Res. 45, 629 (1971).

ZONAL CENTRIFUGATION OF RAT LIVER HOMOGENATES WITH D_2O/H_2O GRADIENTS

John F. Thomson, Sharron L. Nance, and Sandra L. Tollaksen

PURPOSE AND METHODS

We recently described the use of deuterium oxide (D_2O) in preparing gradients for density-gradient centrifugation (1). The advantages of using D_2O, rather than a solute such as sucrose, to vary the density are (a) osmotic effects are negligible, and (b) the increase in viscosity is much less. We showed that when mouse liver homogenates were layered over a gradient in which the sucrose remained constant at 0.29 M, with the concentration of D_2O varying from 0 to 86%, the same separation of mitochondrial enzyme distributions was observed as had been reported with 0.29 to 0.88 M sucrose gradients (1).

Swick et al. (2), had proposed that the apparent heterogeneity of distribution of enzymes in rat liver mitochondria separated by zonal centrifugation (3) could be accounted for in large measure by area-volume considerations. However, there was the possibility that the differences in enzyme distribution reflected damage to the mitochondria as a result of their traveling through

a medium with progressively increasing osmotic pressure. This report is concerned with our confirmation of the results with sucrose gradients by zonal centrifugation of rat liver through D_2O/H_2O gradients.

Most of the methods used have been reported elsewhere (1,3,4). The principal difference was the construction of the gradient. To produce sucrose gradients we used concentrations of sucrose and volumes of solutions that yielded an exponential gradient closely approximating a concentration gradient that was linear with respect to radial distance in the rotor. This approach was not feasible for D_2O gradients, because the volume required in the mixing chamber was such that the maximum concentration of D_2O obtainable would have been only 68%. Thus a smaller volume (400 ml of 0.29 M sucrose in H_2O) was chosen, with 1160 ml of 0.29 M sucrose in D_2O as the reservoir. The nonlinearity of the gradient was accounted for by modification of the computer program.

PROGRESS REPORT

Table 8.2 shows the midpoints and dispersions of seven enzymes associated with rat liver mitochondria, plus total protein as estimated from D_2O/H_2O gradients, together with the midpoint values computed earlier from data obtained with sucrose gradients (3). Although the average values for the midpoints are some 30% higher for the D_2O gradient experiments, the rank ordering of the midpoints is essentially the same. The reason for the higher values calculated for the D_2O gradients is probably the basis of estimation of mitochondrial density and its change with increasing D_2O concentration (1).

CONCLUSIONS

Since the data obtained on the distributions of mitochondrial enzymes by use of zonal centrifugation confirm those previously reported with sucrose gradients, it appears that damage to the mitochondrial membranes by high sucrose concentrations is probably negligible.

[The results of these experiments have been incorporated into a paper recently submitted for publication (5)].

REFERENCES

1. Thomson, J. F., S. L. Nance, and S. L. Tollaksen. Arch. Biochem. Biophys. 160, 130 (1974).
2. Swick, R. W., S. L. Tollaksen, S. L. Nance, and J. F. Thomson. ANL-7635, (1969), p. 209.
3. Swick, R. W., J. L. Stange, S. L. Nance, and J. F. Thomson. Biochemistry 6, 737 (1967).
4. Thomson, J. F., S. L. Nance, and S. L. Tollaksen. Radiat. Res. 45, 629 (1971).
5. Swick, R. W., S. L. Tollaksen, S. L. Nance, and J. F. Thomson. Arch. Biochem. Biophys., in press.

Table 8.2. Parameters of Distribution Curves for Mitochondrial Enzymes of Rat Liver

Assay	D_2O/H_2O Gradient		Sucrose Gradient (3)	
	Midpoint	Dispersion	Midpoint	Ratio
Rotenone-insensitive cytochrome c reductase	1.180 ± 0.0056	0.184 ± 0.0063	-	-
Cytochrome oxidase	1.204 ± 0.0047	0.174 ± 0.0040	0.902	1.335
Succinate dehydrogenase	1.208 ± 0.0033	0.174 ± 0.0036	0.919	1.315
β-Hydroxybutyrate dehydrogenase	1.212 ± 0.0035	0.175 ± 0.0038	0.921	1.315
Glutamate-oxalacetate aminotransferase	1.223 ± 0.0032	0.176 ± 0.0044	0.934	1.309
Protein	1.225 ± 0.0040	0.169 ± 0.0046	0.938	1.306
Malate dehydrogenase	1.226 ± 0.0062	0.180 ± 0.0060	0.941	1.303
Adenylate kinase	1.240 ± 0.0028	0.156 ± 0.0030	-	-

Values are the mean μm ± standard errors, based on 3 or 4 experiments.

INCORPORATION OF LIPOSOMES INTO SPLEEN CELLS

John F. Thomson, Sharron L. Nance, Sandra L. Tollaksen, Elizabeth A. Cerny, and Yueh-Erh Rahman

PURPOSE AND METHODS

When a liposome-encapsulated compound is administered to an animal, the tissue distribution may be appreciably different from that after administration of the same compound in the free form. In the case of encapsulated actinomycin D or of ethylenediaminetetraacetic acid (EDTA), the spleen takes up an appreciable fraction of the injected dose. This report deals with the preliminary separation of spleen cells to establish the cell types that take up the drugs.

Cells were teased from the spleens of six to eight CF#1 female mice killed 1 hour after intravenous injection of either ^{3}H-actinomycin D or ^{14}C-EDTA liposomes. The cells were rinsed and resuspended in 3 ml of isotonic saline, and then were layered over a 42-ml linear gradient of bovine serum

albumin, the concentration ranging from 10 to 30% in 0.9% NaCl. The gradient tube was then centrifuged at 650 rpm in an International PR-2 centrifuge with a swinging bucket rotor No.269, to a total $\omega^2 t$ of 60 x 10^5 radians^2/sec. Fifteen 3-ml fractions were removed, each of which was examined for radioactivity, cell number, and cell type.

PROGRESS REPORT

Microscopic examination of the fractions showed that fractions 4 and 5 (numbered from the top) contained erythrocytes, whereas the majority of the lymphocytes passed through the gradient and were recovered as the pellet in fraction 15.

Figure 8.3 shows the cell counts and the radioactivity determinations on the fractions. It appears that ^{3}H-actinomycin D is associated only with the lymphocytes.

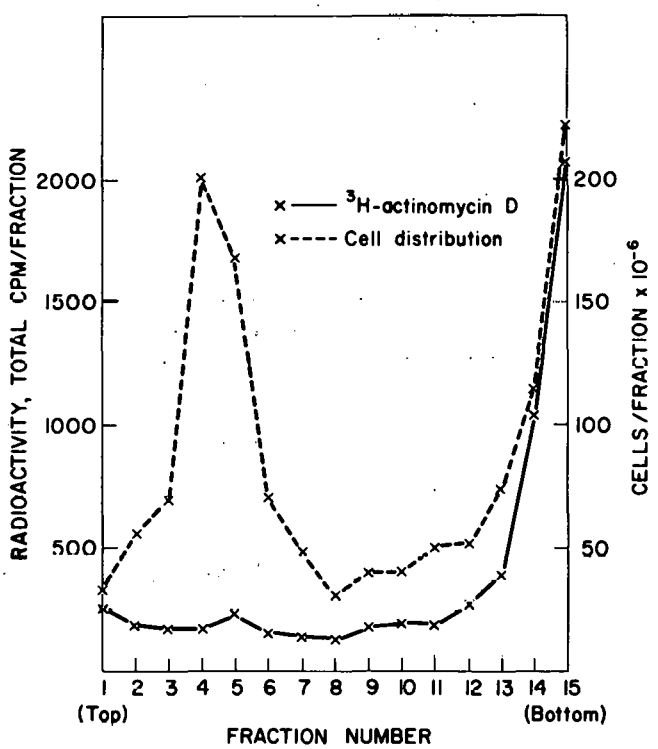

Fig. 8.3. Distribution of cell counts and ^{3}H radioactivity in a suspension of spleen cells prepared from a mouse injected 1 hour previously with liposome-encapsulated ^{3}H-actinomycin D. In this experiment, the actinomycin D was incorporated in the lipid phase of the liposomes.

The results with ^{14}C-EDTA liposomes were essentially identical with those obtained with ^{3}H-actinomycin D except that incorporation into the spleen was more rapid.

CONCLUSIONS

The bovine serum albumin gradient is an effective tool for gross separation of erythrocytes from other cells in the spleen. The results obtained with

this technique show conclusively that liposome-encapsulated actinomycin D is not taken up by erythrocytes. In experiments in which the cells were not rinsed prior to layering, there was very little radioactivity in fraction 1, which represents the original cell suspension; thus it is probable that there was negligible destruction of liposomes and no release of free actinomycin D.

Further work, including electron microscopic examination, will be required to demonstrate the actual presence of liposomes in the lymphocytes of the spleen.

LIVER FRACTIONATIONS USING SUCROSE GRADIENTS TO STUDY MECHANISM OF DRUG RELEASE FROM LIPOSOMES

John F. Thomson, Sandra L. Tollaksen, Sharron L. Nance, Elizabeth A. Cerny, and Yueh-Erh Rahman

PURPOSE AND METHODS

In a recent paper (1), we showed that the toxicity of actinomycin D is drastically reduced when the drug is incorporated into liposomes before being injected into the animal. Although the drug is gradually released from the liposomes, the mechanism of release is not understood.

We used the technique of sucrose gradients for fractionation of liver cells to ascertain whether liposomes become associated with specific subcellular particulates. Fifteen studies were attempted, using ^{3}H-actinomycin D liposomes injected intravenously 1 hour before sacrificing the animals. The actinomycin D was incorporated into the aqueous phase of the liposomes or into the lipid phase.

For each experiment, two livers were homogenized in 12 ml 0.25 M sucrose + 0.0003 M EDTA and filtered through gauze. A sample of the homogenate was set aside; the remainder was centrifuged at 1500 rpm for 10 minutes and washed once. The nuclear pellet was resuspended in saline. The supernatants were combined, and 4 ml aliquots were layered on each of two 42-ml 10-30% sucrose gradients (with EDTA) and were centrifuged $\sim$ 70 minutes at 4100 rpm, for a final cumulative $\omega^2 t$ value of $\sim 76 \times 10^7$ rad^2/second. Fifteen fractions were removed: fraction 1 was 4 ml, fractions 2 through 15 were 3 ml each; the individual fractions from the two gradients were pooled.

Assays run on all the fractions included cytochrome oxidase, uricase, acid phosphatase, glucose-6-phosphatase, ^{3}H or ^{14}C counts, and protein.

PROGRESS REPORT

In every experiment, the largest quantity of radioactivity was associated with the nuclear pellet, the values ranging from 35 to 65% of the total ^{3}H counts. The radioactivity found in the cytoplasm showed distribution patterns paralleling those of uricase and acid phosphatase, the enzymes employed as

markers for peroxisomes and lysosomes, respectively. It is probable that the latter particulate is the one with which the liposomes are predominantly associated. It seems certain that mitochondria (cytochrome oxidase marker) and microsomes (glucose-6-phosphatase marker) are not involved in intracellular transport or metabolism of liposomes.

CONCLUSIONS

On the basis of these experiments, we postulate that the liposomes first become associated with the lysosomes. The lysosomes, by mechanisms not as yet understood, facilitate the breakdown of the liposomes and the release of actinomycin D, which then reaches the nuclei.

It is possible, of course, that liposomes reach the lysosomes and the nuclei more or less simultaneously. However, liposomes have not been observed in the nuclei, and the best evidence indicates that the radioactivity found in the nuclei is free actinomycin D.

It is clear that work will have to be done at different time intervals to support this hypothesis.

REFERENCE

1. Rahman, Y. E., E. A. Cerny, S. L. Tollaksen, B. J. Wright, S. L. Nance, and J. F. Thomson. Proc. Soc. Exp. Biol. Med. 146, 1173 (1974).

BIOCHEMICAL EFFECTS OF X-IRRADIATION ON YEAST CELLS

K. D. Nakamura and F. Schlenk

PURPOSE AND METHODS

In continuation of our earlier studies of cytological and biochemical features of X-irradiated yeast cells (1,2), it proved necessary to establish some basic properties of normal cells with respect to processes of active transport of metabolites by the cytoplasmic and vacuolar membrane. While the variety of metabolites transported by the cytoplasmic membrane of yeast cells is large, relatively few biological compounds have been demonstrated in the vacuole with certainty. Among these is the biological methyl donor, (-)S-adenosyl-L-methionine. After intracellular synthesis, which can be greatly increased by modification of the culture medium, this compound is accumulated by the vacuole to a very high concentration. It can be detected there by ultraviolet photography without disrupting the cell structure.

PROGRESS REPORT

The failure of isolated vacuoles to concentrate S-adenosylmethionine from the surrounding medium (2) suggested that the active transport of this compound

is linked in some fashion to its intracellular biosynthesis. This hypothesis could be tested by observing the ability of intact cells to take up and concentrate in the vacuoles the preformed sulfonium compound supplied in the medium. The failure of the vacuoles of intact cells to concentrate the extraneous material would suggest dependence of the active transport on intracellular biosynthesis. A prerequisite for these experiments was to secure a yeast capable of taking up large quantities of material from the culture medium. A suitable strain of yeast (*Saccharomyces cerevisiae* No. 4094) was obtained from Dr. H. de Robichon-Szulmajster, Gif-sur-Yvette.

The uptake of S-adenosyl-L-methionine by active transport through the cytoplasmic membrane and the vacuolar membrane was fast. Ultraviolet micrography (3) proved the accumulation of the material in the vacuole. Under aerobic conditions, with glucose as an energy source, a hundredfold enrichment in the cells, including the vacuoles, could be observed after 4 hours, by spectrophotometry of the medium, tracer techniques, and ultraviolet micrography of the cells.

This system also permitted the examination of the membrane specificity by supplying related compounds and stereoisomers of (-)S-adenosyl-L-methionine which had been obtained by chemical synthesis or biosynthesis (Table 8.3). In the case of (±)sulfonium racemates, both stereoisomers were taken up, and D-configuration of the amino acid part did not interfere with the active transport of the sulfonium compound, but the closely related S-adenosyl-D-homocysteine was excluded by the cells. Additional indication of the ability of the cytoplasmic and vacuolar membranes of the cells to discriminate is that of a large variety of related sulfur and sulfonium compounds tested (4), only S-methylsulfonium-L-methionine penetrated readily into the cells.

Table 8.3. Uptake of S-Adenosylmethionine and Related Compounds by *S. cerevisiae* 4094[a]

Compounds Examined, (0.2 and 0.6 mM)	Rate of Uptake	Principal Intracellular Location	Recovery of Compound from the Cells
	(4 hr)		%
(-)S-Adenosyl-L-methionine	fast	vacuole	67
Same, no glucose	none	-	-
(±)S-Adenosyl-L-methionine	fast	vacuole	not measured
(±)S-Adenosyl-D-methionine	fast	vacuole	95
(-)S-Adenosyl-L-ethionine	fast	vacuole	87
(-)S-Adenosyl-(S-n-propyl) L-homocysteine	slow	?	-
S-Adenosyl-L-homocysteine	fast	rapid intracellular degradation	<2
S-Adenosyl-D-homocysteine	slow	-	-

[a]Cells from late exponential growth phase (10 mg/ml) in 0.05 M K-phosphate, pH 5; 1.5% glucose; aerobic incubation at 30°C.

REFERENCES

1. Nakamura, K. D., J. L. Dainko, and F. Schlenk. ANL-7970 (1972), p. 94.
2. Nakamura, K. D., J. L. Dainko, and F. Schlenk. ANL-8070 (1973), p. 111.
3. Svihla, G. Ultraviolet microscopy. In: The Encyclopedia of Microscopy, Ed. P. Gray. Van Nostrand-Reinhold Co., New York, 1973, p. 580.
4. Nakamura, K. D., and F. Schlenk. J. Bacteriol. 120, 482 (1974).

ISOLATION AND BIOLOGICAL ACTIVITY OF COMPOUNDS RELATED TO S-ADENOSYLMETHIONINE

F. Schlenk, J. L. Dainko, and K. D. Nakamura

PURPOSE AND METHODS

The increased interest in enzymatic transmethylation, especially of macromolecules such as t-RNAs and proteins, suggested further studies on the specificity of the biological methyl donor, S-adenosyl-L-methionine, and a search for analogues that might be useful as competitive inhibitors in transmethylation systems.

PROGRESS REPORT

In a survey of yeasts, it was found that the biosynthesis of the methylsulfonium donor, L-methionine + ATP → S-adenosyl-L-methionine + PP_i + P_i, is not restricted to L-methionine as the amino acid component. With *Candida utilis* (ATCC 9950), the formation of S-adenosyl-D-methionine from D-methionine and the formation of S-adenosyl-2-methyl-DL-methionine from 2-methyl-DL-methionine was observed. A special strain of *Saccharomyces cerevisiae* (isolated in this Laboratory) reacted with the S-*n*-propyl analogue of methionine, S-*n*-propyl-L-homocysteine, to yield S-adenosyl-(S-*n*-propyl)-L-homocysteine. The latter could be separated from endogenous S-adenosyl-L-methionine by ion exchange chromatography, but the D-stereoisomer and the 2-methylsulfonium compound defied separation from the endogenous biological methyl donor which is an ubiquitous cell constituent.

These two derivatives were prepared, therefore, by chemical synthesis. For this, S-adenosyl-D-homocysteine and S-adenosyl-2-methyl-DL-homocysteine were prepared by reaction of D-homocystine and 2,2'-dimethyl-DL-homocystine with 2',3'-O-isopropylidene-5'-O-toluene-*p*-sulfonyl adenosine (1) after reduction with sodium metal in liquid ammonia. After removal of the isopropylidene group, S-adenosyl-D-homocysteine and S-adenosyl-2-methyl-DL-homocysteine were isolated and methylated with $^{14}CH_3I$. The resulting sulfonium compounds were isolated by chromatography.

Qualitative results of the examination of these alkyl donors in enzyme systems are listed in Table 8.4. The derivatives were found to be active in several systems, and the specificity of the biological methyl donor, S-adenosyl-L-methionine, is not as high as it had been assumed in earlier studies (7).

Table 8.4. S-Adenosyl-L-methionine and Some of Its Derivatives in Enzymatic Transalkylations

Sulfonium Compounds Examined $[^{14}CH_3]$ or $[1\text{-}^{14}C_3H_7]$	Enzyme Systems[a] I	II	III	IV	V
S-Adenosyl-L-methionine	+++	+++	+++	+++	+++
S-Adenosyl-D-methionine	-	+	-	±	+
S-Adenosyl-2-methyl-DL-methionine	+	-	+	?	++
S-Adenosyl-(S-*n*-propyl)-L-homocysteine[b]	±	-	?	-	+

[a]The sources of the enzymes and analytical techniques are described in the literature (2-6).

I: N-Acetylserotonin O-methyltransferase
II: Histamine N-methyltransferase
III: Glycine N-methyltransferase
IV: Guanidinoacetate N-methyltransferase
V: L-Homocysteine S-methyltransferase

[b]Transpropylation was measured in these experiments.

REFERENCES

1. Sakami, W., and A. Stevens. Bull. Soc. Chim. Biol. 40, 1787 (1958).
2. Axelrod, J. Methods Enzymol. 17 B, 764 (1971).
3. Snyder, S. H. Methods Enzymol. 17 B, 838 (1971).
4. Heady, J. E., and S. J. Kerr. J. Biol. Chem. 248, 69 (1973).
5. Cantoni, G. L., and P. J. Vignos. J. Biol. Chem. 209, 647 (1954).
6. Shapiro, S. K. Methods Enzymol. 17 B, 400 (1971).
7. de la Haba, G., G. A. Jamieson, S. H. Mudd, and H. H. Richards. J. Am. Chem. Soc. 81, 3975 (1959).

2-METHYL-DL-HOMOSERINE: A NEW AMINO ACID ANALOGUE

F. Schlenk

INTRODUCTION

The 2-methylamino acids, such as 2-methylaspartic acid, 2-methylmethionine, and 2-methylglutamic acid have played an important role in inhibition studies of amino acid metabolism, for example, deamination, decarboxylation, and incorporation of amino acids into proteins. However, 2-methylhomoserine has not been available, so far, as a homoserine antagonist.

EXPERIMENTAL RESULTS

A convenient way to prepare 2-methylhomoserine from commercial 2-methylmethionine (1) has now been found using the following reactions:

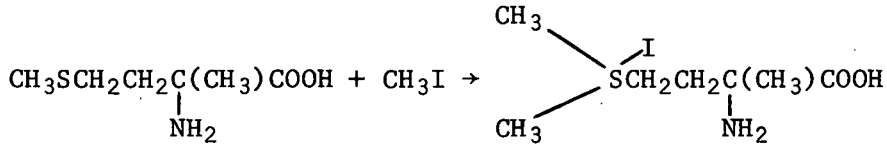

(I)

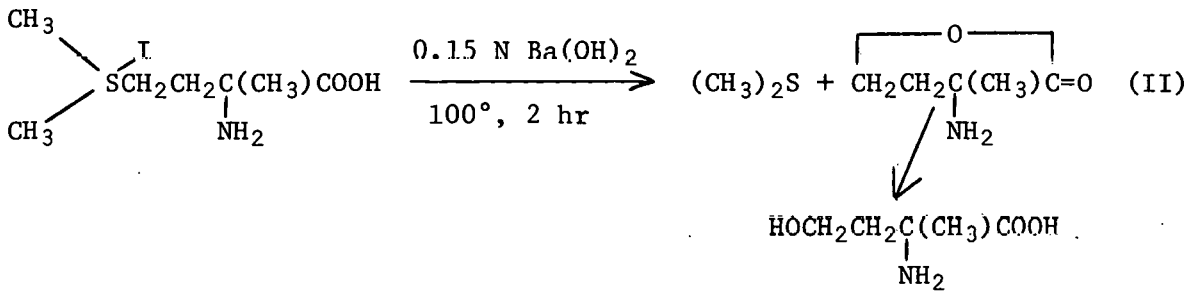

(II)

S-Methyl-2-methyl-DL-methionine sulfonium iodide (the end product of Reaction I) was recrystallized from methanol, and its structure was confirmed by elementary analysis. For conversion to 2-methyl-DL-homoserine lactone and 2-methyl-DL-homoserine (Reaction II), the material was heated in 0.15 N $Ba(OH)_2$ solution for 2 hours. The conversion of the lactone to 2-methyl-DL-homoserine is almost instantaneous under the alkaline conditions. The lactone can be obtained, however, by refluxing 2-methyl-DL-homoserine in 2 N HCl for 2 hours in an oil bath. Evaporation of the acid under reduced pressure, and recrystallization of the residue from acetone gave the lactone hydrochloride.

Elementary analysis of 2-methyl-DL-homoserine gave the expected values, and NMR studies of Dr. S. S. Danyluk corroborated the structure. The various 2-methyl compounds described here are readily distinguished from the corresponding amino acids by paper and thin layer chromatography (Table 8.5).

2-Methyl-DL-homoserine is promising as an antagonist of homoserine in the formation of cystathionine and methionine, and in the reactions leading to aspartic semialdehyde and aspartic acid (2).

REFERENCES

1. Pfister, K., W. J. Leanza, J. P. Conbere, H. J. Becker, A. R. Matzuk, and E. F. Rogers. J. Am. Chem. Soc. 77, 697 (1955).
2. Black S., and N. G. Wright. J. Biol. Chem. 213, 51 (1955).

Table 8.5. Chromatography of Some Amino Acids and Their Derivatives[a]

Compound Examined	R_F Values	
	Paper Chromatography	Thin Layer Chromatography
Methionine	0.54	0.55
2-Methylmethionine	0.66	0.57
S-Methyl-2-methyl-methionine sulfonium iodide	0.12	0.16
Homoserine	0.24	0.35
Homoserine lactone	0.38	0.45
2-Methylhomoserine	0.35	0.40
2-Methylhomoserine lactone	0.47	0.52

[a]Whatman No. 1 paper and Eastman Chromagram Sheets No. 6060 were used with 1-butanol-acetic acid-H_2O (12:3:5, v/v) and ascending technique. The reaction of 2-methylamino acids with ninhydrin is weaker than that of the corresponding amino acids.

EFFECTS OF INDOLEACETIC ACID ON DICTYOSOMES OF APICAL AND EXPANDING CELLS OF OAT COLEOPTILES*

Stanley R. Gawlik and J. Shen-Miller

We found that the auxin-induced growth is mediated through the activation of the dictyosomes (collectively, the Golgi apparatus). Incubation of oat (*Avena sativa*) coleoptile segments in indoleacetic acid-sucrose-phosphate buffer changes significantly the number of dictyosomes in the expanding cells. A further indication of auxin enhancement of dictyosome activity is a decrease in dictyosomal cisternae (flattened membranous sacs). This decrease occurred after 6 minutes of incubation in auxin, and then was followed by a reduction in the organelle number per se. These times are in keeping with the rapid action of auxin-induced cell elongation, and the latent period of geotropism. In the apical cells, the effect of indoleacetic acid is more subtle and complex. The periods of increased dictyosome utiliztion and of increased dictyosome synthesis in auxin-treated segments occur as in the control. These observations indicate that dictyosomes not only have a function in cell elongation, but also may participate in processes such as auxin transport and stimuli perception. The expanding cells have five times as many dictyosomes as the cells in the apex. Dictyosome number within a cell appears to be directly proportional to the length of the cell. The fluctuation of dictyosome number and the effect of auxin on the rate of elongation of individual cells in outer epidermis are discussed.

*Abstract of a paper published in Plant Physiology 54, 217 (1974).

GRAVITY SENSING IN PLANTS: A CRITIQUE OF THE STATOLITH THEORY*

J. Shen-Miller and R. R. Hinchman†

This paper presents a historical overview of plant geotropism and the pros and cons of the statolith theory. It also introduces evidence and interpretations of recent studies of the amyloplast and the dictyosomes (Golgi apparatus). Both organelles are shown to have a correlative function in plant geotropism. At this point, we favor the idea that gravity perception in plants is not the work of a single sensor, but the interaction of several groups of organelles.

---

*Abstract of a paper published in BioScience 24, 643 (1974).

†Environmental Statement Project, Argonne National Laboratory.

GROWTH, CELL WALL PROPERTIES, AND HORMONE TRANSPORT OF MONO- AND DICOTYLEDON PLANTS GROWN ON CLINOSTATS

*J. Shen-Miller, Diane Hunt,** *Michael J. Koziol,*† *and Y. Masuda*‡

PURPOSE AND METHODS

The growth of shoots of oats (a monocot) was reduced (1), and of hypocotyls of sunflower (a dicot) was increased (2) when the plants were germinated and grown on clinostats whose rotation in a vertical plane nullifies the geotropic response of the plants. The two groups of experiments were done at different times and using different growth media. This study was initiated first to determine whether this difference in growth does exist under the same growth conditions; second, to examine the cell wall properties of these plants, and lastly, to check if the growth and cell wall properties of the plant are related to the hormone transport of the plant.

The seeds were soaked and exposed to 24 hours of red light. They were then planted in sand (16% moisture) and placed on the clinostat for an additional 65 hours of growth in the dark. (The control plants were placed on a clinostat which rotated in a horizontal plane.) The length of the oat shoots and sunflower hypocotyls were then measured and the same tissues were killed in boiling ethanol for cell wall extensibility measurements by a tensile testing technique (3).

---

*Spring 1974 participant in the Undergraduate Honors Research Participation Program, St. Francis College, Joliet, Illinois.

†Participant in the 1974 Summer Institute in Biology, Oxford University, Oxford, England.

‡Osaka City University, Osaka, Japan.

For hormone transport studies, the seeds were treated identically. At the end of the 40-hour growth in the dark, donor tubings containing ^{14}C-indoleacetic acid (^{14}C-IAA, 49 mC/mM) were slipped on to apices of oat coleoptiles or sunflower hypocotyls (cotyledons were removed from the sunflower before IAA application). After IAA application the plants were again placed on the clinostat. Radioactivity within the plant was determined at 10-minute intervals following IAA application for a period of 120 minutes.

PROGRESS REPORT

The growth and wall property measurements are tabulated in Table 8.6. We substantiated the earlier finding that "gravity nullification" by clinostat indeed reduces significantly the length of the oat shoots and increases that of the sunflower hypocotyls. However, the shorter, clinostat-exposed oat tissues have a significantly greater potential in cell wall extensibility than their comparable controls. The longer, clinostat-exposed sunflower hypocotyls, on the other hand, have a lower potential in subsequent cell wall extensibility. These data point out that growth indices (such as length) are not necessarily correlated with the cell wall extensibility.

Table 8.6. Length and Cell Wall Properties of Oat Shoots (Coleoptile plus Mesocotyl) and Sunflower Hypocotyls[a]

Plant	Treatment	Length (mm)	Extensibility (mm/g)	Tau[b] (sec)	To[b] (sec)
Oat	Clinostat	30.4	0.0822	0.6168	0.0380
	Control	32.4	0.0784	0.6214	0.0403
	t Test	$P < 0.001$	$P < 0.05$	n.s.[c]	$P < 0.05$
Sunflower	Clinostat	29.6	0.0547	0.6276	0.0401
	Control	26.0	0.0630	0.6288	0.0413
	t Test	$P < 0.01$	$P < 0.01$	n.s.[c]	$P < 0.01$

[a]Values are means derived from a minimum of 200 measurements.

[b]Calculated values, see (3) for methods of derivation.

[c]n.s. = not significant ($P > 0.05$).

Table 8.7 presents data on hormone uptake and transport. Although clinostat treatment significantly increases the uptake of the hormone in both oats and sunflower plants, it significantly decreases the transport of the hormone into the basal region in both plants. The increased uptake in tissues grown on the clinostat could indicate a greater availability of uptake sites or, indirectly, a lower hormone titer. The reduced transport in the oats could explain the reduced growth. We are not able to interpret the transport data of the sunflower in relation to growth. The removal of the sunflower cotyledons could have affected the hormonal transport of the plant.

Table 8.7. ^{14}C-Indoleacetic Acid Uptake and Transport through Oat Coleoptiles and Sunflower Hypocotyls

Transport Time (min)	Oat				Sunflower			
	Uptake[a] (cpm)		Transport[b] (%)		Uptake[a] (cpm)		Transport[b] (%)	
	Clino.	Control	Clino.	Control	Clino.	Control	Clino.	Control
10	540	289	0.3	0.4	2,941	2,844	0.2	0.1
20	659	404	0.4	0.9	4,376	4,112	0.1	0.1
30	921	684	1.4	2.7	4,770	4,992	0.1	0.1
40	531	604	2.2	3.0	5,912	6,109	0.1	0.1
50	1,027	827	6.2	5.2	7,496	6,261	0.2	0.1
60	1,324	773	7.8	9.8	7,719	6,713	0.6	1.0
70	1,136	737	12.6	12.5	8,434	6,876	2.2	2.7
80	1,596	1,103	9.1	12.9	9,458	7,294	2.9	3.8
90	1,314	817	11.9	16.5	7,555	8,202	6.3	6.0
100	1,401	1,305	12.9	17.1	9,290	9,382	6.5	8.9
110	1,762	1,597	12.8	15.8	11,332	9,673	8.4	9.3
120	2,500	1,819	10.5	17.2	10,972	9,070	9.8	10.1
Mean	1,226	913	7.34	8.18	7,522	6,794	3.12	3.53
	$P < 0.001$[c]		$P < 0.01$[c]		$P < 0.05$[c]		$P < 0.05$[c]	

[a]Average donor = 70,382 cpm (oats) and 116,304 cpm (sunflower).

[b]Percentage of transport, based on total uptake, through apical 10 mm of the tissue into the basal region.

[c]By 2-way analysis of variance.

REFERENCES

1. Shen-Miller, J., and S. A. Gordon. Plant Physiol. 42, 352 (1967).
2. Bara, M., and S. A. Gordon. Physiol. Plant. 27, 272 (1972).
3. Yamamoto, R., K. Shinozaki, and Y. Masuda. Plant Cell Physiol. 11, 947 (1970).

PHYTOCHROME INVOLVEMENT IN THE GEOTROPIC RESPONSE OF CORN ROOTS

Jane Shen-Miller, Leah Glessner, * *and Douglas Moffat*†

PURPOSE AND METHODS

Light activates the geotropic response of corn roots. Corn seeds planted in soil kept in the dark show no tropistic response of the root. Using equal quantal exposures at different wavelengths in the visible spectrum, we observed four response peaks (1). The highest peak occurred at the 660 nm region. The dose was high, 2.6×10^{16} quanta$\cdot$cm^{-2}. The present study was undertaken to determine whether a lower dose would elicit similar responses and if the peak responses, particularly that at the 660 nm, could be reversed by a 730 nm irradiation. A reversal after 730 nm exposure could mean the participation of phytochrome.

Corn seeds were germinated and the primary roots were exposed to various wavelengths (350-750 nm) using interference filters of narrow 1/2-band width. The dose used was 3.33×10^{14} quanta$\cdot$cm^{-2} (60 second exposure time). Five hours after irradiation the geotropic curvature of the roots was measured. In a second group of experiments, the irradiated roots were immediately re-irradiated with equal quanta of 730 nm light. The tropistic curvature was measured 5 hours later.

PROGRESS REPORT

Figure 8.4 shows the spectral response of corn roots. The responses at the three peaks, 460, 560, and 660 nm, were significantly different from those at their adjacent valleys (P = 0.01). The response at 660 nm was significantly greater than the other two peaks (P = 0.01). The responses at 460 and 560 nm were not different. Table 8.8 shows the effect of far-red irradiation (730 nm) on the tropistic response of the roots pre-irradiated with 460, 560, or 660 nm light. The 730 nm irradiation significantly reduced the response induced by the 460 and 660 nm irradiation, but had no significant effect on the control (dark) and the 560 nm irradiation response.

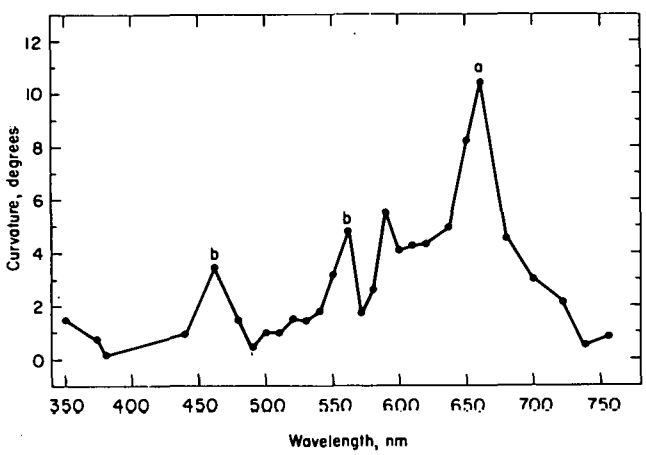

Fig. 8.4. Spectral effect on corn-root geotropism. Equal quantal irradiation, 3.33×10^{14} quanta$\cdot$cm^{-2}, at each wavelength. Peaks with different letters differ significantly at P = 0.01.

A highly purified sample of phytochrome from oat shoots showed absorption peaks in the blue and red region of the spectra (2). Red light converts

---

*Fall 1973 participant in the Undergraduate Honors Research Participation Program, Thiel College.

†Spring 1974 participant in the Undergraduate Honors Research Participation Program, D'Youville College.

Table 8.8. Geotropic Response of Corn Roots at Different Wavelengths as Affected by Postirradiation at 730 nm

Wavelength (nm)	730 nm Postirradiation	Curvature (degrees)	*t* Test
Dark	No	4.03	n.s.†
Dark	Yes	3.44	
460	No	4.45	$P = 0.05$
460	Yes	3.34	
560	No	4.91	n.s.†
560	Yes	4.06	
660	No	8.46	$P = 0.01$
660	Yes	6.80	

†Not significant.
Responses to single irradiation at 560 and 660 nm are significantly greater than their comparable dark controls at $P < 0.01$ and $P < 0.001$, respectively.

phytochrome to a morphologically active form, and this active form can be reversed to the nonactive state by far-red irradiation (2). The reduction in the tropistic response at 460 or 660 nm irradiation followed by 730 nm exposure indicates the involvement of phytochrome as a photoreceptor for root geotropism in corn.

REFERENCES

1. Shen-Miller, J., and J. Lutz. ANL 8070 (1973), p. 125.
2. Shropshice, W., Jr. Photophysiology II, 33 (1972).

PREFERENTIAL ORGANELLE DISTRIBUTIONS DURING GEOTROPIC RESPONSE IN CORN ROOTS

Rand McNitt and Jane Shen-Miller

PURPOSE AND METHODS

Geotropism in corn roots is dependent on light. We have used light as a stimulus or photomorphogenic trigger for the geotropic response and determined the subsequent organelle distributions and associations.

Seeds were germinated in the dark, and the primary roots were exposed for 60 seconds to 5.53×10^{-10} einsteins·cm^{-2} of 660 nm light. Root caps and the 5th mm region (measured from the root apex) of the roots were sampled at 15-minute intervals (over a 2 1/2-hour period) after light exposure.

They were simultaneously fixed with glutaraldehyde and acrolein, post-fixed in OsO_4, and embedded in Spurr's low viscosity embedding medium. Organelles in the tops and bottoms of cell sections in the upper and lower (with respect to gravity) cortical tissue of the 5th mm ("curving zone") of the root were counted. Organelles and organelle associations in the tops and bottoms of cell sections of the central root cap ("geoperceptive site") were also tabulated.

PROGRESS REPORT

In the cortical cells of the curving zone (upper tissues of red-exposed roots), dictyosomes show the greatest preferential distribution in the top (Table 8.9). The cells of the lower tissue show a preferential distribution of dictyosomes toward the bottom. The difference between the top and bottom is greater in the upper cortical tissue of red-exposed roots. This differential between the upper and lower tissue is reduced in the dark controls.

Table 8.9. Average Dictyosome Numbers in the Tops and Bottoms of Cells of the Upper and Lower Cortical Tissue of the 5th mm of Corn Roots[a]

Treatment	Tissue		Time (min) after Light Exposure 1	30	60	90
660 nm	Upper	Top	3.3	2.4	2.8	3.3
		Bottom	2.4	1.5	1.4	1.5
		ΔTop-Bottom	+.9	+.9	+1.4	+1.8
	Lower	Top	2.0	1.7	1.4	2.6
		Bottom	3.4	2.7	2.4	2.6
		ΔTop-Bottom	-1.4	-1.0	-1.0	0
Dark	Upper	Top	2.2	2.1	2.9	2.9
		Bottom	2.0	1.0	2.6	2.1
		ΔTop-Bottom	+.2	+1.1	+.3	+.8
	Lower	Top	2.3	2.0	2.2	2.3
		Bottom	2.6	1.7	2.3	3.0
		ΔTop-Bottom	-.3	+.3	-.1	-.7

[a]Values are means from 30 cells.

As with dictyosomes, the greatest concentration of mitochondria is toward the top of cells of the upper tissue in red-exposed roots, and the preferential distribution is greater in the red-exposed roots than in the dark roots. These preferential distributions of dictyosomes and mitochondria are compatible with the relatively greater growth of upper tissues which results in a downward curvature, positive geotropism.

There is evidence that the central root cap cells are the geosensing cells (1), yet the mechanism of sensing remains unelucidated. We are trying

to identify and quantify ultrastructural changes which occur after light stimulation and concomitantly with the geotropic response in these cap cells.

Although amyloplasts may have a role in gravity perception, their sedimentation in the cap cell is not sufficient to explain the geotropic response. We find that amyloplasts settle to the bottoms of cells in both red-exposed (curving) and dark control (non-curving) roots.

We find that dictyosomes in central root cap cells have a preferential distribution toward the top after red light treatment (Figure 8.5A). A similar distribution seems to characterize the mitochondrial population, also. In addition, a greater percentage of cell nuclei is located in the top half of cells in the red-exposed roots than in the dark controls (Figure 8.5B). The activation of corn-root geotropism by red light indicates the involvement of phytochrome. The contention that phytochrome may become membrane-associated in its active form led us to attempt to characterize the degree of association of the sedimented amyloplasts to the rough ER which occurs as several-layered sheets in the peripheral cytoplasm. We found that a close association (amyloplasts no more than three cisternal thicknesses from the ER) occurs more commonly in the dark control roots, through the first 90 minutes after irradiation (Figure 8.5C). Preferential distributions of organelles within the central root cap cells could cause a message to be transmitted asymmetrically to the elongating cells of the root proper. The growth inhibitor that occurs in corn root caps (2) could conceivably be such a message.

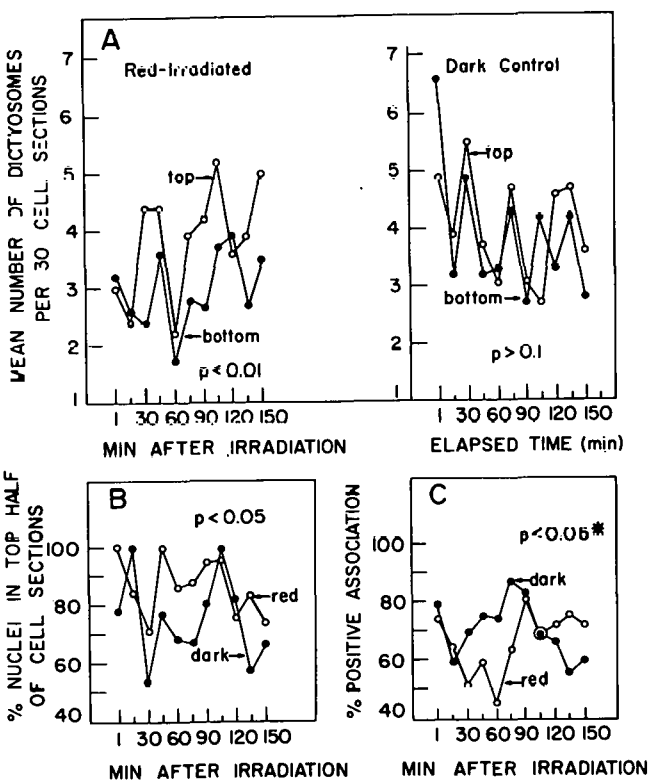

Fig. 8.5. Organelle distribution and association in central root-cap cells (n = 30) of corn after geotropic stimulation. Red = 660 nm irradiation. Data analysed by 2-way analysis of variance. (A) Dictyosomes, (B) Nuclei, (C) ER - amyloplast association (*analysis between 1 and 105 minutes).

REFERENCES

1. Juniper, B. E., S. Groves, B. Landau-Schachar, and L. J. Audus. Nature (London) 209, 93 (1966).
2. Pilet, P.-E. Planta 106, 169 (1972).

ACTION SPECTRA ON PHOTOTROPISM AND GROWTH INHIBITION OF OAT COLEOPTILES

William M. Elliott[*] *and Jane Shen-Miller*

PURPOSE AND METHODS

We have proposed that the first positive phototropic response is the result of a differential transport of the plant hormone (auxin). Subsequently, in examining the dose response and spectral response of hormone movement we found that light does impair the basipetal transport of auxin (1). A reduction of auxin in the growing cells would mean a reduced elongation in these cells. The present study examines whether the dose response and spectral response in growth match those for the phototropic response.

For dose-response experiments of phototropism and growth, oat coleoptiles were exposed either to a unilateral or equilateral blue source (440 nm, interference filter, 1/2-band width - 13.5 nm). Action spectra for phototropism and growth were determined between 360 and 730 nm, also using interference filters, exposing at a dose of 10^{13} photons$\cdot$cm^{-2}, equivalent to 45 ergs$\cdot$cm^{-2} at 440 nm. The curvature response was measured 90 minutes from the time of light exposure and the growth measurements were tabulated as the net growth within a 120-minute period, between 30 and 150 minutes after irradiation.

PROGRESS REPORT

Table 8.10 shows the dose response. Blue light (440 nm) reduces the elongation of the coleoptile. Growth reduction increases with dose. The dose-response trend for growth is comparable to that for phototropism at intensities between 10^{11} and 10^{13} photons$\cdot$cm^{-2}, and differs at higher level of exposures. Choosing a dose level which is near the peak response for phototropism (10^{13} photons$\cdot$cm^{-2}), we next examined the spectral effect on the two responses. Figure 8.6 shows the action spectra. Phototropism and photoinhibition in growth share similar spectral effects between 360-500 nm region of the spectrum. In the longer wavelengths growth seems to be enhanced, while phototropism is unaffected. Such an enhancement in growth is compatible with a reduction in the phototropic curvature and an increase in growth when the coleoptiles were preirradiated with red light (660 nm), Table 8.10. The action spectra indicate that the two responses could share a common photoreceptor. However, the light-growth response appears to be an action of more than one photoreceptor.

[*]Biology Department, Hartwick College, Oneonta, N. Y.

Table 8.10. Dose Response of Growth and Phototropism of Oat Coleoptiles as Induced by 440 nm Irradiation

Photons·cm^{-2}	Net Growth (mm)		Curvature (degrees)	
	No Red	Pre-Red[a]	No Red	Pre-Red[a]
0	2.39	2.32	0.5	-0.2
10^{11}	-	-	-	0.65
2 x 10^{11}	2.15	2.41	5.10	-
10^{12}	-	-	-	10.8
2 x 10^{12}	2.04	2.35	13.0	-
10^{13}	1.88	2.15	18.4	13.0
2 x 10^{13}	-	-	23.7	10.0
5 x 10^{13}	1.84	2.01	14.7	-
10^{14}	1.71	2.04	4.6	3.5
2 x 10^{14}	1.54	2.09	1.6	0.9

[a]660 nm at 10^{16} photons·cm^2.

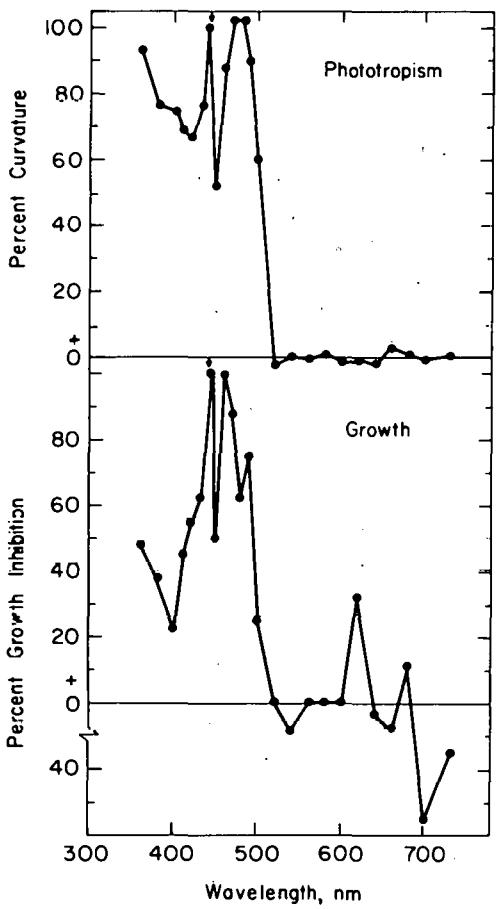

Fig. 8.6. Action spectra of phototropism and growth of oat coleoptiles. The percentages are based on the 440 nm response (arrow). Dose, 10^{13} photons·cm^{-2}. Exposure time, 25 sec.

REFERENCE

1. Shen-Miller, J., P. Cooper, and S. A. Gordon. Plant Physiol. 44, 491 (1969).

9. BIOPHYSICS

SUMMARY

Steven S. Danyluk, Group Leader

Four areas of research are currently being explored in the Biophysics group. These are circadian regulation in eukaryotes and higher organisms, clinical applications of stable isotopes, protein crystallography, and magnetic resonance studies of nucleic acids and drugs. A fifth program in mammalian cell biology, formerly in the group, is now functioning as a separate unit. Although all four programs have a substantial commitment to problems of a fundamental nature, there continues to be a strong emphasis on those systems that relate directly to *in vivo* cellular and organismic functioning, particularly in response to external agents such as radiation, toxic chemicals, and drugs.

One of the major goals of the circadian research is to show how regulation in eukaryotes is connected to specific molecular events at the cellular level. An important step in this direction was made with the discovery that circadian regulation originates at the genome level, a finding now being studied in greater detail in an extensive series of measurements focusing on the roles of food, light and thermal cycle on circadian regulation in synchronous cultures of *Tetrahymena pyriformis*. A facet receiving particular attention is the involvement of intermediary metabolic pathways in circadian regulation. Along this line, preliminary results point to a possible regulatory involvement of biogenic amines in *T. pyriformis*. Results from these studies are laying a foundation for the explanation of circadian regulation in higher organisms including man.

The Argonne program for clinical applications of stable isotopes and mass spectrometry, now in its fifth year of operation, represents an outstanding example of results from fundamental research developing into practical applications. This program has as its main objectives the synthesis of biochemical compounds with potential clinical application, development of new GC-MS instrumentation for detection and quantitative measurement of stable isotope metabolites, and organization of a clinician network to test and validate the usefulness of labeled compounds in diagnostic procedures. Progress was made in the past year in the synthesis and testing of ^{13}C-labeled aminopyrine for measurement of liver microsomal mass. The results with normal volunteers were sufficiently encouraging to warrant follow-up investigations in persons with liver disease. Further work continued on the synthesis of ^{2}H-labeled bile acids and an extensive trial program for chenodeoxycholic acid treatment of gallstone disease was initiated. In a related study, a new class

of biliary lipids, present in concentrations as high as 10% in bile acid samples of patients with abnormal hepatic function, was isolated and identified by chemical synthesis of analogues and GC-MS.

Both the protein crystallography and magnetic resonance programs are concerned with accurate three-dimensional biomolecular structure determinations and the correlation of these structures with biological function. X-ray crystallographic techniques are being used to determine crystal structures for Bence-Jones and parent IgG myeloma proteins to atomic resolution. Argonne's lead in this area of immunoglobulin research was further consolidated by extension of the Bence-Jones structure to 2.3 Å resolution and construction of a scale model for the protein. Diffraction measurements were also used to map out the binding regions in an Mcg Bence-Jones dimer for numerous hapten-like molecules. The results provide the first insight into structural features responsible for the diversity in antibody response.

The magnetic resonance studies continued to focus upon structures, conformations, and interactions of nucleic acid segments, antibiotics and drugs, and certain peptides in aqueous and non-aqueous solutions. A 3-D structure determination, utilizing paramagnetic ion probes, was completed for the chloroquine cation in methanol and revealed rather striking differences from the corresponding free base structure. There are good reasons to believe that the compact, folded structure of the cation is the preferred form for binding to DNA. An extensive long-range proton NMR study of structures for all commonly occurring 2'-, 3'-, and 5'-ribo- and deoxyribonucleotides, completed in the past year, has led to a number of conformational "rules" which will prove invaluable for structure determinations of more complex nucleic acid fragments currently underway. Further progress toward the first complete NMR assignment of a trinucleotide codon spectrum was made with the synthesis of a selectively deuterated A$\overset{*}{p}$ApA ($\overset{*}{}$Ap-, fully deuterated) trimer. The spectrum for this compound combined with an earlier spectrum for *ApApA has permitted assignment of all the base and anomeric H1' protons of ApApA.

Continued efforts by Biophysics group members over the past four years to solicit support for their programs from other governmental agencies met with some success in 1974 with the award of an NIH contract to support one phase of the Clinical Applications of Stable Isotopes program. Several other proposals from group members are in various stages of preparation and review.

BIOPHYSICS STAFF

REGULAR STAFF

Ainsworth, Clinton F. (Scientific Assistant)
Danyluk, Steven S. (Senior Chemist)
Edmundson, Allen B. (Senior Biochemist)
Ehret, Charles F. (Senior Biologist)
Ely, Kathryn A. (Scientific Assistant)
Groh, Kenneth R. (Scientific Assistant)
*Hachey, David L. (Assistant Biochemist)
*Hardman, Karl D. (Assistant Biochemist)
Klein, Peter D. (Senior Biochemist)
Meinert, John C. (Scientific Assistant)
†Schiffer, Marianne (Biophysicist)
*Sinclair, Warren K. (Senior Biophysicist)
*Sutherland, Alexander (Scientific Assistant)
Szczepanik, Patricia A. (Scientific Assistant)
Westholm, Florence A. (Scientific Assistant)

TEMPORARY STAFF DURING 1974

Abola, Enrique (Postdoctoral Appointee)
Antipa, Gregory A. (Postdoctoral Appointee)
Bryant, William F. (Postdoctoral Appointee)
Dobra, Kenneth W. (Postdoctoral Appointee)
Ezra, Fouad S. (Postdoctoral Appointee)
Fiat, Daniel (Visiting Scientist)
Firca, Joseph R. (Postdoctoral Appointee)
Girling, Rowland L. (Postdoctoral Appointee)
Panagiotopoulos, Nicolas C. (Postdoctoral Appointee)
Schoeller, Dale A. (Postdoctoral Appointee)

---

*Terminated during 1974.

†Now Associate Laboratory Director for Biomedical and Environmental Research, and in the Mammalian Cell Biology Group.

BIOMOLECULAR STRUCTURE DETERMINATIONS: MAGNETIC RESONANCE STUDIES OF BIOMOLECULAR STRUCTURES AND INTERACTIONS

Steven S. Danyluk, Fouad Ezra, Daniel Fiat, and Clinton F. Ainsworth

High-resolution nuclear magnetic resonance spectroscopy continues to be the only available experimental approach for the determination of biomolecular conformational features in solution. When combined with supplementary NMR techniques such as paramagnetic ion probes, double resonance, and spin-lattice relaxation times, along with judicious syntheses of derivatives selectively labeled with ^{2}H, ^{13}C, and ^{15}N), exciting possibilities can be foreseen for complete, accurate, 3-dimensional analyses of biomolecular structures in

aqueous solution, and the pinpointing of specific interaction pathways attendant to biological function.

As outlined in previous reports, our overall program evolves along several interconnected lines of research. A major effort is directed toward accurate 3-D structure determinations for nucleic acid constituents in aqueous solution, with ribo- and deoxyribonucleotide fragments being the main focal points. The ultimate goal here is to integrate structural data for simpler oligomeric constituents into a complete composite structural model for naturally occurring t-RNA, m-RNA, and DNA. Information in this area is vitally needed for meaningful assessments of biological interactions involving these molecules.

A second aspect is concerned with accurate 3-D structure determinations for physiologically active antibiotics and drugs whose activity is expressed by initial binding to nucleic acid receptor sites. Of particular interest in this area are the powerful tumor-inhibiting antibiotic, actinomycin D (ACD), and chloroquine (CQ), a drug extensively used in antimalarial chemotherapy. This segment is coordinated with nucleotide structure determinations. Together, these investigations will provide definitive knowledge on conformational determinants of drug-DNA interactions.

A third area of interest is concerned with HRNMR determinations of conformational properties of dipeptides and higher oligopeptides, particularly as they relate to recognition processes between amino acid residues and nucleic acid segments.

Finally, a substantial continuing effort is directed toward the identification of radiation damage sites in nucleic acids, the development of damage-structure correlations, and the investigation of biopolymer motional properties. A number of advances were made in each of these projects in the past year, and these are summarized briefly in following sections.

SYNTHESIS AND NMR SPECTROSCOPY OF SELECTIVELY DEUTERATED NUCLEIC ACIDS: TRINUCLEOSIDE DIPHOSPHATES, *ApApA

Norman S. Kondo, Clinton F. Ainsworth, and Steven S. Danyluk

PURPOSE AND METHODS

Previous work from our group described chemical and enzymatic methods for synthesizing dinucleoside monophosphates containing a fully deuterated nucleotidyl unit at either 3' or 5' loci (1). Synthesis of these selectively labeled compounds permitted complete and unambiguous assignment of all signals in the 220 MHz proton NMR spectra for the protio forms, thereby opening up the possibility of using accurate NMR parameters derived from analysis of the spectra to determine conformational features for these molecules in aqueous solution. The approach is currently being exploited in conformational analyses of adenylyl-(3' → 5')-adenosine (ApA) and uridylyl-(3' → 5')-adenosine (UpA) and other dinucleoside monophosphates.

As the pattern of conformational properties emerges for dimers, a foundation is laid for extending such structural studies to the next higher level of nucleic acid complexity, i.e, trinucleoside diphosphates. The determination of conformational features for trinucleotides is of especial interest since these fragments incorporate all of the structural components present in triplet codons. As with dinucleotides, however, an assignment of proton signals for trinucleotides is ruled out by signal overlap. Accordingly, the purpose of this study was to extend synthetic procedures developed for the preparation of labeled dimers to the synthesis of selectively deuterated trinucleoside diphosphates. The trimer chosen for synthesis was adenylyl-(3' → 5')-adenylyl-(3' → 5')-adenosine, ApApA.

PROGRESS REPORT

A complete assignment of all proton signals of ApApA requires the synthesis of at least four selectively deuterated trimer derivatives, *ApApA, Ap*ApA (or Ap*Ap*A), *Ap*ApA and *ApAp*A (or Ap*Ap*A), where *A represents a fully deuterated nucleotidyl unit. The first two trimers are necessary for assignment of all the base (H_2,H_8) and anomeric H1' signals, while the latter pair is required to complete the ribose signal identification. In the event of significant back-exchange of D-8 atoms further syntheses of D-8ApApA and ApD-8ApA will be necessary to sort out the H-8 signals.

An enzymatic approach was selected for synthesis of trimers from appropriate dinucleotides. Under appropriate conditions of high salt concentration, polynucleotide phosphorylase from *Micrococcus lysodeikticus* can be used to synthesize short chain oligonucleotides, n = 3 and upwards, from starting dinucleoside monophosphates as primer. *ApA, originally synthesized in the dimer study, was incubated with ADP in the presence of enzyme for 24 hours, and the labeled trimer was then isolated by paper chromatography and purified by passing through DEAE - cellulose. The overall yield of *ApApA was close to that reported by Thach (2) for the synthesis of other trimers, and was sufficient to permit NMR measurements.

A comparison of proton spectra for ApApA and *ApApA, Figure 9.1, permits immediate assignment of H2, H1', and H5'(5") signals for the Ap- nucleotide. Tentative assignments are also possible for H2', H3', and H4' signals by taking differences between integrated signal intensities of *ApApA and ApApA in the complex multiplet region at 3.5 to 4.5 ppm. Further confirmation will require measurement of spectra for other combinations of selectively deuterated adenylate trimers (cf. above). Along this line, a synthesis has been completed very recently of an Ap*ApA trimer and NMR spectral measurements are currently underway.

One of the most surprising results revealed by the *ApApA spectrum was a greater shielding of H2 for Ap- than for base protons of -ApA residues. This unexpected result runs counter to a prediction, based on consideration of stacked trimer possibilities and crystal structures (poly A), that base protons of -pAp- should be most shielded. The NMR result is clearly incompatible with a symmetric trimer structure and further suggests that base-stacking may be a non-cooperative phenomenon, i.e., ΔH for a stacking interaction is sequence dependent. Finally, these preliminary measurements serve to point out the pitfalls of making spectral assignments based on hypothetical "favored" conformations for trimers.

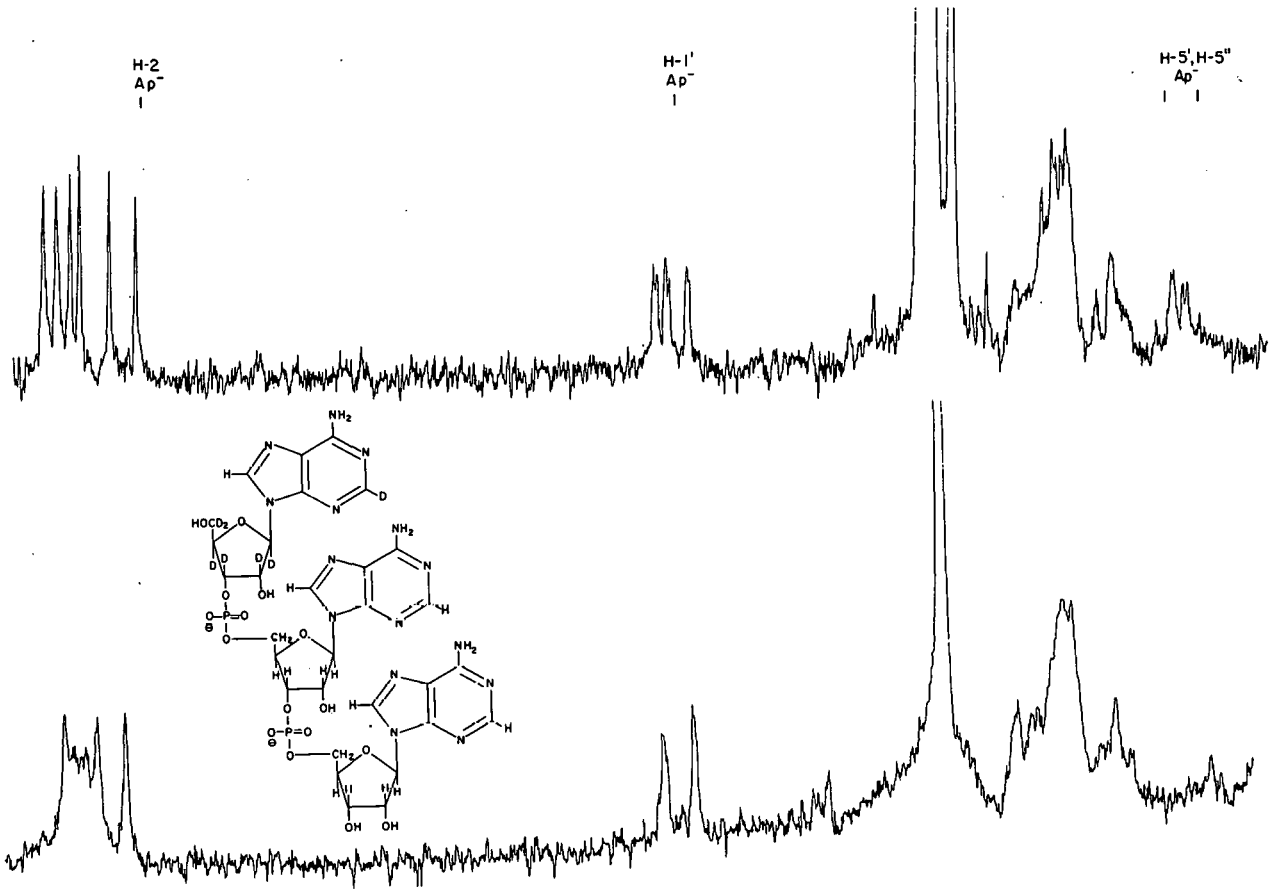

Fig. 9.1. The 220 MHz proton magnetic resonance spectra for ApApA (upper spectrum) and *ApApA (lower spectrum). Spectra were measured at 18°C under similar conditions of concentration and pH.

REFERENCES

1. Kondo, N. S., and S. S. Danyluk. J. Am. Chem. Soc. 94, 5121 (1972).
2. Thach, R. E. In: Procedures in Nucleic Acid Research, Vol. 1. Eds. G. L. Cantoni and D. R. Davies. Harper and Row, New York, 1966, p. 520.

EPR STUDIES OF FREE RADICALS IN γ-IRRADIATED NUCLEIC ACIDS

Fouad Ezra and Steven S. Danyluk

PURPOSE AND METHODS

Radiation damage in DNA is manifested as single or double strand breaks, cross-linkage, breakage of hydrogen bonds, and base degradation. This molecular damage in turn causes an impairment in transcription and replication processes, and may be responsible for chromosome abnormalities and cell death. One of the central questions in radiation damage of nucleic acids is the nature of mechanisms involved in the interaction of ionizing radiation with the target molecule.

It is generally believed that the initial effect of ionizing radiation is the production of electrons and positive ions from which free radical species are subsequently formed. Formation of free radicals in nucleic acid constituents has accordingly been extensively studied by electron paramagnetic resonance (EPR). In most cases, radicals produced at the base moieties have been identified accurately (1). Comparatively little attention has been given to the ribose phosphate moiety; however, there is strong evidence, from pulse radiolysis and chemical analysis of end products, that damage in DNA is indeed sustained at the ribophosphate backbone.

Several attempts have been made to detect and identify radiation-induced radical intermediates produced at sites other than the base, but assignments of EPR signals have not been definitive in these studies. It has been proposed, for example, that a weak doublet (splitting, 115-125 G) present in irradiated samples of dinucleotides and several mononucleotides is due to a phosphate type radical (2). This assignment has been challenged recently by Van de Worst and coworkers (3) who attribute the doublet to the outer lines of a 1:2:1 triplet due to a $R\dot{C}H_2$ type radical. However, the conditions (irradiation time, dose, etc.) under which the two studies were carried out differ sufficiently so as to preclude a definitive assignment. A further complicating factor in both cases was the presence of a large, broad signal arising from base radicals. In order to circumvent this difficulty and to provide further confirmatory evidence for phosphate and/or ribose group free radicals, an EPR study was undertaken of the effects of γ-irradiation on fully deuterated nucleotides and dinucleoside monophosphates in the crystalline state.

The rationale for these experiments is straightforward. If the weak doublet originally observed in protonated dinucleotides and several mononucleotides arises from a phosphorus centered radical, then no alteration of the splittings should occur upon irradiation of fully deuterated counterparts. On the other hand, if the radical is of the $R\dot{C}H_2$ type, then in deuterated nucleotides it should show an approximately symmetric 5-line pattern with a separation of about 35 G between the outermost lines.

PROGRESS REPORT

As an initial test of the preceding hypothesis, a mixture of fully deuterated 2' and 3'-uridine monophosphates (UMD-2',3') was separated chromatographically from an RNA hydrolysate extracted from fully deuterated algae. The nucleotide mixture was purified, lyophilized, and then irradiated at 77°K under vacuo with γ-rays from a ^{60}Co source. A similar protocol was

followed in the preparation of irradiated protonated UMP-2' and UMP-3' (sodium salts purchased from Sigma Chemical). Total doses ranged from 1 to 20 Mrads in both cases.

EPR spectra, measured at X-band for protonated and fully deuterated nucleotides at 77°K, are shown in Figure 9.2. For the protio sample, Figure 9.2(a), the broad, slightly assymmetric doublet (g = 2.0034) results from electron addition at the uridine ring (2) and, as expected, is reduced to a broadened singlet with unresolved splitting in the deuterated sample, Figure 9.2(b). The doublet of low intensity, cf. arrows, Figure 9.2(a), and splitting of 128G is similar to those detected for other protonated mono- and dinucleoside monophosphates (2). These signals have been attributed to a phosphorus type radical $RO(RO')\dot{P}O_2$, with an unpaired spin localized on one or both of the non-ester oxygens (2).

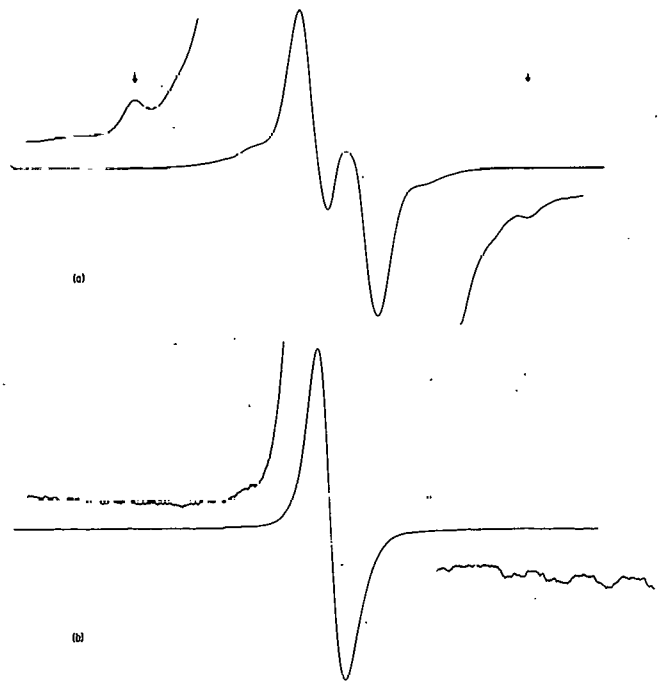

Fig. 9.2. First derivative X-band ESR spectrum of γ-irradiated 2' and 3'-UMP (Na Salt) mixture obtained at 77°K. (a) Protonated sample, microwave power (mp) = 0.05 mW, modulation amplitude (ma) - 1.0 G, receiver gain (rg) = 2×10^3. Wing lines, mp = 1.0 mW, ma = 2.5 G, rg = 4×10^3. (b) Deuterated sample, mp = 0.05 mW, ma = 1.0 G, rg = 1.6×10^3. Wing lines, mp = 2.0 mW, ma = 5 G, rg = 8×10^3.

Examination of Figure 9.2(b) reveals no comparable doublet for the deuterated sample and no evidence of a multiplet pattern expected for $R\dot{C}D_2$. Furthermore, variation of the microwave power did not produce any significant change in the basic spectrum shown in Figure 9.2(b). This unexpected result for deuterated nucleotides raises serious questions regarding the formation of $RO(R'O)\dot{P}O_2$ or $R\dot{C}H_2$ type radicals in γ-irradiated nucleic acids. Neither of these possibilities can be accommodated by the present results. One explanation of the discrepancies could be the influence of counter ions present in the vicinity of the ribose phosphate moiety, a likelihood indicated by preliminary measurements on nucleotides prepared by different procedures. Studies are currently underway to assess this influence and to resolve the questions raised by the deuterated radicals.

REFERENCES

1. Muller, A., and J. Hutterman. Ann. N. Y. Acad. Sci. 222, 411 (1973).
2. Bernhard, W. A., and S. S. Danyluk. Radiat. Res. 53, 169 (1973).
3. Van de Vorst, A., Y. Lion, and C. M. C. Bacq. Int. J. Radiat. Biol. 24, 605 (1973).

NUCLEAR MAGNETIC RESONANCE STUDIES OF NUCLEIC ACID STRUCTURES IN SOLUTION: 5'-RIBO- AND DEOXYRIBONUCLEOTIDES*

David B. Davies† *and Steven S. Danyluk*

An extensive proton NMR study is reported for all common purine and pyrimidine-5'-ribo- and deoxyribonucleotides at 220 MHz. Spectra for these nucleotides were measured in D_2O solutions at 20 ± 2°C and signal assignments made with the aid of selected ^1H-^1H and ^{31}P-^1H decoupling experiments. Complete sets of accurate chemical shifts and coupling constants were derived for each nucleotide by iterative procedures and yielded close agreement between observed and calculated spectra.

The NMR parameters have been utilized in a quantitative evaluation of several key nucleotide conformational features including equilibrium conformations of ribose and deoxyribose rings, preferred exocyclic group orientations, and base-ribose ring orientation. A quantitative conformational analysis was made for the D-ribose and D-deoxyribose rings of all the 5'-ribonucleotides following procedures analogous to those developed recently by Altona and Sundaralingam. The analysis is based on an assumption of a rapidly equilibrating mixture between N type [C(3')-*endo*, C(2')-*exo*] and S type [C(2')-*endo*, C(3')-*exo*] conformers, N ⇌ S. With the aid of graphical plots, quantitative estimates were made of pseudorotational angle, P, degree of pucker, T, and ring conformer populations. The results show that the pseudorotational parameters (P, T) do not vary significantly between nucleotides and are generally within ranges found in the crystalline state. An S-type conformation is favored in both ribo- and deoxyribonucleotides at 20° with the equilibrium lying somewhat more in favor of the S-conformer in the latter, i.e., 70:30 versus 60:40. Possible effects of electronegativity change upon pseudorotational parameters were explored and it was concluded that no particular advantage is gained by using adjusted Karplus expressions for individual ring molecular fragments at the present accuracy of measured coupling constants.

A conformational analysis was also made of rotamer populations about exocyclic C(4')-C(5') and C(5')-O(5') bonds. In each instance rapid interconversion was assumed between three classical staggered rotamers, *gg*, *gt*, *tg*. Numerical analysis of the NMR data led to the result that the *gg* rotamer is markedly preferred above both C(4')-C(5') and C(5')-O(5') bonds in all the 5'-nucleotides studied. This preference is somewhat greater in ribonucleotides and appears to be correlated with furanose ring conformation. The

---

*Abstract of a paper published in Biochemistry 13, 4417 (1974).

†Visiting Scientist, Birkbeck College, London.

exocyclic side-chain accordingly exists predominantly in an all *trans* bonding arrangement with the phosphate group directed over the ribose ring of the nucleotide. Taken together, these results point to a surprising constancy of ribose-phosphate conformational features throughout the entire series of 5'-nucleotides. Moreover, comparison with crystallographic results shows that solution structures differ only slightly from those in the crystalline state. Although the results are apparently consistent with recent hypothesis of a "rigid" nucleotidyl structural unit, it is important to note that nucleotide structures in solution are actually a dynamical average of a number of rapidly interconverting conformers.

Finally, sizeable deshieldings observed for base protons of 5'-ribo and deoxyribonucleotides relative to corresponding 2'- and 3'-derivatives and the surprisingly large deshieldings of ribose ring protons in purine relative to pyrimidine 5'-nucleotides are both compatible with a preferred *anti* orientation of base and ribose rings about the glycosidic bond in these nucleotides. The ribose proton deshieldings in purine nucleotides are qualitatively accounted for by the effect of "in-plane" purine ring diamagnetic anisotropy. It is concluded that 5'-nucleotides exist in a dynamic equilibrium between two preferred ranges of *anti* conformations, i.e., *anti* $\rightleftharpoons$ *anti*-S.

NUCLEAR MAGNETIC RESONANCE STUDIES OF 2'- AND 3'-RIBONUCLEOTIDE STRUCTURES IN SOLUTION*

David B. Davies[†] *and Steven S. Danyluk*

A systematic 220 MHz proton NMR study has been made of all common purine and pyrimidine-2'(3')-ribonucleotides in D_2O solutions at 20 ± 2°C. Spectra for the entire series were measured under similar conditions of concentration, temperature, and ionic strength, thereby facilitating intercomparisons of spectral properties. Spectral assignments were accomplished with the aid of selected ^{31}P-^{1}H decoupling experiments and accurate values of NMR parameters were derived by simulation-iteration procedures.

A detailed analysis of the coupling constants and chemical shifts permitted a determination of conformational properties for ribose rings, exocyclic carbinol and phosphate groups, and the orientation of base-ribose rings. Following procedures described elsewhere, an evaluation was made of ribose ring pseudorotational parameters for each 2'(3')-nucleotide. The results show that both the degree of pucker and pseudorotational angle vary only slightly throughout the entire series of molecules, and lie within ranges found in the crystalline state. Furthermore, the ribose rings are in rapid equilibrium between N type [C(3')-*endo*, C(2')-*exo*] and S type [C(2')-*endo*, C(3')-*exo*] conformers, N $\rightleftarrows$ S, with an S type conformer favored in purine-2'(3')-ribonucleotides ($\sim$ 60:40) while pyrimidines exhibit approximately

*Abstract of a paper to be published in Biochemistry, 1974-75.

[†]Visiting scientist, Birkbeck College, London.

equal compositions. Thus, the phosphate location on the ring has less of an effect on ring properties than does the nature of the base ring.

An analysis is also reported of rotamer equilibria about C(4')-C(5'), C(2')-O(2'), and C(3')-O(3') bonds. For the former the NMR coupling constant data are consistent with a predominant *gg* rotamer (∿ 70%) with *gt* and *tg* rotamers populated to the extent of ∿ 20% and ∿ 10% respectively. No correlation of the type seen for 5'-nucleotides appears to exist between C(4')-C(5') *gg* population and ribose ring equilibrium composition. For 2'-nucleotides the ^{31}P-H(2') coupling data indicate a preferred C(3')*g*, C(1')*t* conformer about C(2')-O(2') in agreement with ^{13}C NMR results. A less definitive rotamer analysis follows from observed $J_{^{31}P,H(3')}$ values, but when these results are combined with relevant chemical shift data for deoxynucleosides and nucleotides, the evidence strongly points to essentially free rotation and approximately equal rotamer populations about C(3')-O(3').

Chemical shift differences between purine and pyrimidine 2'(3')-ribonucleotides are qualitatively accounted for in "in-plane" purine diamagnetic anisotropy effects. Also, the greater magnitude for purine deshieldings in 2'(3')-nucleotides relative to 5'-nucleotides is explained by a more favored *syn:anti* ratio in the former, in line with recent Nuclear Overhauser results.

Comparison of the present work with earlier results for 5'-nucleotides reveals a remarkable consistency in almost all of the conformational features for the basic nucleotidyl unit throughout the entire range of mononucleotides. An important exception is the difference in rotamer behavior for exocyclic phosphate groups in 5'- and 3'-nucleotides. The greater rotational freedom in the latter has important consequences for conformational properties of dinucleotides and higher nucleic acid polymers.

AN NMR RELAXATION STUDY OF POLYNUCLEOTIDE-NUCLEOTIDE INTERACTIONS*

D. O. Van Ostenburg,† *R. L. Spiewak,*† *and S. S. Danyluk*

A study has been made of the influence of polyuridylic acid (poly U) - adenosine (A) interactions upon the NMR proton relaxation behavior of H_2O protons in aqueous solutions doped with Mn^{++} ions. Factors investigated included the effect of adenine oligonucleotide chain length, nucleoside concentration, and temperature upon the relaxation behavior of H_2O. The results show that in all cases where solution and temperature conditions favor 2 poly U:A triple strand formation, a significant enhancement in H_2O relaxation rate occurs over that for poly U or nucleotide solutions alone. Moreover, plots of relaxation enhancement versus temperature show well-defined transition regions with the enhancement approaching values for free poly U above the transition temperature, T_m. The data also show that T_m increases with

---

*Abstract of paper to be published in Bioinorganic Chemistry.

†Department of Physics, DePaul University, Chicago.

increasing adenosine concentration and oligomer chain length. No comparable changes are observed for poly U solutions containing guanosine or cytidine derivatives. The increased relaxation rate in 2 poly U:A solutions is consistent with a more rigid secondary structure in the complex than in poly U; melting of this structure leads to an increase in polymer segmental mobility and a corresponding decrease in relaxation rate. The "melting" transitions and variation of T_m with concentration and chain length have been interpreted quantitatively in terms of recent statistical models and yield values of $\Delta H = -20 \pm 3$ kcal/mole (base triplet) and $\Delta S = -63 \pm 10$ cal/mole °K (base triplet) in satisfactory agreement with results of optical studies.

CIS-TRANS CONFORMATIONAL DEPENDENCE OF THE CARBOXYLATE pK IN GLYCYLSARCOSINE*

Richard A. Morton† *and Steven S. Danyluk*

A study is reported of the influence of pD upon the 220 MHz proton n.m.r. spectrum of the dipeptide glycylsarcosine (Gly-Sar) in D_2O at 23°C. Variation of pD produces characteristic changes in chemical shifts for Gly-Sar and an analysis of the pD - chemical shift curves shows that the carboxyl pK differs significantly in *cis* and *trans* conformers, having values of 3.01 ± 0.03 and 3.39 ± 0.03, respectively. From a consideration of molecular models and theoretical calculations, it is concluded that the pK difference arises from a closer juxtaposition of terminal carboxyl and amino groups in the *cis* isomer.

---

*Abstract of a paper published in Canadian Journal of Chemistry 52, 2348 (1974).

†McMaster University, Hamilton, Ontario.

THE ARGONNE PROGRAM FOR CLINICAL APPLICATIONS OF STABLE ISOTOPES AND MASS SPECTROMETRY

Peter D. Klein, Patricia A. Szczepanik, David L. Hachey, and Dale A. Schoeller

The Argonne Program for Clinical Applications of Stable Isotopes and Mass Spectrometry is now in its fifth year of collaboration with clinical investigators who require the safety of nonradioactive tracers of hydrogen, carbon, nitrogen, and oxygen for their studies on pregnant women, on premature and newborn infants, on young children, and on individuals requiring repeated tracer studies. This program seeks to generate wider use of stable isotopes by identifying the compounds which, if available with stable isotopic labeling, could find significant research or diagnostic application; by pressing the developmental transition from laboratory prototype to commercial product; and

most important, by recruiting additional clinicians through the joint publication of successful collaborative applications in clinical journals. At the same time, the collaborative network of participants in this program serves an important weathervane function, indicating needs and trends which can guide commercial suppliers of labeled compounds and instrument manufacturers engaged in development of instrumentation for these uses.

A significant offshoot in the area of instrumentation has been the initiation of high-sensitivity $^{13}CO_2$ measurement as a common end technique for the use of ^{13}C-labeled substrates in clinical diagnosis. These measurements promise to reduce the quantity of material required in patient studies and thereby reduce the cost of such procedures substantially.

In association with the instrumentation for isotope ratio measurements in organic molecules, this program has developed a unique facility for electron impact and chemical ionization mass spectroscopy which is providing new means of identifying and quantitating unusual bile acids encountered in the treatment of gallstones by oral therapy with chenodeoxycholic acid. A new program, expected to enroll some 1000 patients at ten treatment centers around the country for an extended evaluation of this treatment, will make extensive use of these capabilities in our program.

INITIAL STUDIES ON THE DEMETHYLATION OF ^{13}C AMINOPYRINE AS A MEASURE OF LIVER MICROSOMAL MASS IN HUMANS

Dale Schoeller, John Schneider, * *and Peter D. Klein*

PURPOSE AND METHODS

It is well established that the mixed oxidase function of liver microsomes plays a major role in drug detoxification. To date, no good estimate of the total active microsomal mass is available, and as a result it is not possible to predict the patient's response to the dosage of drug to be administered: the dose may be too small or too large. Recently, Lauterburg and Bircher (1) have shown that the rate of demethylation of ^{14}C-dimethylamino-antipyrine (as measured by the appearance of $^{14}CO_2$ in respiratory CO_2) was proportional to liver mass in the rat and followed Lineweaver-Burke plots against substrate concentration. The rate was reduced in proportion to liver mass removed by partial hepatectomy and stimulated 8-fold by pretreatment of the animal with phenobarbital, a known microsomal induction agent. Our purpose in developing the use of ^{13}C-labeled aminopyrine is a means of estimating a patient's ability to detoxify drugs and as a measure of hepatic function in normal and disease states. Using the nonradioactive labeling, the safety of such testing could enable its use in children and pregnant women.

The demethylation rate can be determined by measuring the rate of $^{13}CO_2$ liberation after administration of the drug labeled in the methyl positions

* University of Chicago.

with ^{13}C. $^{13}CO_2$ production is determined by measurements of the $^{13}C/^{12}C$ abundance in expired CO_2 using a dual collector isotope ratio mass spectrometer (2,3).

PROGRESS

Research to date has dealt with the problems of sample collection, the sensitivity of the ratio determination, and the acquisition of data on normal subjects. The CO_2 in expired air is collected by bubbling the breath through 10 ml of 2N NaOH in the bottom of a 250 ml round bottomed flask. The use of smaller containers such as scintillation vials was found to produce variable CO_2 trapping efficiency, resulting in inconsistent values. The effectiveness of the procedure (which would be used in clinical practice and field applications) was compared with the standard method of freezing out CO_2 from breath by passing the gas stream through a trap cooled to liquid nitrogen temperature. Table 9.1 shows that CO_2 collected in 2N NaOH solutions is depleted by 13 °/₀₀ with respect to the values obtained by collection in liquid nitrogen. This depletion is very similar to previously published values by Craig (4) and is attributed to kinetic isotope effects at the gas-liquid interface. Despite this fractionation effect, the use of NaOH solutions as trapping media for CO_2 samples still serves as an effective means of collecting CO_2; except for the point at 15 minutes, the $^{13}CO_2$ increase following administration of ^{13}C labeled aminopyrine is identical for the two methods within the limits of experimental error. The deviation at 15 minutes is attributed to a small difference in sampling times.

Table 9.1. Comparison of ^{13}C Abundance in CO_2 Samples Collected in Aqueous 2N NaOH and by Cryogenic Trapping in Liquid Nitrogen Following ^{13}C Aminopyrine Administration in the Human

Time after Administration of ^{13}C Aminopyrine	CO_2 Collected in NaOH	CO_2 Collected in Liquid N_2	Difference
Minutes	°/₀₀[a]	°/₀₀	°/₀₀
0	1.3	-11.6	-12.9
15	14.8	- 0.9	-15.7
30	14.2	2.2	-12.0
60	-	- 0.9	-
90	9.3	- 2.6	-11.9
120	8.7	- 3.9	-12.9
150	8.5	- 4.0	-12.5

The average deviation of all instrumental measurements was 1.4 °/₀₀.

a °/₀₀ = $\left[\frac{(^{13}C/^{12}C)_{unknown} - (^{13}C/^{12}C)_{reference}}{(^{13}C/^{12}C)_{reference}}\right] \times 10^3$

The sensitivity of this procedure is limited by the uncertainty or standard deviation of the determinations. When replicate samples are measured, either within the same study or at weekly intervals, the values obtained have a standard deviation of 0.6 °/₀₀. This is of the same magnitude as the short-term fluctuations in ^{13}C abundance in respiratory CO_2 in the absence of labeled substrate. Thus the minimum change in abundance with a significance of $P = 0.05$ is 2.5 °/₀₀.

To date, three normal subjects with no history of liver disease have been tested. Each subject was given an oral dose of 4,4',dimethyl-^{13}C aminopyrine at a dosage of 2 mg/kg body weight and samples of respiratory CO_2 were collected over a 3-hour period. The changes in $^{13}CO_2$ abundance, compared to a baseline value obtained before substrate administration, are shown in Figure 9.3. Within two hours, 11% to 22% of the labeled material appeared as $^{13}CO_2$ in these three patients, and all showed rates of demethylation that could be readily and accurately determined by changes in the $^{13}CO_2$ abundance. Thus the dosage selected for this test is probably adequate to provide the desired diagnostic information.

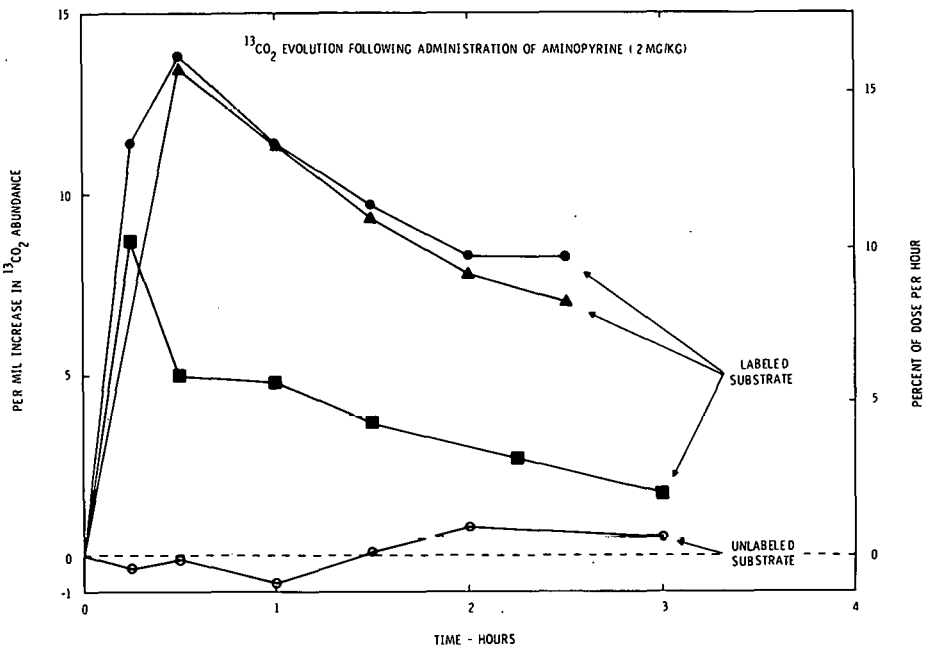

Fig. 9.3. The per mil changes in the expired $^{13}CO_2$ after the administration of either ^{13}C labeled aminopyrine (closed forms) or natural abundance aminopyrine (open circles). The standard deviation of the ratio determination is 0.6 per mil.

CONCLUSION

Measurement of respiratory $^{13}CO_2$ abundance following administration of 4,4',dimethyl-^{13}C aminopyrine to normal volunteers has been carried out. Even at the small dosage employed, an increase in ^{13}C abundance, reflecting demethylation of the aminopyrine by the liver, could be detected. The utility of this procedure in diagnosis of liver disease and drug-drug interaction will be the subject of further investigation.

REFERENCES

1. Lauterburg, B., and J. Bircher. Gastroenterology 65, 556 (1973).
2. McKinney, C. R., J. M. McCrea, S. Epstein, H. A. Allen, and H. C. Urey. Rev. Sci. Instrum. 21, 724 (1950).
3. Nier, A. O. Rev. Sci. Instrum. 18, 398 (1947).
4. Craig, H. Geochim. Cosmochim. Acta 3, 53 (1953).

BILE ACID ALKYL ETHERS: EVIDENCE FOR A NEW CLASS OF BILIARY LIPIDS IN HUMAN BILE

D. L. Hachey, P. A. Szczepanik, P. D. Klein, A. M. Tercyak, * *and J. B. Watkins**

PURPOSE AND METHODS

Bile acids most commonly occur in man as the hydroxylated glycine or taurine conjugates of 5β-cholanic acid. In addition, the hydroxyl group is subject to bacterial oxidation in the large intestine and sulfation in the liver. We now have evidence for a third hydroxyl transformation of bile acids: O-alkylation of the hydroxyls to form alkyl ethers.

In 1966 Eneroth, Gordon and Sjövall (1) reported traces of an unidentified compound in the trihydroxy fraction of human fecal bile salts. This compound exhibited a mass spectrum with a base peak at m/e 299 and an ion characteristic of trihydroxy bile acids at m/e 253. This material had a relative retention time of 2.86 on QF-1, but it could not be oxidized to a triketo cholic acid. We have found evidence for this same compound, in concentrations as high as 10%, in biliary bile acid samples from premature infants, children with cystic fibrosis, and cholecystectomized adults. We have tentatively identified both 3α-ethoxy and 3α-methoxy-7α,12α-dihydroxy-5β-cholanic acid by gas chromatography-mass spectrometry (GC-MS) using both electron impact and chemical ionization tecniques. Additional proof of structure was provided by chemical synthesis of both analogs.

*Children's Hospital Medical Center, Boston.

PROGRESS REPORT

We obtained a bile sample from a male child tentatively identified as having cystic fibrosis. The sample was subjected to Folch extraction to remove phospholipids and neutral sterols, hydrolysis in aqueous sodium hydroxide, and separation of the free acids into dihydroxy and trihydroxy fractions by thin layer chromatography. The fraction migrating slightly ahead of the dihydroxy bile acids was collected and derivatized for GC-MS as the methyl ester acetate derivative. Electron impact (EI) ionization results in a mass spectrum (Figure 9.4) that has a base ion at m/e 299 [M^+ - side chain - (2 HOAc)] and an intense ion at m/e 253 [M^+ - side chain - EtOH - (2 x HOAc)] which is characteristic of trisubstituted bile acids. In addition, there are minor ions at m/e 368 [M^+ - (2 x HOAc) - 46], m/e 414 [M^+ - (2 x HOAc)] and m/e 428 [M^+ - HOAc - 46]. The chemical ionization (CI) spectrum exhibits a base peak at m/e 415 [MH^+ - (2 x HOAc)] and intense ion at m/e 369 [MH^+ - (2 x HOAc) - 46]. Additionally, there are several smaller peaks at m/e 387 [MH^+ - (2 x HOAc) - 28], m/e 429 [MH^+ - HOAc - 46], m/e 475 [MH^+ - HOAc] and m/e 489 [MH^+ - 46]. There is no molecular ion in either the CI or EI spectra. The characteristic loss of 46 amu from both clusters of ions (i.e., m/e 253 and 299 which lose the side chain, and m/e 368 and 414 which retain the side chain) was puzzling at first, but is consistently only with elimination of ethanol (MW = 46) from the intact steroid nucleus. The mass spectra, both EI and CI, unfortunately provide no clue to the position of the ethoxy group. The intense ion at m/e 299 (EI) suggests to us that the ethoxy group may be in the 3 position by comparison with other known derivatives (e.g., trimethylsilyl, trifluoroacetate and acetate).

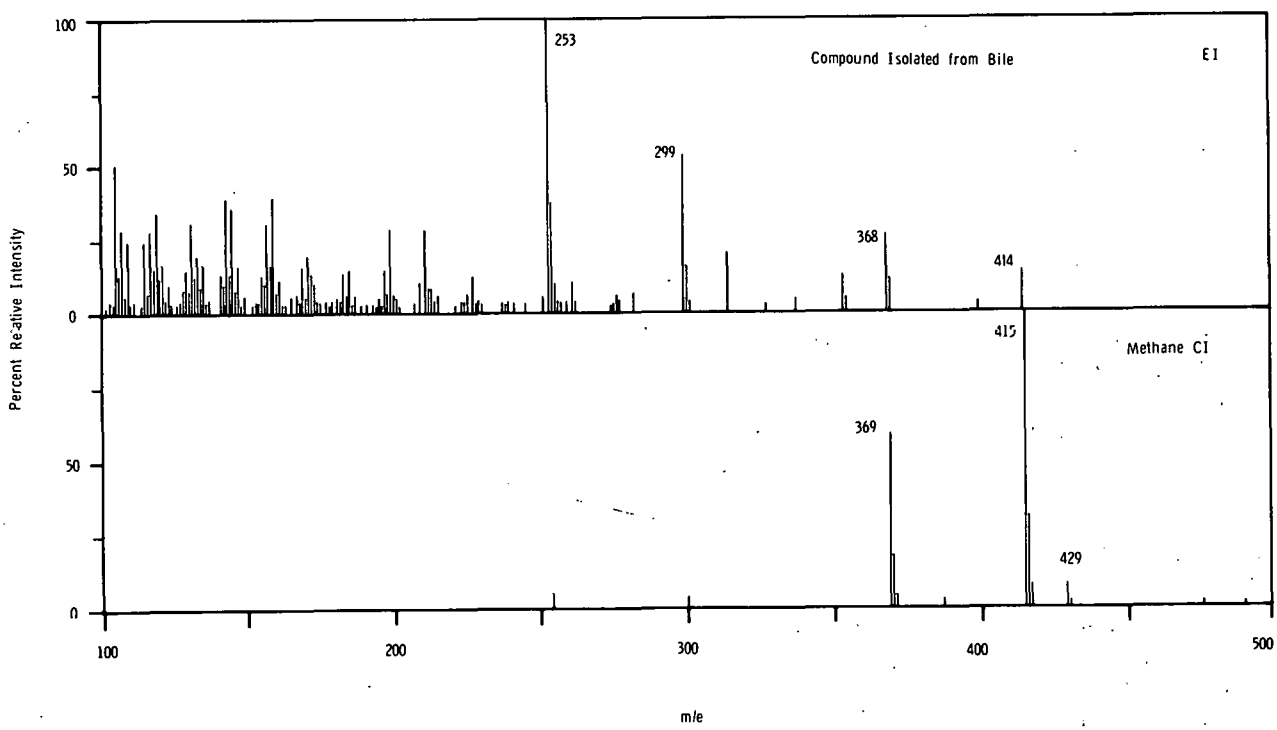

Fig. 9.4. Electron impact (top) and chemical ionization mass spectra (bottom) of an unusual bile acid isolated from the bile of a child with cystic fibrosis.

Additional proof of structure was sought through chemical synthesis of the 3α-ethoxy and 3α-methoxy-7α,12α-dihydroxy-5β-choloric acids. These compounds were prepared from methyl 3-keto-7α,12α-dihydroxy-5β-cholanate as shown in Figure 9.5. The hydroxyls were protected by forming the acetate derivative and the ketone was reduced to the alcohol with sodium borohydride. The mixture of α and β epimers was separated to give methyl 3α-hydroxy-7α, 12α-diacetoxy-5β-cholanate. The methyl and ethyl ethers were prepared by treatment of the 3α-hydroxy compound with trimethyloxonium hexafluorophosphate or triethyloxonium tetrafluoroborate, respectively. The products were purified by preparative thin layer chromatography. The methyl and ethyl ethers were characterized by high resolution NMR spectroscopy and by both EI and CI mass spectrometry and are consistent with the assigned structures. The mass spectrum of the synthetic compound is virtually identical to the spectrum of the compound isolated from bile (Figure 9.4). The spectrum of 3α-methoxy-7α,12α-dihydroxy-5β-choloric acid is also identical to that of a compound isolated from bile.

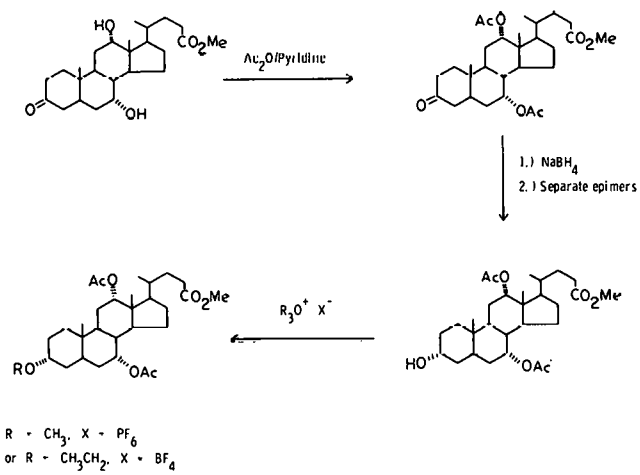

Fig. 9.5. Synthesis of methoxy and ethoxy analogs of 3α-alkoxy bile acids.

Further work is under way to define the extent of occurrence of the bile acid alkyl ethers in man, to determine their origin, to identify possible positional isomers and to determine if a homologous series (i.e., methoxy, ethoxy, and propoxy) occurs in nature. This work will involve preparing synthetic standards of all the positional isomers of the methoxy, ethoxy and propoxy compounds, defining the gas-liquid chromatographic behavior, and obtaining EI and CI spectra of these compounds.

CONCLUSION

We now have evidence for a new class of biliary lipids which occur in man. The bile acid alkyl ethers do not appear to be artifactual in origin, but to date have only been identified in bile obtained from patients with possibly abnormal hepatic function. More work will be required to define the extent of occurrence in nature, to identify homologs and positional isomers, and to determine the biological origin. Bile acid samples provided by treatment centers associated with the National Cooperative Gallstone Study should provide a rich source of material for extending this study.

REFERENCE

1. Eneroth, D., B. Gordon, and J. Sjövall. J. Lipid Res. 7, 524 (1966).

MEDICAL APPLICATIONS OF STABLE ISOTOPES*

Peter Klein, Patricia Szczepanik, David Hachey, and William Bryant

Increasing ethical concern over the use of radioactivity in human research studies as well as a general concern about reduction of radiation exposure in the total population has spurred the development of stable isotope techniques in clinical research and diagnosis. Among those needs best met by stable isotopes are studies where no usable radioisotope exists (e.g., ^{15}N, ^{18}O); studies where it is preferable not to administer ^{3}H or ^{14}C (e.g., obstetric, neonatal, and pediatric research) or where their use would require inordinate amounts; clinical pharmacological studies of drug metabolism and kinetics, especially in juvenile patients and studies requiring quantitation of tissue constituents and metabolites at the picomolar (10^{-12}) to femtomolar (10^{-15}) level. Stable isotopes are incorporated into labeled compouds by conventional syntheses employing simple molecules such as $^{2}H_2$, $^{13}CO_2$, and $^{15}NH_3$, in which the enrichment of heavy isotope is 60-99%. Detection and quantitation of stable isotopically labeled molecules is best achieved by gas chromatography-mass spectrometry and intensive instrumental development is making substantial progress in adapting such instrumentation to clinical requirements. Three lines of application are attracting clinical interest: studies of metabolic disorders in premature and full term infants, young children, and pregnant women; development of ^{13}C-labeled analogues of compounds used in $^{14}CO_2$ "breath test" for lactase deficiency, intestinal bacterial overgrowth, pancreatic insufficiency, or estimation of hepatic microsomal mass; and reverse isotope dilution assays for plasma levels of neurotransmitters, prostaglandins and drug metabolites. Stable isotope usage to date parallels and reflects the early clinical applications of ^{3}H and ^{14}C but the unique advantages of nonradioactive tracers suggest that they will gain acceptance as independently powerful research tools.

*Abstract of a paper to be published in International Journal of Nuclear Medicine.

SYNTHESIS AND BIOLOGIC STABILITY IN MAN OF 11,12-^{3}H- AND 11,12-^{2}H-LABELED CHENODEOXYCHOLIC AND LITHOCHOLIC ACIDS*

A. E. Cowen,[†] *A. F. Hofmann,*[†] *D. L. Hachey, P. J. Thomas,*[†] *D. T. E. Belobaba,*[†] *P. D. Klein, and L. Tökes*[‡]

Deuterium- and tritium-labeled chenodeoxycholic acid and lithocholic acid were prepared by catalytic reduction of their respective Δ^{11-12} derivatives. Structures of the intermediates and their isotopic purity were determined by chemical ionization and electron impact mass spectrometry and by nuclear magnetic resonance spectroscopy. When ^{3}H-labeled bile acids were incubated with human feces under anaerobic conditions, no loss of label occurred, indicating stability of the label to bacterial enzymes. When ^{3}H-labeled bile acids were administered simultaneously with ^{14}C-labeled bile acids to healthy subjects, the ^{3}H/^{14}C ratio in bile remained identical to that administered, and ^{3}H was excreted solely in feces, demonstrating the stability of the label during enterohepatic cycling and intestinal passage in healthy man. Bile acids labeled with 11,12-^{2}H or 11,12-^{3}H appear ideal for metabolic studies in man.

---

*Abstract of a paper submitted to the Journal of Lipid Research.

[†]Mayo Clinic and Mayo Foundation, Rochester, Minnesota.

[‡]Institute of Organic Chemistry, Syntex Research, Palo Alto, California.

FORMATION OF BILE ACIDS IN MAN: METABOLISM OF 7α-HYDROXY-4-CHOLESTEN-3-ONE IN NORMAL SUBJECTS WITH AN INTACT ENTEROHEPATIC CIRCULATION*

Russell F. Hanson,[†] *Patricia A. Szczepanik, Peter D. Klein, Eugene A. Johnson,*[†] *and Gale C. Williams*[†]

The formation of bile acids in man is thought to involve a series of reactions in which the initial steps are the same for both cholic acid and chenodeoxycholic acid. The point of bifurcation of the pathway is postulated to occur after the formation of 7α-hydroxy-4-cholesten-3-one. To test the hypothesis that the entire synthesis of both bile acids proceeds through this intermediate, we studied the metabolism of labeled 7α-hydroxy-4-cholesten-3-one in eight normal subjects with an intact enterohepatic circulation.

If all the production of cholic acid and chenodeoxycholic acid takes place via 7α-hydroxy-4-cholesten-3-one, the areas under the SA decay curves of cholic acid and chenodeoxycholic acid should be identical following a single injection of this labeled intermediate. However, in 6 of the 8 subjects

---

*Abstract of a paper submitted to the Journal of Biological Chemistry.

[†]University of Minnesota, Minneapolis.

studied, the area under the cholic acid SA decay curve was significantly less than the area under the chenodeoxycholic acid SA decay curve.

These results indicate that the production of cholic acid in man may not always involve the intermediate 7α-hydroxy-4-cholesten-3-one.

N-METHYLATION OF PURINES AND PYRIMIDINES*

William F. Bryant and Peter D. Klein

A rapid, convenient method for the N-methylation of purines and pyrimidines has been developed. When the purine or pyrimidine is dissolved in DMSO and treated with sodium methoxide and methyl iodide, quantitative conversion to the N-permethylated product occurs. Thymine, adenine, 6-methylaminopurine, xanthine, and uric acid have been derivatized in this manner. In the case of thymine, xanthine, and uric acid, no evidence of O-methylation has been observed. The chemical ionization and electron impact mass spectra of the methylated products are presented. Spectrophotometric analysis of the product from the methylation of thymine indicates quantitative conversion to 1,3-dimethylthymine.

---

*Abstract of a paper to be published in Analytical Biochemistry.

METABOLISM OF 2,4-^{3}H-14α-METHYL-5α-ERGOST-8-ENOL and 2,4-^{3}H-5α-ERGOSTA-8,14-DIENOL IN CHLORELLA ELLIPSOIDEA*

L. B. Tsai,† *G. W. Patterson,*† *C. F. Cohen,*‡ *and P. D. Klein*

5α-Ergosta-8,14-dienol and 14α-methyl-5α-ergost-8-enol were chemically synthesized from ergosterol and labeled with tritium at the C-2 and C-4 positions. Both labeled sterols, when incubated with growing cultures of *Chlorella ellipsoidea*, were converted to ergost-5-enol but not to C-27 or C-29 sterols. *C. ellipsoidea* thus has the capability of removing the C-14 methyl group and converting the 8(9) and 8,14 double bond systems to the 5(6) position. Brassicasterol produced by this organism is not labeled in these experiments, indicating that it is not derived from a saturated side chain precursor.

---

*Abstract of a paper in Lipids 9, 1014 (1974).

†University of Maryland, College Park.

‡Agricultural Research Service, U.S.D.A., Beltsville, Maryland.

CIRCADIAN CYBERNETICS; SUMMARY

Charles F. Ehret

Eukaryotes are structurally distinguishable from prokaryotes by the presence of multirepliconic genomes distributed upon euchromosomes in true nuclei; by the presence of large and semi-autonomous cytoplasmic organelles (some of which, the kinetosomes, show axial periodicities of 9); and by the presence of unique and, to our surprise, apparently ubiquitous regulatory routes in intermediary metabolism (the catecholamine and indolamine pathways). They are functionally distinguishable by their capacities for circadian regulation in the infradian growth mode. Any comprehensive understanding of eukaryotic regulation must ultimately encompass each of these distinguishing, and probably interrelated, properties; any basic approach to circadian regulation must take each into account. Recent work, including our own, has shown that gene action is fundamental to circadian regulation (1). Our present interest is to learn how gene action and short-lived enzymes [e.g., tyrosine aminotransferase (2)] may be coupled to exert circadian phase control over the energy reserves in infradian cells (3). In the past year, our studies at the cellular level have focused upon the roles of light, food, and thermal cycles with particular emphasis upon phase relationships between light and respiration, and the use of tryptophan as a circadian synchronizer in cultures not limited by oxygen. In other studies at the cellular level, another link was firmly established between the circadian cell cycle and the ultradian cell division cycle, in that the time required for entry into the latter (i.e., "lag") is a function of the circadian phase of the infradian inoculum. Attempts to show that the biogenic amines norepinephrine, epinephrine, and serotonin play a key role in the circadian regulation of glycolysis even at the cellular level have begun with refinements in their isolation from *Tetrahymena*. At the organismic level, a study of the phase control of the mammalian clock through the application of chronobiotics and molecular level strategies has continued.

REFERENCES

1. Ehret, C. F. Adv. Biol. Med. Phys. 15, 47 (1974).
2. Ehret, C. F., and V. R. Potter. Int. J. Chronobiol. 2, (in press) (1974).
3. Sutherland, A., G. A. Antipa, and C. F. Ehret. J. Cell. Biol. 58, 240 (1973).

A CONCISE CIRCADIAN GLOSSARY

Charles F. Ehret

Circa diem--"About a day" (Latin).

Circadian, ultradian, infradian--Approximately a day; less than a day; more than a day (1).

Zeitgeber--Synchronizer, entraining agent, or forcing oscillation that can entrain a biological rhythm (2).

G-E-T effect--A graphical representation of the conditions under which the protozoa *Gonyaulax, Euglena,* and *Tetrahymena* can manifest circadian oscillations; these conditions, which are shared by all eukaryotes, have been generalized as the circadian-infradian rule (q.v.) (3,4).

Circadian-infradian rule--A eukaryotic cell is incapable of endogenous circadian oscillations during the ultradian (fast exponential) mode of growth; a cell, in switching its state from the ultradian to the infradian mode, is capable of circadian outputs in the latter mode. The circadian component of an infradian culture is readily revealed by light synchronization (3,4).

Chronon--A polycistronic DNA replicon common to all eukaryotes and naturally selected to be of such length as to rate-limit the eukaryotic infradian cell cycle of RNA transcription to circadian periods; a component of the circadian escapement in the Chronon theory of Ehret and Trucco (5).

Chronon theory--The circadian clock escapement includes two component functions: [1] the sequential transcription component, or chronon, which is relatively temperature-independent during infradian growth, and [2] chronon recycling and initiation (5,6).

Chronotype--The temporal phenotype of an organism (4).

Chronobiotic--A drug that may be used to alter the biological time structure by rephasing a circadian rhythm (7).

Circadian transcriptotype--The circadian chronotype of temporally characteristic gene products (4).

Free running rhythms--Self-sustained undamped oscillations under constant conditions (2).

FS--Programmed feeding cycle (feed-starve) (4).

FS 8:16--FS with food present for 8 hours and absent for 16 hours (4,8,9).

LD--Programmed light-dark cycle (2).

LD 10:14 (100:0.1)--LD with 10 hours of light at 100 lux and 14 hours of darkness at 0.1 lux (2).

CW--Programmed thermal cycle (cool-warm).

CW 7:17°(26.5:29)--CW with 7 hours at 26.5°C and 17 hours at 29°C.

SSDDCC--Constant starvation, darkness, and temperature.

Period (T)--Time after which a definite phase of an oscillation recurs (2).

Phase shift--A single displacement of an oscillation along the time axis (2).

Phase-response curve--The relationship between the amount and direction of a phase shift, and the phase within which a stimulus (*Zeitgeber*) is applied (2).

Circadian cybernetics--The discipline of chronobiology concerned with biological regulation that includes time constants within the ultradian-infradian domain (4).

Other Standard Abbreviations: y = year, m = month, w = week, d = day, h = hour, mi = minute, s = second (10).

REFERENCES

1. Halberg, F. Annu. Rev. Physiol. 31, 675 (1969).
2. Aschoff, J., Ed. Circadian Clocks, North-Holland Publ., Amsterdam 1965.
3. Ehret, C. F., and J. J. Wille. In: Photobiology of Microorganisms, Ed. Per Halldal. Wiley, New York, 1970, p. 369.
4. Ehret, C. F. Adv. Biol. Med. Phys. 15, 47 (1974).
5. Ehret, C. F., and E. Trucco. J. Theor. Biol. 15, 240 (1967).
6. Barnett, A., C. F. Ehret, and J. J. Wille. In: Biochronometry, Ed. M. Menaker. National Academy of Sciences, Washington, D. C. 1971, p. 637.
7. Halberg, F., E. Halberg, and N. Montalbetti. Quad. Med. Quant. Sperimentazione Clin. Controllata 7, 7 (1969).
8. Potter, V. R., E. F. Baril, M. Watanabe, and E. D. Whittle. Fed. Proc., Fed. Am. Soc. Exp. Biol. 27, 1238 (1968).
9. Ehret, C. F., and V. R. Potter. Int. J. Chronobiol. 2 (in press) (1974).
10. Halberg, F., and G. S. Katinas. Int. J. Chronobiol. 1, 36 (1973).

CIRCADIAN CYBERNETICS; PROPERTIES OF EUKARYOTIC CELLS DURING INFRADIAN GROWTH

I. CIRCADIAN CHRONOTYPIC DEATH IN HEAT-SYNCHRONIZED INFRADIAN MODE CULTURES OF TETRAHYMENA*

John C. Meinert, Charles F. Ehret, and Gregory A. Antipa†

Continuous cultures of *Tetrahymena* in the infradian ("slow-exponential") growth mode can be entrained to give circadian rhythms of cell division by the application of thermal cycles of 24 hours duration. The degree to which these cultures are synchronized (synchronization index) is dependent upon the cycling of other environmental agents, such as food, light, and oxygen, whose phase angles to the circadian cell cycle influence the quality of synchronization. In well-synchronized oxygen-limited cultures, a circadian rhythm in cell death (circadian chronotypic death) is seen when the culture's oxygen requirements periodically exceed the oxygen support limit of the environment.

---

*Abstract of a paper to be published in Microbial Ecology.

†Present address: Wayne State University, Detroit.

II. CIRCADIAN RESPIRATORY RHYTHM OF LIGHT-ENTRAINED TETRAHYMENA PYRIFORMIS W GROWN ON SOLID AGAR

Kenneth W. Dobra and Charles F. Ehret

Respiration studies of liquid cultures are frequently made more difficult by the physical parameters of the liquid to gas equilibria involved in the measures. Thus, it is necessary to determine not only the solubility of O_2 and CO_2 in the particular culture medium, but also the rate of transfer of oxygen into the medium (and CO_2 out of the medium), which are functions of the surface to volume ratio, the concentration gradients, and the amount of agitation (1,2). If a culture is not limited by the availability of nutrient, the cells will continue to divide until the transfer of oxygen becomes limiting. Since the culture has a large capacity to dissolve CO_2 and a poor transfer of O_2, the ability to perceive rapid changes in cellular respiration is severely limited.

The ideal system is one that can reduce the diffusion distance and transfer time of oxygen, reduce the solubility of CO_2, and improve the surface to volume ratio to its maximum. These conditions are closely approximated when *Tetrahymena* are grown on solid, enriched, proteose-peptone agar plates. Under this condition, the cells form a monolayer on the surface of the agar about 10 μm thick with a very thin overlay of moisture. Respiration is determined by combining a number of plates in a non-sterile chamber that has a volume only slightly greater than the combined volume of the plates. A standard gas of known O_2 and CO_2 content is pumped through the chamber by a Cole Parmer peristaltic pump which maintains both flow and pressure at constant

levels. As the gas exits the chamber it is passed through a Beckman CO_2 analyzer and a Beckman O_2 analyzer for measurement of respiratory gases in a manner similar to that described by Neal and Jones (3). Respiration on a per cell basis can be determined by removing one or more plate cultures from a chamber, counting the cells, and measuring the change in the respiratory output due to their absence.

Figure 9.6 is the record of CO_2 output from a chamber containing ten 60-mm diameter plates inoculated with about 1.5×10^5 cells/plate. The flow, maintained at a rate of 300 ml/min, was vented to the atmosphere, and a daily cycle consisting of 8 hours of light, 16 hours of darkness (LD 8:16) was imposed. The temperature was maintained at 30°C ± 0.25°C.

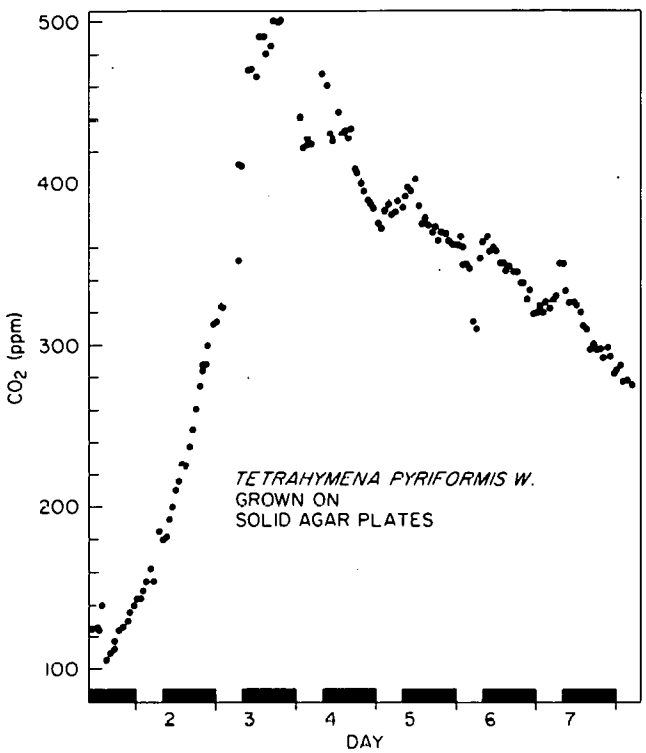

Fig. 9.6. The circadian respiratory rhythm of light-entrained *Tetrahymena* showing CO_2 output in ppm/300 ml/minute. Dark bars represent the dark phase of the light-dark cycle.

The cells attained a level of about 7×10^6 cells/plate, or a total of 7×10^7 cells in each of three replicate chambers which were monitored serially (4) for one week. The CO_2 output was found to be higher during the light than the dark phase of the daily LD cycle.

During the middle of the light phase, 1.8×10^7 cells were removed and the difference in the CO_2 was found to be 400 ppm, which transforms to 6.6 µl $CO_2/10^6$ cells/min. A similar measurement during the middle of the dark phase revealed that the respiratory output of CO_2 was only 50% of the light-phase level (3.7 µl $CO_2/10^6$ cells/min). In a similar study in which the cultures were allowed to free-run in continuous darkness following 2 days of entrainment, there was a greater output of CO_2 during the time corresponding to the light phase of the circadian cycle.

Further studies utilizing this system will attempt to quantitate the respiratory parameters in response to irradiance levels and phase relationships of LD cycles during different modes of growth. In this way, it will be possible to determine if such classical *zeitgebers* as light, temperature, and oxygen availability are able to reset cellular rhythmicity by means of altering the energy capabilities of the cells.

REFERENCES

1. Antipa, G. A., and K. W. Dobra. ANL-8070 (1973), p. 166.
2. Finn, R. K. Biochemical and Biological Engineering Sciences, Vol. 1, Ed. N. Blakebrough. Academic Press, New York, 1972, p. 69.
3. Neal, W. K., and R. M. Jones. Anal. Biochem. 49, 88 (1972).
4. Dobra, K. W., C. F. Ehret, and W. Eisler, ANL-8070 (1973), p. 168.

III. TOWARD THE USE OF TRYPTOPHAN AS A CIRCADIAN ZEITGEBER IN NUTRIENT-LIMITED INFRADIAN SYSTEMS AT THE CELLULAR LEVEL

Kenneth R. Groh and Charles F. Ehret

In mammalian dietary studies, tryptophan stands apart from the other essential amino acids for its signal role in enzyme induction and in circadian regulation. Tryptophan determines the circadian rhythm of tyrosine aminotransferase activity (1); influences the level of certain neurotransmitters such as serotonin (2), known already to be under circadian control (3); and, in a general way, appears to regulate the inducibility of enzymes not even involved in tryptophan metabolism (4). Because of our interest in the regulatory significance of catecholamines and indolamines at the cellular level, and because we already knew that food was as strong a circadian zeitgeber in feed-starve (FS) cycles in cellular systems as it is in mammals, we decided to test the effectiveness of daily addition and dilution of tryptophan alone from a defined medium to see if it would suffice as a circadian entraining agent in a cellular system using *Tetrahymena pyriformis*.

In the course of the investigation we made several unexpected observations regarding the effect of tryptophan on the growth of *Tetrahymena pyriformis*. Using a completely defined medium (5), generation times of 4-5 hours in the ultradian mode of growth at 26.5°C are typical. However, the order of addition of the medium constituents is of extreme importance. Tryptophan must be added at the time of addition of the other amino acids in the preparation of the medium. If it is added after the other ingredients, the resulting defined medium fails to sustain normal growth (Figure 9.7A).

It has been shown that tryptophan solutions irradiated with near-UV produce toxic products (TP) that can inhibit prokaryotic (6,7), as well as eukaryotic growth (8). To determine whether such toxic products inhibit growth in *T. pyriformis* W, we added various concentrations of TP (produced by irradiation of tryptophan at 365 nm for 4 hours) either as the only source of available tryptophan or in addition to the concentration usually present. The results

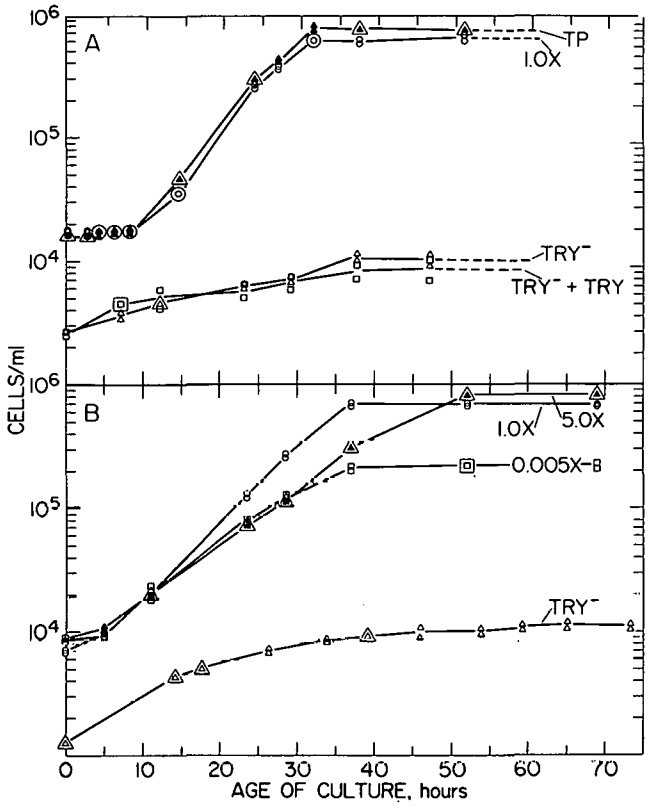

Fig. 9.7. The relationship between cell concentration and time after inoculation, showing the influence of tryptophan (try) in defined medium (DM) on ultradian growth rates and on infradian cell levels attained by *Tetrahymena pyriformis* W. (A) TP = DM that contained "toxic products," produced by irradiating a tryptophan solution; 1 X - DM full strength; TRY^- = tryptophan-deficient DM; TRY^- + TRY - a tryptophan deficient DM to which tryptophan was later added in concentration sufficient to make 1 X DM. (B) 5 X = DM containing try at 5 times normal strength; 1.0 X, etc., as above. At every sampling time, duplicate cultures were sampled.

suggest that tryptophan toxic products are not responsible for the absence of growth on defined medium when tryptophan is not added with the other amino acids (Figure 9.7A).

Because tryptophan is an essential amino acid for *Tetrahymena pyriformis*, both generation time and final cell concentration in the infradian mode should be dependent upon the amount of tryptophan present. This dependancy is important if tryptophan is to be used as a zeitgeber for circadian studies. For these reasons batch cultures of *Tetrahymena* containing varying amounts of tryptophan (0.005-5.0 X, X = 1.5×10^{-4} g/ml) were inoculated and cell titers measured throughout growth. It was found that minimum ultradian generation time and final control level infradian cell concentrations are obtained when 1/20 of the normal 1.5×10^{-4} g/ml tryptophan is present (Figure 9.7B). Below this tryptophan concentration both generation time and final cell concentration are reduced. On the other hand, tryptophan concentrations above 1.5×10^{-4} g/ml inhibit growth in the ultradian mode by extending the generation time. However, even though defined medium (DM) with 5 X tryptophan increases the ultradian generation time from 4 hours to 6 1/2 hours, the ultimate infradian cell titer is slightly but significantly higher than that reached with DM containing 1 X tryptophan. From these studies tryptophan appears to be a workable agent for circadian FS entrainment at the cellular level. Because of its already defined role in the synthesis and regulation of requisite biogenic amines in mammals, it is likely that manipulation of tryptophan concentrations by asymmetric program feeding in continuous cultures within a circadian framework will lead to elucidation of these pathways at the cellular level. These studies are now in progress.

REFERENCES

1. Wurtman, R. J., W. J. Shoemaker, and F. Larin. Proc. Nat. Acad. Sci. U.S.A. 59, 800 (1968).
2. Fernstrom, J. D., and R. J. Wurtman. Sci. Am. 230, 84 (1974).
3. Black, I. B., and J. Axelrod. Biochemical Actions of Hormones, Vol. 1, Ed. G. Litwack. Academic Press, New York, 1970, p. 135.
4. Peraino, C., R. L. Blake, and H. C. Pitot. J. Biol. Chem. 240, 3039 (1965).
5. Holz, G. G., J. Erwin, and R. J. Davis. J. Protozool. 6, 149 (1959).
6. Yoakum, G., W. Ferron, A. Eisenstark, and R. B. Webb. J. Bacteriol. 119, 62 (1974).
7. Yoakum, G., and A. Eisenstark. J. Bacteriol. 112, 653 (1972).
8. Zigman, S., and J. D. Hare. Abstracts of 2nd Ann. Meeting of Am. Soc. for Photobiol. p. 101 (1974).

IV. A CIRCADIAN RHYTHM IN THE INDUCIBILITY OF ULTRADIAN CELL DIVISION IN OXYGEN AND IN NUTRIENT-LIMITED INFRADIAN CELLS

Charles F. Ehret, John C. Meinert, Gregory A. Antipa, and Kenneth W. Dobra*

The duration of the transition between the infradian (slow exponential or "stationary") mode of growth (I) and the ultradian (fast exponential) mode (U) is frequently referred to as "lag," i.e., the interval between inoculation and the beginning of rapid growth in batch culture. In oxygen-limited cultures of *Tetrahymena pyriformis*, this I → U transition takes approximately 3 hours, is induced by oxygen, blocked by classical inhibitors of aerobic respiration, and is another example of the "Pasteur effect" (1). Earlier work had already provided evidence that light entrained continuous cultures in the infradian mode of growth showed a circadian rhythm in this manifestation of the Pasteur effect (2). The present study extends the earlier observations in showing that they apply as well not only during another method of entrainment (WC, thermal cycling) (3), but also during the periods of free-run following entrainment, and in nutrient limited cultures, with oxygen in excess, stimulated to begin the I → U transition into rapid cell division by the addition of nutrient.

Infradian cultures of *Tetrahymena pyriformis* W were entrained by daily thermal (CW) and feed-starve (FS) cycling in a 10-liter continuous culture system (1). Although dissolved oxygen was less than 0.1% in the oxygen-limited runs, cells were not so severely limited as to show chronotypic death (3). Subcultures (100 ml) of the large continuous culture were taken every 2 hours during the 2 days of entrainment [CW 7:17(26.5:29); FS 14:10 (8 x/h and 4 x/h in F: 2 x/h in S)] and for 2 ensuing days in which the "free-running" large continuous culture received no circadian environmental cues (CC 26.5°C, FF 4 X h^{-}). Each subculture was then maintained as a vigorously aerated batch

*Present address: Wayne State University, Detroit.

culture for intervals in excess of 8 hours. During these intervals the light scattering capacity of each subculture was measured in an automatic multi-system nephelometer every 30 minutes (4). In some experiments, a correlation was made between cell titer and light scatter. As shown in Figure 9.8, the magnitude of inducibility of cell division in the first 5 hours after aeration is bimodal and is strongly dependent upon the circadian phase of cells in the large culture, in which the average generation time ($\overline{GT}$) was over 82 hours. Comparable results were observed in circadian entrained infradian cultures in which the probability of cell division was less than 5% per day, indicating clearly the continuing presence in all of the cells of circadian-phase-dependent cell division information. When the nutrient level of an oxygen-limited, large continuous culture was decreased by diluting the defined medium to 0.25 full strength, the dissolved oxygen rose from < 0.1% to over 10% and the infradian culture became nutrient-limited. The addition of 4X medium to subcultures then induced the ultradian mode in a circadian pattern similar to that seen following oxygen induction. The light scatter results taken together with cell count data after induction are consistent with the view that infradian cells are not resting, but are instead dynamically and cyclically active. (We regard "G_o" as a myth). Such active cells always enter the cell division cycle ($G_1 \rightarrow S \rightarrow (G_2) \rightarrow M$) from a specific circadian phase of the circadian cell cycle ($P_1 \rightarrow T \rightarrow P_2$) (5). This forces lag to behave as a circadian function in an induced infradian population, provided that the cells of the population are in circadian synchrony. If the infradian population is asynchronous at the time of induction (as is commonly the case) then lag becomes an integral function of the circadian phase angles of all participating cells.

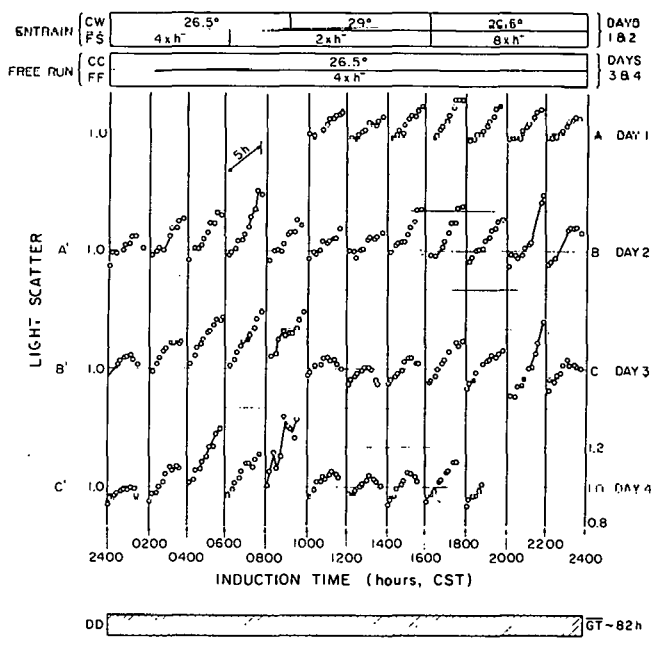

Fig. 9.8. Circadian rhythm of the Pasteur effect in *Tetrahymena*, showing the relationship between the circadian phase of a continuous infradian culture of cells and the increases in light scatter induced by aeration over a 5-hour interval in 41 separate subcultures. On days 1 and 2, the separate graphs for 19 aerated subcultures are shown, each one derived from the oxygen-limited infradian culture during its entrainment (WC, FS, shown above the abscissae). On days 3 and 4, 22 subcultures derived from the infradian culture during inducible and non-inducible phases of two of its free-running periods are shown.

REFERENCES

1. Ehret, C. F., J. Barnes, and K. Zichal. Chronobiology, Eds. L. Scheving, F. Halberg, and J. E. Pauly. Igaku Shoin Ltd., Tokyo, 1974, p. 44.
2. Ehret, C. F., and G. Antipa. J. Protozool. 19 (Suppl.), 27 (1972).
3. Meinert, J. C., C. F. Ehret, L. Rocha, and N. Warren. ANL-8070 (1973), p. 170.
4. Ehret, C. F., W. J. Eisler, and G. Antipa. ANL-7870 (1971), p. 103.
5. Ehret, C. F. Adv. Biol. Med. Phys. 15, 47 (1974).

V. THE ISOLATION AND IDENTIFICATION OF BIOGENIC AMINES IN CULTURES OF TETRAHYMENA PYRIFORMIS W

K. W. Dobra, C. F. Ehret, M. Lips, and N. Foltz†*

In recent years the role of biogenic amines has been found to be considerably more complex than that of simple neurotransmitters. The importance of epinephrine in the activation of the cyclic AMP regulation of glycogen metabolism in mammalian skeletal muscle (1) is perhaps the most significant example.

Longitudinal studies (time series) involving very accurate and precise determinations of the levels of biogenic amines in continuous, rhythmic cultures, with time, are necessary to determine if the biogenic amines play a regulatory role in the protozoan culture systems as in mammalian skeletal muscle. Since we already know that there are circadian oscillations in the levels of glycogen (2) and in CO_2 production and O_2 utilization (3) in rhythmic cultures of *Tetrahymena*, we are encouraged to propose that the regulatory involvement of biogenic amines in the circadian rhythm may be quite significant, especially in light of the role in circadian regulation already assigned to catecholamines (4) and indolamines (5) in mammalian systems.

Methods used for extraction of amines from *Tetrahymena* (6) have proved unsatisfactory for a precise longitudinal study because they require a large number of cells and because the maximum recovery is about 85% for catecholamines (7) and 50% for indolamines (8). The development of more quantitative and reproducible extraction procedures was therefore necessary.

The extraction procedure developed for the isolation of catecholamines was a modification of the method outlined by Crout (9). The main modification was that the alumina, following absorption of the catecholamines at pH 10, was placed on a millipore filter apparatus with a 0.45-μm filter and washed with distilled water followed by collection in acid, rather than

*Participant in the 1974 Summer Institute in Biology, Illinois Institute of Technology.

†Participant in the 1974 Summer Institute in Biology, University of Illinois, Urbana.

elution from a column. This procedure achieved a more complete recovery and used smaller sample volumes. The total amount of catecholamines was then measured by relative fluorescence with the trihydroxyindole method.

The indolamines were extracted by a modification of the method of Kariya and Aprison (10). An acetone formate extract was homogenized and lyophilized. The dried material was then extracted with n-butanol, spotted on a cellulose acetate thin layer chromatographic plate, and developed for 3 hours in a solvent consisting of butanol, glacial acetic acid, and water (4:1:1). The spots were visualized either under ultraviolet light or by means of a modification of Erhlich's reagent which uses *p*-dimethylaminocinnamaldehyde in concentrated HCl. The spots with the same Rf as standard serotonin were then eluted from the cellulose acetate and read in a Farrand spectrofluorometer at activation 295, emission 535.

Table 9.2 summarizes the results of the extraction procedures outlined in the methods section on both authentic biogenic amines and amines extracted from cultures of *Tetrahymena pyriformis*. The recovery of catecholamines was excellent and highly reproducible. The recovery of indolamines was difficult because of the many steps in the isolation, the instability of serotonin in solutions above pH 6.8, and the quenching of fluorescence due to the presence of fine particles of cellulose acetate. Care must be taken to carry out all steps at 0°C, and in subdued light. Although some changes, such as the significantly higher level of intracellular tryptophan found in infradian cultures than in ultradian, suggest the involvement of exogenous tryptophan on cellular metabolism, the changes expected in the levels of endogenous biogenic amines in infradian cultures are expected to be subtle and confidence in the percentage of recovery is essential if these are to be detected.

Table 9.2. Recovery and Identification of Biogenic Amines

Compound	Source	Concentration	Recovery %	Fluorescence Peaks Activation	Emission
Epinephrine	Standard[a]	10-1000 ng	95-100	395	505
Norephinephrine	Standard	10-1000 ng	95-100	395	505
Epinephrine + Norepinephrine	Tetrahymena	180-400 ng/g cells	95-100	412	510
Serotonin	Standard	10^{-6}-10^{-3} g	90-95	295	535
Indole with Same Rf as Serotonin	Tetrahymena	330 ng/g cells	90-95	305	535

[a]Sigma Chemical Company

The methods outlined above provide the necessary high yields for measuring the low levels of biogenic amines present in *Tetrahymena* and, with the appropriate internal standards, provide a method of determining the synthesis and control of catecholamines and indolamines in longitudinal studies of continuous culture systems.

REFERENCES

1. Robison, G. A., R. Butcher, and E. W. Sutherland. Cyclic AMP, Academic Press, New York, 1970.
2. Antipa, G. A., C. F. Ehret, and J. C. Meinert. ANL-7970 (1972), p. 140.
3. Dobra, K. W., and C. F. Ehret. Circadian cybernetics; properties of eukaryotic cells during infradian growth, II. This Report, Section 9.
4. Black, I., and J. Axelrod. In: Biochemical Actions of Hormones, Vol. 1, Ed. Gerald Litwack. Academic Press, New York 1970, p. 135.
5. Fernstrom, J. D., and R. J. Wurtman. Sci. Am. 230, 84 (1974).
6. Brizzi, G., and J. Blum, J. Protozool. 17, 553 (1970).
7. Janakidevi, K., V. C. Dewey, and G. W. Kidder. J. Biol. Chem. 241, 2576 (1966).
8. Blum, J. J. Proc. Nat. Acad. Sci. U.S.A. 58, 81 (1967).
9. Crout, R. J. In: Standard Methods in Clinical Chemistry, Vol. 3, Ed. D. Siligson. Academic Press, N. Y., 1961, p. 62.
10. Kariya, T., and M. Aprison. Anal. Biochem. 31, 102 (1969).

CIRCADIAN CYBERNETICS; CHRONOTYPIC PROPERTIES OF THE MAMMALIAN CLOCK

I. CIRCADIAN CHRONOTYPIC INDUCTION OF TYROSINE AMINOTRANSFERASE AND DEPLETION OF GLYCOGEN BY THEOPHYLLINE IN THE RAT*

Charles F. Ehret and Van R. Potter†

The short-lived hepatic enzyme tyrosine aminotransferase (L-tyrosine-2-oxoglutarate aminotransferase, EC 2.6.1.5) is chronotypically inducible by theophylline with a circadian pattern for as long as three days in starved rats (Sprague-Dawley) kept in constant dim-light. Liver glycogen can be completely depleted by theophylline in starved rats at any circadian phase, but since glycogen in uninjected rats continues to oscillate chronotypically at very low levels, injected rats show a circadian pattern of theophylline-induced glycogen release.

---

*Abstract of a paper to be published in the International Journal of Chronobiology, Volume 2, 1974.

†McArdle Laboratory for Cancer Research, University of Wisconsin, Madison.

II. CHRONOTYPIC ACTION OF THEOPHYLLINE AND OF PENTOBARBITAL AS CIRCADIAN ZEITGEBERS IN THE RAT*

Charles F. Ehret, Van R. Potter,† and K. W. Dobra

In the rat the deep body temperature rhythm, monitored by telemetry, can be reset in a predictable direction by a stimulant (theophylline) and by a depressant (pentobarbital). When the drugs are applied immediately before or during the early active phases of the circadian cycle, the rhythm is set back (phase delay). When applied later, past the thermal peak, theophylline, but not pentobarbital, shifts the rhythm ahead (phase advance). Theophylline and pentobarbital, in addition to their already established pharmacological properties, are thereby defined as *chronobiotics*: drugs that may be used to alter the biological time structure by rephasing a circadian rhythm.

---

*Abstract of a paper to be published in Science.

†McArdle Laboratory for Cancer Research, University of Wisconsin, Madison.

III. THE SEPARATE AND SIMULTANEOUS USE OF FOOD AND OF THEOPHYLLINE AS CHRONOBIOTICS IN THE RAT

Charles F. Ehret and Kenneth W. Dobra

Since food in feed-starve (FS) cycles is itself a powerful circadian zeitgeber for the rat, we wondered whether the chronobiotic action of theophylline, already demonstrated in free-running rats (DDSS) (1), could be used to supplement that shown by food alone when administered at a new circadian phase angle. The circadian rhythm of deep body temperature was measured by implant telemetry in rats entrained by program feeding (30% protein, FS 7:17) and light cycling (DL 17:7).* The responses of five rats to mixed zeitgebers were compared for a week following ten days of FS, DL entrainment (Figure 9.9). At the start of day 11, the dark phase was extended 8 hours (top bar, Figure 9.9) and DL 17:7 continued as before, but with a phase-shift ($\Delta\Phi$ delay) in the light cycle. The results are describable in times of early transients (days 11-13) and "net effect" by day 14, which we "fix-in-phase" by 2 days of DDSS on days 15 and 16. The influence of food alone is dramatically shown by rats I and II. Rat I enjoyed a prolonged extension of feeding (FF) after the last F phase of day 10, and under the influence of the new DLFF cycle alone its thermal acrophase shifted late only gradually through 3 or 4 days of transients, much like the long transients observed during DL induced phase delay in the ad lib (FF) mouse and rat (2,3,4). Rat II experienced instead a day of starvation and prolonged SS until entry into FF on the first D phase

---

*See: A concise circadian glossary, by C. F. Ehret, this Report, Section 9, for definition of abbreviations.

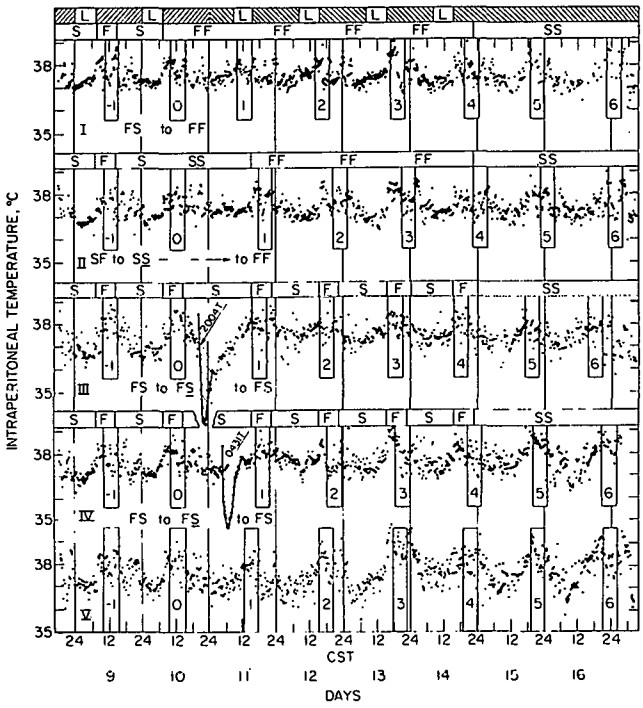

Fig. 9.9. Chronobiotic effects of food and of theophylline in the rat, as shown by telemetry tracings of body temperatures in 5 rats (I-V) over 8 days. During the preceding 8 days (not shown) and the first 2 days illustrated, the animals were entrained by daily programs of feeding (FS 7:17) and illumination (DL 17:7). On day 10 the dark phase was prolonged (top bar) and DL was then resumed as before, but with an 8 hour phase delay. Shifts in feeding protocols are shown separately in the respective frames; rats III and IV received theophylline (75 mg/kg) at the times indicated by arrows. Theophylline induced phase shifts are clearly detectable even in the presence of other powerful zeitgebers (food and light cycles).

of the new DL cycle. Under these conditions rat II locked rapidly into its new cycle by the second day. Rats III-V experienced no day of starvation, but only an S phase prolonged by 8 hours, followed by the new FSDL. The response of rat V was almost exactly like that of rat I, and several days were needed for the thermal acrophase to achieve its phase-shift. Theophylline given at 2004 to rat III caused a lasting net-phase advance of 5 or 6 hours, as predicted by the phase advances seen in an earlier study (1). Theophylline given at 0431 caused, as predicted, a phase delay in the early transients, thereby reducing time required to lock into the newly imposed DLFS cycle. In conclusion, the clock-resetting capacity of theophylline can be detected even in the presence of two other powerful zeitgebers, food and light.

REFERENCES

1. Ehret, C. F., V. R. Potter, and K. W. Dobra. Science, in press.
2. Halberg, F., W. Nelson, W. Runge, and O. H. Schmitt. Fed. Proc., Fed. Am. Soc. Exp. Biol. 26, 599 (1967).
3. Haus, E., and F. Halberg. Rassegna Neurologia Vegetativa 23, 83 (1969).
4. Lindberg, R. E., E. Halberg, F. Halberg, and P. Hayden. Space Life Sci. 14, 240 (1973).

BIOMOLECULAR STRUCTURE DETERMINATION: X-RAY CRYSTALLOGRAPHIC STUDIES OF IMMUNOGLOBULINS

Allen B. Edmundson, Marianne Schiffer, Rowland L. Girling, Enrique E. Abola, Joseph R. Firca, Kathryn R. Ely, and Florence A. Westholm

PURPOSE AND METHODS

Both the serum IgG immunoglobulin and the urinary Bence-Jones protein from a patient (Mcg) with multiple myeloma have been crystallized in forms suitable for X-ray diffraction experiments. IgG immunoglobulins in both myelomatous and normal sera consist of two light chains (MW 22,000 to 23,000) and two heavy chains (MW 50,000 to 55,000) linked by interchain disulfide bonds. Bence-Jones proteins are excreted light chains, and their presence in urine is pathognomonic of multiple myeloma. The isolation of crystalline IgG and Bence-Jones proteins from one patient is particularly significant because the amino acid sequence of the IgG light chain constituent is identical with that of the Bence-Jones protein only when the proteins are obtained from the same individual. This combination provides a unique system for the determination of the three-dimensional structure of an antibody molecule. The high resolution study that is possible with the Bence-Jones protein can complement and extend the low resolution study attainable with the myeloma protein.

Preliminary results of the crystallographic study of the myeloma protein have been reported (1), and the structural determinations of the Bence-Jones protein at 6 Å (2) and at 3.5 Å (3) resolution have been described. In the past year data collection on crystals of the myeloma protein was initiated, and a search for isomorphous heavy-atom derivatives was begun. The structural study of the Bence-Jones protein was extended to 2.3 Å. The electron density map was interpreted, and a scale model of the protein was constructed with Watson-Kendrew skeletal models. The amino acid sequence data kindly furnished by Fett and Deutsch at the University of Wisconsin was indispensable for the construction of the atomic model.

Three-dimensional data for both crystals were collected with an automated Picker diffractometer by procedures discussed in previous Annual Reports (4). The IgG myeloma protein crystallizes from water or dilute ($\sim$ 0.01 M) phosphate or borate buffers in the orthorhombic space group $C222_1$, with a = 87.8, b = 111.3, and c = 186.3 Å. The crystallographic asymmetric unit is the half-molecule (MW = 75,000), with four complete molecules in the unit cell.

The Bence-Jones protein crystallizes from ammonium sulfate in the space group $P3_121$, with unit cell dimensions of a = 72.3 and c = 185.9 Å. The asymmetric unit is the dimer (MW = 46,000), of which six are present in the unit cell.

The structural determination indicated that the Bence-Jones dimer is represented by two modules of electron density (see Figure 9.10). The large module consists of the amino-terminal regions ("domains") of the two monomers and the small module contains the two carboxyl-terminal regions. The amino region is composed of 111 amino acid residues, while the carboxyl domain contains 105 residues. The two domains are connected by an extended chain

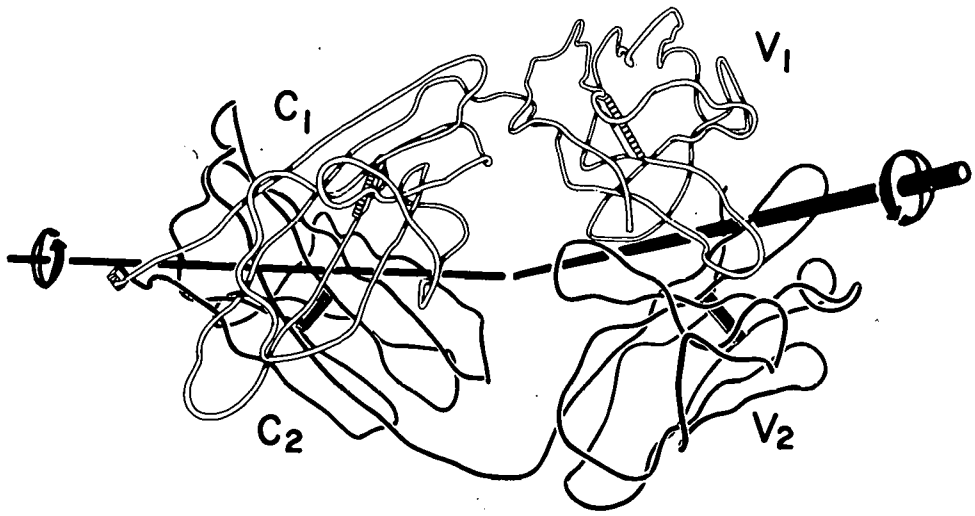

Fig. 9.10. Tracing of a photograph of a model of the Bence-Jones dimer, with the local pseudo-twofold axes of rotation included. Monomer 1 is shown in white and monomer 2 in black. The amino or "variable" domains are labeled V, and the carboxyl or "constant" domains are labeled C, with the appropriate subscript for monomer 1 or 2. The pseudo-twofold axis on the right passes through the center of the main binding cavity in the solvent channel between the V domains.

(the "switch" region). Sites for the binding of antigens or haptens are found only in the amino domains. In the Bence-Jones dimer, these sites are associated with the amino acid residues lining the solvent channel between the two amino domains. The presence of this solvent channel is mainly responsible for the difference in size between the modules of the amino and carboxyl domains, as observed at 6 Å resolution.

As a step toward understanding how antigens or haptens are bound, 2,4-dinitrophenyl compounds and other small hapten-like molecules were diffused into crystals of the Bence-Jones dimer. The locations of the binding regions were determined by crystallographic techniques and related to the three-dimensional structure of the dimer.

PROGRESS REPORT*

Data collection and the heavy-atom search for the myeloma protein are still in the preliminary stages, and definitive statements on the progress of the work will be deferred.

The skeletal model of the Bence-Jones dimer contains more than 3000 non-hydrogen atoms, and photographs are generally very complicated. Therefore, we prefer to show tracings of the polypeptide chains, together with schematic drawings of interesting parts of the molecule. Such a tracing is

*Parts of this report were taken from an abstract of a published paper (5).

presented in Figure 9.10, with the local pseudo-twofold axes of rotation included. The amino domains from different proteins vary in amino acid sequence and are called "variable" (V), while the carboxyl domains in proteins from the same class and species have a relatively "constant" (C) sequence. Within the V domains are "hypervariable" sequences, some of which appear to be essential for antigen-binding.

In last year's Annual Report (4), we described the basic immunoglobulin "fold." Each domain consists of two layers, one with three antiparallel segments of polypeptide chains, and the second with four antiparallel chains. The two layers are connected by an intrachain disulfide bond near the center of each domain. The 2.3 Å map shows that each layer has a pleated sheet (beta) structure. The domains are roughly cylindrical, and have been described as "beta barrels." Inside each barrel are hydrophobic side chains, while the exterior surfaces are covered with polar groups.

The pseudo-twofold axis between the V domains in Figure 9.10 passes down the middle of the solvent channel in which the binding sites are located. In Figure 9.11, which is a schematic drawing of the main binding cavity at the tip of the dimer, the view is down the pseudo-twofold axis. The cavity is shaped like a truncated cone, 15 Å in diameter at the entrance and 10 Å across at the base (floor). The distance from the entrance to the floor along the pseudo-twofold axis is about 17 Å. The solvent passes through an opening in the floor into an ellipsoidal pocket. Constituents of the hypervariable regions line the main cavity but not the pocket.

Hapten-like molecules which bind along the solvent channel include dinitrophenyl compounds, ε-dansyllysine, colchicine, 1,10-phenanthroline, methadone, morphine, meperidine, 5-acetyluracil, caffeine, theophylline, menadione (vitamin K_3), and triacetin. Binding occurs in two sites (A and B) in the main cavity and one site (C) in the pocket. Site A is located near the cavity entrance, which is ringed with aromatic side chains interspersed with polar groups. This ring is composed of Tyr-34, Tyr-51, Glu-52, and Tyr-93 of both monomers, and Asp-97 of monomer 2. Only the residues from monomer 2 are associated with site A. In the crystal lattice, the site (A') adjacent to monomer 1 and potentially equivalent to site A is blocked by constituents of a symmetry-related dimer. The side chain of Leu-110 from monomer 2 of this second molecule protrudes into site A', and occupies a position between Tyr-34 and Glu-52. Site B is situated at a deeper level, and extends from the Phe-99 side chains near the middle of the main cavity to four aromatic residues (Tyr-38 and Phe-101) at the base. Four seryl residues (36 and 91) are available for hydrogen bonding in site B. Sites A and B can be covalently labeled with 1-fluoro-5-iodo-2,4-dinitrobenzene, which reacts to the same extent with Tyr-34 and Tyr-38 of monomer 2. The total quantities of bound dinitrophenylleucine or triacetin are also evenly divided between sites A and B. Methadone and ε-dansyllysine bind only in site A, while caffeine and theophylline prefer site B. Bis(dinitrophenyl)lysine is not removed from sites A and B by soaking the crystals in buffered ammonium sulfate for 2 weeks, but ε-dinitrophenyllysine is displaced by the same treatment. The pocket containing site C is lined primarily by hydrophobic groups, including those of Tyr-38, Pro-46, Tyr-89, and Phe-101 of both monomers. 5-Acetyluracil binds isomorphously and with high occupancy in site C. Menadione, meperidine, 1,10-phenanthroline, *p*-nitrophenylphosphorylcholine, phenylmercuric compounds, and ω-bromoheptanoate also bind in significant quantities in site C. However,

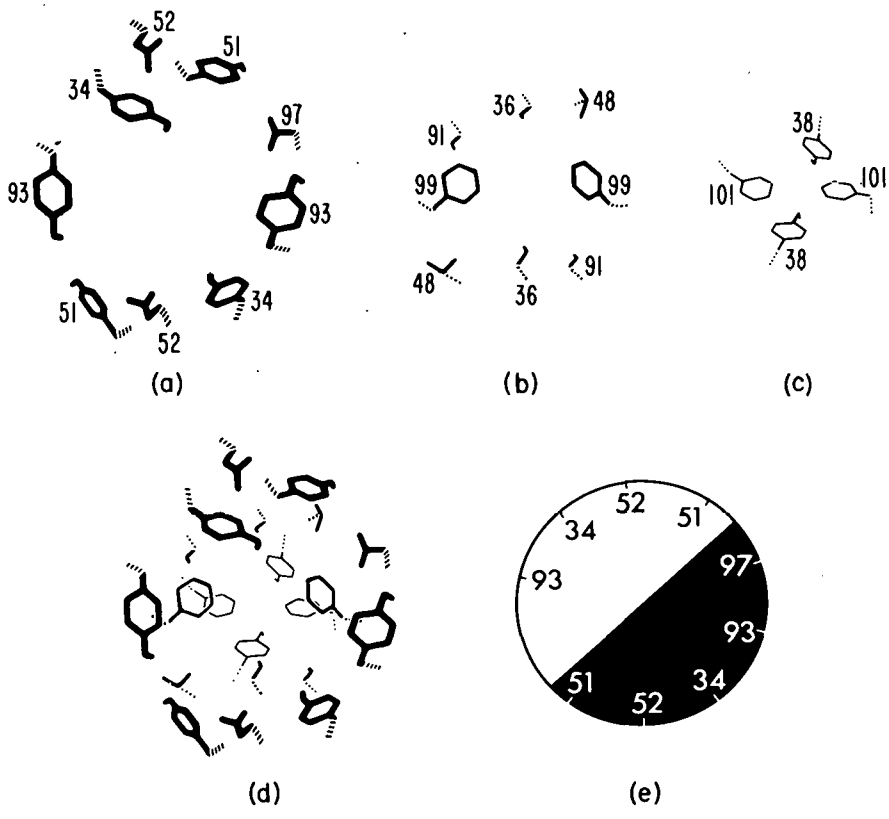

Fig. 9.11. Schematic and composite drawings of the side chains lining the main binding cavity of the Bence-Jones dimer. The bond between the α and β carbon atoms is represented by a striated line. (a) The entrance to the cavity that is lined by Asp-97, Tyr-93, Tyr-34, Glu-52 and Tyr-51 from monomer 2 (reading clockwise), and by Tyr-93, Tyr-34, Glu-52, and Tyr-51 from monomer 1. Binding site A is close to Tyr-34 of monomer 2. (b) Intermediate level in the cavity. The Phe-99 side chains are about 10-11 Å from the entrance. The side chains of Ser-36, Ser-91, and Val-48 lie between Phe-99 and the base. Binding site B is located in this region. (c) The base ("floor") of the cavity, about 16-17 Å from the entrance, consisting of Tyr-38 and Phe-101 from the two monomers. (d) Composite drawing of the cavity lining. (e) Key to the distribution of the side chains between monomer 1 (white half of circle) and monomer 2 (black half).

the crystals are physically damaged by these compounds, and the difference Fourier maps show additional troughs and peaks in the vicinity of site C. In the case of menadione, the changes were interpreted in terms of a displacement of a section of polypeptide chain between Lys-44 and Ala-45 in monomer 2 of the native protein. This chain is involved in one of the few interactions between the amino domains. It appears that a large entering

group with the appropriate affinity can induce a fit in the deeper sites by disrupting such weak interactions along the solvent channel.

The electron density maps at 3.5 and 2.3 Å reveal striking differences in the conformations of the two monomers in the Bence-Jones dimer. A comparison of the dimer with human and murine Fab (antigen binding) fragments studied by Poljak et al. (6) and by Padlan, Davies et al. (7) shows that monomer 2 (see Figure 9.10) closely resembles the light chains in the Fab fragments. Monomer 1 is similar to the heavy chain components of the fragments. This surprising finding contrasts with the situation in the IgG myeloma protein, in which the two light chains are identical in conformation. The Mcg proteins therefore provide unequivocal evidence that different conformations can be derived from the same amino acid sequence. If the Bence-Jones monomers were identical in conformation, the binding sites would not exist as we see them in the electron density maps.

The Bence-Jones dimer binds the hapten-like molecules in sites comparable in location to the corresponding binding sites in the Fab fragments. As expected from the differences in specificities, the sites are different in size and in some residues in immediate contact with the hapten-like molecules. Moreover, the dimers of V domains of other Bence-Jones proteins have cavities similar to those of the Mcg dimer and the Fab fragments. These V domain dimers are the subjects of accompanying abstracts of work in which Marianne Schiffer participated in her year's leave of absence in Munich.

CONCLUSIONS

An atomic model of the Bence-Jones dimer has been constructed, and the general features of the structure have been described. We have presented evidence that the Mcg Bence-Jones dimer binds hapten-like molecules in sites comparable to those in functional antibodies. With the monomers displaying different conformations (one resembling heavy chains), which directly relate to the capability for hapten binding, we suggest that the Bence-Jones dimer can serve as a model for a primitive antibody. The presence of multiple binding sites and different binding specificities provide strong support for economy of the immune response to the challenge of the vast number of possible antigenic determinants.

REFERENCES

1. Edmundson, A. B., M. Schiffer, M. K. Wood, K. D. Hardman, K. R. Ely, and C. F. Ainsworth. Cold Spring Harbor Symp. Quant. Biol. 36, 427 (1971).
2. Edmundson, A. B., M. Schiffer, K. R. Ely, and M. K. Wood. Biochemistry 11, 1822 (1972).
3. Schiffer, M., R. L. Girling, K. R. Ely, and A. B. Edmundson. Biochemistry 12, 4620 (1973).
4. Edmundson, A. B., M. Schiffer, R. L. Girling, and K. R. Ely. ANL-8070 (1973), p. 152.
5. Edmundson, A. B., K. R. Ely, R. L. Girling, E. E. Abola, M. Schiffer, F. A. Westholm, M. D. Fausch, and H. F. Deutsch. Biochemistry 13, 3816 (1974).
6. Poljak, R. J., L. M. Amzel, H. P. Avey, B. L. Chen, R. P. Phizackerley, and F. Saul. Proc. Nat. Acad. Sci. U.S.A. 70, 3305 (1973).
7. Padlan, E. A., D. M. Segal, T. F. Spande, D. R. Davies, S. Rudikoff, and M. Potter. Nature (London), New Biol. 245, 165 (1973).

CRYSTAL AND MOLECULAR STRUCTURE OF A DIMER COMPOSED OF THE VARIABLE PORTIONS OF THE BENCE-JONES PROTEIN REI*

Otto Epp,[†] *Peter Colman,*[†] *Heinz Fehlhammer,*[†] *Wolfram Bode,*[†] *Marianne Schiffer, Robert Huber,*[†] *and Walter Palm*[‡]

The structure of the variable part of a κ-type Bence-Jones protein Rei has been determined at a resolution of 0.28 nm. It forms a dimer in the crystal related by a local diad, held together by hydrogen bonding interactions of residues Tyr-36, Gln-38, Ala-43, Pro-44, Tyr-87, Gln-89, and Phe-98, which are largely conserved in light chains. The structure consists of two hydrogen-bonded sheets covering a hydrophobic interior made up of mostly conserved amino-acid side chains. Approximately 50% of the residues form β-pleated sheets. Several of the pleated sheet strands are connected by hair-pin bends, which contain glycine residues conserved in most light chains. The arrangement of the hypervariable segments, especially in comparison with the Fab structure, suggests that the V dimers form a primitive antibody. The folding of the polypeptide chain and the spatial relationship of the two monomers appear to be the same as in the λ-type Bence-Jones protein dimer and the Fab fragment.

---

*Abstract of a paper published in The European Journal of Biochemistry 45, 513 (1974).

[†]Max-Planck-Institut für Biochemie, Martinsried, und Physikalisch-Chemisches Institut der Technischen Universität, Munchen.

[‡]Institut für Medizinische Biochemie der Universität, Graz.

THE STRUCTURE DETERMINATION OF THE VARIABLE PORTION OF THE BENCE-JONES PROTEIN AU*

H. Fehlhammer,[†] *M. Schiffer, O. Epp,*[†] *P. M. Colman,*[†] *E. E. Lattman,*[‡] *P. Schwager,*[†] *and W. Steigemann*[†]

The structure of a κ-type Bence-Jones protein variable fragment Au has been determined by molecular replacement methods using the known structure of another Bence-Jones variable fragment Rei [Epp et al. (1974) Eur. J. Biochem. 45, 513]. The crystallographic *R* factor is 0.31 for about 4000 significantly measured reflections between 6.8 to 2.5 Å. The Au proteins form a dimer across a crystallographic twofold axis. The spatial relationship of the two monomers, the conformation of the backbone, and of the internal residues are extremely similar to those found in Rei.

---

*Summary of a paper published in Biophys. Struc. Mechanism 1, 139 (1975).

[†]Max-Planck-Institut für Biochemie, Martinsried, und Physikalisch-Chemisches Institut der Technischen Universität, München.

[‡]Present address: Rosenstiel Institute, Brandeis University.

THIS PAGE

WAS INTENTIONALLY

LEFT BLANK

10. MAMMALIAN CELL BIOLOGY

SUMMARY

Mortimer M. Elkind, Group Leader

Mammalian cells grown in culture are used to study mechanisms of response to radiation (ionizing, ultraviolet, and near ultraviolet) and to chemical agents (mutagens, oncogens, and drugs used in cancer therapy). While *in vitro* studies with such material are not expected to reflect all the factors important in *in vivo* responses, in a number of respects they lend themselves to more incisive observations than do animal systems. This is particularly true when molecular mechanisms are of interest such as those involved in cytotoxicity, mutagenesis, and oncogenesis. A further advantage of cultured cells is that they can be synchronized, thus permitting a detailed examination of cyclic events important to cell growth and division.

Studies of the action of N-ethylmaleimide (NEM), as an inhibitor of repair, have been extended from synchronous Chinese hamster cells to synchronous human HeLa cells. These studies show a similar mode of action in both cell types lending support to the notion that conclusions may be extracted from such observations that are of fairly general applicability to mammalian cells. Radiation studies with NEM are being extended to hypoxic cells to inquire if NEM is effective relative to oxygen-independent damage. Observations relative to survival, DNA synthesis, and DNA strand elongation--resulting from the addition products to DNA when cells are exposed to near UV in the presence of psoralen--have been extended. These complement ongoing studies in the Carcinogenesis group (Section 5 of this Report) of the carcinogenic action on mouse skin resulting from near UV after the skin was treated with the furocoumarin psoralen. They also complement ongoing studies of DNA damage-repair processes due to ionizing radiation. Near UV (365 nm) has also been used to determine the relative frequency of frank single-strand scissions in DNA versus alkali-labile lesions in bacteriophage T4 DNA. The cross-linking ability of ^{3}H decay in adenine-2-^{3}H also has been studied with bacteriophage T4. The influence of hyperthermia, in regard to cell killing and DNA damage, was examined in reference to radiation (ionizing and UV) and the DNA mono-alkylator methyl methanesulfonate. The results indicate that hyperthermia interferes with repair processes and enhances damage expression; consequently hyperthermia could be a useful adjuvant in the treatment of cancer with radiation and chemicals. The modes of action of two chemotherapeutic agents--actinomycin D and nitrogen mustard--have been examined at the level of X-irradiation induced DNA damage and its repair. And lastly, the relevance of cell-based responses, deriving in part from the aforementioned studies, has been extended to analyses of the treatment of cancer with radiation.

The future program will continue to emphasize the exploitation of cultured mammalian cells for the study of the growth, division, and metabolic processes of normal and transformed cells, and how cultured cells are affected by radiation, various chemicals and drugs, and environmental pollutants. Such studies are essential to our understanding of the basic biology of mammalian cells and how various kinds of environmental factors, including radiation, alter the biology of such cells. In addition, studies of this type potentially are of practical value in helping to assess the hazards to humans and other biota of noxious environmental agents, and in improving the treatment of cancer.

MAMMALIAN CELL BIOLOGY STAFF

REGULAR STAFF

Dibelka, Diana R. (Scientific Assistant)
Elkind, Mortimer M. (Senior Biophysicist)
Geroch, Mary E. (Scientific Assistant)
*Kokaisl, Gloria A. (Scientific Assistant)
Ley, Ronald D. (Assistant Biophysicist)
Liu, Chin-Mei (Scientific Assistant)
Long, Melvin D. (Scientific Assistant)
†Sinclair, Warren K. (Senior Biophysicist)

TEMPORARY STAFF DURING 1974

Han, Antun (Visiting Scientist)
Kimler, Bruce F. (Postdoctoral Appointee)

---

*Now in Radiological and Environmental Research Division, Argonne National Laboratory.

†Associate Laboratory Director for Biomedical and Environmental Research.

SENSITIZATION OF SYNCHRONIZED HeLa CELLS TO X-RAYS BY N-ETHYLMALEIMIDE

Antun Han, Warren K. Sinclair, and Bruce F. Kimler*

PURPOSE AND METHODS

The lethal response of synchronized mammalian cells to X-radiation exhibits two peaks of resistance; one in early G_1 and another in late S, while cells at the G_1/S border and in mitosis are sensitive. In cells with a short G_1, such as Chinese hamster V79 cells, only the peak of resistance in late S

---

*Associate Laboratory Director for Biomedical and Environmental Research.

is evident. In a model proposed by Sinclair (1) it is postulated that two factors control the variations in lethal response. The first factor is DNA synthesis and the second factor, so far unidentified, has been called "Q." The latter could reflect a fraction of the intracellular sulfhydryl. These two components of the model were determined in Chinese hamster V79 cells (1). However, an important feature of the model remained to be tested; is there only one Q factor, i.e., is the process controlling the response during inhibition of DNA synthesis the same as that responsible for the peak of resistance in early G_1 in long G_1 cell lines? To explore this aspect of the model, experiments with synchronized HeLa cells were performed.

Synchronous populations of HeLa cells were obtained by harvesting log phase cells under controlled conditions. The plates containing about 1 to 1.5 x 10^6 log phase cells per dish were shaken on a reciprocating, horizontal-action shaker for 1 minute. After shaking, the suspension was removed and the contents of many plates were pooled. Suitable aliquots of the synchronous population were used to determine the cell concentration and the mitotic index (which ranged from 50-75%). Tests were performed to determine the degree of synchrony; namely, the mitotic index and pulse labeling with ^{3}H-thymidine.

For cell survival, clones were scored after postirradiation incubation for 14-16 days.

Cultures were irradiated with 250 kVp X-rays (HVL 0.9 mm Cu) dose rate of 149 rads/min at room temperature.

Fresh N-ethylmaleimide (NEM, from Sigma Chemical Company, St. Louis, Mo.) was dissolved in phosphate-buffered saline (PBS) and maintained in darkened bottles during the experiment. The concentration of NEM used was 0.75 μM, the same as that used in the experiments with V79 Chinese hamster cells (1). Toxicity data show that the agent is about equally effective as a sensitizer in both cell lines at the same concentration. Cells were irradiated at room temperature and in the presence of NEM, irradiation being applied 10 minutes after the addition of NEM. The total length of exposure to NEM was 30 minutes.

PROGRESS REPORT

The results of two typical experiments (Figure 10.1) show the typical age response pattern for HeLa cells with two resistant peaks, one in early G_1 and the other in late S. The age response of HeLa cells in the presence of 0.75 μM NEM shows sensitization of early G_1 cells, and late S cells. There is no effect, however, on G_1-S cells. Late S cells are sensitized in almost the same manner as shown earlier for V79 cells (1). The toxicity of 0.75 μM NEM in HeLa cells is also very similar to that in Chinese hamsters (2).

Survival curves, with and without NEM, were determined at representative ages; namely, mitosis (0 hr); early G_1 (3.0 hr); G_1-S (9.0 hr); and late S (18.0 hr). The survival curve parameters are summarized in Table 10.1.

Evidently in these cells, the effect is mainly on the shoulder rather than the slope. This supports the notion that NEM interferes with repair

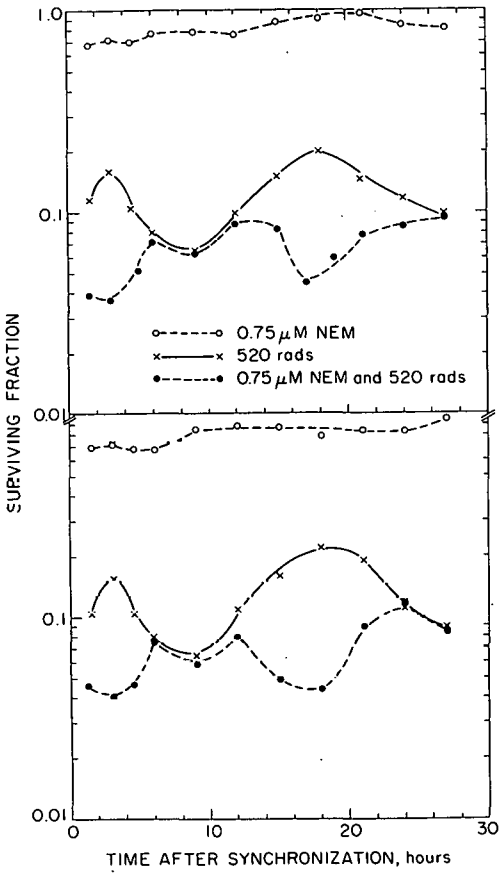

Fig. 10.1. The effect of 0.75 μM NEM on age response of HeLa cells irradiated with 520 rads of X-rays.

Table 10.1. Survival Curve Parameters of HeLa Cells X-Irradiated in PBS or NEM

Stage of the Cycle	Time after Synchroniz. (hours)		Overall Extrapolation Number*	D_q^*	D_o
M	0	PBS	2.1	113 rads	123 rads
		NEM	2.1	113 rads	123 rads
G_1	3.0	PBS	9.0	293 rads	113 rads
		NEM	4.6	180 rads	99 rads
G_1 - S	9.0	PBS	3.0	151 rads	113 rads
		NEM	3.0	151 rads	113 rads
late S	18.0	PBS	10.0	293 rads	123 rads
		NEM	3.0	132 rads	118 rads

*Values not corrected for multiplicity ($\bar{N} \simeq 1.8$-2.0).

processes. It has been suggested in connection with the findings in Chinese hamster cells that repair kinetics of G_1 and S cells are different, as shown

by the addition of NEM (2). Similar results (not shown) have now been obtained in HeLa cells. In both cell lines, recovery occurs more rapidly in S cells than in G_1 cells; irradiated HeLa cells becoming insensitive to the addition of NEM within 2 hours, while irradiated G_1 cells need approximately 6 hours, again a result very similar to that found in Chinese hamster cells.

Based upon these results obtained with HeLa cells, we can conclude that besides DNA synthesis, there is only one other factor, Q, that controls the sensitivity, and the two-component model appears valid (1). This factor Q is responsible for the first resistant peak seen in early G_1 and contributes to the second resistant peak seen in late S. The possible identity of Q has been discussed elsewhere (2).

REFERENCES

1. Sinclair, W. K. Curr. Topics Radiat. Res. Q. 7, 264 (1972).
2. Sinclair, W. K. Radiat. Res. 55, 41 (1973).

SENSITIZATION OF HYPOXIC CHINESE HAMSTER CELLS TO X-IRRADIATION BY N-ETHYLMALEIMIDE

Bruce F. Kimler, Warren K. Sinclair, and Mortimer M. Elkind*

As an extension of previous work (1) on the sensitization of oxygenated Chinese hamster cells to X-irradiation by N-ethylmaleimide (NEM), a technique has been established in this laboratory for rendering cells hypoxic. Chinese hamster cells are grown in a glass prescription bottle which can be fitted with a Lucite valve, de-oxygenated by flowing nitrogen through the valve into the bottle, and maintained at a low oxygen tension after closing the valve. The relative effects of hypoxia, with and without NEM, on cell responses to X-rays are being studied with asynchronous cells and with synchronous cells harvested from log-phase cultures.

It was expected that oxygen would have essentially a dose-modifying effect--hypoxic cells requiring a higher dose to achieve the same lethality as oxygenated cells--with an oxygen enhancement ratio (OER) of approximately three. This was observed with asynchronous cells X-irradiated both in the presence and in the absence of NEM (0.75 μM). Thus, the possibility is supported that NEM sensitizes Chinese hamster cells irradiated in the absence of oxygen via a mechanism similar to, if not the same as, that in the presence of oxygen.

REFERENCE

1. Sinclair, W. K. Radiat. Res. 55, 41 (1973).

---

*Associate Laboratory Director for Biomedical and Environmental Research.

DNA DAMAGE AND ITS REPAIR IN HYPERTHERMIC MAMMALIAN CELLS: RELATION TO CELL KILLING*

E. Ben-Hur† *and Mortimer M. Elkind*

A pronounced enhancement of cell killing is observed with mammalian cells maintained hyperthermic during and/or after X-irradiation, methyl methanesulfonate (MMS) treatment, ultraviolet (UV) light irradiation, or incorporation of radioisotopes into DNA. The target molecule for all these agents is thought to be DNA.

Temperatures from 37°C up to 41°C enhance cell killing mainly by interfering with the repair of sublethal damage. Higher temperatures enhance lethal damage expression. Sedimentation studies of cellular DNA using alkaline sucrose gradients reveal damage to DNA expressed as single-strand breaks and damage to a DNA complex. Following X-irradiation, hyperthermia up to 42°C enhances the repair of single-strand breaks and slows the repair of the DNA complex. After MMS treatment, hyperthermia also slows the repair of MMS-induced single-strand breaks. Temperatures above 41°C, applied for a few hours after either X-irradiation of MMS treatment, cause an endonucleolytic-type of degradation of the DNA. It is suggested that inhibition of the repair of sublethal damage by hyperthermia is due to the interference with the repair of the DNA complex. Enhancement of the expression of lethal damage could be due to hyperthermia-induced DNA degradation.

These results, taken together with the increased heat sensitivity reported for at least some cancer cells compared to normal cells, raise the possibility that the efficacy of the radiotherapy and/or the chemotherapy of cancer could be enhanced when combined with hyperthermia.

---

*Abstract of a paper published in Radiation Research 59, 6 (1974).

†The Hebrew University, Hadassah Medical School, Jerusalem, Israel.

DAMAGE-REPAIR STUDIES OF THE DNA FROM X-IRRADIATED CHINESE HAMSTER CELLS*

Mortimer M. Elkind

Sedimentation studies of DNA released from Chinese hamster cells lysed on top of an alkaline sucrose gradient have shown these principal points. 1) After short lysis periods (e.g., ∿ 60 min, ∿ 25°C), the DNA from unirradiated cells sediments as a two-peaked pattern. The relative position of these peaks is strongly speed dependent. 2) With increasing lysis time, DNA lost from one peak (the "complex") appears in the other (the "main peak") and the same transition is effected, for a given lysis time, if prior to lysis cells are X-rayed with small doses (100 to 700 rads). Since such doses are in the

---

*Abstract of a paper to be published in the Proceedings of the ICN-UCLA Conference on DNA Repair, Squaw Valley, Calif. February 24-March 2, 1974, Plenum Publishing Corporation, New York.

high survival range (∿ 80% to ∿ 3% respectively), an association between damage to the complex and survival is suggested. And 3) the complex contains lipid as well as DNA. Cosedimentation of these materials is lost after doses that resolve the complex into main peak DNA while incubation for repair results in a reformation of the complex plus cosedimentation of lipid and DNA.

INDUCTION OF ALKALI-LABILE LESIONS IN DENATURED T4 DNA BY 365 nm RADIATION

Ronald D. Ley

We previously have reported that a near ultraviolet (UV) wavelength (365 nm) induces single-strand breaks in *Escherichia coli* DNA *in vivo* and in extracted T4 phage DNA (1). However, since the breakage determinations were made by sedimentation of the irradiated DNA in alkaline sucrose gradients (pH 12.5) we could not distinguish between actual UV-induced discontinuities in the DNA and UV-induced alkali-labile lesions. In an attempt to determine if the breaks observed were in fact alkali-labile lesions the following experiment was performed. High molecular weight T4 DNA was denatured by exposure to a high pH (∿ 12.5) and then neutralized prior to irradiation at 365 nm. Following irradiation, the denatured DNA was either sedimented in a neutral sucrose gradient, without further treatment, or first subjected to a pH of ∿ 12.5, then neutralized, and then sedimented in neutral sucrose. If the irradiated, denatured DNA was immediately sedimented without further treatment a breakage efficiency of ∿ 1×10^{-7} breaks per 10^8 daltons per Jm^{-2} was observed. However, if the irradiated DNA was exposed to a high pH before sedimentation the breakage efficiency was calculated to be ∿ 18×10^{-7} breaks per 10^8 daltons per Jm^{-2}. [This value is comparable to the breakage efficiency (24×10^{-7} breaks per 10^8 daltons per Jm^{-2}) we reported for the irradiation of native phage DNA as determined by sedimentation in alkaline sucrose (1).] Thus it would appear that 365 nm radiation induces in denatured DNA true single-strand breaks in alkali-labile lesions in a ratio of ∿ 1:18. It seems reasonable, therefore, to predict that the 365 nm-induced breaks observed in native T4 DNA are, for the most part, alkali-labile lesions. However, this remains to be confirmed by direct observation.

REFERENCE

1. Tyrrell, R. M., R. D. Ley, and R. B. Webb. Photochem. Photobiol. 20, 395 (1974).

POSTREPLICATION REPAIR OF DNA CONTAINING PSORALEN CROSS-LINKS IN CHINESE HAMSTER CELLS*

E. Ben-Hur† *and Mortimer M. Elkind*

Chinese hamster cells exposed to near ultraviolet (NUV) light (315 nm) in the presence of 4,5',8-trimethylpsoralen are killed exponentially after an initial dose range in which sublethal damage is accumulated. Cells are able to repair sublethal damage, although at a slower rate than after X-irradiation. Photochemically, psoralen produces mono- and di-adducts with pyrimidine bases in DNA. The latter form interstrand cross-links and their rate of production is about one-eighth that of mono-adducts. If, after a first treatment consisting of psoralen-plus-NUV, a second NUV exposure is given without psoralen, mono-adducts in DNA are converted to cross-links. Using this procedure, a correlation was found between the rate of DNA cross-linking and cell killing. This suggests that psoralen cross-links in DNA are the principal lesions leading to cell death.

Psoralen-plus-NUV treatment severely inhibits DNA synthesis. When the DNA synthesized immediately after treatment is sedimented through an alkaline sucrose gradient, its size is found to be decreased in a dose-dependent manner. The reduction in size is about equal to the number of psoralen adducts in the DNA. When cells are incubated for a few hours after treatment, the newly synthesized DNA increases in size until it is similar to that of DNA from untreated cells. The time required for this increase is proportional to the NUV dose.

These findings are interpreted in terms of the postreplication repair of DNA. DNA polymerase leaves gaps in nascent DNA opposite psoralen adducts. Subsequently these gaps are filled in by old DNA (recombination repair) as suggested for bacteria; by *de novo* DNA synthesis as postulated for mammalian cells; or both.

---

*Abstract of a paper to be published in the Proceedings of the XI International Cancer Congress, Excerpta Medica, 20-26 October 1974, Florence Italy.

†The Hebrew University, Hadassah Medical School, Jerusalem, Israel.

INDUCTION OF INTERSTRAND DNA CROSS-LINKS BY THE DECAY OF TRITIUM AT THE 2 POSITION OF ADENOSINE

*Ronald D. Ley, Frank Krasin, and S. R. Person**

Previous studies (unpublished data) in the Department of Biophysics of Pennsylvania State University indicated that the tritium decay of incorporated

---

*Department of Biophysics, Pennsylvania State University, University Park, Pennsylvania.

adenosine-2-^{3}H resulted in interstrand cross-linking in DNA. Studies with bases (purines and pyrimidines) labeled with tritium in a position other than the 2 position of adenosine showed decay-induced single-strand breaks in the labeled DNA, but no evidence of the induction of cross-links. Thus the ability of a tritium decay to induce a DNA cross-link appears to require that the tritium atom reside at the 2 position of adenosine. Subsequently, we have measured the efficiency for DNA cross-link induction by incorporated adenosine-2-^{3}H and the efficiency for induction of single-strand breaks. Both processes, cross-linking and single-strand breakage, occur in DNA that contains adenosine-2-^{3}H.

T4 bacteriophage were labeled in their DNA by infection of *Escherichia coli* PS-5 (a purine requiring mutant) grown in medium supplemented with adenosine-2-^{3}H. The labeled T4 phage were purified by banding in a CsCl density gradient, and purified DNA was obtained by extraction with hot phenol. The DNA was stored at -196°C to allow decays to accumulate. Following various periods of storage, the fraction of DNA that would renature after heat denaturation was determined. As would be expected, the amount of renaturable DNA increased (due to the induction of cross-links) with the accumulation of tritium decays. From the rate at which the non-renaturable DNA is converted to renaturable DNA we have calculated that tritium decay from adenosine-2-^{3}H results in cross-link formation with an efficiency of $\sim$ 0.75 cross-links per decay. An accurate determination of cross-linking efficiency is complicated by the induction of single-strand breaks by tritium decay. In order to estimate the efficiency of single-strand break induction we compared sedimentation profiles from alkaline sucrose gradients of DNA labeled with adenosine-2-^{3}H or with guanosine-8-^{3}H. The accumulation of low molecular weight DNA as a function of number of decays occurred at about the same rate for DNA labeled in the 8 position of guanosine or the 2 position of adenosine. Since tritium decay from the 8 position of guanosine was observed to have a single-strand breakage efficiency of $\sim$ 8% it would seem that a similar efficiency for break induction was occurring for adenosine-2-^{3}H labeled DNA. This is only a qualitative observation and a quantitative measurement remains to be made. However, tritium decay at the 2 position of adenosine does result in interstrand DNA cross-linking at a high efficiency ($\sim$ 0.75 cross-links per decay). In comparable experiments with stored DNA that contained guanosine-8-^{3}H, we observed no cross-link formation and an efficiency for single-strand break induction of $\sim$ 8%.

DNA DAMAGE-REPAIR STUDIES OF CHEMOTHERAPEUTIC AGENTS AND RADIATION*

Mortimer M. Elkind

Because of the central role of DNA in the processes of growth, division, and function of cells, the nucleus and in particular the DNA contained therein has usually been assumed to be the major target of radiation damage. Similarly, DNA has frequently been implicated as the target of lethal action of chemical

---

*Abstract of a paper to be published in the Proceedings of the XI International Cancer Congress, Excerpta Medica, 20-26 October 1974, Florence, Italy.

agents known to affect the properties of DNA. In the latter category are mono- and bifunctional alkylating agents and base-pair intercalators.

To help cross-illuminate the molecular action of DNA interactive agents, two chemotherapeutic drugs have been studied separately and in conjunction with X-radiation. Actinomycin D intercalates between complementary base pairs and nitrogen mustard binds primarily to purines producing a number of addition products including interstrand cross-links.

Relative to cell killing and the damage-repair processes involved, it was found that actinomycin D and radiation are synergistic. Nitrogen mustard and radiation, however, produce lethal effects which are only additive. While the effects on DNA sedimentation of these two drugs are quite different from each other, relative to DNA damage due to radiation their actions on DNA are consistent with their differences in affecting radiation cell killing.

ISOSURVIVAL CURVES: THEIR DEPENDENCE ON THE SHAPE OF SINGLE-CELL SURVIVAL CURVES AND OTHER FACTORS*

Mortimer M. Elkind

A single-dose survival curve of the damage accumulation type implies that the corresponding isosurvival plot (i.e., total dose to reach a given level of survival as a function of number of fractions) is an ascending curve concave downward. If the initial slope of the survival curve is zero, the total dose of the isosurvival curve increases without limit. A nonzero negative initial slope causes the isosurvival plot to plateau, other things being equal. The steeper the initial slope, the lower the total dose to reach the plateau, and hence, the broader the plateau. Thus, the importance of a "single-hit" component of cell killing is the consequence that over a range of number of fractions, the total dose to reach a given level of survival is essentially invariant.

In general, a similar result can be obtained if, as a fractionation sequence progresses, the remaining surviving cells become more "sensitive," or equivalently fewer than all of them have to be inactivated to reach the same level of biological effectiveness. At least three processes could contribute to such an enhanced sensitivity. 1) Progressive loss of repair of potentially lethal damage as non-cycling cells are brought into cycle during the course of fractionation. 2) Progressive immunological inactivation of surviving cells in the instance of tumors with appropriate antigenic properties. And 3) progressive reoxygenation of initially hypoxic tumor cells. Two or all three of the foregoing may be operative in a given case. In terms of the effective single-cell survival curve, all three cases operationally would represent enhanced single-cell "sensitivity" during the course of fractionation.

---

*Abstract of a paper to be published in the Proceedings of the 6th L. H. Gray Conference, September 16-20, 1974, London, England.

11. MOLECULAR GENETICS

SUMMARY

Herbert E. Kubitschek, Group Leader

The overall program in Molecular Genetics is directed toward an integrated understanding of the nature of genetic material, and its organization, function, regulation, and replication in the living cell. Studies in these areas are essential to understanding radiation effects on genetic material as well as other complex biological phenomena. While it is generally known that most of the information required for cellular processes is encoded in chromosomal DNA, that chromosomes must duplicate coordinately with other cellular events during the cell cycle, and that the cell must, in turn, retrieve information from the chromosome in an orderly way, only the first of these steps has been worked out in satisfactory detail. The nature of cellular DNA replication, for example, still remains unsolved.

Present programs are particularly concerned with the nature and action of lethal and mutagenic lesions in DNA and the mechanisms by which these are produced by radiation or by decay of radioisotopes incorporated in DNA. Studies of radioisotope decay provide the advantages that the original lesion is localized in the genetic material and the immediate physical and chemical changes that occur at decay are known. We have related specific types of DNA damage to characteristic decay properties of several radioisotopes. Incorporated ^{125}I, for example, induces a double-stranded break in DNA with almost every decay, but causes remarkably little damage of any other kind to the DNA.

Other kinds of genetic lesions are produced by visible light, near-UV, and far-UV, and must therefore be studied separately. Our understanding of the mechanisms of action of these different lesions is aided greatly by the use of radiation-sensitive and resistant mutants, as well as by the use of techniques of molecular biology. These techniques are now also being extended, in collaboration with the Aging Research group, to studies of the genetics of antibody formation in mouse myeloma cells to distinguish between mutational and recombinational mechanisms as the source of antibody diversity.

In recent years, studies of lethal and mutagenic lesions induced by near-UV have already led to several significant findings here. It was shown that pyrimidine dimers produced by near-UV can be lethal lesions; that, like X-rays, near-UV also induced single-strand breaks in addition to pyrimidine dimers; and that near-UV can be used to enhance the effect of X-rays. Two findings are especially notable: DNA repair enzymes are inactivated by near-UV, and inactivation of cells and DNA by near-UV appears to occur through

synergistic photochemical reactions involving both near-UV and shorter radiations. These findings have broad implications for human populations exposed to sunlight, since they indicate that reductions in atmospheric shielding of solar radiation would lead to greatly magnified biological effects.

Biochemical studies of bacterial chromosome replication center primarily on a *quasi-in vitro* system in which newly replicated genes are assayed for biological activity by transformation. This approach shows promise for elucidating mechanisms involved in the initiation of DNA replication. The system also is useful for studies of DNA repair. It has been used to demonstrate that the photoproduct of tryptophan produced by near-UV inhibits a repair activity of DNA polymerase I, the 5' to 3' exonuclease II activity, without affecting the polymerase activity of this enzyme. This is the first biochemical evidence for involvement of exonuclease II in DNA replication.

In slowly growing bacteria, the timing of DNA replication has been examined by a new method that depends upon the capacity of cells to divide in the absence of protein synthesis once a round of DNA replication is completed. The results support our earlier conclusions that DNA replication in these bacteria is very similar to that in eukaryotes, with the usual G_1, S, and G_2 periods, and suggest that the fundamental control mechanisms for DNA replication are the same in bacteria and in eukaryotes.

MOLECULAR GENETICS STAFF

REGULAR STAFF

[*] Allen, Katherine H. (Scientific Associate)
Brown, Mickey S. (Scientific Assistant)
Krisch, Robert E. (Biophysicist)
Kubitschek, Herbert E. (Senior Biophysicist)
Matsushita, Tatsuo (Assistant Geneticist)
Prioleau, John C. (Scientific Assistant)
Sauri, Catherine J. (Scientific Assistant)
[†] Shotola, M. Anita (Scientific Assistant)
[†] Spanski, Sandra (Scientific Assistant)
Venters, Dace (Scientific Assistant)
Webb, Robert B. (Bacteriologist)

TEMPORARY STAFF DURING 1974

[‡] Koch, Arthur L. (Visiting Scientist)
Krasin, Frank (Postdoctoral Appointee)
Robb, Frank T. (Postdoctoral Appointee)
Yoakum, G. H. (Postdoctoral Appointee)

---

[*] Now in Neutron and Gamma-Ray Toxicity Studies.

[†] Terminated during 1974.

[‡] Argonne Universities Association Distinguished Appointment for 1974-1975.

ESTIMATION OF THE D PERIOD FROM RESIDUAL DIVISION AFTER EXPOSURE OF EXPONENTIAL PHASE BACTERIA TO CHLORAMPHENICOL*

Herbert E. Kubitschek

Values of the *D* period, between termination of chromosome replication and cell division, were determined from measurements of residual cell division after exposure to chloramphenicol of exponential phase cultures of *Escherichia coli* B/r and K12 and of *Salmonella typhimurium*. The results obtained by this method were almost identical with earlier results for *E. coli* B/r obtained from measurements of DNA content per cell. For each method, values of the *D* period were independent of growth rate, and the average value of $D = 26.1 \pm 1.2$ minutes obtained by residual division is in good agreement with the value of 25 minutes obtained earlier. These results indicate that the method of residual division provides a good measure of the duration of the *D* period. Values of *D* were also independent of growth rate for both of the other strains.

---

*Abstract of a paper published in the Journal of Molecular and General Genetics 135, 123 (1974).

GENETIC CONTROL OF LEUCINE PERMEASE SYSTEMS IN E. COLI

Frank Robb

Leucine transport into *E. coli* takes place through two quite distinct major permease systems. The high affinity system is specific to L-leucine, and the low affinity (LIV) system is shared by isoleucine and valine. These affinities have provided the basis for a program of mutant selection designed to separate the two systems genetically and to identify the components of each system. The selection of mutants resistant to analogues of leucine has provided the key to obtaining transport deficient strains. The analogue 5,5,5-trifluoroleucine (TFL) is toxic to *E. coli* and probably enters via both major permease systems, since it is a competitive inhibitor of both high and low affinity transport. A mutant defective in both systems would be very difficult to isolate, since a double mutation might be required to provide resistance. Instead, we have isolated the high affinity system as described below.

The strain EO-0319, obtained from D. Oxender (University of Michigan), has elevated levels of leucine specific permease activity, and also elevated levels of the periplasmic leucine specific binding protein, a possible component of leucine transport. Spontaneous TFL-resistant mutants, strains TFL 32 to TFL 49, were selected in the presence of 30 µg of L-isoleucine per ml. These were then tested by the radial streak method to determine which were dependent on isoleucine for TFL resistance, and then grown in liquid culture overnight to test whether a transport deficiency was present. Leucine transport

was tested in the presence and absence of 200 μM L-isoleucine. Since only the high affinity system is active in the presence of saturating isoleucine, this assay system permits separation of the high and low affinity systems. The ratio of leucine specific/LIV activity can be readily calculated; this ratio is not dependent on cell density in mid-logarithmic cultures, and provides a useful measure for assaying regulation or deficiency of the leucine permeases.

PROGRESS REPORT

The majority of transport mutants examined had specific deficiencies in the high affinity system. Two mutants (TFL 33 and TFL 35) had pleiotropic lowering of both leucine permeases, possibly due to the alteration of some common regulatory component. A single mutant (TFL 49) retained leucine specific activity and lost LIV activity. A second series of mutants was selected and characterized. The cultures were treated with the frameshift mutagen ICR 170E. Frameshift mutations cause a very high frequency of chain termination events, and in this case the missing polypeptide might be purified and identified. The periplasmic proteins from these mutants were analysed by SDS polyacrylamide gel electrophoresis, on very thin slabs. This technque, described by Ames (1), permits molecular weight estimates of proteins from bacterial extracts. The mutant extracts were found to be missing a 39,000 molecular weight polypeptide that was prominent in wild-type extracts. The molecular weight of purified leucine specific binding protein is 39,000 by several techniques (2). It is probable that the leucine specific binding protein is absent in these mutants. These results provide the most direct evidence to date for the involvement of the leucine specific binding protein in active transport. In addition, leucine binding activity of the periplasmic extracts was tested by equilibrium dialysis. The mutant extracts had less binding activity, and were inhibited completely by 25 μM isoleucine, indicating the absence of leucine specific binding. The wild-type extracts reached partial saturation at 25 μM isoleucine but leucine specific binding was still present.

Kinetic studies were done on the residual transport activity of the mutants. Leucine transport was inhibited by isoleucine to a much greater extent in the mutants than in the wild-type. In mutants a residual of approximately 20% of total leucine transport remained in the presence 200 μM isoleucine. The residual transport activity was resistant to TFL inhibition in mutants but not in wild-type. It is probable that this residual transport activity represents a minor system for leucine uptake not previously reported, and it is provisionally called the leucine specific system II. This new system was insensitive to inhibition by threonine, valine, and methionine.

Future studies on the regulation of leucine transport may use these mutants as a model system without leucine specific system I. It is probable that the two major uptake systems have a common evolutionary origin (2), and thus possible that regulation is coupled.

REFERENCES

1. Ames, G. F. J. Biol. Chem. 249, 634 (1974).
2. Furlong, C. University of California, Riverside. Personal communication (1974).

LEUCINE UPTAKE DURING THE CELL CYCLE

Frank Robb

An attempt was made to examine leucine transport during different phases of the cell cycle, using *E. coli* strain BUG 6. This strain has a temperature sensitive block in cell division, and cells grow into long "filaments" at the non-permissive temperature, 42°C. Leucine transport of BUG 6 was examined during temperature shift experiments.

PROGRESS REPORT

The non-permissive temperature was previously reported by Shen and Boos to lead to repression of galactose binding proteins and galactose transport. Overall leucine transport was repressed during long (8 hr) growth 42°C. Since Shen and Boos' result depended on efficient uptake of ^{14}C leucine into 8-hr filaments, and since he did not examine leucine uptake, his results are suspect.

Another method was devised to obtain synchronously dividing cells. Exponential BUG 6, growing at 34°C, were transferred to 42°C for 1 or 2 hours. During this time all the cells grew but did not divide. Then, after shifting these small filamentous cells back to 34°C, the population immediately underwent synchronous division. There were only minor perturbations of leucine uptake during this division, and no variation of the ratio of leucine specific to LIV (low affinity system) transport.

In another experiment, D_2O/H_2O gradient centrifugation was used to separate "cells from small filaments," with the help of G. Blumberg (Microbiology Department, Indiana University). The cells recovered from the gradients had very little leucine transport activity.

In summary, it has yet to be shown that transport of leucine is regulated coordinately with the cell cycle.

REFERENCE

1. Shen, B. H. P., and W. Boos. Proc. Nat. Acad. Sci. U. S. A. 70, 1481 (1973).

EFFECTS OF RADIOISOTOPE DECAY IN MICROORGANISMS

I. EFFECTS OF ^{125}I DECAY IN COLIPHAGE T4

Robert E. Krisch and Catherine J. Sauri

Radioactive isotopes incorporated into the genetic material of viable bacteria or bacteriophage cause death or genetic damage in an increasing number of organisms as radioactive decay proceeds. The goal of our experiments is to relate such biological effects to specific physical and chemical changes of decaying atoms, as well as to physicochemical damage to the genetic material.

PURPOSE AND METHODS

Iodine-125 decays by electron capture, causing extensive fragmentation of small organic molecules, presumably by means of electrostatic forces resulting from the vacancy cascades and multiple ionizations that accompany decay (1). In our experiments ^{125}I was incorporated into the DNA of coliphage T4 in the form of 5-iododeoxyuridine (IUDR), an analogue of thymidine. We have previously demonstrated an extremely high lethal efficiency per decay, $\alpha(\text{lethal}) = 0.6$, for ^{125}I decay in T4 phage, and an even higher efficiency for the induction of double-strand breaks (DSB's) in the DNA of phage T4, $\alpha(\text{DSB}) = 1.0$ (2). The breakage efficiency was determined by the sedimentation in neutral sucrose gradients of phenol-extracted DNA from stored phage. These experiments further showed that α(DSB) was independent of storage temperature during decay (+4°C vs.-196°C) and also independent of whether storage was as intact phage or as free DNA.

These results, along with the unit efficiency for the induction of DSB's, strongly suggested that the observed DNA breakage is due to local ^{125}I decay effects rather than to the ionizing radiation emitted during decay. The reason for the difference between α(lethal) and α(DSB) is not yet clear and is under current investigation.

PROGRESS REPORT

More recent experiments have been carried out to examine the origin of the DSB's from ^{125}I decay in T4 DNA in another way. External, low LET ionizing radiation is known to cause about 20 single-strand breaks (SSB's) in DNA per DSB (3). In contrast, if the DSB's from ^{125}I decay were due solely to local molecular damage, we would predict only two SSB's per DSB (one SSB on each of the two opposite strands of the DNA double helix). In our experiments, ^{125}I-labeled T4 DNA was stored at -196°C either tightly packed as intact phage, or greatly extended as extracted DNA. These storage conditions should maximize and minimize, respectively, the self-irradiation dose from ionizing radiation to a phage genome from an ^{125}I decay. After varying amounts of decay, both single- and double-strand breaks were measured, using alkaline and neutral sucrose gradients, respectively. We confirmed our earlier finding that there was one DSB per ^{125}I decay for either intact phage or extracted DNA. However, there were 3-4 SSB's per genome equivalent per decay for intact phage compared with nearly two SSB's per decay for extracted DNA.

CONCLUSIONS

These experiments narrowly bracket the frequency of occurrence of SSB's from ^{125}I decay in T4 DNA. Because of the low ratio of SSB's/DSB's for intact phage, they provide very strong evidence that the severe damage to phage DNA from ^{125}I decay is primarily due to local molecular damage from the decay. They further demonstrate that ^{125}I decay in extracted DNA can induce DSB's with maximum efficiency ($\alpha = 1.0$) while inducing no SSB's at all, other than the two that, together, constitute each DSB. This latter finding indicates that external ionizing radiations play essentially no role in the severe damage to phage DNA from the decay of incorporated ^{125}I.

REFERENCES

1. Carlson, T. A., and R. M. White. J. Chem. Phys. 38, 2930 (1963).
2. Krisch, R. E., and R. D. Ley. Int. J. Radiat. Biol. 25, 21 (1974).
3. Bohne, L., T. Coquerelle, and V. Hagen. Int. J. Radiat. Biol. 17, 205 (1970).

II. EFFECTS OF ^{125}I DECAY IN *E. COLI*

Robert E. Krisch and Frank Krasin

PURPOSE AND METHODS

We have previously examined the lethal effects of ^{125}I in four different strains of *E. coli* with varying genetic deficiencies in DNA repair and different sensitivities to other forms of radiation (1). These strains showed corresponding differences in sensitivity to killing from ^{125}I decay. In view of our finding that ^{125}I decay induces double-stranded breaks (DSB's) in coliphage DNA with approximately unit efficiency (part I), these differences in killing efficiency suggested a remarkable capability by wild-type *E. coli* to repair DSB's induced in its DNA, since unrepaired DSB's in the bacterial genome are presumably incompatible with survival.

In order to study directly the induction and repair of DSB's in the DNA of *E. coli* and their correlation with survival, we have adapted a technique for the isolation of intact or nearly intact bacterial genomes (2). The technique involves treatment of cells on the surface of a neutral sucrose gradient with lysozyme and detergent.

In addition, we have recently developed a purification technique that now enables us to obtain accurate measurements of the specific activity of ^{125}I-labeled bacterial DNA. This technique involves a sequence of enzymatic treatments followed by passage through a hydroxyapatite column. The DNA concentration is then measured by a very sensitive fluorometric method (3) and the radioactivity is measured by a standard gamma scintillation detector.

PROGRESS REPORT

With these techniques, we are correlating the induction of DSB's in bacterial DNA by ^{125}I decay with loss of viability. *E. coli* K12 AB2487, a *recA* mutant, is compared with the corresponding *rec*$^+$ strain, AB2497. Results to date are consistent with an efficiency of 1.0 per decay for the induction of DSB's by ^{125}I decay in either bacterial strain, as found earlier for ^{125}I decay in the DNA of T4 phage. However, the results to date for bacteria are subject to considerably greater uncertainty than the results for phage, due to technical problems caused by the much larger bacterial genome. The lethal efficiencies per decay appear to be approximately 1.0 for the *recA* mutant and 0.3 to 0.5 for the wild-type, strongly suggesting that there is repair of DSB's in the *rec*$^+$ strain, but not in the *recA* mutant. Preliminary physicochemical assays for repair have been carried out with both strains by incubating samples of stored, labeled cells for 1 hour in rich medium prior to DNA extraction and comparing the results of these assays with those on unincubated cells. The results have been difficult to interpret because of extensive DNA breakdown induced in the *recA* cells by the experimental procedure. Nevertheless, these experiments do provide evidence for significant repair of ^{125}I-induced DSB's in wild-type cells and no evidence at all for repair in the *recA* cells. These observations suggest that biological repair of DSB's is a crucial factor in the survival of wild-type *E. coli* labeled with ^{125}I and that a pathway requiring a functioning *recA* gene is involved in such repair.

REFERENCES

1. Krisch, R. E. Int. J. Radiat. Biol. 21, 167 (1972).
2. Bonura, T. Stanford University, Stanford. Personal communication (1973).
3. Le Pecq, J. Methods Biochem. Anal. 20, 41 (1971).

III. EFFECTS OF ^{14}C DECAY IN COLIPHAGE T4

Robert E. Krisch

PURPOSE AND METHODS

Carbon-14 decays by the emission of a beta particle of relatively low mean energy (0.045 MeV). The biological effects of this decay have not been widely studied but are of considerable interest because of the ubiquitous occurrence of ^{14}C in the biosphere. We have incorporated ^{14}C into the DNA of thymidine-deficient *E. coli* by supplying it in the growth medium as thymidine-2-^{14}C. A comparison of killing and damage to DNA is being attempted with coliphage T4 grown on ^{14}C-labeled *E. coli*.

PROGRESS REPORT

An experiment has been running for more than a year in which T4 phage, labeled with a measured (average) number of ^{14}C atoms per phage genome, have

been stored at -196°C and periodically assayed for loss of viability and for the induction of DSB's in DNA. The techniques for measuring DNA breakage seem to be considerably more sensitive and reproducible than those for measuring loss of viability. Results to date indicate that α(DSB) for ^{14}C decay in T4 is between zero and 0.01, with 95% confidence. As far as we know, this is the first data anywhere on DNA scission by ^{14}C decay.

LETHAL AND MUTAGENIC EFFECTS OF NEAR-ULTRAVIOLET RADIATION

Robert B. Webb

Pyrimidine dimers (1,2) and single-strand breaks (or alkali-labile bonds) (3) are induced in bacterial DNA by 365 nm radiation. Furthermore, the photoreactivation (PR) enzyme (4) and dark-repair enzyme (5) can be damaged by 365 nm radiation within the biological dose range. Damage to dark-repair mechanisms would be expected to enhance the biological effects of repairable DNA lesions. The absence of PR after 365 nm inactivation in wild-type and *uvr* (5,6), together with the strong oxygen dependence for lethality in these strains (7), suggests that dimers may not be important lethal lesions for these strains. Further elucidation of lethal and mutagenic lesions induced in DNA by near-ultraviolet radiation was obtained by examining the oxygen dependence and photoreactivation of these lesions in *Escherichia coli* B/r Hcr.

Radiation at 365 nm was provided by a 2.5 kW Hg/Xe arc lamp coupled to a 500 nm Bausch and Lomb monochromator with a Corning 0-52 filter to reduce stringently the stray radiation of wavelengths shorter than 350 nm. Anoxia was provided by passing prepurified nitrogen over copper filings heated to 500°C. Photoreactivation light was provided by a 500 W quartz iodine lamp in a slide projector. Procedures have been described (1,8).

PROGRESS REPORT

Oxygen dependence and photoreactivation of lethality and mutagenicity by 365 nm radiation in *Escherichia coli* B/r Hcr (a strain deficient in excision repair) are shown in Figure 11.1. The large oxygen enhancement for lethality shown is typical of this strain and the related repair proficient strain B/r (7). The oxygen dependence for the induction of mutation of tryptophan independence is strikingly different from that for lethality. At relatively low doses, less than 3×10^6 J m^{-2}, the induced mutant frequencies are significantly reduced in the presence of oxygen; but at high dosages, the mutant yield appears to be greater in the presence of oxygen. This relationship is a result of mutation induction curves that were approximately dose squared when oxygen was present and almost linear in its absence (Figure 11.1).

Photoreactivation of lethal and mutagenic lesions induced by 365 nm radiation also is shown in Figure 11.1. Survival was slightly less after the aerobically irradiated cell suspensions were exposed to photoreactivating illumination. Cells inactivated under anoxic conditions showed a small but significant PR sector. In contrast to the small PR effect on lethal lesions

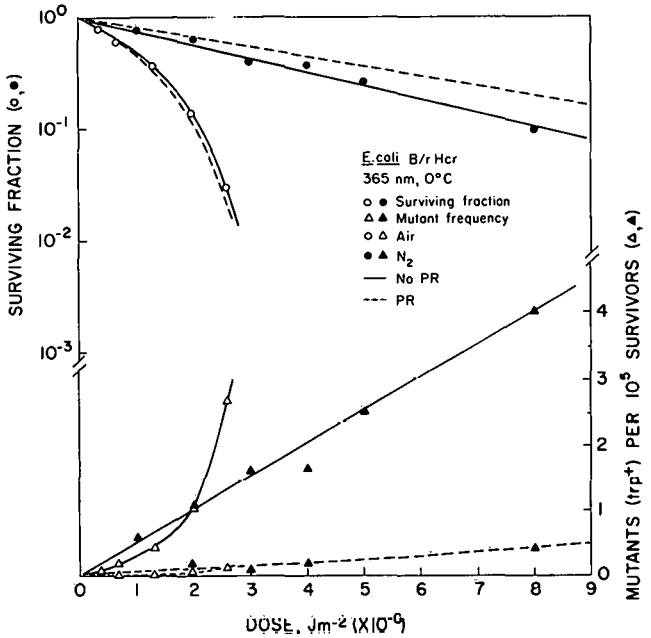

Fig. 11.1. Inactivation and mutation to tryptophan independence induced in *E. coli* B/r Hcr by 365 nm radiation (0°C). Irradiance, 1200 W m^{-2}. Photoreactivation illumination (380-430 nm), 30 min at 100 W m^{-2} (25°C).

induced in both the presence and absence of oxygen, mutational lesions were reduced almost to the spontaneous background by exposure of the 365 nm irradiated cells to photoreactivating light. Photoreactivation of the mutational lesions demonstrates that the PR enzyme was not inactivated in these stationary phase cells at the dosages given. In log phase cells PR enzyme activity is effectively inactivated by a dose of 2 x 10^6 J m^{-2}, but stationary phase cells contain more PR enzyme molecules than log phase cells (2), so larger doses of 365 nm radiation would be required to inactivate all PR activity in stationary phase cells. If photoreactivation is taken as evidence for pyrimidine dimers, data shown in Figure 11.1 are evidence that reversion to tryptophan independence induced by high fluences of 365 nm radiation occurs through the production of pyrimidine dimers.

The relationship between mutagenicity and lethality in strain B/r Hcr at 254 nm and 365 nm is depicted in Figure 11.2. Under aerobic conditions, mutation induction relative to killing is six times more efficient at 365 nm than at 254 nm. Under anoxic conditions, mutation induction at 365 nm is 18 times more efficient than at 254 nm relative to lethal effects. It is evident that the mutagenic effect of dimers relative to their lethal action differs greatly under these three sets of conditions.

The small oxygen dependence for the 365 nm inactivation of *E. coli* K12 AB2480, a UV sensitive strain deficient in both excision and recombination repair of pyrimidine dimers, is shown in Figure 11.3. The large photoreactivation sector of 0.75 shown by these results, and reported previously (1), is evidence that pyrimidine dimers are the major 365 nm lethal lesion for this double mutant strain. The small oxygen dependence shown can be entirely accounted for by the nonphotoreactivable sector of lethal damage. Thus the photoreactivable (dimer) component of lethal damage is the same in the presence and absence of oxygen. These results indicate that the induction of pyrimidine dimers at 365 nm is not enhanced by oxygen.

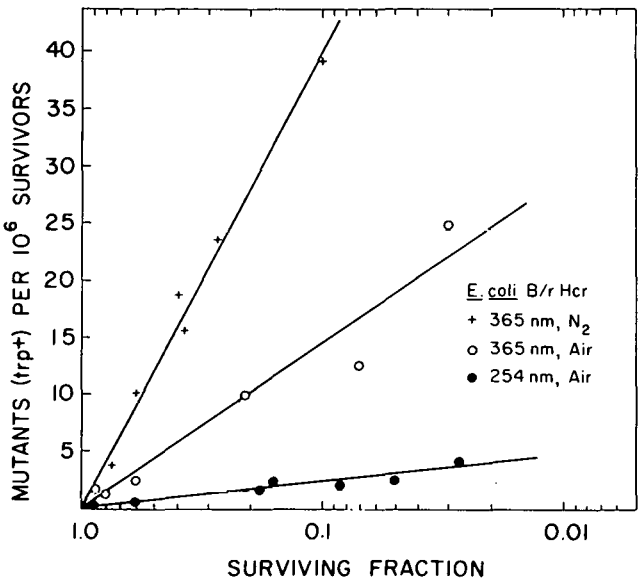

Fig. 11.2. Relationship between lethality and mutagenesis (tryptophan independence) at 254 nm and 365 nm in *E. coli* B/r Hcr.

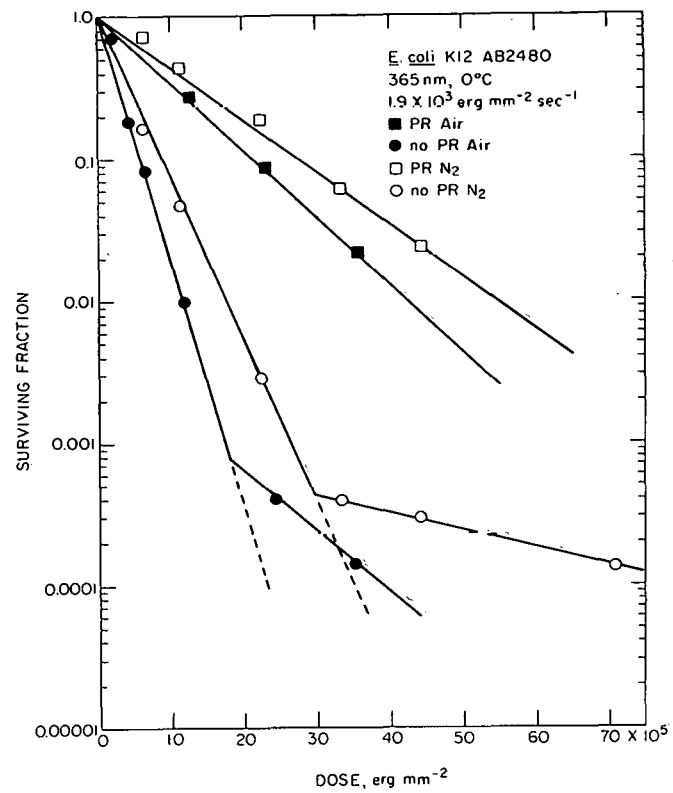

Fig. 11.3. Photoreactivation after 365 nm inactivation (0°C) of *E. coli* K12 AB2480 in the presence and absence of oxygen. Irradiance at 365 nm, 300 W m^{-2}. Photoreactivation illumination (380-430 nm), 30 min at 20 W m^{-2} (25°C).

Dimers are induced by 365 nm radiation and clearly account for a major part of the inactivation in strains deficient in both excision and recombination repair (Figure 11.3). However, lesions other than dimers probably cause most of the 365 nm inactivation in repair proficient and *uvr* mutant strains. Consistent with this mechanism is the observation that single-strand breaks (or alkali-labile bonds) are induced in DNA by 365 nm radiation (3). Single-strand breaks were not detected when cells were irradiated under anoxic

conditions. The large oxygen dependence of near-UV inactivation suggests that single-strand breaks may be the major lethal lesion induced by 365 nm radiation in repair proficient and *uvr*$^-$, *rec*$^+$ strains.

Damage to repair systems may be oxygen dependent. If so, some but not all of the oxygen dependence for 365 nm lethality could be accounted for by enhanced damage to repair systems.

There are striking differences between near-UV mutation induction in chemostat cultures by low chronic exposures (9) and in stationary phase suspensions subjected to large acute lethal fluences at very high irradiances (Figure 11.1). It is likely that mutagenesis at continuous low irradiances of near-UV (< 6 J $m^{-2}s^{-1}$) is caused by different lesions from mutations induced by very high irradiance (1000 J $m^{-2}s^{-1}$) in stationary phase cells. Mutational lesions induced at high irradiances are photoreactivable (Figure 11.1), implicating pyrimidine dimers. It is unlikely that dimers are involved in low irradiance mutagenesis, as the very small numbers of dimers that might be induced at the near-UV fluences used would be largely photorepaired concomitantly. If the chromophore(s) responsible for low irradiance mutagenesis are light labile and destroyed quickly by the high acute irradiances used, the low irradiance chromophore(s) would be not be expected to contribute significantly to the high irradiance responses observed.

REFERENCES

1. Brown, M. S., and R. B. Webb. Mutat. Res. 15, 348 (1972).
2. Tyrrell, R. M. J. Bacteriol. 115, 450 (1973).
3. Tyrrell, R. M., R. D. Ley, and R. B. Webb. Photochem. Photobiol. 20, 395 (1974).
4. Tyrrell, R. M., R. B. Webb, and M. S. Brown. Photochem. Photobiol. 18, 249 (1973).
5. Tyrrell, R. M., and R. B. Webb. Mutat. Res. 19, 361 (1973).
6. Brown, M. S., and R. B. Webb. Biological consequences of pyrimidine dimers induced by near-ultraviolet radiation. This Report, Section 11.
7. Webb, R. B., and J. R. Lorenz. Photochem. Photobiol. 12, 283 (1970).
8. Webb, R. B., and M. S. Brown. Photochem. Photobiol., in press.

BIOLOGICAL CONSEQUENCES OF PYRIMIDINE DIMERS INDUCED BY NEAR-ULTRAVIOLET RADIATION

Mickey S. Brown and Robert B. Webb

PURPOSE AND METHODS

Past studies have given evidence for the presence of pyrimidine dimers in *Escherichia coli* cells following near-ultraviolet radiation (1,2), but gave little or no evidence for photoreactivation (PR) of wild-type strains and *uvr* strains when irradiated in air. Damage to the PR enzyme was suggested to account for the absence of PR after 365 nm inactivation in these strains (2).

It was also possible, however, that synergistic reaction between the PR and near-UV wavelengths obscured the PR effect, especially since strong synergistic interactions are known to occur between different near-UV wavelengths (3).

To examine these possibilities, we tested for an aerobic synergistic interaction between the inactivating wavelength (365 nm) and the photoreactivating wavelength (405 nm) and investigated the role of oxygen in this interaction. In addition, we tested for damage to the PR enzyme by 365 nm radiation.

Strains of bacteria used were *E. coli* K12 AB1157 (wild-type) and *E. coli* K12 AB1886 (*uvr*). The assay method for near and far-UV was the same as described previously (1). PR was carried out using a wavelength of 405 nm with the mercury - xenon lamp (Hanovia 2.5 kW) in combination with a predispersion prism (Schoeffel) and a 500 nm grating monochromator (Bausch and Lomb). For PR irradiation under anoxia the cells were flushed with nitrogen before and during irradiation to eliminate oxygen.

PROGRESS REPORT

Evidence of a synergistic interaction of 365 nm and PR light is demonstrated in Figure 11.4 in which survival is shown as a function of time of exposure to PR light (405 nm). PR illumination does not cause inactivation of the more resistant wild-type strain (*E. coli* K12 AB1157) when the cells are exposed to only PR light at a dose rate of 350 W m^{-2} (3,500 ergs·mm^{-2}·sec^{-1}). However, when these cells were exposed to 365 nm radiation prior to PR illumination in air additional inactivation was obtained. Figure 11.4 also shows that synergistic response is greater at 25°C than at 0°C.

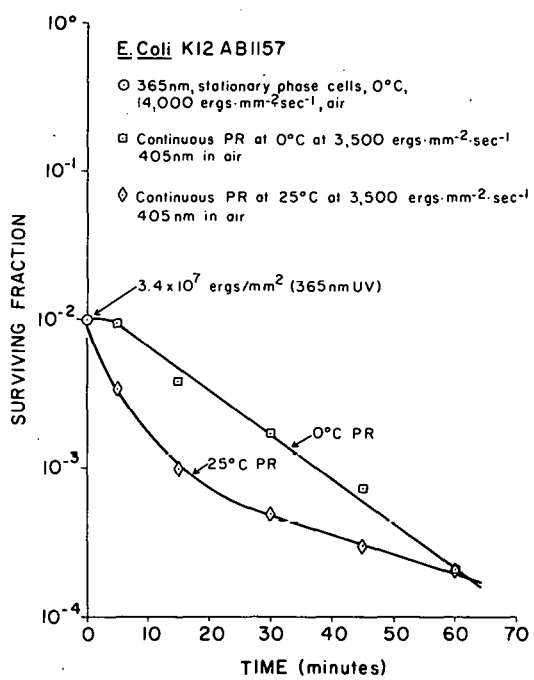

Fig. 11.4. Inactivation of *E. coli* K12 AB1157 (wild-type) by 365 nm irradiation at 0°C followed by continuous photoreactivating light (405 nm) at 0°C and 25°C. Photoreactivation irradiance was 3,500 ergs·mm^{-2}·sec^{-1}.

When the 365 nm inactivation was followed by a 405 nm exposure under anoxic conditions (N_2), synergism was no longer observed. Similar results were obtained using 405 nm produced by a monochromator instead of 405 nm radiation.

Figures 11.5 and 11.6 show that after inactivating doses of 365 nm radiation neither of the two strains of *E. coli* (stationary phase) differing in their repair capabilities showed photorepair upon exposures to PR light under anoxic conditions. However, upon exposures to PR light following 254 nm irradiation, a significant degree of repair was demonstrated. Photorepair was even more effective when cells were exposed both to 365 nm and 254 nm UV prior to PR light (Figures 11.5 and 11.6). All the maximum photorepair was reached at moderate PR doses. It is evident that functional PR enzyme remained after the 365 nm doses given in these stationary phase cells. These results rule out damage to the PR enzyme as the basis of absence of photorepair after 365 nm inactivation. However, these data do not contradict the previous findings that biological doses of 365 nm radiation inactivated the PR enzyme in exponential phase cells (2,4), as stationary phase cells contain more PR enzyme molecules.

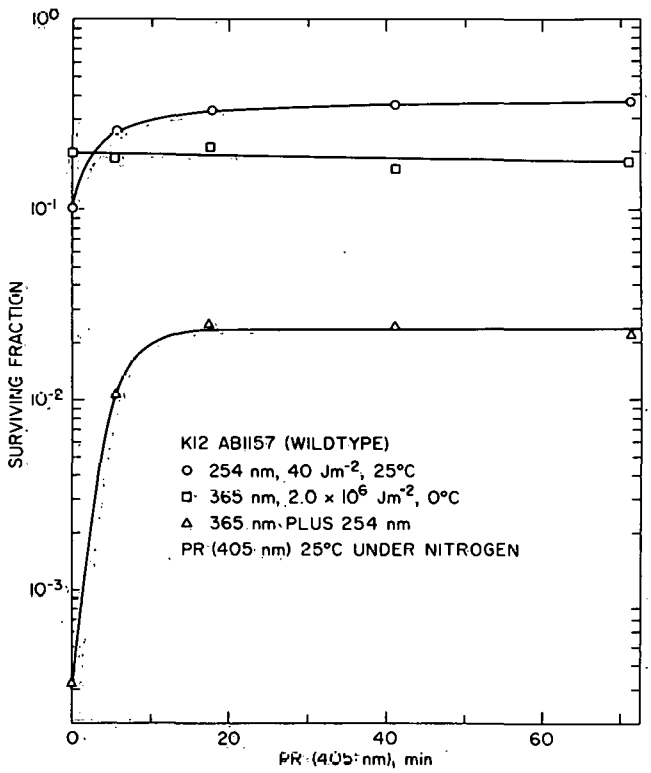

Fig. 11.5. Inactivation of *E. coli* K12 AB1157 by 254 nm (25°C), by 365 nm (0°C), and by 365 nm (0°C) plus 254 nm (25°C) irradiation followed by continuous photoreactivation (25°C) under nitrogen.

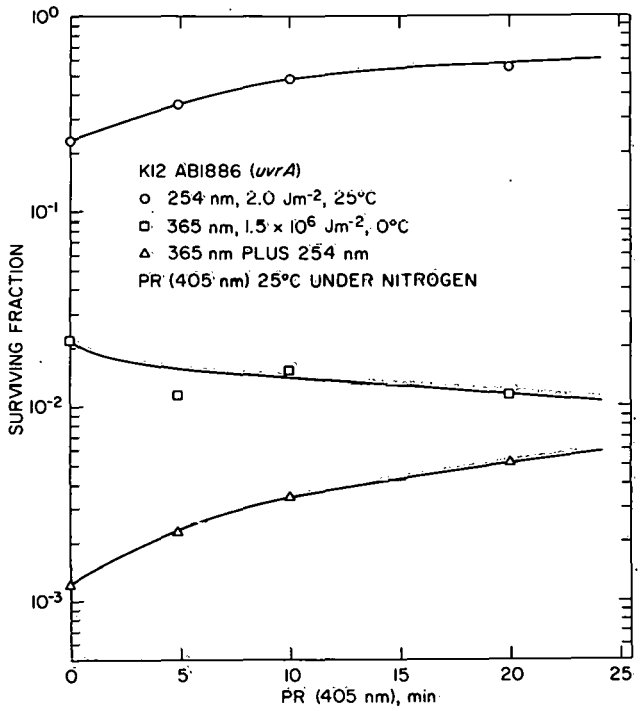

Fig. 11.6. Inactivation of *E. coli* K12 AB1866 (*uvr*) by 254 nm (25°C), by 365 nm (0°C), and by 365 nm plus 254 nm irradiation followed by continuous photoreactivation (25°C) under nitrogen.

CONCLUSIONS

The PR response following a combination of 365 nm and 254 nm radiations indicates the presence of functional PR enzyme not observed when these wild-type and *uvr* cells are exposed to 365 nm alone. The results further indicate that an oxygen dependent synergistic interaction occurs between 365 nm and 405 nm wavelengths, but this effect does not account for the absence of PR under anoxic conditions. These results suggest that pyrimidine dimers induced at 365 nm may be repaired more efficiently by dark repair mechanisms than are dimers induced at 254 nm.

REFERENCES

1. Brown, M. S., and R. B. Webb. Mutat. Res. 15, 348 (1972).
2. Tyrrell, R. M., R. B. Webb, and M. S. Brown. Photochem. Photobiol. 18, 249 (1973).
3. Peak, M. J., J. G. Peak, and R. B. Webb. Photochem. Photobiol. 21, 129 (1975).
4. Brown, M. S., and R. B. Webb. ANL-8070 (1973), p. 202.

ACTION SPECTRA OF INACTIVATION OF RECOMBINATIONLESS STRAINS OF SALMONELLA TYPHIMURIUM AND ESCHERICHIA COLI*

Donna Mackay,[†] *A. Eisenstark,*[‡] *and M. S. Brown*

Action spectra for lethality of both stationary and logarithmically growing cells of recombinationless (*recA*) mutants of *Salmonella typhimurium* and *Escherichia coli* were obtained. Maximum sensitivity was observed at 260 nm which corresponds to the maximum absorbance of DNA. However, a shoulder occurred in the 280-300 nm range that departed significantly from the absorption spectrum of DNA. Between 240 nm and 313 nm, 90 to 99% of the cells were killed exponentially, but 1 to 10% of the population was resistant. At wavelengths longer than 320 nm, the shapes of inactivation curves departed significantly from those at wavelengths shorter than 320 nm. Survival curves at wavelengths longer than 320 nm had a strongly shouldered shape. The special sensitivity of *recA* mutants to broad spectrum near-UV radiation may be due to synergistic effects of different wavelengths. Parallels between the inactivation of *recA* mutants and the induction of photoproducts of L-tryptophan toxic for *recA* mutants suggest that photoproducts from endogenous tryptophan may be involved in the high sensitivity of these strains to broad spectrum near-UV radiation.

---

*Abstract of a paper to be submitted to Photochemistry and Photobiology.

[†]Kansas State University, Manhattan.

[‡]University of Missouri, Columbia.

PHOTOREACTIVATION AFTER 365 nm INACTIVATION OF STRAINS OF ESCHERICHIA COLI DIFFERING IN REPAIR CAPABILITY*

Robert B. Webb, Mickey S. Brown, and Rex M. Tyrrell

Photoreactivation (PR) after 365 nm inactivation was attempted in four strains of *Escherichia coli* differing in repair capability. Photoreactivation was observed in the *recA* strains K12 AB2480 and K12 AB2463 indicating a significant role of pyrimidine dimers in the lethal action of 365 nm radiation in these strains. Significant PR was not observed in the *uvr* strain, K12 AB1886, or in the wild-type strain, K12 AB1157, after 365 nm inactivation. Biological evidence indicated that in stationary phase cells the PR enzyme is not inactivated by fluences of 365 nm radiation of 2×10^6 J m^{-2} or less. Mechanisms are presented to account for the failure to observe PR at 365 nm doses less than 2×10^6 J m^{-2} in rec^+ strains.

---

*Abstract of a paper to be submitted to Mutation Research.

NEAR-UV PHOTOPRODUCT(S) OF L-TRYPTOPHAN: AN INHIBITOR OF MEDIUM DEPENDENT REPAIR OF X-RAY INDUCED SINGLE-STRAND BREAKS IN DNA WHICH ALSO INHIBITS REPLICATION GAP CLOSURE IN E. COLI DNA*

G. Yoakum, A. Eisenstark,† *and R. B. Webb*

Near-UV photoproducts of L-tryptophan (TP), which are especially toxic for recombination deficient (*rec*) mutants, were found to inhibit medium dependent repair of X-ray induced single-strand breaks. This inhibitor also slows the rate of closure of replication gaps suggesting that these two processes may have a common pathway (or share a required step which TP can inhibit).

---

*Abstract of a paper submitted for publication in Molecular Mechanisms for the Repair of DNA. Plenum Publishing Corporation, New York.

†University of Missouri, Columbia.

TRYPTOPHAN PHOTOPRODUCT(S): SENSITIZED INDUCTION OF STRAND BREAKS (OR ALKALI-LABILE BONDS) IN BACTERIAL DNA DURING NEAR-UV IRRADIATION*

George H. Yoakum

The experiments presented here provide evidence that photooxidation products of the amino acid L-tryptophan sensitize bacterial DNA, increasing the rate of 365 nm induction of DNA-strand breaks (or alkali-labile bonds). Evidence is also presented which demonstrates that these sensitized DNA lesions contribute to the inactivation of *Escherichia coli* W3110 wild-type, and P3478 *polA1*. These results suggest that photooxidation products of endogenous L-tryptophan act as an internal sensitizer responsible for near-UV radiation induced oxygen-dependent DNA-strand breaks (or alkali-labile bonds) in cellular DNA.

---

*Abstract of a paper to be published in the Journal of Bacteriology.

MULTIPLE MUTATIONS INDUCED IN BACILLUS SUBTILIS BY ULTRAVIOLET LIGHT

*H. E. Kubitschek and G. Venema**

PURPOSE AND METHODS

As reported last year (1), UV-induced mutations to resistance to bacteriophage T5 in *Escherichia coli* strain WP2 Hcr follow a dose-squared response, in agreement with present interpretations that UV-induced mutagenesis occurs as a recombinational event. The results indicated that the two UV-induced lesions responsible for mutagenesis were separated, on the average, by about 200 nucleotide pairs. Because this estimate is the minimal average spacing of these mutagenic lesions, it seemed that UV may frequently induce recombinations over greater ranges of the genome. Experiments were designed to test this possibility with *Bacillus subtilis*. The genetic map of this organism contains a number of antibiotic markers in a localized region replicated very early in the cell cycle. Mutations to high-level (1 mg/ml) streptomycin resistance were induced by exposure of *B. subtilis* strain 1G23 *trp, uvr* to UV. Streptomycin resistant mutants were then individually examined for resistance to each of the other antibiotics, rifampicin, neomycin, kanomycin, erythromycin, and lincomycin.

It was necessary to test between the possibilities that resistance to more than a single antibiotic might arise either from a single mutation of a transport gene that decreased the sensitivity of a cell to several antibiotics or, alternatively, that mutations occurred at each of the observed antibiotic resistance loci. This was accomplished by extracting DNA from each mutant strain tested and using this DNA to transform a recipient strain sensitive at each of the antibiotic loci. Transformant frequencies were measured for resistance to one or more of the antibiotics. In some experiments, streptomycin-resistant transformant colonies were replicated to plates containing another antibiotic.

PROGRESS REPORT

Of 136 streptomycin resistant colonies examined, 135 were multiple mutants resistant to one or more of the other antibiotics rifampicin, neomycin, kanomycin, or erythromycin. Some UV-induced mutants were resistant to each of these antibiotics. However, none were resistant to lincomycin, which has a locus located at a greater distance along the genetic map. An important feature of the antibiotic resistance patterns of these mutants is that resistance did not occur at random. Instead these patterns invariably were bunched in the manner that would be predicted from one double crossover event.

Seven multiple mutants for streptomycin, neomycin, and kanomycin resistance were examined by transformation. In every case, transformant frequencies for resistance to only one of the antibiotics were much greater than those for

* Genetics Institute, University of Groningen, The Netherlands. Work performed while first author was on leave from Argonne National Laboratory.

simultaneous resistance to two or more of the antibiotics; that is, very few of the transformants carried resistance to more than a single antibiotic. Thus the induced mutations are separable, and represent mutation at each of the individual antibiotic resistance loci. In addition, streptomycin resistant transformants were examined for erythromycin resistance by replica plating, and these mutations also were separable.

CONCLUSIONS

The interpretation that UV induces mutations in *B. subtilis* 1G23 by an error-prone recombinational process that can extend over several cistrons is supported by the three kinds of observations reported above.

1. All but one of 136 UV-induced mutants were multiply mutated, in two or more cistrons.
2. Mutational patterns in multiple mutants invariably agreed with predictions of a double crossover event.
3. Transformation tests showed that the mutations were separable, and had occurred at each of the individual antibiotic loci.

REFERENCE

1. Kubitschek, H. E. ANL-8070 (1973), p. 198.

TESTS FOR DEOXYRIBONUCLEIC ACID SYNTHESIS IN TOLUENIZED BACILLUS SUBTILIS CELLS*

Tatsuo Matsushita and Noboru Sueoka†

Several tests were devised to further characterize deoxyribonucleic acid (DNA) synthesis in toluenized *Bacillus subtilis* cells. Vigorous agitation of toluenized cells (localization test) demonstrated that the DNA replication is exclusively a cell-associated process. A DNA "repair" condition was also applied to toluenized cells and shown to be distinct from DNA replication in its DNA polymerase I dependency and its ability to synthesize DNA on a template which is either cell associated or free, outside the cell. This repair condition was used in conjunction with the localization test to demonstrate the penetration of deoxyribonuclease I and possibly DNA polymerase I into toluenized cells. Therefore, we suggest that the localization test can be used to test the penetration of proteins into toluenized cells for both the DNA repair and replication processes.

---

*Abstract of a paper published in the Journal of Bacteriology 118, 974 (1974).

†University of Colorado, Boulder.

DNA POLYMERASE II-DEPENDENT DNA SYNTHESIS IN TOLUENIZED BACILLUS SUBTILIS CELLS*

Tatsuo Matsushita

Toluenized cells have been used to study semi-conservative DNA replication in both *E. coli* and *B. subtilis*. In *B. subtilis*, this ATP-dependent process represents only elongation of preexisting replication forks. There is no chromosome initiation or background repair under these conditions. However DNA repair can be induced in toluenized *B. subtilis* by introducing exogenous DNase I to nick the chromosome while simultaneously inhibiting DNA replication with sulfyhydryl group reagents such as *p*-chloromercuribenzoic acid (PCMB). Under this "repair condition," the *polA*$^+$ strain 168TT shows DNA repair in both the presence and absence of ATP but *polA*$^-$ mutant strains NB841 and HA101(59)F show no DNA synthesis. This suggests a *polA* repair function in *B. subtilis* analogous to *E. coli*.

Attempts to duplicate this repair synthesis assay by substituting 6-(p-hydroxyphenylazo)-uracil (HPUra), a known replication inhibitor for PCMB, unexpectedly revealed residual ATP-stimulated DNA synthesis in the NB841 *polA*$^-$ mutant. Since 770 μM HPUra completely inhibits ATP-stimulated DNA synthesis (replication) in the absence of DNase I, this residual DNA synthesis could not be due to incomplete inhibition of DNA replication. We conclude that this HPUra-resistant, DNase I-stimulated activity in toluenized *polA*$^-$ cells is exclusively due to DNA polymerase II activity since HPUra is known to inhibit DNA replication in toluenized *B. subtilis* cells and inhibits only DNA polymerase III *in vitro*. Thus, in the absence of polymerase I and by inhibiting polymerase III with HPUra, polymerase II-mediated DNA synthesis can be demonstrated in toluenized *B. subtilis polA*$^-$ cells. This polymerase II synthesis occurs when exogenous DNase and ATP are added. It appears as if the polymerase II-mediated repair in toluenized *B. subtilis* is similar to the UV-stimulated polymerase II-mediated repair demonstrated by Masker and Hanawalt in toluenized *E. coli* which is also ATP-dependent and which they suggest is responsible for "long patch" repair.

Preliminary studies in a *B. subtilis* mutant GSY 1006 (*his*-25, *trp*-16, *recA*) show a much higher toluenized cell DNA repair in the presence of HPUra and exogenous DNase I, correlating with the "reckless" phenotype of this mutant. The DNA repair in this case is probably mediated by both polymerase I and II since this strain is *polA*$^+$. Under these conditions there appears to be little difference in the amount of DNA repair in the presence or absence of ATP in this mutant. Studies are now in progress to determine the mechanism behind this unusual behavior of DNA repair in toluenized *recA* cells.

---

*Abstract of a paper to be published in Molecular Mechanisms for Repair of DNA, Plenum Publishing Corporation, New York.

THE PERMANENT LOSS OF CHROMOSOME INITIATION IN TOLUENIZED B. SUBTILIS CELLS*

Scott Winston† *and Tatsuo Matsushita*

Initiation of DNA replication is absent in *B. subtilis* cells permeabilized by toluene. A permeabilized-washed system was developed in *B. subtilis* which maintained the characteristics of the toluenized cell system in the absence of toluene. This system was used to see if initiation would recover in toluenized cells after removal of toluene. The lack of initiation in the permeabilized-washed cells indicated a permanent loss of initiation in cells treated with toluene. Protein synthesis was also inhibited permanently by toluene treatment indicating damage to translation as a possible mechanism for loss of initiation in toluenized cells.

---

*Abstract of a paper submitted to Journal of Molecular Biology.

†Spring 1974 participant in the Undergraduate Honors Research Participation Program, University of Rhode Island, Kingston.

THE ROLE OF PolA 5'-3' EXONUCLEASE ACTIVITY IN E. COLI CHROMOSOMAL REPLICATION

*Tatsuo Matsushita, George H. Yoakum, and David W. Rooney**

The enzyme *E. coli* DNA polymerase I, or the "Kornberg Enzyme," is a product of the *polA* gene and contains several enzymatic activities, the most widely studied being the DNA polymerization reaction. We have been concerned with what was once considered a less important activity, the 5'-3' exonuclease (exonuclease II), and report that we have biochemical evidence that suggests this activity is an extremely important DNA replication enzyme. Our biochemical evidence consists of the simple *in vitro* observation that tryptophan photoproduct(s) (TP) inhibits *polA* exonuclease II activity with absolutely no inhibition of *polA* polymerizing activity. This observation is significant because of the known biological activity of TP on DNA replication. This compound(s) is selectively lethal for *rec* mutants and completely inhibits DNA replication in not only *recA* but also in *polA*. The TP effect on DNA replication was shown to be involved in gap closure between small DNA replication intermediates (Okazaki pieces), since TP inhibited the conversion of Okazaki pieces into large molecular weight DNA. This TP effect on gap closure *in vivo* could be explained as (1) inhibiting DNA polymerization to close the gaps, or (2) inhibiting exonucleolytic removal of the RNA primer from the Okazaki DNA piece. Our *in vitro* data with purified *E. coli* DNA polymerase I show no effect of TP on polymerizing activity and effectively eliminate this activity as the site of action of TP *in vivo*. However, the specific inhibition of exonuclease II by TP *in vitro* is an exciting observation since it not only identifies the probable site of action of TP *in vivo* but provides strong

---

*Faculty Research Participant, Saint Louis University.

biochemical evidence for the involvement of exonuclease II in chromosome replication. Furthermore, the inhibition suggests the exonuclease is involved in gap closure between Okazaki pieces and perhaps participates by removing the RNA primer from the Okazaki piece. Therefore TP is a novel biochemical tool for studying the RNA primer role in DNA replication, a subject of great current interest in the DNA replication field.

A STUDY OF MUTATION RATE IN THE IMMUNOGLOBULIN VARIABLE REGION*

Pattle Pun,† *David Thompson,*‡ *Tatsuo Matsushita, and Bernard N. Jaroslow*

PURPOSE AND METHODS

It is not known whether the germ cells contain only a small number of structural genes that code for antibody specificity or whether the germ line contains a gene for each specific antibody. If antibody diversity in the variable (V) region of the immunoglobulin light chain is generated by mutational or recombinational processes (1), it is possible that there are certain sites in the immunoglobulin structural genes that mutate with a high frequency and thus are comparable to the hot spots observed in the bacteriophage chromosome (2). We are testing this possibility by comparing rates of mutation in the variable (V) and constant (C) regions of immunoglobulin produced by somatic cells after exposure to mutagens.

To compare mutation rates in V and C regions of an immunoglobulin we must have antibody produced by a single clone of cells. An excellent model system is the homogeneous population of light chain (the "Bence-Jones" protein) excreted by Balb/c mice carrying the transplantable myeloma line MOPC-41. Mice with this myeloma excrete free type *K* Bence-Jones protein in urine.

Our experimental plan to induce mutation and determine whether it occurs at the V or C region will proceed as follows:

1) Mutagenesis. Mutagens will be added to mass cultures of MOPC-41 myeloma cells.

2) Preparation of monospecific antisera. Antisera to the original MOPC-41 Bence-Jones protein will be absorbed with appropriate myeloma proteins which share antigens with MOPC-41 to give a variety of monospecific antisera to the detectable antigens in the V and C regions.

3) Replica-plating and selection of mutants. Using the principle of the Lederberg replica-plating technique (3), we will grow the clones of mutagen-

---

*Work partially supported by Research Corporation, Minneapolis, Minnesota.

†Visiting Research Associate, Wheaton College.

‡Visiting Student Associate, Wheaton College.

treated cells in replicate agar overlay plates (4) and an appropriate anti-serum will be added to each. A precipitate will form around the clone that produces the original antigen, whereas none will appear around the mutated clone. The replicates, using different classes of specific antisera, will characterize each clone and will identify the location of any mutation.

4) Verification of mutations. The clone will be grown and injected into mice to produce tumors which in turn produce large amounts of Bence-Jones protein for more detailed investigation and verification of the mutation.

PROGRESS REPORT

Progress has been made in obtaining specific antisera to the V and C regions. The MOPC-41 Bence-Jones protein (BJP) has been purified using DEAE-sephadex chromatography. We have identified the purified BJP as MOPC-41 specific using the Ouchterlony test and have determined the purity as greater than 90% by SDS-polyacrylamide gel electrophoresis. We have also obtained specific rabbit antiserum to the V and C regions using purified MOPC-41 BJP or commercial BJP. After immunizing with MOPC-41, mouse specific antibodies are removed by strain RPC-20 *lambda* light chain absorption. A further absorption with MOPC-321 *kappa* light chain removes anti-C and a specific anti-V (for MOPC-41) antiserum results.

Anti-C (for MOPC-41) has been similarly obtained by immunizing with MOPC-321 *kappa* and removing mouse-specific determinants with RPC-20 *lambda*. Since MOPC-321 *kappa* has the same C-region as MOPC-41 (also a *kappa* C) but a different V-region, the antiserum will be specific for only the C-region when MOPC-41 BJP is used as antigen. We have also developed the technique for hydrolyzing MOPC-41 BJP into the V and C regions and have used these fragments to demonstrate the specificity of our absorbed rabbit antisera.

We have made progress in developing a replica-plating technique for selecting V and C-region mutations. Since MOPC-41 has proven difficult to culture, we have achieved only partial success in serial passage with three passages accomplished. We have developed the agar overlay technique so that we can now detect primary cultures of MOPC-41 cells with the absorbed rabbit antiserum. The primary cultures secrete enought BJP so that a precipitin line is easily detected by our technique.

To summarize progress in the preparation of monospecific antisera against all the V and C-region determinants, we have established the basic methodology. We have obtained anti-V and anti-C antisera containing antibody against MOPC-41 determinants and absorbed with mouse antigens. We will repeat this procedure and obtain anti-V and C-region antisera from other mouse myeloma strains, and continue cross-absorptions of all the antisera with other BJP's. Because of our progress in this area, we can now start accumulating the necessary number of monospecific antisera needed for mutant selection.

In the replica-plating of the mutagenized cells and selection of mutants, we have made significant progress in culturing the cells and in developing the overlay technique of selection. Although the culturing techniques will need further refinement in order to establish successfully and to subculture clones, we have basically accomplished the groundwork for the mutant selection

system. The technique for making replicas for clones is the remaining major technique (in this area) to be developed.

CONCLUSION

In addition to yielding information on the genetic mechanism of antibody formation, this system should prove invaluable as a convenient eukaryotic mutagen testing system. Mutagenicity has generally been determined in bacteria, whereas carcinogenicity has been tested directly in animal tumor systems. Although ultimate carcinogens are found to be mutagenic, there has been a lack of correlation between mutagen and carcinogens, arising from the need for some compounds to be "metabolized" to the ultimate carcinogenic compound by animal enzymes absent in bacteria. Our myeloma system will allow correlation between mutagens and carcinogens and should be useful for identifying both. The potential effects of these compounds on the generation of antibody diversity can also be studied and may reveal some interesting relationships between neoplasia and antibody formation.

REFERENCES

1. Cold Spring Harbor Symp. Quant. Biol. Volume 32, 1967.
2. Benzer, S. Proc. Nat. Acad. Sci. U. S. A. 47, 403 (1961).
3. Lederberg, J., and E. M. Lederberg. J. Bacteriol. 63, 399 (1952).
4. Coffino, P., and M. D. Scharff. Proc. Nat. Acad. Sci. U. S. A. 68, 219 (1971).

12. LABORATORY ANIMAL FACILITIES

SUMMARY

Robert J. Flynn, Assistant Director for Animal Facilities

The objective of the Animal Facilities group is to provide sufficient and appropriate animals and animal management so that the Division's research programs have the greatest chance of successful conclusion. Animal facilities personnel also provide specialized professional support (pathology, microbiology, radiography, surgery) to other groups within the Division. This support can be identified in reports found elsewhere in this publication.

LABORATORY ANIMAL FACILITIES STAFF

REGULAR STAFF

Brennan, Patricia C. (Biologist)
Fritz, Thomas E. (Veterinary Pathologist)
Flynn, Robert J. (Senior Veterinarian)
Keenan, William G. (Scientific Assistant)
Poole, Calvin M. (Veterinarian)
Simkins, Richard C. (Scientific Assistant)
Tolle, David V. (Scientific Assistant)

THE SUPPLY AND MAINTENANCE OF DEFINED ANIMALS

I. STATUS OF THE COLONY

Robert J. Flynn, Calvin M. Poole, Patricia C. Brennan, and Thomas E. Fritz

The June 30, 1974 animal inventory, including the number and kinds of animals produced or acquired and maintained in the Division's animal facilities during the past fiscal year, is presented in Table 12.1.

The studies involving these animals during this period may be identified by referring to other parts of this report. Animals produced within the Division's facilities are usually designated with the suffix "Anl" (for Argonne National Laboratory).

Table 12.1. Animal Inventory, Animals Acquired, and Animals Produced, Fiscal Year 1974

Common Name	Scientific Name	Inventory as of June 30, 1974	Total Acquired July 1, 1973 to June 20, 1974	Total Produced at Argonne July 1, 1973 to June 30, 1974
Mouse	*Mus musculus*			
SPF		38,401	100	36,108
Conventional		3,270	4,116	6,215
Wild		325	0	200
Whitefooted Mouse	*Peromyscus leucopus*	1,296	4	534
Brush mouse	*Peromyscus boylei*	1	0	0
California mouse	*Peromyscus californicus californicus*	22	0	0
California mouse	*Peromyscus californicus insignis*	229	0	60
Canyon mouse	*Peromyscus crinitus*	3	0	0
Cactus mouse	*Peromyscus eremicus*	4	0	0
Florida mouse	*Peromyscus floridanus*	19	0	0
Cotton mouse	*Peromyscus gossypinus*	57	0	15
Northern pygmy mouse	*Baiomys taylori*	21	0	15
Palestine spiny mouse	*Acomys cahirinus*	8	8	0
Rat	*Rattus norvegicus*	647	2,076	0
Black rat	*Rattus rattus*	18	0	3
Multimammate mouse	*Praomys natalensis*	89	0	69
Rice Rat	*Oryzomys palustris*	2	0	0
Cotton rat	*Sigmodon hispidus*	10	10	0
Golden hamster	*Mesocricetus auratus*	2	2	0
Chinchilla	*Chinchilla laniger*	5	0	0
Rabbit	*Oryctolagus cuniculus*	16	12	0
Dog (beagle)	*Canis familiaris*	591	0	254

II. THE DEVELOPMENT OF INBRED CATALASE MUTANT MICE

Calvin M. Poole, Robert N. Feinstein, and Robert J. Flynn

The program to introduce the acatalasemic locus (Cs^b) and the hypocatalasemic locus (Cs^c) into the C3Hf/An1 and C57BL/6 An1 inbred strains of mice was continued.

Development of these inbred mutant strains involves initial crosses between the mutants and the selected inbred strains with subsequent backcrosses between mutant carriers and stocks from the appropriate inbred strains. Mutant carriers are determined by tests of the blood catalase levels. Whenever possible only mutant carriers from large litters (eight or more animals weaned) with the physical appearance of the inbred strains are used for further breeding. Eight generations of backcrosses and eight subsequent sibling matings between mutant homozygotes are required to produce an inbred mutant that is genetically comparable to the catalase-normal inbred strain.

Eight backcross generations and in excess of eight sibling-mated generations in the C3Hf/An1-Cs^b program have been completed and the development of this strain is now completed. The fourth sibling-mated generation has been reached in the C57BL/6 An1-Cs^b program and the fifth sibling-mated generation in the C3Hf/An1-Cs^c and C57BL/6 An1-Cs^c programs. Ten to fifteen breeding pairs of each mutant inbred line are being maintained.

Several studies involving these special strains of mice are planned. One requires substantial numbers of C3Hf/An1-Cs^b mice and their catalase-normal counterparts, C3Hf/An1 mice. It also requires comparable numbers of each strain with and without the mammary tumor milk factor. Since cesarean-derived C3Hf mice are free of the mammary tumor agent it was necessary to develop a program to reinfect them. Naturally infected C3H/He females were obtained and milk from them was given by intraperitoneal inoculation to a few cesarean-derived C3Hf/An1-Cs^b and C3Hf/An1 females. They were then mated to sibling males. At subsequent lactations milk from these inoculated females was tested for the presence of the mammary tumor factor.* Offspring from females positive for the factor were set up in sibling matings. After several months work, we can now report that we have significant numbers of all four strains in production and the planned experiment will soon be initiated.

---

*Testing performed by Dr. Dan H. Moore, Institute for Medical Research, Camden, New Jersey.

THIS PAGE

WAS INTENTIONALLY

LEFT BLANK

13. EDUCATIONAL ACTIVITIES

POSTGRADUATE TRAINING

During 1974, a total of 32 postdoctoral appointees, visiting scientists, and research associates contributed to the research programs of the Division. Nine of these were new appointments in 1974, three less than the number who finished their assignments during the year.

The temporary appointees, their schools, and the staff members with whom they were affiliated are as follows:

Enrique E. Abola	University of Pittsburgh	A. B. Edmundson
Gregory A. Antipa	University of Illinois, Urbana	C. F. Ehret
William F. Bryant	Iowa State University	P. D. Klein
Jerome C. Cater*	University of Glasgow	B. N. Jaroslow
Kenneth W. Dobra	Indiana University, Bloomington	C. F. Ehret
Fouad S. Ezra	University of Rochester	S. S. Danyluk
Daniel Fiat†	Weizman Institute of Science	S. S. Danyluk
Joseph R. Firca	University of Cincinnati	A. B. Edmundson
Rowland L. Girling	University of South Carolina	A. B. Edmundson
Raymond A. Guilmette*	New York University	A. Lindenbaum
David L. Hachey‡	University of California, Santa Barbara	P. D. Klein
Antun Han†	Laboratory for Experimental Cancerology (Yugoslavia)	W. K. Sinclair/ M. M. Elkind
Ray R. Hinchman	University of Chicago	J. Shen-Miller
Margaret M. Jonah	Columbia University	Y. E. Rahman
Bruce F. Kimler	University of Texas	W. K. Sinclair/ M. M. Elkind
Arthur L. Koch†	Indiana University, Bloomington	J. F. Thomson/ H. E. Kubitschek
Frank Krasin	Pennsylvania State University	R. E. Krisch
Chung K. Lee	University of Illinois, Urbana	M. P. Finkel
Ronald D. Ley‡	Oregon State University	R. E. Krisch

*Research Associate

†Visiting Scientist

‡Now Assistant Scientist

Ronald G. Lindahl	Wayne State University	R. N. Feinstein
Rand E. McNitt	University of North Carolina	J. Shen-Miller
J. Emory Morris*	State University College of New York, Brockport	C. Peraino
D. Stuart Nachtwey†	University of Oregon	J. F. Thomson/ E. J. Ainsworth
Kenji D. Nakamura	Oregon State University	F. Schlenk
Nicolas C. Panagiotopoulos	University of Pittsburgh	A. B. Edmundson
John E. Parks	University of Wisconsin, Madison	A. Lindenbaum
Frank T. Robb	University of California, Riverside	H. E. Kubitschek
Dale A. Schoeller	Indiana University, Bloomington	P. D. Klein
John P. Stone	Wayne State University	W. P. Norris
Francis A. Williamson‡	Purdue University	J. Shen-Miller
Vivian V. Yang	University of Chicago	S. P. Stearner
George H. Yoakum	University of Missouri, Columbia	T. Matsushita

In addition, there were 12 Faculty Research Participation appointments, supported by the Argonne Center for Education Affairs (CEA); these appointments enable college and university faculty members to participate in the research activities of the Laboratory in order to broaden their perspectives for teaching and research on their home campuses. The names of the Faculty Research Participants during 1974, their schools, and their staff sponsors were as follows:

Ronald J. Doyle	University of Louisville	H. E. Kubitschek
William M. Elliott	Hartwick College, New York	J. Shen-Miller
Owen H. Hilding	University of Illinois Medical Center	G. Svihla
Norman S. Kondo	Federal City College, Washington, D. C.	S. S. Danyluk
Eugene W. McArdle	Northeastern Illinois University	C. F. Ehret
William F. Millington	Marquette University	J. Shen-Miller
J. Emory Morris*	State University College of New York, Brockport	C. Peraino
Daniel G. Oldfield	DePaul University	R. J. M. Fry
Ronald M. Rogowski	Northwestern University	P. D. Klein
David W. Rooney	St. Louis University	T. Matsushita
John F. Schneider	University of Chicago	P. D. Klein
Thomas A. Victor	Northwestern University	S. S. Danyluk

*Visiting Scientist, and also Faculty Research Participant

†Visiting Scientist

‡Research Associate

SUMMER GRADUATE STUDENT PROGRAM IN BIOLOGY

Seventeen students from 12 different universities were enrolled in the 1974 program. Dr. D. Stuart Nachtwey of Oregon State University served as coordinator of the course, in cooperation with Dr. E. John Ainsworth. The program, which ran for 12 weeks, consisted of 15 "core" lectures in radiation biology by Dr. Nachtwey, followed by a specialized series of lectures given by Drs. R. J. Michael Fry, W. E. Kisieleski, and Christopher A. Reilly, Jr. Each student spent the remainder of his time working in a laboratory of a staff member. Most of the students received academic credit for the course from their home institutions.

The students, their schools, and their staff supervisors were as follows:

Elaine H. Callahan	Monmouth College	Y. E. Rahman
Ronald J. Douglas	St. Louis University	G. A. Sacher
Kenneth G. Draper	Northern Illinois University	P. C. Brennan
James I. Fast	Northern Illinois University	M. P. Finkel
Norma L. Foltz	University of Illinois, Urbana	C. F. Ehret
Michael W. Garner	University of Illinois, Urbana	W. P. Norris
Michael P. Hagan	University of Illinois, Urbana	M. M. Elkind
Patricia M. Irving	University of Wisconsin, Milwaukee	C. Jordan
Michael J. Koziol	Balliol College, England	J. Shen-Miller
Ping-Kwong Lai	University of Illinois, Urbana	R. J. M. Fry
Michael D. Lips	Illinois Institute of Technology	C. F. Ehret
Warren D. Lo	Northwestern University Medical School	B. N. Jaroslow
Ronald McNight	University of Maryland	T. Matsushita
David N. Paddock	Illinois State University	R. Devine
Gregory J. Schweger	San Diego State University	Y. E. Rahman/ J. F. Thomson
Suad S. Wanna	University of Illinois, Urbana	R. B. Webb
Jack C. Wiaz	University of Illinois Chicago Circle	T. E. Fritz

OTHER GRADUATE PROGRAMS

Five graduate students were Laboratory Graduate Participants working in the Division on research for their PhD degrees in a program administered by the Center for Educational Affairs. The Laboratory Graduate Participants and their staff sponsors were as follows:

Howard W. Braham	Ohio State University	G. A. Sacher
John P. Christopher	Oregon State University	C. Peraino
Alfred G. Garcia	Northern Illinois University	R. J. M. Fry
Roy M. Vigneulle	University of Illinois, Urbana	E. J. Ainsworth
George H. Yoakum*	University of Missouri	R. B. Webb

A related program, called Thesis Parts, allows graduate students to perform pertinent parts of their research at Argonne. In 1974, seven students held such appointments in the Division:

Allan R. Britt	San Diego State University	W. E. Kisieleski
James I. Fast†	Northern Illinois University	M. P. Finkel
Andrew J. Fischinger	University of Illinois, Medical Center	S. S. Danyluk
Kenneth R. Groh	University of Chicago	R. J. M. Fry
Patricia M. Irving†	University of Wisconsin, Milwaukee	J. Shen-Miller
Terry F. Werner	St. Louis University	E. J. Ainsworth
Charles J. Zeller	Northern Illinois University	R. J. M. Fry

In addition, Michael J. Belluzzi, Northeastern Illinois University, held a Guest Graduate Student appointment under the supervision of Dr. C. F. Ehret.

UNDERGRADUATE TRAINING

During 1974, a total of 19 college undergraduates received training in the Division of Biological and Medical Research through the CEA-sponsored Spring, Summer, and Fall Honors Research Participation Programs. The students, their schools, and their staff supervisors are listed below:

SPRING PROGRAM

Diane Hunt	College of St. Francis, Joliet	J. Shen-Miller
Rosanne K. Fidelus	College of St. Francis, Joliet	B. N. Jaroslow
William D. Mawby	Defiance College	Y. E. Rahman
Douglas H. Moffat	D'Youville College	J. Shen-Miller
Helen G. Muhlbauer	Barnard College	Y. E. Rahman
Scott E. Winston	University of Rhode Island	T. Matsushita

*Also Postdoctoral Appointee.

†Also participant in the Summer Graduate Student Program in Biology.

SUMMER PROGRAM

Joe L. Allen	Southern University	R. J. M. Fry
Linda G. Daniel	Clark College	P. C. Brennan
Yvonne D. Leonard	Oakwood College	J. Shen-Miller
Jose V. Pardo	University of Miami	A. B. Edmundson
Catherine Whiteside	Benedict College	S. A. Tyler

FALL PROGRAM

Yvonne M. Arcus	Knox College	B. N. Jaroslow
Barbara E. Carr	Ohio State University	J. Shen-Miller
Nancy G. Doan	St. Olaf College	A. Lindenbaum
Andrea J. Dungy	Voorhees College	E. J. Ainsworth
Kathryn D. Held	Thiel College	M. M. Elkind
Paul G. Kremser	Carleton College	A. B. Edmundson
Jacquelynne L. Perou	Carleton College	R. B. Webb
Martha L. White	Indiana State University, Terre Haute	P. C. Brennan

ANL YOUTH PUBLIC EMPLOYMENT PROGRAM

Five high school students from the Chicago metropolitan area participated in this program, which is supported by the U. S. Department of Labor. The students and their supervisors were:

Jeannette Crowder	R. B. Webb
Roberto Mojica	M. P. Finkel
Ostuard Rodas	M. P. Finkel
Eleanor Stegall	P. H. Duffy
Beverly Woods	M. S. Brown

JOINT ARGONNE-UNIVERSITY APPOINTMENTS

During 1974, 19 staff members held a total of 31 faculty appointments at universities in the Chicago area. These appointments comprise limited teaching activities, generally of a specialized nature, at the graduate level, which involve regular contact with students. They have led to cosponsorship of graduate students and to collaborative research efforts with faculty members, some of which are described in this report.

The affiliations were as follows:

University of Chicago

Mortimer M. Elkind	George A. Sacher
Robert N. Feinstein	Fritz Schlenk
R. J. Michael Fry	Warren K. Sinclair
Peter D. Klein	

University of Illinois at Chicago Circle

Douglas Grahn
Bernard N. Jaroslow
Herbert E. Kubitschek
Carl Peraino
Fritz Schlenk
Warren K. Sinclair
John F. Thomson

Loyola University

Thomas E. Fritz
Bernard N. Jaroslow
Walter E. Kisieleski
Arthur Lindenbaum
Marcia W. Rosenthal
George A. Sacher

Northern Illinois University

R. J. Michael Fry
Douglas Grahn
Karl D. Hardman
Bernard N. Jaroslow
Herbert E. Kubitschek
Carl Peraino
Y. E. Rahman
Fritz Schlenk
Warren K. Sinclair
John F. Thomson
Robert B. Webb

NINTH ANNUAL AUA-ANL BIOLOGY SYMPOSIUM

The 1974 Symposium, "Mechanisms of Oncogenesis," was held at Argonne National Laboratory on November 11-13, under the joint sponsorship of the Division of Biological and Medical Research, the Division of Radiological and Environmental Research, and the Center for Educational Affairs. Drs. R. J. Michael Fry and John H. Marshall were co-chairmen.

The program of the symposium, held in memory of Dr. Solon A. Gordon, was designed to introduce first- and second-year graduate students to the problems of carcinogenesis. Eighteen presentations covered the nature of cancer; aspects of chemical, viral, and radiation induction of cancer; molecular lesions and host factors related to tumorigenesis; and the genetics of cancer at the level of man, the chromosome, and the gene locus.

The symposium was directed toward graduate students, primarily but not exclusively from member institutions of the Argonne Universities Association. Over 360 students and faculty members attended and participated in discussions.

14. PUBLICATIONS

JOURNAL ARTICLES

Ben-Hur, E., and M. M. Elkind. Thermal sensitization of Chinese hamster cells to methyl methanesulfonate: Relation of DNA damage and repair to survival response. Cancer Biochem. Biophys. 1, 23-32 (1974).

Cairnie, A. B., D. Grahn, H. B. Rayburn, F. S. Williamson, and R. J. Brown. Teratogenic and embryolethal effects in mice of fission-spectrum neutrons and γ-rays. Teratology 10, 133-140 (1974).

Colman, P. M., O. Epp, H. Fehlhammer, W. Bode, M. Schiffer, E. E. Lattman, T. A. Jones, and W. Palm. X-ray studies on antibody fragments. FEBS Lett. 44, 194-199 (1974).

Davies, D. B., and S. S. Danyluk. Nuclear magnetic resonance studies of 5'-ribo- and deoxyribonucleotide structures in solution. Biochemistry 13, 4417-4434 (1974).

Edmundson, A. B., K. R. Ely, R. L. Girling, E. E. Abola, M. Schiffer, F. A. Westholm, M. D. Fausch, and H. F. Deutsch. Binding of 2,4-dinitrophenyl compounds and other small molecules to a crystalline λ-type Bence-Jones dimer. Biochemistry 13, 3816-3827 (1974).

Epp, O., P. Colman, H. Fehlhammer, W. Bode, M. Schiffer, R. Huber, and W. Palm. Crystal and molecular structure of a dimer composed of the variable portion of the Bence-Jones protein REI. Eur. J. Biochem. 45, 513-524 (1974).

Everett, M. Dose-response curves for radish seedling phototropism. Plant Physiol. 54, 222-225 (1974).

Frigerio, N. A. Poisson and non-poisson behavior of radioactive systems. Nucl. Instrum. Methods 114, 175-177 (1974).

Frigerio, N. A., and R. S. Stowe. Computer production of randomized examinations. J. Med. Ed. 49, 286-288 (1974).

Gawlik, S. R., and J. Shen-Miller. Effects of indoleacetic acid on dictyosomes of apical and expanding cells of oat coleoptiles. Plant Physiol. 54, 217-221 (1974).

Gordon, S. A., and E. M. Buess. Correlative inhibition of root emergence in the gamma-irradiated coleus leaf--III. Effects of auxin on the radiation-induced changes in RNA, RNA metabolism, and rooting. Radiat. Bot. 13, 283-286 (1973).

Gordon, S. A., P. Kremer, and S. Venketeswaran. Growth and cytological responses to white and far-red light of *Haplopappus* cells in suspension culture. Radiat. Bot. 14, 17-22 (1974).

Hachey, D. L., P. A. Szczepanik, O. W. Berngruber, and P. D. Klein. Syntheses with stable isotopes: Synthesis of deuterium and ^{13}C labeled bile acids. J. Labelled Compd. 9, 703-719 (1974).

Hepner, G. W., A. F. Hofmann, J. R. Malagelada, P. A. Szczepanik, and P. D. Klein. Increased bacterial degradation of bile acids in cholecystectomized patients. Gastroenterology 66, 556-564 (1974).

Hinchman, R. R., and S. A. Gordon. Amyloplast size and number in gravity-compensated oat seedlings. Plant Physiol. 53, 398-401 (1974).

Jaroslow, B. N., K. M. Suhrbier, and T. E. Fritz. Decline and restoration of antibody-forming capacity in aging beagle dogs. J. Immunol. 112, 1467-1476 (1974).

Klein, P. D. Clinical applications of stable isotopes at Argonne National Laboratory. Chicago Medicine 77, 127-130 (1974).

Klein, P. D. Applications of stable isotopes to drug research: Present status and future prospects. Pure Chemicals "Daiichi" 5, 59-69 (1974).

Krisch, R. E. Lethal and genetic effects of radiophosphorus decay in bacteriophages SP82G and T7. Int. J. Radiat. Biol. 25, 261-276 (1974).

Krisch, R. E., and R. D. Ley. Induction of lethality and DNA breakage by the decay of iodine-125 in bacteriophage T4. Int. J. Radiat. Biol. 25, 21-30 (1974).

Kubitschek, H. E. Constancy of the ratio of DNA to cell volume in steady-state cultures of *Escherichia coli* B/r. Biophys. J. 14, 119-123 (1974).

Kubitschek, H. E. Replication and repair of UV-induced mutational lesions in chemostat cultures of *Escherichia coli* WP2 Hcr. Mutat. Res. 23, 297-309 (1974).

Kubitschek, H. E. Estimation of the *D* period from residual division after exposure of exponential phase bacteria to chloramphenicol. Mol. Gen. Genet. 135, 123-130 (1974).

Ley, R. D., and R. E. Krisch. Lethality and DNA breakage from ^{32}P and ^{33}P decay in bacteriophage T4. Int. J. Radiat. Biol. 25, 531-537 (1974).

McDowell, R. E., D. Feir, and R. E. Ecker. RNA synthesis during the development of the bug, *Oncopeltus faciatus*. Insect Biochem. 4, 295-301 (1974).

Menon, M., B. N. Jaroslow, and R. Koesterer. The decline of cell-mediated immunity in aging mice. J. Gerontol. 29, 499-505 (1974).

Morris, J. E., C. Peraino, and D. Strayer. Molecular weight of rat liver ornithine-ketoacid aminotransferase. Proc. Soc. Exp. Biol. Med. 147, 706-709 (1974).

Mushlin, P. S., and C. Peraino. Effects of dietary phenobarbital on the binding of 2-acetylaminofluorene to rat liver nuclear DNA. Proc. Soc. Exp. Biol. Med. 145, 859-862 (1974).

Nakamura, K. D., and F. Schlenk. Examination of isolated yeast cell vacuoles for active transport. J. Bacteriol. 118, 314-316 (1974).

Nakamura, K. D., and F. Schlenk. Active transport of exogenous *S*-adenosylmethionine and related compounds into cells and vacuoles of *Saccharomyces cerevisiae*. J. Bacteriol. 120, 482-487 (1974).

Pritchard, D. J., C. A. Reilly, Jr., M. P. Finkel, and J. C. Ivins. Cytotoxicity of human osteosarcoma sera to hamster sarcoma cells. Cancer 34, 1935-1939 (1974).

Rahman, Y. E., E. A. Cerny, S. L. Tollaksen, B. J. Wright, S. L. Nance, and J. F. Thomson. Liposome-encapsulated actinomycin D: Potential in cancer chemotherapy. Proc. Soc. Exp. Biol. Med. 146, 1173-1176 (1974).

Rahman, Y. E., M. W. Rosenthal, E. A. Cerny, and E. S. Moretti. Preparation and prolonged tissue retention of liposome-encapsulated chelating agents. J. Lab. Clin. Med. 83, 640-647 (1974).

Rowe, D. W., E. B. McGoodwin, G. K. Martin, M. D. Sussman, D. Grahn, B. Faris, and C. Franzblau. A sex-linked defect in the cross-linking of collagen and elastin associated with the mottled locus in mice. J. Exp. Med. 139, 180-192 (1974).

Sacher, G. A. Biomedical gerontology. Gerontologist 14, 268-270 (1974).

Sacher, G. A., and E. F. Staffeldt. Relation of gestation time to brain weight for placental mammals: Implications for the theory of vertebrate growth. Am. Nat. 108, 593-615 (1974).

Shen-Miller, J. Obituary of Dr. Solon Albert Gordon 1916-1973. Radiat. Bot. 14, 65-68 (1974).

Shen-Miller, J., and R. R. Hinchman. Gravity sensing in plants: A critique of the statolith theory. BioScience 24, 643-651 (1974).

Sherwin, J. E., and S. A. Gordon. Linear velocity of cyclic adenosine 3', 5-monophosphate transport in corn coleoptiles. Plant Physiol. 53, 416-418 (1974).

Sherwin, J. E., and S. A. Gordon. The effect of auxin on the incorporation of [^{3}H]thymidine into the DNA of pea epicotyls. Planta 116, 65-72 (1974).

Stearner, S. P., and E. J. B. Christian. Dose protraction and acute radiation mortality in the chicken: A reappraisal of injury accumulation kinetics. Radiat. Res. 57, 121-131 (1974).

Szczepanik, P. A. The mass spectra of some 5'-alkyl substituted 5'-thioadenosine trimethylsilyl derivatives. Org. Mass Spectrom. 9, 631-633 (1974).

Thomson, J. F., S. L. Nance, and S. L. Tollaksen. Density-gradient centrifugation of mouse liver mitochondria with H_2O/D_2O gradients. Arch. Biochem. Biophys. 160, 130-134 (1974).

Thomson, J. F., S. L. Nance, and S. L. Tollaksen. Preparation of peroxisomes from mouse liver by rate-zonal centrifugation. Proc. Soc. Exp. Biol. Med. 145, 1174-1177 (1974).

Tsai, L. B., G. W. Patterson, C. F. Cohen, and P. D. Klein. Metabolism of 2,4-^{3}H-14α-methyl-5α-ergost-8-enol and 2,4-^{3}H-5α-ergosta-8,14,dienol in *Chlorella ellipsoidea*. Lipids 9, 1014-1017 (1974).

Tyrrell, R. M. The interaction of near U.V. (365 nm) and X-radiations on wild-type and repair-deficient strains of *Escherichia coli* K12: Physical and biological measurements. Int. J. Radiat. Biol. 25, 373-390 (1974).

Tyrrell, R. M., R. D. Ley, and R. B. Webb. Induction of single-strand breaks (Alkali-labile bonds) in bacterial and phage DNA by near UV (365 nm) radiation. Photochem. Photobiol. 20, 395-398 (1974).

Yoakum, G. H., W. Ferron, A. Eisenstark, and R. B. Webb. Inhibition of replication gap closure in *Escherichia coli* by near-ultraviolet light photoproducts of L-tryptophan. J. Bacteriol. 119, 62-69 (1974).

BOOKS, REPORTS, AND PROCEEDINGS

Ainsworth, E. J., R. J. M. Fry, D. Grahn, F. S. Williamson, P. C. Brennan, S. P. Stearner, A. V. Carrano, and J. H. Rust. Late effects of neutron or gamma irradiation in mice. In: Biological Effects of Neutron Irradiation. International Atomic Energy Agency, Vienna, IAEA-SM-179/1, 1974, pp. 359-379.

Danyluk, S. S., and N. S. Kondo. A selective labeling approach to NMR studies of nucleic acid structures. In: Proceedings of the Fifth International Symposium on Magnetic Resonance, Bombay, India, January 14-18, 1974, p. 14A48.

Edmundson, A. B., K. R. Ely, R. L. Girling, E. E. Abola, M. Schiffer, and F. A. Westholm. Structure and binding properties of a λ-type Bence-Jones dimer. In: Progress in Immunology II, Vol. 1, Eds. L. Brent and J. Holborow. North-Holland Publishing Company, Amsterdam, 1974, pp. 103-113.

Edmundson, A. B., M. Schiffer, K. R. Ely, and M. K. Wood. Structural features of immunoglobulin light chains. Progress in Molecular and Subcellular Biology, Vol. 3, Ed. F. E. Hahn. Springer-Verlag, Berlin, 1973, pp. 159-182.

Ehret, C. F. The sense of time: Evidence for its molecular basis in the eukaryotic gene-action system. In: Advances in Biological and Medical Physics, Vol. 15. Eds. W. Harris and C. Tobias. Academic Press, Inc., New York, 1974, pp. 47-77.

Ehret, C. F., J. H. Barnes, and K. E. Zichal. Circadian parameters of the infradian growth mode in continuous cultures: Nucleic acid syntheses and oxygen induction of the ultradian mode. In: Chronobiology, Eds. L. E. Scheving, F. Halberg, and J. E. Pauly. Igaku Shoin Ltd., Tokyo, 1974, pp. 44-50.

Ehret, C. F., and E. W. McArdle. The structure of *Paramecium* as viewed from its constituent levels of organization. In: *Paramecium*: A Current Survey. Ed. W. J. Van Wagtendonk. Elsevier Scientific Publishing Co. New York, 1974, pp. 263-338.

Elkind, M. M. Repair mechanisms related to DNA integrity (and survival) in mammalian cells. In: Advances in Radiation Research, Biology and Medicine, Vol. 1, Eds. J. F. Duplan and A. Chapiro. Gordon and Breach, London, 1973, pp. 23-38.

Elkind, M. M., and E. Ben-Hur. DNA damage in mammalian cells and its relevance to lethality. In: Proceedings of the Fourth Symposium on Microdosimetry, Verbania-Pallanza (Italy) 24-28. IX. (1973).

Fry, R. J. M., C. L. Weber, W. E. Kisieleski, M. L. Griem, and F. D. Malkinson. Study of cell proliferation of the hair follicle. In: Advances in Radiation Research, Biology and Medicine, Vol. 3, Eds. J. F. Duplan and A. Chapiro. Gordon and Breach, London, 1973, pp. 853-860.

Jaroslow, B. N., and M. M. Miller. Late effects of irradiation on immune responsiveness of aging mice. In: Advances in Radiation Research, Biology and Medicine, Vol. 3, Eds. J. F. Duplan and A. Chapiro. Gordon and Breach, London, 1973, pp. 1381-1393.

Kubitschek, H. E. Operation of selection pressure on microbial populations. In: Evolution in the Microbial World, Symposia of the Society for General Microbiology, No. XXIV. Cambridge University Press, London, 1974, pp. 105-130.

Kubitschek, H. E. Biophysics. In: Britannica Book of the Year, 1974, pp. 419-420.

Noakes, J. E., and W. Kisieleski. Spark combustion of ^{3}H and ^{14}C labeled samples suitable for liquid scintillation counting. In: Liquid Scintillation Counting: Recent Developments, Eds. P. E. Stanley and B. A. Scoggins. Academic Press, Inc., New York, 1974, pp. 125-137.

Sacher, G. A. Dose dependence for life shortening by X-rays, gamma rays and fast neutrons. In: Advances in Radiation Research, Biology and Medicine, Vol. 3, Eds. J. F. Duplan and A. Chapiro. Gordon and Breach, London, 1973, pp. 1425-1432.

Sacher, G. A. Use of zoo animals for research on longevity and aging. In: Research in Zoos and Aquariums, A symposium held at the Forty-ninth Conference of the American Association of Zoological Parks and Aquariums, Houston, Texas, October 6-11, 1973. National Academy of Sciences, Washington, D. C., 1975, pp. 191-198.

Sacher, G. A. Aging. Encyclopaedia Britannica, Vol. 1, Encyclopaedia Britannica, Inc., Chicago, 1974, pp. 299-304.

Sinclair, W. K. Introductory remarks and the role of sulfhydryls in the cell cycle response of mammalian cells to X-rays. In: Advances in Radiation Research, Biology and Medicine, Vol. 2, Eds. J. F. Duplan and A. Chapiro. Gordon and Breach, London, 1973, pp. 861-868.

Sinclair, W. K. Modification of cell cycle response of synchronous mammalian cells to ionizing radiation by inhibition of repair. In: Control of Proliferation in Animal Cells. Cold Spring Harbor Conferences on Cell Proliferation, Vol. 1, Eds. B. Clarkson and R. Baserga. Cold Spring Harbor Laboratory, 1974, pp. 985-994.

ABSTRACTS

Ainsworth, E. J. Effects of single or fractionated doses of neutron or gamma-radiation on hematopoietic stem cells. Radiat. Res. 59, 49 (1974).

Ainsworth, E. J., and R. J. M. Fry. Life shortening effects of fractionated doses of fission neutron or gamma radiation. Radiat. Res. 59, 314-315 (1974).

Archer, J. F., and W. K. Sinclair. Some of the binding sites of the radiosensitizer N-ethylmaleimide in Chinese hamster cells. Radiat. Res. 59, 79 (1974).

Ben-Hur, E., and M. M. Elkind. DNA damage and its repair in hyperthermic mammalian cells: Relation to enhanced cell killing. Radiat. Res. 59, 6-7 (1974).

Brennan, P. C., and E. J. Ainsworth. Radiation effects on host defense mechanisms. Radiat. Res. 59, 252 (1974).

Britt, A. R., and W. E. Kisieleski. The oxidation and combustion of ^{32}P and ^{36}Cl in preparation for Cerenkov liquid scintillation counting. Abstracts of 167th National Meeting of the American Chemical Society, Los Angeles, California, March 31-April 5, 1974, abstract No. 41.

Brockwell, P. J., and R. J. M. Fry. Stochastic models for cell kinetics and the analysis of labelling experiments. Biometrics 29, 837 (1973).

Brown, M. S., and R. B. Webb. Photoreactivation and oxygen dependence after 365 nm ultraviolet irradiation of *Escherichia coli*. Abstracts of 74th Annual Meeting of the American Society for Microbiology, Chicago, Ill., May 12-17, 1974, p. 50.

Christian, E. J. B., and S. P. Stearner. Radiation-effects on circulatory efficiency. Radiat. Res. 59, 135 (1974).

Cowen, A. E., A. F. Hofmann, P. J. Thomas, P. D. Klein, and L. Tökés. An improved preparation of tritium and deuterim labeled bile acids: Synthesis and validation. Gastroenterology 66, 679 (1974).

Finkel, M. P., C. A. Reilly, Jr., B. O. Biskis, and D. J. Pritchard. Tumor induction in Syrian hamsters by extracts of human bone tumors. XIth International Cancer Congress, Abstracts 1, 242-243 (1974).

Fritz, T. E., and W. P. Norris. Pathologic responses of the beagle dog to protracted exposure to ^{60}Co gamma-rays. Radiat. Res. 59, 145 (1974).

Fry, R. J. M., E. J. Ainsworth, E. Staffeldt, A. Sallese, and K. Allen. The effect of radiation on the incidence of pulmonary tumors in $B6CF_1$ mice. Radiat. Res. 59, 222 (1974).

Hachey, D. L., P. A. Szczepanik, J. B. Watkins, A. M. Tercyak, and P. D. Klein. Bile salt alkyl ethers: Evidence for a new class of biliary lipids in human bile. Gastroenterology 67, 795 (1974).

Han, A., W. K. Sinclair, and B. F. Kimler. The sensitization of X-irradiated HeLa cells by N-ethylmaleimide. Radiat. Res. 59, 79 (1974).

Hanson, R. F., J. N. Isenberg, P. D. Klein, G. C. Williams, P. Szczepanik, and H. L. Sharp. Defective metabolism of trihydroxycoprostanic acid (THCA) to cholic acid (CA) in two siblings with a familial liver disease: An apparent deficiency of 24-hydroxylase. Gastroenterology 67, 796 (1974).

Jaroslow, B. N., K. M. Suhrbier, and R. J. M. Fry. Increasing radiosensitivity of ileum crypt cells of ground squirrels during arousal from hibernation. Radiat. Res. 59, 138 (1974).

Jaroslow, B. N., K. M. Suhrbier, R. J. M. Fry, and S. A. Tyler. Immunosuppression by lymphomas in aging mice. Gerontologist 14, 33 (1974).

Jonah, M. M., W. E. Kisieleski, and Y. E. Rahman. Differential tissue uptake of liposomes prepared by varying lipid constituents and incorporated drugs. J. Cell Biol. 63, 158a (1974).

Ley, R. D., R. M. Tyrrell, and R. B. Webb. Induction of single-strand breaks (or alkali-labile bonds) in DNA by 365 nm radiation. Abstracts of 2nd Annual Meeting of American Society for Photobiology, Vancouver, B. C., Canada, July 22-26, 1974, p. 101.

Lindenbaum, A., and M. W. Rosenthal. Separate and combined effects of DTPA and glucan in removal of monomeric and polymeric plutonium from the dog liver. Radiat. Res. 59, 132-133 (1974).

McNitt, R. E., L. Glessner, and J. Shen-Miller. Spectral effects on corn-root geotropism and preferential distribution of organelles. Plant Physiol. Annual Supplement, 46 (June, 1974).

Miller, M., E. M. Cooke, and E. J. Ainsworth. Effects of neutron or gamma dose fractionation on the hematological response of mice. Radiat. Res. 59, 50 (1974).

Nakamura, K. D., F. Schlenk, and H. de Robichon-Szulmajster. Active transport of S-adenosylmethionine from the medium into the vacuole of *Saccharomyces cerevisiae*. Abstracts of The Annual Meeting of the American Society for Microbiology, 1974, p. 154.

Norris, W. P., and T. E. Fritz. Response of the beagle dog to protracted exposure to ^{60}Co gamma-rays. Radiat. Res. 59, 145 (1974).

Peak, M. J., J. G. Peak, and R. B. Webb. Synergism between wavelengths of near-ultraviolet radiation in the inactivation of transforming DNA. Abstracts of 2nd Annual Meeting of American Society for Photobiology, Vancouver, B. C., Canada, July 22-26, 1974, p. 100.

Rahman, Y. E., and J. F. Thomson. Liposome-encapsulation of actinomycin D. Increased effectiveness in treatment of mice bearing Ehrlich ascites tumor. Pharmacologist 16 (2) (1974).

Reilly, C. A., Jr., P. J. Dale, and M. P. Finkel. *In vivo* interference of naturally occurring murine bone tumor viruses. Abstracts of The Annual Meeting of the American Society for Microbiology, 1974, p. 232.

Reilly, C. A., Jr., and M. P. Finkel. Biological relationships of three murine bone tumor viruses. Abstracts of the XIth International Cancer Congress, 1974, Vol. 2, p. 82.

Rosenberg, I. H., L. Palladino, D. Hachey, and P. D. Klein. Synthesis of two forms of deuterium-labeled folic acid for studies of absorption and utilization in man. Gastroenterology 66, 862 (1974).

Rosenthal, M. W., and Y. E. Rahman. Liposome-encapsulated DTPA in plutonium therapy. Radiat. Res. 59, 134 (1974).

Sacher, G. A. An examination of the time parameter that governs the effect of fractionation on life shortening. Radiat. Res. 59, 313 (1974).

Sacher, G. A., M. Gabriel, and S. A. Tyler. Markov chain model for chromosome aberrations and cell lethality. Radiat. Res. 59, 296-297 (1974).

Shen-Miller, J. Spectral sensitivity of corn root geotropism. Proceedings of the 8th International Conference on Plant Growth Substances, Tokyo, Japan, August 1973, p. 147.

Sinclair, W. K. Mammalian cell sensitization, repair and the cell cycle. Radiat. Res. 59, 164-165 (1974).

Spokas, J. J., F. S. Williamson, and G. L. Holmblad. A small ionization chamber for measurement of neutron and photon dose. Radiat. Res. 59, 53-54 (1974).

Stearner, S. P., E. J. B. Christian, and R. L. Devine. Structural changes in the microvasculature in the aging, irradiated mouse. Radiat. Res. 59, 136 (1974).

Stearner, S. P., and R. L. Devine. Fine structural changes in the microvasculature of the mouse pinna: Aging and radiation injury. Proceedings of the 32nd Annual Meeting of the Electron Microscopy Society of America, St. Louis, Mo., August 12-16, 1974. Ed. C. J. Arceneaux. Claitors Publ. Div., Baton Rouge, 1974.

Svihla, G., M. Sanderson, and G. Sacher. Comparative biology of aging, optic and vagus nerves of *Peromyscus leucopus* and *Mus musculus*. Gerontologist 14, 36 (1974).

Tolle, D. V., T. E. Fritz, and W. P. Norris. Myeloproliferative disorder in the beagle--a consequence of continuous low dose exposure to ^{60}Co gamma irradiation. Abstracts of 3rd Annual Meeting of the International Society for Experimental Hematology, Houston, Texas, March 31 - April 3, 1974, p. 32.

Tyler, S. A., W. P. Norris, and G. A. Sacher. Design analysis for a low-level gamma-ray experiment under two alternative dose-effect assumptions. Radiat. Res. 59, 146 (1974).

Tyler, S. A., G. A. Sacher, and E. F. Staffeldt. Genetic variance components for sensitivity of inbred and hybrid mice to chronic gamma-irradiation. Radiat. Res. 59, 130 (1974).

Watkins, J. B., P. Szczepanik, J. B. Gould, P. Klein, and R. Lester. Bile salt metabolism in the premature infant: Influence of prenatal dexamethasone and phenobarbital. Proceedings of Meeting, Pediatric Research (May, 1974).

Watkins, J. B., A. M. Tercyak, P. Szczepanik, and P. D. Klein. Bile salt kinetics in cystic fibrosis (CF): Influence of pancreatic enzyme replacement. Gastroenterology 67, 835 (1974).

Webb, R. B. Genetic effects of near-ultraviolet radiation (NUV). Abstracts of 2nd Annual Meeting of American Society for Photobiology, Vancouver, B. C., Canada, July 22-26, 1974, pp. 46-47.

Webb, R. B., and M. S. Brown. Biological consequences of pyrimidine dimers and single-strand breaks induced in bacterial DNA by 365 nm UV. Radiat. Res. 59, 235-236 (1974).

Wright, B. J., and G. Svihla. Liposome-encapsulated actinomycin D and increased effectiveness in Ehrlich ascites tumor cell killing, a morphological study. J. Cell Biol. 63, 380 (1974).

Yoakum, G. H. Synergism of near-UV photoproducts of L-tryptophan and 365 nm radiation for the induction of "alkali-labile" bonds in bacterial DNA. Abstracts of 2nd Annual Meeting of the American Society for Photobiology, Vancouver, B. C., Canada, July 22-26, 1974, pp. 100-101.

Yoakum, G., W. Ferron, A. Eisenstark, and R. Webb. Stabilization of *E. coli* replication gaps by photoproducts of L-tryptophan. Abstracts of 74th Annual Meeting of the American Society for Microbiology, Chicago, Illinois, May 12-17, 1974, p. 162.

15. SEMINARS DURING 1974

During the first half of 1974, the Division of Biological and Medical Research seminar committee consisted of Drs. E. J. Ainsworth, S. S. Danyluk, M. W. Rosenthal, F. Schlenk, and R. E. Krisch, Chairman. For the 1974-1975 seminars, the committee consisted of Drs. S. S. Danyluk, R. N. Feinstein, T. Matsushita, C. A. Reilly, Jr., and E. J. Ainsworth, Chairman.

In the Fall of 1974, the seminar format was changed to provide a greater opportunity for questions and in-depth discussions of the seminar speaker's subject. An informal afternoon colloquium with the speaker was instituted to supplement the formal seminar, which was shifted to 11:00 A.M. from 3:00 P.M.

The seminar program for 1974, selected by the committee on the basis of recommendations from the staff, was as follows:

Dr. F. Mauro, Laboratory of Animal Radiation Biology, CNEN, CSN
"Studies of Drug Effects on Plateau Phase Mammalian Cells"
January 7, 1974

Dr. A. Han, Central Institute for Tumors and Allied Diseases, Zagreb, Yugoslavia and the Division of Biological and Medical Research, ANL
"Ultraviolet Light Induced DNA-to-Protein Crosslinking in Mammalian (HeLa) Cells"
January 17, 1974

Dr. Clement E. Furlong, University of California
"The Periplasmic Binding Proteins of *Escherichia coli* and *Salmonella typhimurium*"
January 24, 1974

Dr. Ronald W. Hart, Oak Ridge National Laboratory
"Biological Results of Disturbance to Cellular Homeokinetics"
January 31, 1974

Dr. Noel R. Rose, Wayne State University, School of Medicine
"Genetic Aspects of Autoimmune Thyroiditis"
February 7, 1974

Dr. E. Costa, Laboratory of Preclinical Pharmacology
"Multiple Ion Detection in the Study of Putative Synaptic Transmitters"
February 14, 1974

Dr. Friedrich Deinhardt, Rush-Presbyterian-St. Luke's Medical Center
"Oncogenic Simian Herpesviruses and Epstein-Barr Virus of Man: The Significance of their Similarities and Differences"
February 21, 1974

Dr. J. J. Trentin, Baylor University College of Medicine
"Control of Hematopoietic Stem Cell Differentiation, and Genetic Resistance to Bone Marrow Transplantation"
February 28, 1974

Dr. Paul D. Forbes, Temple University Health Sciences
"Carcinogenesis by Ultraviolet Light"
March 7, 1974

Dr. Philip Hanawalt, Stanford University
"Molecular Mechanisms for the Repair of DNA"
March 14, 1974

Dr. Donald F. Steiner, The University of Chicago
"Studies on the Biosynthesis of Insulin and Other Polypeptides"
March 21, 1974

Dr. D. W. van Bekkum, Radiobiological Institute, The Netherlands
"Hemopoietic Stem Cells in Relation to Leukemia"
March 28, 1974

Dr. J. D. Chapman, Atomic Energy of Canada Limited; Whiteshell Nuclear Research Establishment
"Modification of Cellular Radiation Sensitivity by Exogenous Chemicals"
April 4, 1974

Dr. Charles M. King, Michael Reese Hospital
"Modification of Tissue Macromolecules by Carcinogenic Aromatic Amines"
April 9, 1974

Dr. Zhores Medvedev, National Institute for Medical Research, USSR
"Peaks of Longevity in the USSR, Biological and Social Aspects"
April 15, 1974

Dr. Alexander Nakeff, Mallinckrodt Institute for Radiology
"Recent Advances in the Humoral Regulation of Megakaryocyte and Platelet Production: An Overview"
April 25, 1974

Prof. Frank Blatt, Michigan State University
"The Action Potential in Algae"
April 26, 1974

Dr. Webster S. S. Jee, University of Utah College of Medicine
"Diphosphonates, an Approach to the Therapy of Osteoporosis"
May 2, 1974

Dr. Ronald Paque, University of Illinois at the Medical Center
"Transfer of Delayed Type Hypersensitivity with Subcellular Components of Sensitized Lymphoid Cells"
May 9, 1974

Prof. W. F. Forbes, University of Waterloo
"Some Recent Advances in Smoking and Health Studies"
May 17, 1974

Mini-Symposium, May 23, 1974, in Honor of Dr. Theodore N. Tahmisian

Dr. Harold W. Beams, University of Iowa, Moderator
"Electron Microscopy and Biological Ultrastructure"

Prof. Hewson Swift, University of Chicago
"Electron Microscopy of DNA Molecules"

Dr. Albert J. Dalton, National Cancer Institute
"Ultrastructural Characterization of Oncorna (Oncogenic RNA) and Related Viruses"

Dr. Richard G. Kessel, University of Iowa
"Biological Applications of Scanning Electron Microscopy"

Dr. J. Robert Stewart, University of Utah Medical Center
"Clinical and Experimental Aspects of Radiation-Induced Heart Disease"
May 30, 1974

Dr. Stan D. Vesselinovitch, University of Chicago
"Hepatocarcinogenesis and Diurnal Variation in Macromolecular Replication"
June 6, 1974

Dr. Samuel S. Epstein, Case Western Reserve University
"Adverse Health Effects from Chemical Pollutants of the Environment: Science and Public Policy"
June 13, 1974

Dr. J. Broerse, Radiobiological Institute TNO
"Preliminary Results of Fast Neutron Radiotherapy"
June 20, 1974

Dr. Lawrence Goodfriend, McGill University
"Chemistry of a Low Molecular Weight Ragweed Pollen Allergen Ra5, and Association of Responsiveness to Ra5 with HL-A7 Cross-reacting Group"
June 27, 1974

Prof. Carroll M. Williams, Harvard University
"Photoperiodic Behavior Controlling Dormancy and Development in Silkmoths"
August 6, 1974

Dr. Francesco Bresciani, University of Naples, Italy
"Early Molecular Stages of Estrogen Interaction with Responsive Cells"
September 13, 1974

Dr. Melvin L. Griem, University of Chicago
"Effects of Radiation and Chemotherapeutic Agents on Hair Growth"
September 26, 1974

Dr. Abraham Worcel, Princeton University
"Studies on the Folded Chromosome of *E. coli*"
October 4, 1974

Prof. Arthur L. Koch, Indiana University
"Energy Coupling to Membrane Transport"
October 31, 1974

Dr. Arnold J. Levine, Princeton University
"Adenovirus and SV40 Early Proteins Involved in DNA Replication and Viral Transformation"
November 21, 1974

Dr. Harvey V. Samis, Jr., Masonic Medical Research Laboratory
"Aging: Errors and Regulatory Capability"
December 5, 1974

Dr. Robert Rein, State University of New York at Buffalo
"Interactions Between Nucleic Acid Constituents and Structure of Nucleic Acids"
December 12, 1974

Dr. Ross Nigrelli, Osborn Laboratories of Marine Sciences New York Aquarium
"Longevity and Aging in Fish"
December 19, 1974

In addition, several informal seminars in specialized subjects were held during the year. Most of the speakers were members of the Divisional staff; on occasion scientists from other institutions, primarily in the Chicago area, also presented seminars, as follows:

Dr. Page R. Painter, University of California
"Protein Burden and Control of Cell Growth"
January 30, 1974

Dr. Abraham Eisenstark, University of Missouri
"The Role of L-Tryptophan and Life Processes"
February 5, 1974

Dr. L. Dumas, Northwestern University
"Effects of Host Mutations on Bacteriophage ϕX-174 DNA Replication"
February 20, 1974

Dr. Katherine L. Knight, University of Illinois Medical Center
"Genetic Control of Antibody Biosynthesis"
March 13, 1974

Dr. Dieter Mergenhagen, Harvard University
"The Biological Clock in a Single Cell Acetabularia"
April 8, 1974

Dr. Francis C. Neuhaus, Northwestern University
"Translocation Reactions in the Biosynthesis of Bacterial Cell Walls"
April 17, 1974

Dr. Steve Hsieh, University of Wisconsin
"Mechanism for the Biosynthesis of Dimethylselenide from Selenite"
May 10, 1974

Dr. Clarence Kado, University of California
"Studies of the Mechanism of Tumorigenesis in Higher Plants by *Agrobacterium tumefaciens*: Role of DNA"
May 16, 1974

Dr. Deepak Bastia, University of Colorado
"Initiation and Termination of DNA Replication of Phage λ"
May 20, 1974

Dr. Richard E. Ecker, Vitose Corporation
"A Kinetic Model for Determining Amino Acid Pool Size and Role of Protein Synthesis in Rapidly Synthesizing Cells"
June 18, 1974

Dr. George S. Dimitrievich, University of Chicago
"Effects of Fast Neutrons and X-ray Irradiation"
June 26, 1974

Dr. B. S. Mawhinney, University of London, England
"Radiation Effects on the Thyroid in the Chick Embryo"
July 9, 1974

Dr. Marilena Bianchi, European Organization for Nuclear Research, Switzerland
"RBE at Low Doses and Dose Rates of PuBe 14 MeV and 400 MeV Neutrons"
July 25, 1974

Dr. Joannes A. G. Davids, Biology Group Reactor Centrum Nederland, Patten; The Netherlands
"Status of the Neutron Radiobiology Program at Reactor Centrum, Nederland"
July 26, 1974

Dr. Hanoch Slor, Tel-Aviv University, Israel
"Studies of Excision of Thymine Dimers Using Extracts of Mammalian Cells"
September 10, 1974

Dr. Alvin Markovitz, University of Chicago
"A Pleiotropic Mutation Controlling Radiation Sensitivity, Polysaccharide Synthesis (*gal* operon), and Bacteriophage Lambda Development"
October 16, 1974

Dr. Robert Roth, Illinois Institute of Technology
"Genetic Control of Replication During Meiosis in Yeast"
October 30, 1974

Dr. Conrad Woldringh, Universiteit Van Amsterdam Laboratorium, The Netherlands
"Morphological Aspects of Cell Division in *E. coli* B/r"
November 6, 1974

Dr. I. A. Newman, University of Tasmania, Australia
"Electric Measurements on Oats and Phytochrome Transformation"
November 14, 1974

Dr. Lucia Rothman-Denes, University of Chicago
"Replication of DNA Virus"
November 27, 1974

Dr. Stephen Benjamin, Lovelace Foundation
"Pathological Studies in the Lovelace Inhalation Program"
December 6, 1974

Dr. James D. Yager, Dartmouth College
"DNA Repair as One Aspect of the Initiation of Carcinogenesis"
December 10, 1974

Dr. M. C. Henry, IIT Research Institute
"Role of Particles in Respiratory Carcinogenesis Bioassay"
December 17, 1974

AUTHOR INDEX

☆ U.S. GOVERNMENT PRINTING OFFICE: 1975—652-279